Bauhaus-Universität Weimar

Graduiertenkolleg 1462

Evaluation of the coupling between an analytical and a numerical solution for boundary value problems with singularities

Bewertung der Kopplung zwischen analytischen und numerischen Lösungen für Randwertaufgaben mit Singularitäten

DISSERTATION

zur Erlangung des akademischen Grades
Doctor rerum naturalium
an der Fakultät Bauingenieurwesen
der
Bauhaus-Universität Weimar

vorgelegt von

Dmitrii Legatiuk

geboren am 01.05.1988 in Tula, Russland

Gutachter:
1. Prof. Dr. rer. nat. habil. Klaus Gürlebeck
2. Prof. Maria Irene Almeida Falcão
3. Prof. Dr. Wolfgang Sprößig

Tag der Disputation: 17. Februar 2015

The miracle of the appropriateness of the language of mathematics for the formulation of the laws of physics is a wonderful gift which we neither understand nor deserve. We should be grateful for it and hope that it will remain valid in future research and that it will extend, for better or for worse, to our pleasure, even though perhaps also to our bafflement, to wide branches of learning.

Eugene Wigner

Zusammenfassung

In der Praxis muss man sich häufig mit Problemen befassen, die verschiedene Arten von Singularitäten (z.B. Risse, Lücken etc.) beinhalten. Um diese Probleme mit numerischen Methoden zu bearbeiten, ist es notwendig, einige Anpassungen in der Nähe der Singularität vorzunehmen. Die bekannteste numerische Methode ist die Finite-Elemente-Methode, welche es erlaubt, eine Näherungslösung für singuläre Probleme mit Hilfe von Netzverfeinerungen zu konstruieren.

Eine Alternative zu den numerischen Methoden sind die funktionentheoretischen Methoden, welche die Konstruktion einer exakten Lösung eines Randwertproblems mit einer Singularität erlauben. Aufgrund der Tatsache, dass diese Methoden auf einige kanonische Gebiete beschränkt sind, ist deren tatsächliche Anwendung sehr begrenzt.

Die Idee dieser Doktorarbeit ist es, eine Methode zu entwickeln, die die Vorteile sowohl der FEM, als auch der funktionentheoretischen Methoden in einem einzigen Verfahren miteinander kombiniert. Diese Verbindung wird durch das Konstruieren einer exakten Lösung einer Differentialgleichung in einem kleinen Gebiet nahe der Singularität und durch die Kopplung dieser analytischen Lösung mit der Finite-Elemente-Lösung in dem verbleibenden Teil des Gebietes realisiert.

Diese Arbeit zeigt einen Weg auf, wie man eine stetige Kopplung zwischen den beiden Lösungen konstruiert. Die Stetigkeit ist durch einen speziellen Interpolationsoperator gesichert, der auf dem Interface zwischen den beiden Lösungen definiert wird.

Die eindeutige Lösbarkeit des dazugehörigen Interpolationsproblems ist in dieser Arbeit bewiesen. Erste Schritte der Konvergenzanalyse und der Fehlerabschätzung werden durchgeführt und bewiesen. Verschiedene numerische Beispiele einschließlich eines tatsächlichen Beispiels aus der Ingenieurpraxis werden vorgestellt. Diese Arbeit lässt erkennen, dass eine solche Kopplungsmethode das Potential besitzt, ein nützliches Instrument für praktische Anwendungen zu werden. Insbesondere die Arbeit mit der analytischen Lösung nahe der Singularität lässt eine bessere lokale Konvergenzrate in dieser Region erwarten.

Abstract

Often in practice one has to deal with problems containing different types of singularities (crack, gaps, etc.). To handle such problems by numerical methods one needs to perform some adaptations in the region near the singularity. The finite element method is the most popular numerical method among the others, which allows to construct an approximate solution for singular problems after a certain level of refinement.

An alternative to numerical methods are the function theoretic methods, which allow to construct an exact solution to a boundary value problem with a singularity. But due to the fact that these methods are restricted to some canonical domains, their real applications are rather limited.

The idea of this thesis is to propose a method which can combine the advantages of the FEM and the function theoretic methods in one procedure. This combination is realised by constructing an exact solution to a differential equation in the small region near a singularity and by coupling this analytical solution with the finite element solution in the remaining part of a domain.

This thesis shows a way how to construct a continuous coupling between two solutions. The continuity is ensured by a special interpolation operator, which is constructed on the interface between the two solutions. The unique solvability of the corresponding interpolation problem is proved in this thesis. First steps in the convergence analysis and the error estimation are performed and proved. Several numerical examples including a realistic example of the engineering practice are presented. This work indicates that such a method of coupling has a potential to become a useful tool in practical applications. The idea is that by working with the analytical solution near the singularity one can expect a better convergence rate in this region.

Acknowledgments

I would like to express my deepest thanks to my supervisor Professor Klaus Gürlebeck for his support throughout my work in Weimar. His open mind, his endless ideas and his inspiration for mathematics, which I've learned from him. It is a great honour for me to be his student.

Special thanks must go to Professor Guido Morgenthal for the possibility to work on a real engineering problem. Without his great engineering experience the applied part of this thesis wouldn't be possible.

I would like to send my particular thanks to Professor Maria Irene Falcão for opening for me the world of conformal mappings and their applications in elasticity during my stay in Braga.

I would also like to thank Professor Uwe Kähler for inviting me to Aveiro and providing me valuable support in the approximation theory, and for the great time during my stay.

Especially I would like to thank Tina Liesigk for her invaluable help in the organisation of my life in Weimar, and for strong linguistic and administrative support.

Thanks are also due to Doctor Reinhard Illge for his great experience in didactics and language, which helped me in the way of writing this thesis.

I'm grateful to Professor Frank Werner for the opportunity to join the great team of the GRK 1462.

I'm also grateful to the German Research Foundation (DFG) for the financial support of my research.

Contents

Chapter 1

Introduction

During the modelling of different physical phenomena in engineering practice we often have to deal with problems containing different types of singularities: cracks, gaps, interfaces between different materials, geometric irregularities, singular boundary conditions, etc. Such problems typically require more sophisticated techniques to construct a solution which will describe the singularity correctly. These techniques will vary depending on the considered problem, and therefore at the present moment it is not possible to construct a general method which will cover all possible cases. For that reason this thesis deals with the linear elastic fracture mechanics on the macro scale, i.e. with the corresponding boundary value problem with a singularity coming from a crack tip.

The fracture mechanics considers bodies with cracks and inclusions, and one of the main interests is the description of the behaviour of mechanical parameters (displacements, strains, stresses, etc.) in the region near these irregularities. One of the first works in that direction was done by Westergaard in [Westergaard 1939], where he has shown an influence of a crack on the stress distribution in an infinite body. With developing of new technologies and new materials the study of fracture became more and more important task in research and in engineering practice. A huge amount of works has been published in this field, for an overview we refer to some classical works, like [Anderson 2005, Broek 1984, Liebowitz 1968] and the references therein. The book of Liebowitz [Liebowitz 1968] is of particular importance, because in that book the crucial role of the complex function theory in the construction of analytical solutions was shown. Even Westergaard has constructed the analytical solution for an infinite plane with a crack by the help of the complex-valued functions. But only in [Liebowitz 1968] the significance of the complex function theory was shown in all its majesty.

Another crucial work in the direction of applications of the complex function theory is related to the name of Kolosov, and to the name of his student Muskhelishvili. In his doctoral thesis Kolosov [Kolosov 1909] has introduced a representation of a general solution to a problem of plane elasticity in terms of two independent analytic functions of one complex variable z. Later on Muskhelishvili in his book [Mußchelischwili 1971], has given a strong mathematical foundation for the proposed method of solution. He has developed ideas not only for the method introduced by Kolosov, but he has shown a

remarkable series of examples for applications of classical tools from the complex function theory, such as Cauchy integral formula and conformal mappings.

The analytical solution based on the complex function theory gives us a high accuracy of the solution in the neighbourhood of the singularity. Because of using exact solutions of the partial differential equations all details of the mathematical model are preserved. The disadvantage of the complex analytic approach is that the full linear elastic boundary value problem can be solved explicitly only for some elementary (simple) or canonical domains. By that reason the alternative to analytical methods – numerical methods, become a very popular tool for practical calculation.

The finite element method is the most popular numerical method which is used for solving practical problems in different fields of engineering. But to deal with problems which contain a singularity one has to make some adaptations and improvements to get an acceptable result. For instance, in the case of mesh-based methods one has to perform an additional refinement in the region near the singularity. Another approach is to introduce a special singular element, see for example [Zienkiewicz & Taylor 2000], where a set of basis functions is enriched by functions which show correct asymptotic behaviour near the singularity. The extended finite element method is based on that idea [Fleming et al. 1997]. In the recent years a lot of possible adaptations of the finite element method were studied. Among the others the Extended and Generalized Finite Element methods are the most popular at the moment, an extensive review on these methods can be found in [Belytschko et al. 2009].

These modern computational methods give us a lot flexibility in the modelling of fracture and in solving singular problems. But they are also not free of disadvantages:

(i) the functions which are used to enrich the standard finite element basis are based on some well-known analytical solutions from the fracture mechanics for canonical domains, like for example, a crack in an infinite plane. But in a bounded domain one has to take into account boundary conditions which will influence the behaviour of the analytical solution near the singularity. By the construction the well-known analytical solutions for infinite bodies cannot represent this influence of the boundary conditions;

(ii) by using in a certain region the enrichment function we typically loose the continuity between the enriched elements and the standard elements. This problem was solved by introducing a new version of the FEM, the Generalized Finite Element Method [Melenk 1995], an overview of this method can be found in [Babuška et al. 2004];

(iii) the third disadvantage is that the constructed solution near the singularity is not an exact solution to the differential equation in that region. This disadvantage can be crucial if one is interested in more detailed analysis of the fracture process and wants to calculate some physical quantities (for example, strain energy, stress intensity factors, etc.). Because from the fracture mechanics it is known, that these quantities can be easily calculated exactly if the solution is an analytic function.

But in the case of the finite element approximation a solution is never an analytical function, and therefore all these physical quantities can be only approximated.

Another point of view on the problem is to try to construct a coupled method: to use the analytical solution in a small region near the singularity and couple it with the finite element solution in the remaining part of a domain. The first attempt in the direction of a coupling of the complex function theory and the finite element method was done by Piltner in his PhD thesis [Piltner 1982]. The idea of Piltner was to introduce a special finite element containing a crack or a hole. The solution inside of this special element is constructed by the complex function theory, and a coupling with standard finite elements is realised via nodes on the boundary of the special element. This approach was further developed in his works [Piltner 1985, Piltner 2003, Piltner 2008].

Piltner has shown promising results obtained by his method, but a continuous coupling between two solutions was still missing. Because the solution between two nodes was assumed to be a piecewise linear or a piecewise quadratic function, which is not true for the analytical solution based on holomorphic functions. Therefore a global solution has jumps passing this boundary, and from the point of view of quality this is not completely satisfying to improve the approximation of a point singularity (zero-dimensional) of the displacement field and as a result the displacement field has a one-dimensional jump.

To overcome the problem of a discontinuous coupling between the two solutions we introduce a method of coupling in this thesis. The main goal of this approach is to obtain a global continuity for the displacement field in the whole domain. To get the desired continuity we introduce a new type of finite elements, the so-called coupling elements, which are based on the special interpolation operator. In the works of Piltner the coupled method was realised based on a variational formulation in the whole domain. But in the proposed method we construct the shape functions in the special element based on a strong solution of a differential equation in the field near the singularity. In this case these shape functions for the finite element approximation satisfy the differential equation in the special element.

Another goal of the proposed method is to use the classical version of the finite element method. This goal is related to the simplicity of the method, that one can use the most canonical form of the FEM and one can obtain anyway a continuous coupling. This approach is different to the GFEM, which requires more sophisticated technique for the numerical integration. Another difference to the GFEM is that in the proposed method the special functions (analytic functions) are not simply multiplied with the vertex "hat" functions, but are used in the constructions of the finite element shape functions. By this construction the shape functions satisfy the differential equation in the region near the singularity.

Another reason for the classical FEM is a very fundamental mathematical basis which was developed in [Ciarlet 1978, Ciarlet & Raviart 1971]. Because our main goal is not only to show a few numerical examples for test problems, but to construct a theory for the proposed method of coupling. Particular interest is to obtain the error estimate for the coupling, which can be considered as a measure of a quality for the coupling.

According to these goals this thesis is organised as follows. Chapter 2 gives an introduction to the linear elasticity theory. The last section of this chapter is devoted to discussion of boundary value problems in nonsmooth domains and the regularity of the exact solution in this case.

Chapter 3 introduces the complex and the hypercomplex function theory, and their application to boundary value problems of the linear elasticity. The analytical solution to a crack tip problem is constructed in this chapter.

Chapter 4 shows a way how to get the desired coupling. One of the most important results here is the main interpolation theorem, which is proved for an arbitrary node distribution. To make the method more applicable the possible strategy for a refinement is discussed here. Finally the construction of the shape function is illustrated.

Chapter 5 presents the most fundamental results of the thesis in the direction of the error estimation and convergence analysis of the proposed method. Two different strategies for convergence analysis are proposed and proved in this chapter. An alternative proof of the main interpolation theory is also shown in this chapter. Finally the coupling error is estimated here.

Chapter 6 shows several numerical examples, which serve to study possible ways for improvements of the proposed method. In this chapter two examples are considered: a test example with the known exact solution, and a realistic example of a full-size concrete hinge. The obtained results show the potential of the proposed scheme.

In the final Chapter 7 a summary of the work presented is given, conclusions are drawn and possible ways of the future research are provided.

Chapter 2

Fundamentals of linear elasticity theory

The goal of this chapter is to introduce fundamentals of linear elasticity theory. Basic concepts and equations of a continuum mechanics will be introduced with restriction to linear elastic isotropic bodies. We will show a general statement of boundary value problems, which can be formulated in linear elasticity. In the framework of this thesis we will consider boundary value problems in a plane and also in a three dimensional case. For that reason we will formulate everything for spatial elasticity theory, and in the following chapters about plane problems some formulae can be repeated if necessary. The general theory of continuum mechanics can be found in many books, like for instance, in the classical Russian book of [Ilyushin 1971]. The content of this chapter is based on ideas from [Ilyushin 1971, Lurie 1965, Mußchelischwili 1971].

2.1 Main ideas of continuum mechanics

Continuum mechanics considers bodies of such size, that their small parts dV will contain a sufficiently large number of particles. Therefore for these small parts one can introduce definitions of macroscopic quantities like density of body, displacements, velocities, accelerations, outer forces, internal energy and others in sense of mean values. The fact that all mean values are considered as true values is the idealisation of a real physical body in the continuum mechanics. Quantity and mathematical nature of the introduced mean values must be sufficient to describe an internal state of a body and an interaction between bodies. Continuum mechanics considers mainly mechanical and thermal interactions and deformations of small volumes, but when, a so-called, the multi-field problem is formulated then influences of electromagnetic fields, chemical reaction, etc. are also taken into account.

To describe physical states and processes the continuum mechanics uses the three-dimensional Euclidean space with different coordinate systems and the classical time. Physical processes must be independent on the choice of a coordinate system. According to that, mathematical objects which characterise the physical processes must be independent

on the particular choice of the coordinate system, and physical laws must be described by these objects through mathematical relations, which are invariant under coordinate transform.

The main mathematical objects in the continuum mechanics are tensors of different orders: zeroth order – scalars (density, energy, etc.), first order – vectors (radius vector, heat flow, velocity etc.), second order (strain tensor, stress tensor, etc.). All of these tensors are considered to be continuously differentiable with respect to coordinates and to time, and therefore they are bounded with their derivatives in the volume of a body. The physical state of an elastic body can be described by the following physical quantities: forces acting on the continuum, displacements, and strains. These physical quantities are related by a coupled system of partial differential equations: equations of motion, constitutive equations and kinematic equations, which form the system of equations of the linear elasticity.

A material continuum which was originally in equilibrium and occupied a volume v with a surface o reaches a new equilibrium state whose volume and surface are denoted by V and O respectively. The first state is referred to as the initial state (volume v), whilst the second state is called the final state (volume V). We will use these notations throughout this chapter.

2.2 Stresses and outer forces

Let us consider a continuum in its final state. The forces acting on the continuum can be classified as external or internal forces. External forces represent actions on the continuum particles by bodies which are not included in the considered volume V. The external forces may be surface forces (a pressure for instance) and/or volume forces (the gravity force). The force which acts on each particle of the continuum is called a mass force. The mass force which is acting on the mass contained in the volume dV is called the volume force.

Consideration of the equilibrium of a continuum is based upon two statements:

 (i) when the whole continuum is in equilibrium, then any arbitrary part of this contin-
     uum is also in equilibrium (the free-body principle);

 (ii) the equilibrium conditions for a rigid body are the necessary conditions of equilib-
      rium of the considered part of the continuum (the principle of solidification).

Let us mentally divide the volume V into two volumes V_1 and V_2. Let O' denote the surface separating the two volumes and O_1 denotes the part of O which bounds the volume V_1. In addition to the external forces acting on the continuum in volume V_1 we should consider the reaction forces of the continuum in volume V_2 on volume V_1. If we do not include the latter forces, then the necessary conditions of equilibrium of the external forces, which are mass forces in V_1 and surface forces on O_1, are, in general, not satisfied. These forces should be equilibrated by the forces and moments of the interaction forces distributed over the separating surface O'. It is assumed that the distribution of these forces over the surface dO of the surface O' is statically equivalent to the force $\boldsymbol{\sigma}_n dO$,

6

the orientation of the surface dO being prescribed by a unit normal vector $\mathbf{n}$ directed outwards from V_1, see Fig. 2.1.
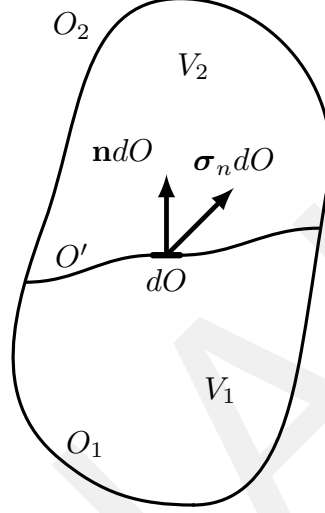

Figure 2.1: Elementary volume of a medium

Therefore, for any oriented surface $\mathbf{n}\,dO$ at any location in the continuum, there exists a force $\boldsymbol{\sigma}_n dO$ (a vector) which is the force exerted on $\mathbf{n}\,dO$ by the part "above" this surface. By virtue of the principle of action and reaction we have

$$\boldsymbol{\sigma}_{-n}dO = -\boldsymbol{\sigma}_n dO.$$

This interaction of the part of the continuum defines the field of internal forces, or in other words, the stress field in continuum. Not only the quantitative characteristics of the stress field vary from point to point, as in scalar fields, but it is also not possible to indicate a certain direction at any point, as in vector fields. The quantity prescribing the stress field must determine the vector $\boldsymbol{\sigma}_n dO$ at any point of the field and for any oriented surface $\mathbf{n}\,dO$ at this point (or vector $\boldsymbol{\sigma}_n$ in terms of vector $\mathbf{n}$). This means that the physical state referred to as the stress field is determined by a quantity which relates vector $\boldsymbol{\sigma}_n$ to vector $\mathbf{n}$. Adopting a linear relationship between these vectors means that this quantity is a tensor of the second rank. This tensor is referred to as the stress tensor and denoted as $\tilde{\boldsymbol{\sigma}}$ whilst its components in a Cartesian coordinate system $\{O; x_1 x_2 x_3\}$ are denoted as σ_{ij}. The vector $\boldsymbol{\sigma}_n$ is determined by multiplication from the left of $\tilde{\boldsymbol{\sigma}}$ by $\mathbf{n}$

$$\boldsymbol{\sigma}_n = \mathbf{n} \cdot \tilde{\boldsymbol{\sigma}}. \tag{2.1}$$

Multiplication from the right of $\tilde{\boldsymbol{\sigma}}$ by $\mathbf{n}$, i.e. $\tilde{\boldsymbol{\sigma}} \cdot \mathbf{n}$, would only affect the notation of components of tensor $\tilde{\boldsymbol{\sigma}}$.

The coordinate representation of the relationship (2.1) is given by the following form

$$\left. \begin{array}{rcl} \sigma_{n_1} &=& \sigma_{11}n_1 + \sigma_{21}n_2 + \sigma_{31}n_3, \\ \sigma_{n_2} &=& \sigma_{12}n_1 + \sigma_{22}n_2 + \sigma_{32}n_3, \\ \sigma_{n_3} &=& \sigma_{13}n_1 + \sigma_{23}n_2 + \sigma_{33}n_3. \end{array} \right\} \tag{2.2}$$

7

Assuming $\mathbf{n} = \mathbf{i}_1$, so that $n_1 = 1$, $n_2 = 0$, $n_3 = 0$ yields the vector of force acting on the unit area with the outward normal $\mathbf{i}_1$. Let us refer to this as stress vector $\boldsymbol{\sigma}_1$. Its projection onto the axes of system $\{O; x_1 x_2 x_3\}$, i.e. $\sigma_{11}, \sigma_{12}, \sigma_{13}$ are termed stresses, where σ_{11} is called the normal, whilst σ_{12} and σ_{13} are called shear stresses. By analogy we introduce stress vectors $\boldsymbol{\sigma}_2$ and $\boldsymbol{\sigma}_3$ on the surfaces whose normals are the unit vectors of coordinate axes $\mathbf{i}_2$ and $\mathbf{i}_3$, respectively. In the matrix of components of tensor $\tilde{\boldsymbol{\sigma}}$

$$\begin{pmatrix} \sigma_{11} & \sigma_{12} & \sigma_{13} \\ \sigma_{21} & \sigma_{22} & \sigma_{23} \\ \sigma_{31} & \sigma_{32} & \sigma_{33} \end{pmatrix},$$

the diagonal and non-diagonal elements present respectively normal and shear stresses. Fig. 2.2 displays an elementary parallelepiped whose edges are parallel to the coordinate axes and the stresses on its three faces.
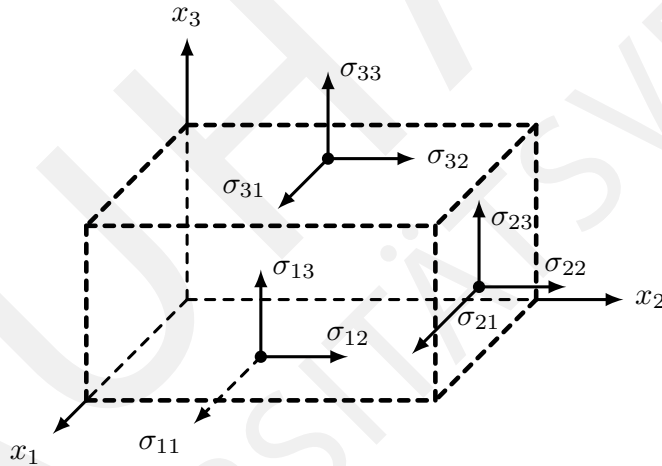
Figure 2.2: An elementary parallelepiped and the stresses on its faces

Let us consider an arbitrary volume V_* bounded by a surface O_*. It is assumed that V_* lies completely within a volume V, and O_* has no common points with a surface O. The surface forces distributed over O_* which are internal for V and external for V_* are caused by the stress state described by the tensor $\tilde{\boldsymbol{\sigma}}$. They are given by the basic relationship (2.1) in which $\mathbf{n}$ denotes the unit vector of the external normal to O_*.

There are two groups of necessary conditions of equilibrium, namely equations of equilibrium in the volume V and those on the surface O. The equations of equilibrium in the volume express the condition of vanishing principal vector and the principal moment of the mass and surface forces in an arbitrary volume V_* within volume V. By expressing these conditions we finally obtain the equation (for all of the details we refer to [Lurie 1965])

$$\operatorname{div} \tilde{\boldsymbol{\sigma}} + \rho \mathbf{K} = 0, \tag{2.3}$$

8

where $\rho\,\mathbf{K}$ is a volume force. This is the first equation of equilibrium for a continuum. The second equation of equilibrium is the symmetry of tensor $\tilde{\boldsymbol{\sigma}}$

$$\tilde{\boldsymbol{\sigma}} = \tilde{\boldsymbol{\sigma}}^{\mathrm{T}}. \tag{2.4}$$

Equilibrium equations for a continuum, eqs. (2.3) and (2.4), are written here in an invariant form. In Cartesian coordinates these equations have the form of three differential equations of statics of a continuum

$$\left.\begin{aligned}
\frac{\partial\sigma_{11}}{\partial x_1} + \frac{\partial\sigma_{21}}{\partial x_2} + \frac{\partial\sigma_{31}}{\partial x_3} + \rho\,K_1 &= 0, \\[2mm]
\frac{\partial\sigma_{12}}{\partial x_1} + \frac{\partial\sigma_{22}}{\partial x_2} + \frac{\partial\sigma_{32}}{\partial x_3} + \rho\,K_2 &= 0, \\[2mm]
\frac{\partial\sigma_{13}}{\partial x_1} + \frac{\partial\sigma_{23}}{\partial x_2} + \frac{\partial\sigma_{33}}{\partial x_3} + \rho\,K_3 &= 0,
\end{aligned}\right\} \tag{2.5}$$

and three equations expressing symmetry of the stress tensor

$$\sigma_{23} = \sigma_{32}, \qquad \sigma_{31} = \sigma_{13}, \qquad \sigma_{12} = \sigma_{21}. \tag{2.6}$$

The equilibrium equations (2.5) contain six components of the symmetric stress tensor. Clearly, equations (2.5) are only necessary conditions for equilibrium, obtaining sufficient conditions inevitably requires consideration of a physical model of the continuum (elastic solid, viscous fluid etc.). The problem of equilibrium of a continuum is statically indeterminate.

Equilibrium equations on the surface O bounding the volume V are obtained from the basic relationship (2.1) where $\boldsymbol{\sigma}_n$ is replaced by force $\mathbf{F}$ distributed over O

$$\mathbf{n} \cdot \tilde{\boldsymbol{\sigma}} = \mathbf{F}.$$

Another form of this equality is

$$n_1\boldsymbol{\sigma}_1 + n_2\boldsymbol{\sigma}_2 + n_3\boldsymbol{\sigma}_3 = \mathbf{F}$$

or

$$\left.\begin{aligned}
n_1\sigma_{11} + n_2\sigma_{21} + n_3\sigma_{31} &= F_1, \\
n_1\sigma_{12} + n_2\sigma_{22} + n_3\sigma_{32} &= F_2, \\
n_1\sigma_{13} + n_2\sigma_{23} + n_3\sigma_{33} &= F_3,
\end{aligned}\right\}$$

where n_s denotes projections of the unit vector $\mathbf{n}$ on the coordinate axes.

The principal values of the stress tensor, referred to as principle stresses, are equal to the roots σ_1, σ_2, σ_3 of its characteristic equation

$$P_3(\sigma) = |\sigma_{sk} - \delta_{sk}\sigma| = \begin{vmatrix} \sigma_{11} - \sigma & \sigma_{12} & \sigma_{13} \\ \sigma_{21} & \sigma_{22} - \sigma & \sigma_{23} \\ \sigma_{31} & \sigma_{32} & \sigma_{33} - \sigma \end{vmatrix} = 0.$$

The algebraic invariants of the stress tensor have the following form

$$
\begin{aligned}
I_1(\tilde{\boldsymbol{\sigma}}) &= \sigma_{11} + \sigma_{22} + \sigma_{33} = \sigma_1 + \sigma_2 + \sigma_3, \\
I_2(\tilde{\boldsymbol{\sigma}}) &= \sigma_{11}\sigma_{22} + \sigma_{11}\sigma_{33} + \sigma_{22}\sigma_{33} - \sigma_{12}^2 - \sigma_{13}^2 - \sigma_{23}^2, \\
I_3(\tilde{\boldsymbol{\sigma}}) &= \det \sigma_{ij} = \sigma_1 \sigma_2 \sigma_3.
\end{aligned}
$$

2.3 Displacements and strains

Let us consider two infinitesimally close points M and N in a volume v (see Fig. 2.3)

$$
\overline{OM} = \mathbf{r} = \mathbf{i}_s x_s, \quad \overline{ON} = \mathbf{r} + d\mathbf{r} = \mathbf{i}_s(x_s + dx_s),
$$

where $\mathbf{i}_s$ denotes the unit basis vectors of the coordinate axes. Their positions M' and N'
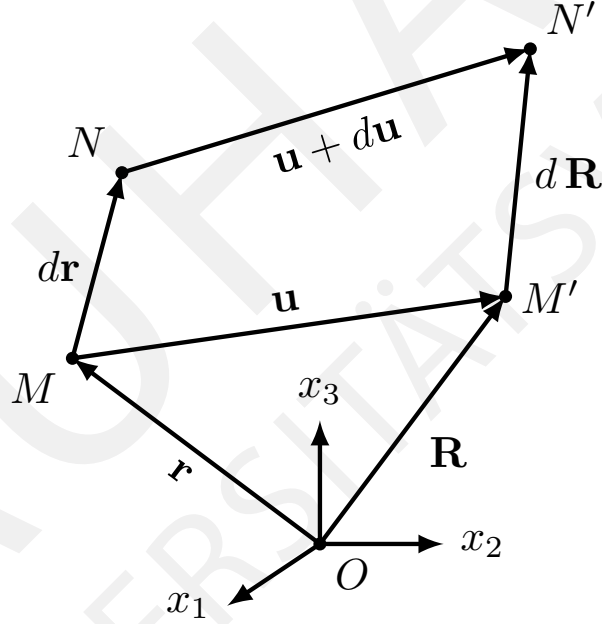
Figure 2.3: Radii vectors of two infinitesimally close points

in volume V are given by the following radii vectors

$$
\left.
\begin{aligned}
\overline{OM'} &= \mathbf{R} = \mathbf{r} + \mathbf{u} = \mathbf{i}_s(x_s + u_s), \\
\overline{ON'} &= \mathbf{R} + d\mathbf{R} = \mathbf{r} + d\mathbf{r} + \mathbf{u} + d\mathbf{u} = \mathbf{i}_s(x_s + dx_s + u_s + du_s).
\end{aligned}
\right\}
$$

Here $d\mathbf{u}$ represents the vector of the relative displacement of two infinitesimally close points in the medium. Then we have

$$
d\mathbf{u} = \frac{d\mathbf{u}}{d\mathbf{r}} \cdot d\mathbf{r} = (\nabla \mathbf{u})^{\mathrm{T}} \cdot d\mathbf{r} = d\mathbf{r} \cdot \nabla \mathbf{u}.
$$

10

The tensor $\frac{d\mathbf{u}}{d\mathbf{r}}$, which is the derivative of the vector $\mathbf{u}$ with respect to direction $\mathbf{r}$, can be set as the sum of its symmetric and skew-symmetric parts

$$\frac{d\mathbf{u}}{d\mathbf{r}} = \frac{1}{2}\left(\frac{d\mathbf{u}}{d\mathbf{r}} + \nabla\mathbf{u}\right) + \frac{1}{2}\left(\frac{d\mathbf{u}}{d\mathbf{r}} - \nabla\mathbf{u}\right) = \tilde{\boldsymbol{\varepsilon}} + \tilde{\boldsymbol{\Omega}}. \tag{2.7}$$

The first component determines a symmetric tensor of second rank which is called the linear strain tensor

$$\tilde{\boldsymbol{\varepsilon}} = \frac{1}{2}\left(\frac{d\mathbf{u}}{d\mathbf{r}} + \nabla\mathbf{u}\right) = \frac{1}{2}\left[(\nabla\mathbf{u})^{\mathrm{T}} + \nabla\mathbf{u}\right].$$

The matrix of the components of this tensor is set in the form

$$\begin{pmatrix} \varepsilon_{11} & \varepsilon_{12} = \dfrac{1}{2}\gamma_{12} & \varepsilon = \dfrac{1}{2}\gamma_{13} \\[2mm] \varepsilon_{21} = \dfrac{1}{2}\gamma_{21} & \varepsilon_{22} & \varepsilon_{23} = \dfrac{1}{2}\gamma_{23} \\[2mm] \varepsilon_{31} = \dfrac{1}{2}\gamma_{31} & \varepsilon_{32} = \dfrac{1}{2}\gamma_{32} & \varepsilon_{33} \end{pmatrix}. \tag{2.8}$$

The expressions for components $\varepsilon_{ij} = \varepsilon_{ji}$ in terms of the derivatives of the displacement vector are as follows

$$\varepsilon_{11} = \frac{\partial u_1}{\partial x_1}, \quad \varepsilon_{12} = \frac{1}{2}\left(\frac{\partial u_1}{\partial x_2} + \frac{\partial u_2}{\partial x_1}\right),$$

$$\varepsilon_{22} = \frac{\partial u_2}{\partial x_2}, \quad \varepsilon_{23} = \frac{1}{2}\left(\frac{\partial u_2}{\partial x_3} + \frac{\partial u_3}{\partial x_2}\right), \tag{2.9}$$

$$\varepsilon_{33} = \frac{\partial u_3}{\partial x_3}, \quad \varepsilon_{31} = \frac{1}{2}\left(\frac{\partial u_3}{\partial x_1} + \frac{\partial u_1}{\partial x_3}\right).$$

In linear elasticity theory the diagonal components of matrix (2.8) relate to extensions, while the non-diagonal components γ_{ij} are referred to as shearing strains.

The second term in formula (2.7) is the skew-symmetric tensor of second rank

$$\tilde{\boldsymbol{\Omega}} = \frac{1}{2}\left(\frac{d\mathbf{u}}{d\mathbf{r}} - \nabla\mathbf{u}\right) = \frac{1}{2}\left[(\nabla\mathbf{u})^{\mathrm{T}} - \nabla\mathbf{u}\right]$$

with the following matrix of the components

$$\begin{pmatrix} 0 & \omega_{12} = -\omega_3 & \omega_{13} = \omega_2 \\ \omega_{21} = \omega_3 & 0 & \omega_{23} = -\omega_1 \\ \omega_{31} = -\omega_1 & \omega_{32} = \omega_1 & 0 \end{pmatrix}.$$

Here the quantities

$$\omega_1 = \frac{1}{2}\left(\frac{\partial u_3}{\partial x_2} - \frac{\partial u_2}{\partial x_3}\right), \quad \omega_2 = \frac{1}{2}\left(\frac{\partial u_1}{\partial x_3} - \frac{\partial u_3}{\partial x_1}\right), \quad \omega_3 = \frac{1}{2}\left(\frac{\partial u_2}{\partial x_1} - \frac{\partial u_1}{\partial x_1}\right)$$

11

represent the projections of vector $\boldsymbol{\omega}$ referred to as the vector of rotation. This vector accompanies tensor $\tilde{\boldsymbol{\Omega}}$.

In the linear elasticity theory the components of tensor $\tilde{\boldsymbol{\varepsilon}}$ and the rotation vector $\boldsymbol{\omega}$ are assumed to be small

$$\left|\frac{\partial u_s}{\partial x_k}\right| \ll 1, \quad |\varepsilon_{sk}| \ll 1, \quad |\omega_s| \ll 1.$$

A typical problem of linear elasticity consists of determining the displacement vector (or its projections u_s) in terms of the prescribed linear strain tensor $\tilde{\boldsymbol{\varepsilon}}$. This involves an integration of the system of six differential equations (2.9). The components of the strain tensor $\tilde{\boldsymbol{\varepsilon}}$ in this system are assumed to be continuous together with the derivatives of the first and second order. The number of equations (six) exceeds the number of the unknowns (three), thus the problem will have a solution only when certain additional conditions are imposed on the components of tensor $\tilde{\boldsymbol{\varepsilon}}$. This can be illustrated by the following example. Let us assume that a medium is divided into elementary blocks. Let each block be subjected to a deformation in the form of small extensions and small shears of the original right-angled block. The obtained bodies can be a continuous (i.e. without gaps) medium only by properly matching the deformation of separate block. This occurs when a displacement vector $\mathbf{u}$ exists such that it is continuous along with the derivatives up to at least third order and the prescribed tensor $\tilde{\boldsymbol{\varepsilon}}$ is its deformation. These conditions are, so called, Saint-Venant's compatibility conditions, and they have the following form

$$\frac{\partial^2 \varepsilon_{11}}{\partial x_2^2} + \frac{\partial^2 \varepsilon_{22}}{\partial x_1^2} = \frac{\partial^2 \gamma_{12}}{\partial x_1 \partial x_2}, \quad \frac{\partial}{\partial x_1}\left(\frac{\partial \gamma_{12}}{\partial x_3} + \frac{\partial \gamma_{31}}{\partial x_2} - \frac{\partial \gamma_{23}}{\partial x_1}\right) = 2\frac{\partial^2 \varepsilon_{11}}{\partial x_2 \partial x_3},$$

$$\frac{\partial^2 \varepsilon_{22}}{\partial x_3^2} + \frac{\partial^2 \varepsilon_{33}}{\partial x_2^2} = \frac{\partial^2 \gamma_{23}}{\partial x_2 \partial x_3}, \quad \frac{\partial}{\partial x_2}\left(\frac{\partial \gamma_{23}}{\partial x_1} + \frac{\partial \gamma_{12}}{\partial x_3} - \frac{\partial \gamma_{31}}{\partial x_2}\right) = 2\frac{\partial^2 \varepsilon_{22}}{\partial x_3 \partial x_1}, \quad (2.10)$$

$$\frac{\partial^2 \varepsilon_{33}}{\partial x_1^2} + \frac{\partial^2 \varepsilon_{11}}{\partial x_3^2} = \frac{\partial^2 \gamma_{13}}{\partial x_1 \partial x_3}, \quad \frac{\partial}{\partial x_3}\left(\frac{\partial \gamma_{31}}{\partial x_2} + \frac{\partial \gamma_{23}}{\partial x_1} - \frac{\partial \gamma_{12}}{\partial x_3}\right) = 2\frac{\partial^2 \varepsilon_{33}}{\partial x_1 \partial x_2}.$$

In practice the first invariant of the strain tensor plays particularly an important role, which is defined as follows

$$\vartheta = I_1(\tilde{\boldsymbol{\varepsilon}}) = \operatorname{div} \mathbf{u}.$$

This invariant has a physical meaning of the dilatation.

2.4 Constitutive equations

The objective of the static analysis of a continuum is to search for that state, among all feasible states of stress (satisfying the equations of statics throughout the volume and on the surface), which is actually realised for the adopted physical model of a particular medium. This model is determined by the constitutive law, namely, for a large number of

media it consists of prescribing relations between the stress tensor and the strain tensor. In the linear elasticity theory it is a linear relationship between the stress tensor and the strain tensor. For a linear elastic body this relationship presents a system of linear equations relating the components of these tensors and expresses the generalised Hooke's law. Also the temperature appears in the expression for the constitutive law.

Prescribing the constitutive law leads to a closed system of differential equations which allows one to determine the state of stress in the body and the displacement vector of the particles of the medium.

The constitutive law of the linear-elastic body under an isothermal deformation process $(\theta = 0)$ is written down in the form

$$\tilde{\boldsymbol{\sigma}} = \lambda \vartheta \tilde{\mathbf{E}} + 2\mu \tilde{\boldsymbol{\varepsilon}}, \tag{2.11}$$

where $\tilde{\mathbf{E}}$ is the unit tensor, λ and μ are the constant moduli of elasticity called the Lamé moduli.

By using eq. (2.11) one can easily express the strain tensor $\tilde{\boldsymbol{\varepsilon}}$ in terms of the stress tensor $\tilde{\boldsymbol{\sigma}}$. We have

$$I_1(\tilde{\boldsymbol{\sigma}}) = \sigma = (3\lambda + 2\mu)\vartheta = 3k\vartheta, \quad \vartheta = \frac{\sigma}{3\lambda + 2\mu},$$

so that

$$\tilde{\boldsymbol{\varepsilon}} = \frac{1}{2\mu} \left(\tilde{\boldsymbol{\sigma}} - \frac{\lambda}{3\lambda + 2\mu} \sigma \tilde{\mathbf{E}} \right). \tag{2.12}$$

Equalities (2.11) and (2.12) express the generalised Hooke's law. The behaviour of a material is prescribed by means of two constants and this is a consequences of assumptions on the medium isotropy and smallness of the components of tensor $\nabla \mathbf{u}$ enabling one to keep only a linear term in the general quadratic dependence between the aligned tensors $\tilde{\boldsymbol{\sigma}}$ and $\tilde{\boldsymbol{\varepsilon}}$.

Equations (2.11) and (2.12) are written in terms of the components of tensors $\tilde{\boldsymbol{\sigma}}$ and $\tilde{\boldsymbol{\varepsilon}}$ in the following way

$$\sigma_{11} = \lambda \vartheta + 2\mu \varepsilon_{11}, \quad \sigma_{12} = 2\mu \varepsilon_{12} \quad \text{etc.,}$$

$$\varepsilon_{11} = \frac{1}{2\mu} \left(\sigma_{11} - \frac{\lambda}{3\lambda + 2\mu} \sigma \right), \quad \varepsilon_{12} = \frac{1}{2\mu} \sigma_{12} \quad \text{etc.} \tag{2.13}$$

Lamé's moduli are used in theoretical papers whereas in the technical literature they are replaced by other moduli of elasticity, most commonly by Young's modulus E and Poisson's ratio ν. In order to introduce these parameters we separate the term with σ_{11} in eq. (2.13) for ε_{11}

$$
\begin{aligned}
\varepsilon_{11} &= \frac{1}{2\mu} \left[\sigma_{11} \left(1 - \frac{\lambda}{3\lambda + 2\mu} \right) - \frac{\lambda}{3\lambda + 2\mu} (\sigma_{22} + \sigma_{22}) \right] = \\
&= \frac{\lambda + \mu}{\mu(3\lambda + 2\mu)} \left[\sigma_{11} - \frac{\lambda}{2(\lambda + \mu)} (\sigma_{22} + \sigma_{33}) \right].
\end{aligned}
$$

Using the notation

$$\frac{\mu\,(3\lambda + 2\mu)}{\lambda + \mu} = E, \qquad \frac{\lambda}{2\,(\lambda + \mu)} = \nu \qquad (2.14)$$

the generalised Hooke's law (2.13) reduces to the form

$$\left.\begin{aligned}
\varepsilon_{11} &= \frac{1}{E}\left[\sigma_{11} - \nu\,(\sigma_{22} + \sigma_{33})\right], & \varepsilon_{12} &= \frac{1}{2\mu}\sigma_{12}, \\[2mm]
\varepsilon_{22} &= \frac{1}{E}\left[\sigma_{22} - \nu\,(\sigma_{33} + \sigma_{11})\right], & \varepsilon_{23} &= \frac{1}{2\mu}\sigma_{23}, \\[2mm]
\varepsilon_{33} &= \frac{1}{E}\left[\sigma_{33} - \nu\,(\sigma_{11} + \sigma_{22})\right], & \varepsilon_{13} &= \frac{1}{2\mu}\sigma_{13}.
\end{aligned}\right\}$$

Using eq. (2.14), the expressions for Lamé's moduli, in terms of E and ν, are put in the form

$$\mu = \frac{E}{2\,(1 + \nu)}, \qquad \lambda = 2\mu\frac{\nu}{1 - 2\nu}.$$

2.5 Boundary value problems of linear elasticity

The basic equations governing elasticity theory can be classified into three groups of relationship. The first group is presented by the equations of statics in volume V

$$\operatorname{div}\tilde{\boldsymbol{\sigma}} + \rho\,\mathbf{K} = 0, \qquad (2.15)$$

relating six components of the symmetric stress tensor $\tilde{\boldsymbol{\sigma}}$ by three equations.

The second group of equations determines the linear strain tensor $\tilde{\boldsymbol{\varepsilon}}$ in terms of the displacement vector $\mathbf{u}$

$$\tilde{\boldsymbol{\varepsilon}} = \frac{1}{2}\left[\nabla\mathbf{u} + (\nabla\mathbf{u})^{\mathrm{T}}\right]. \qquad (2.16)$$

Here we have six equations determining the components of the linear strains tensor by means of the first derivatives of the displacement vector.

The constitutive law for a linear elastic body is formulated in the third group of six equations. For an isotropic solid in an isothermal or adiabatic process this law, referred to as Hooke's law, is written in the form

$$\tilde{\boldsymbol{\sigma}} = 2\mu\left(\frac{\nu}{1 - 2\nu}\vartheta\,\tilde{\mathbf{E}} + \tilde{\boldsymbol{\varepsilon}}\right) \qquad (2.17)$$

or in the form of the inverse relations

$$\tilde{\boldsymbol{\varepsilon}} = \frac{1}{2\mu}\left(\tilde{\boldsymbol{\sigma}} - \frac{\nu}{1 + \nu}\sigma\,\tilde{\mathbf{E}}\right).$$

14

The three groups contain a total of fifteen equations, which is the same number of unknowns – twelve components of two symmetric tensors of second rank $\tilde{\boldsymbol{\sigma}}$ and $\tilde{\boldsymbol{\varepsilon}}$ and three components of vector $\mathbf{u}$.

The conditions on the surface need to be added to the system of equations (2.15)-(2.17) determining the behaviour of the linear elastic body in its volume. These conditions prescribe either the surface forces or the displacement of the surface points. These distinguish the internal problem for the elastic body bounded from outside from the external problem for an unbounded medium with a cavity or cavities. For each of these problems one states three types of problems.

In the first problem a kinematic boundary condition is posed. In a volume V the displacement vector is sought such that it takes a prescribed value on the surface O bounding this volume

$$\mathbf{u}|_O = \mathbf{u}_*(x_1, x_2, x_3).$$

Evidently, coordinates x_1, x_2, x_3 are related by the surface equation.

The second boundary value problem is the static one. Given the distribution of surface forces $\mathbf{F}$, the boundary condition implies the equilibrium equation on the surface

$$\mathbf{n} \cdot \tilde{\boldsymbol{\sigma}}|_0 = \mathbf{F}.$$

The third boundary value problem is the mixed one. A kinematic condition is posed on part O_1 of the surface, whereas on the other part O_2 a static boundary condition holds

$$\left.\begin{aligned} \mathbf{u}|_{O_1} &= \mathbf{u}_*(x_1, x_2, x_3), \\ \mathbf{n} \cdot \tilde{\boldsymbol{\sigma}}|_{O_2} &= \mathbf{F}. \end{aligned}\right\}$$

Remark 1. In this thesis we will follow the classification of the boundary value problem which we have shown. But in literature one can find another classification, where the first boundary value problem is the static one, and the second is the kinematic problem (see for example [Mußchelischwili 1971]).

Two ways of solving the problems of elasticity theory are known. The first one implies determining the displacement vector $\mathbf{u}$. Using this it is not difficult to calculate the strain tensor $\tilde{\boldsymbol{\varepsilon}}$ in terms of $\mathbf{u}$ and thus the stress tensor in terms of $\tilde{\boldsymbol{\varepsilon}}$. This is the only way when the first boundary value problem is considered. However, this way is not always the simplest one and in many cases the way of solving the problem in terms of stresses is favoured. Then one poses the question of seeking a statically possible stress tensor $\tilde{\boldsymbol{\sigma}}$ such that the corresponding strain tensor $\tilde{\boldsymbol{\varepsilon}}$ satisfies the compatibility condition.

By solving the basic equations of the linear elasticity with respect to displacement vector we obtain the Lamé equation

$$\mu \, \Delta \mathbf{u} + (\lambda + \mu)\mathrm{grad}\,\mathrm{div}\,\mathbf{u} + \rho \mathbf{K} = 0, \tag{2.18}$$

or in the form of projections onto the axes of the Cartesian coordinate system

$$
\left.
\begin{aligned}
(\lambda + \mu)\, \frac{\partial \vartheta}{\partial x_1} + \mu \Delta u_1 + \rho K_1 &= 0, \\[2ex]
(\lambda + \mu)\, \frac{\partial \vartheta}{\partial x_2} + \mu \Delta u_2 + \rho K_2 &= 0, \\[2ex]
(\lambda + \mu)\, \frac{\partial \vartheta}{\partial x_3} + \mu \Delta u_3 + \rho K_3 &= 0,
\end{aligned}
\right\}
$$

where

$$
\vartheta = \operatorname{div} \mathbf{u} = \frac{\partial u_1}{\partial x_1} + \frac{\partial u_2}{\partial x_2} + \frac{\partial u_3}{\partial x_3}. \tag{2.19}
$$

2.6 Boundary value problems in nonsmooth domains

Apart from theoretical studies on elasticity theory and continuum mechanics, which can be found in many books, for instance [Malvern 1969, Sokolnikoff 1946], a lot of research was done in the direction of applications of this theory to engineering problems. Corresponding results covering not only elasticity, but also plasticity can be found, for instance, in [Timoshenko & Goodier 1951, Ilyushin & Lensky 1959], for more details we recommend to work with the references therein.

In many of these studies only simplified engineering models are considered, it means that methods of solution are constructed only for some canonical and very classical examples of engineering practice. But it's also a well-known fact that some kind of irregularities in a body, like for instance a crack, can lead to a significant changes in a stress distribution. One of the first works in that direction was done by Westergaard in [Westergaard 1939], where he has shown an influence of a crack on a stress distribution in an infinite body. Later on his significant results lead to a special part of the continuum mechanics, called the fracture mechanics. The fracture mechanics considers bodies with cracks and inclusions, and it's focusing on finding the influence of these irregularities on overall stress distribution in the body. To get an overview of results in this field we refer to some classical works, like [Anderson 2005, Broek 1984, Liebowitz 1968].

In 1965 Lurie in his book [Lurie 1965] has shown that solutions must be constructed more carefully not only in the case of cracks or inclusions, but even for more common boundary irregularities like sharp corners or wedges (see Fig. 2.4). Thus he has shown that the boundary of a domain has a significant influence on the solution of a boundary value problem. And therefore many of the classical methods which work perfectly for smooth domains (domains without corners) cannot be easily applied for solution of a boundary value problem in nonsmooth domains.

Corresponding to the present time the problem of behaviour of a solution (usually called a regularity of solution) for nonsmooth domains is a highly important topic. The importance comes from the fact, that nowadays the majority of engineering problems is
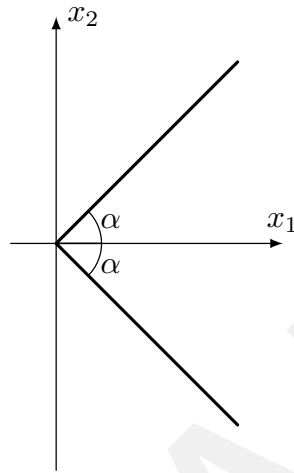
Figure 2.4: Corner with an opening angle 2α

solved by numerical methods, and typically the theory of convergence of these methods is based on the regularity of the exact solution. Therefore the quality of error estimates strongly depends on the quality (regularity) of the exact solution.

With developing the theory of Sobolev spaces the question of regularity of a solution of a boundary value problem in domains with boundary singularities starts to attract mathematicians to work in this direction. One of the first works in this field were done by Kondratiev in the sixties. To avoid a long list of references we refer only to the summary of his results, which can be found in his book with Borsuk [Borsuk & Kondratiev 2006] and the reference therein. By these works it has become clear that the methods of analysis of boundary value problems in smooth domains cannot be applied to the case of nonsmooth domains. Kondratiev has studied the problem of regularity in the L^2 space by applying the method of the Mellin transformation. His results were extended to arbitrary L^p spaces and other functional spaces by Kozlov, Maz'ya, and Roßmann. The summary of their results can be found in the books [Kozlov et al. 1997, Kozlov et al. 2001]. Instead of working with the Mellin transformation, Maz'ya worked with operator theory. According to his results the order of singularity can be obtained by studying the eigenvalues of an operator pencil of a differential equation.

Particularly in [Kozlov et al. 2001] the authors have considered the Lamé system of isotropic elasticity in an angle and a cone with vertex at the origin. In that case the displacement field $\mathbf{u}$ near an isolated vertex has the form $\mathbf{u} = r^\alpha u(\omega)$, where r denotes the distance to the vertex and ω are spherical coordinates in the base of the cone. The knowledge of α and u enables one to determine not only the asymptotics of stresses near conic points, but also the regularity of a weak solution in scales of Sobolev spaces. The pairs (α, u) can be characterised as eigenvalues and eigenvectors of an operator in a

domain on the unit sphere. This pencil is Fredholm. By considering general singularities

$$r^\alpha \sum_{k=0}^{s} \frac{1}{k!} (\log r)^k u^{s-k}(\omega)$$

one arrives at generalised eigenfunctions of the pencil. In the book [Maz'ya & Soloview 2010] these results were also extended to the integral equations in domains with singularities at the boundary.

The generality of the results obtained by Kondratiev and Maz'ya makes it difficult to apply them for analysis of specific problems appearing in real-life applications. But in the 1980s their results were applied and improved by P. Grisvard in his books [Grisvard 1985] and [Grisvard 1992]. Instead of working with the most general case, he has considered polygonal domains with mixed boundary conditions, which is the most common case appearing in engineering practice. Particularly Grisvard has considered a domain Ω in a plane case with polygonal boundary and Ω has only one reentrant corner of measure $\omega > \pi$ at the origin defined by $0 < \theta < \omega$ in the appropriate polar coordinates r, θ. He has shown that the solution $\mathbf{u}$ of the Poisson equation can be decomposed into the sum

$$\mathbf{u} = \mathbf{u}_{\mathrm{R}} + c\,\mathbf{S}$$

of

(i) a regular part $\mathbf{u}_{\mathrm{R}} \in W^{2,2}(\Omega)$ whose behaviour is not affected by the presence of corners and

(ii) a singular part $c\,\mathbf{S}$ where $\mathbf{S}$ is the explicit model singular solution

$$\mathbf{S} = r^\alpha \sin(\alpha\,\theta)$$

where $\alpha = \frac{\pi}{\omega}$ and c is a constant depending only on the data f in the Poisson equation.

In his books Grisvard has presented a series of results on the regularity of a solution of such problems not only in two dimensional geometry, but also in three dimensional case, where the nonsmooth domain is represented by a polyhedron. More precisely, he has studied the edge behaviour which may be described by a three dimensional domain with one reentrant wedge whose edge is the $z'Oz$ axis, defined by $O < \theta < \omega$ in the appropriate cylindrical coordinates r, θ, z. There the solution can be decomposed into the sum

$$\mathbf{u} = \mathbf{u}_{\mathrm{R}} + (K \star c)\mathbf{S}$$

of

(i) a regular part $\mathbf{u}_{\mathrm{R}} \in W^{2,2}(\Omega)$ and

(ii) a singular part $(K \star c)\mathbf{S}$ where $K = \frac{r}{\pi(r^2 + z^2)}$ is a fixed Poisson kernel while c is an arbitrary element of the fractional order Sobolev space $W^{1-\frac{\pi}{\omega},2}(\mathbb{R})$.

Another specification of the results was presented in a paper [Rössle 2000] where the theories of Maz'ya, and Grisvard were applied to a study of a corner singularity for the Lamé equation (2.18) in a plane. This paper has presented a dependence of a regularity of a solution on an opening angle of a corner. Another important theoretical results were presented in [Costabel & Dauge 2002] where more general elliptic systems were considered. The authors have considered so-called Agmon-Douglis-Nirenberg systems and they have proved that for such general elliptic systems with the same boundary condition on both sides of the crack, the singularity exponents of all singular functions satisfying the differential equation have the form $\frac{1}{2} + k$ with integer k. For systems of elasticity with general material law they have obtained the results proved by Maz'ya in [Kozlov et al. 2001].

From these theoretical studies it has become clear, that methods of solution of boundary value problems must be adapted in a proper way to be able to describe a singularity caused by nonsmoothness of a domain. This task becomes even more difficult if we take into account that domains appearing in the engineering practice are not of a simple geometry, and therefore a possible application of analytic methods is rather limited. As an alternative to the analytical methods an adaptation of numerical methods is intensively studied during last years [Fleming et al. 1997]. The so-called Extended and Generalised Finite Element methods are the most popular at the moment, an extensive review of these methods can be found in [Belytschko et al. 2009]. The main idea of these methods is to introduce a set of so-called enrichment functions, which serve to obtain a correct asymptotic behaviour of a solution near the singularity. These enrichment functions are added then to a standard finite element basis in a small region around the singularity. Such a construction allows to use all flexibility of the classical finite element method. But this approach also has several disadvantages:

(i) The enrichment functions are based on some well-known analytical solutions from the fracture mechanics, therefore they have a correct asymptotic behaviour. But the well-known analytical solutions are constructed for canonical problems, like a crack in an infinite plate. But in a bounded domain one has to take into account boundary conditions which will influence the behaviour of the analytical solution near the singularity. By the construction the well-known analytical solutions for infinite bodies cannot represent this influence of the boundary conditions.

(ii) By introducing the enrichment functions in a certain region we typically loose the continuity between the enriched elements and the standard elements. To overcome this problem the Generalized Finite Element Method was introduced by Melenk in his PhD thesis [Melenk 1995]. In the GFEM, the introduction of the special functions into the approximation is done by a simple multiplication of the special function with the vertex "hat" functions based on the linear or the bilinear finite element shape functions, as in the partition of unity methods [Babuška et al. 1996, Melenk 1997]. For the details of a construction of this method we refer to a paper [Strouboulis et al. 2001] and an overview of this method [Babuška et al. 2004].

(iii) The third main disadvantage is that even in the case of a conformal coupling with

the standard finite elements the constructed solution in the field near an inclusion or a crack is not an exact solution to the differential equation in that region. This disadvantage is not so obvious since any of the finite element methods gives us the best approximation of the analytical solution with respect to certain norms. But if one wants to calculate some physical quantities which are not given directly by the best approximation (for example, strain energy, stress intensity factors, etc.), then a set of local refinements could be necessary. Such local refinements significantly increase computational costs, but if one has an exact solution to a differential equation, then it would be possible to calculate these quantity of interest without additional refinement.

Due to the above mentioned disadvantages and based on the fact that before the nineties not so many various versions of the finite element method were available some researchers were looking for an approach which could combine advantages of the finite element and the analytical solution. One example of such a combination was introduced by Piltner in his PhD thesis [Piltner 1982], where he has introduced a special finite element containing a crack or a hole. This special element is based on an analytical solution, which is constructed by the complex function theory. A coupling with standard finite elements is realised via nodes on the boundary of the special element, see Fig. 2.5. This approach was further developed in his works [Piltner 1985, Piltner 2003, Piltner 2008]. In [Piltner 2003] a singular behaviour of stresses near a corner depending on an opening angle was studied. This results coincide with more theoretical work in [Rössle 2000], but were done from more applied point of view by working only with method of the complex function theory, which we will explain and use in chapter 3.
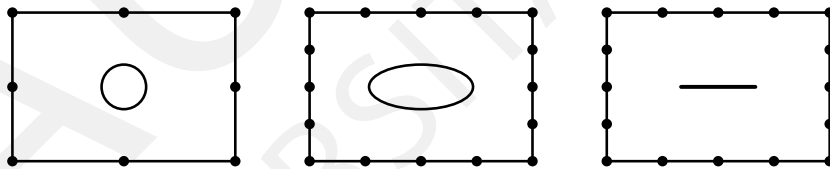
Figure 2.5: Finite elements with a circular/elliptic hole and with an internal crack according to [Piltner 2003]

Piltner has shown promising results obtained by his method, but a continuous coupling between two solution was still missing. Since he has coupled two solution only by values at the nodes on the boundary of the special element a global solution has jumps passing this boundary. The analytical solution in the special element is a purely analytic function, and the finite element solution is based on spline function, therefore they cannot be equal on the boundary between them except values at some specific points. Looking at the quality of the solution it is not completely satisfying that one improves the approximation of a point singularity (zero-dimensional) of the displacement field and as a result the displacement field has a one-dimensional jump.

To overcome the problem of discontinuity between an analytical and a finite element solution we propose in the next chapters of this thesis a new method for coupling. Similar

to the approach of Piltner we introduce a special element which is located near a singularity. Instead of using a special element which contains a crack completely, we work with the special element which covers only a crack tip, see Fig. 2.6. This approach gives us more adaptivity of the method, particularly we can cover the case of a surface crack, which cannot be solved by the approach of Piltner.

Crack
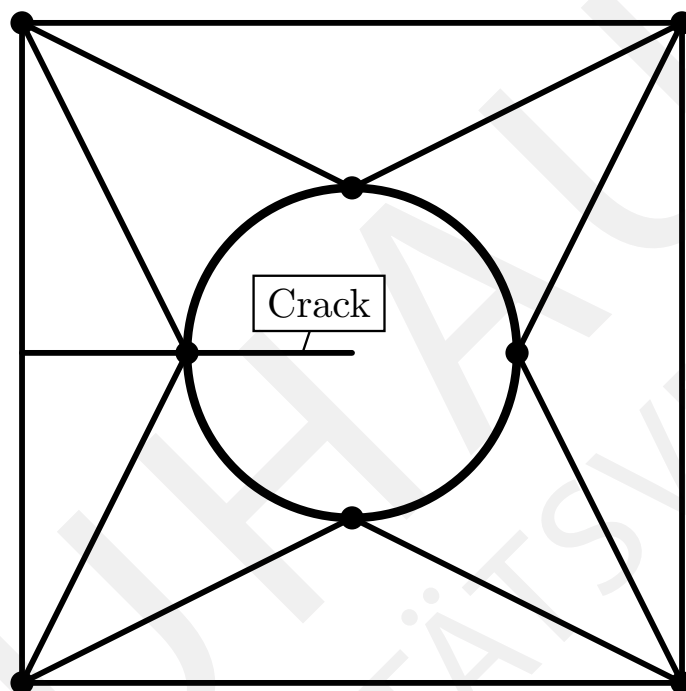
Figure 2.6: Special element for a continuous coupling between two solutions

The main goal of this method is to get the global continuity of the solution, i.e. to couple the analytical solution with the finite element solution continuously not only via nodes at the boundary between two solution, but through the whole interaction interface. To obtain this continuity we will construct the coupling elements (curved triangles in Fig. 2.6), which are based on a special interpolation operator preserving the analytical solution on the interface.

Another goal of the proposed method is to use the classical version of the finite element method. This goal is related to the simplicity of the method, that one can use the most canonical form of the FEM and one can obtain anyway a continuous coupling. This approach is different to the GFEM, which requires more sophisticated technique for the numerical integration. Another difference to the GFEM is that in the proposed method the special functions (analytic functions) are not simply multiplied with the vertex "hat" functions, but are used in the constructions of the finite element shape functions. By this construction the shape functions satisfy the differential equation in the region near the singularity. Throughout the next chapters we will explain and develop the ideas of that method with more details.

Chapter 3

Application of function theoretic methods to linear elasticity problems

A lot of different analytical and numerical methods are available to construct solutions to problems of linear elasticity in the plane. Among the other analytical methods (like for instance, series expansion approach, fundamental solutions, etc.) one of the oldest and well established are the methods based on the complex function theory. This approach is based on the complex representation of the stress function, and the pioneering work in this direction was done by G. W. Kolosov [Kolosov 1909]. In his doctoral thesis he has shown a representation of a general solution to a problem of plane elasticity in terms of two independent analytic functions of one complex variable z, which are also called the complex potentials (see for instance [Green & Zerna 1968] or [Bower 2010]).

The next fundamental work in this direction was done by N. I. Muskhelishvili, who was a student of Kolosov. In his book [Mußchelischwili 1971], the first edition was published in 1931, he has given a strong mathematical foundation for a proposed method of solution. He has developed ideas not only for the method introduced by Kolosov, but he has shown a remarkable series of examples for application of classical tools of complex function theory, such as Cauchy integral formula and conformal mappings.

The methods of complex function theory are not limited only to boundary value problems of linear elasticity, but they are in particular interesting for boundary value problems with singularity, like in fracture mechanics (a crack tip singularity). One of the first works in this field was done by H.M. Westergaard [Westergaard 1939], where he has used a complex-valued function as a stress function. Muskhelishvili in his book has shown how the same solution can be obtained by using the Kolosov-Muskhelishvili formulae. Later on in the book of Liebowitz [Liebowitz 1968] applications of the complex function theory to problems of fracture mechanics were discussed in detail. The advantage of the complex functions approach is an exact representation of the behaviour of a solution near the singularity. But a drawback of this approach is a limitation to standard (canonical) domains. Domains which are coming from real engineering practice are of more complicated shape. For such domains it's a very complicated task to construct an analytical solution satisfying the boundary values, and in many cases this task is unsolvable. To overcome

this limitation we propose another strategy: to construct an analytical solution to a crack tip problem and couple it continuously with one of the well known numerical methods, like the finite element method, for the part of body which is free of singularity.

In this chapter we will introduce the methods of the complex function theory. Also in this chapter we will introduce the basic idea of the proposed method for coupling of an analytical and a finite element solution. To proceed with coupling ideas, at first we need to construct analytical solutions to a crack tip problem in two dimensional case.

3.1 Kolosov-Muskhelishvili formulae for linear elasticity problems

In sequel we will consider the equations of elasticity theory without volume forces. In this case components of stress tensor can be expressed in terms of one additional function, so called the stress function or the Airy function, which plays a crucial role in plane elasticity.

In this case the equilibrium equations are written as follow

$$\frac{\partial \sigma_{11}}{\partial x_1} + \frac{\partial \sigma_{12}}{\partial x_2} = 0,$$

$$\frac{\partial \sigma_{21}}{\partial x_1} + \frac{\partial \sigma_{22}}{\partial x_2} = 0.$$
(3.1)

The first of these equation represents a necessary and sufficient condition for the existence of a function $B(x_1, x_2)$, which satisfies the following conditions

$$\frac{\partial B}{\partial x_1} = -\sigma_{12},$$

$$\frac{\partial B}{\partial x_2} = \sigma_{11}.$$

The second equation from (3.1) is a necessary and sufficient condition for the existence of a function $A(x_1, x_2)$, which satisfies the following conditions

$$\frac{\partial A}{\partial x_1} = \sigma_{22},$$

$$\frac{\partial A}{\partial x_2} = -\sigma_{12}.$$

The comparison of the two equations for $\sigma_{12} = \sigma_{21}$ shows that

$$\frac{\partial A}{\partial x_2} = \frac{\partial B}{\partial x_1},$$

and it follows the existence of a function $U(x_1, x_2)$, such that

$$A = \frac{\partial U}{\partial x_1}, \qquad B = \frac{\partial U}{\partial x_2}.$$

After the substitution of these values for $A(x_1, x_2)$ and $B(x_1, x_2)$ into previous equation we see that there always exists a function $U(x_1, x_2)$. Components of stress tensor can be written by using this function as follows

$$\sigma_{11} = \frac{\partial^2 U}{\partial x_2^2}, \qquad \sigma_{12} = -\frac{\partial^2 U}{\partial x_1 \partial x_2}, \qquad \sigma_{22} = \frac{\partial^2 U}{\partial x_1^2}. \tag{3.2}$$

This fact was first discovered by G.B. Airy in 1862. The function $U(x_1, x_2)$ is called the stress function or the Airy function.

Since functions $\sigma_{11}, \sigma_{12}, \sigma_{22}$ are univalent continuous with their derivatives up to second order, the function $U(x_1, x_2)$ must have continuous derivatives up to fourth order, and these derivatives starting from second order must be univalent functions in the whole domain occupied by a body.

Of course, the inverse formulation is also true: if a function $U(x_1, x_2)$ has the mentioned properties, then the components $\sigma_{11}, \sigma_{12}, \sigma_{22}$ which are given by (3.2) will satisfy also equations (3.1). But it doesn't mean immediately, that these components are related with some possible strain state. To assure that we need to fulfil the compatibility conditions (2.10), which can be rewritten in terms of stresses

$$\Delta\left(\sigma_{11} + \sigma_{22}\right) = 0,$$

or taking into account that

$$\sigma_{11} + \sigma_{22} = \Delta U(x_1, x_2),$$

we get finally

$$\Delta\Delta U(x_1, x_2) = 0 \quad \text{or} \quad \frac{\partial^4 U}{\partial x_1^4} + 2\frac{\partial^4 U}{\partial x_1^2 \partial x_2^2} + \frac{\partial^4 U}{\partial x_2^4} = 0.$$

This equation is called the biharmonic equation, and the solution of it is a biharmonic function.

If a stress function $U(x_1, x_2)$ is given, then corresponding stresses are given by (3.2). But displacements still need to be determined. So, we need to find functions u_1, u_2 from the equations

$$\lambda\vartheta + 2\mu\frac{\partial u_1}{\partial x_1} \quad = \quad \frac{\partial^2 U}{\partial x_2^2},$$

$$\lambda\vartheta + 2\mu\frac{\partial u_2}{\partial x_2} \quad = \quad \frac{\partial^2 U}{\partial x_1^2}, \tag{3.3}$$

$$\mu\left(\frac{\partial u_2}{\partial x_1} + \frac{\partial u_1}{\partial x_2}\right) \quad = \quad -\frac{\partial^2 U}{\partial x_1 \partial x_2}.$$

24

After the solution of the first two equations with respect to $\frac{\partial u_1}{\partial x_1}, \frac{\partial u_2}{\partial x_2}$ we have

$$2\mu\frac{\partial u_1}{\partial x_1} = \frac{\partial^2 U}{\partial x_2^2} - \frac{\lambda}{2(\lambda + \mu)}\Delta U,$$

$$2\mu\frac{\partial u_2}{\partial x_2} = \frac{\partial^2 U}{\partial x_1^2} - \frac{\lambda}{2(\lambda + \mu)}\Delta U.$$

If we denote

$$\Delta U = P,$$

and substitute in the first equation $P - \frac{\partial^2 U}{\partial x_1^2}$ instead of $\frac{\partial^2 U}{\partial x_2^2}$, and doing the same with the second equation, we obtain

$$2\mu\frac{\partial u_1}{\partial x_1} = -\frac{\partial^2 U}{\partial x_1^2} + \frac{\lambda + 2\mu}{2(\lambda + \mu)}P,$$

$$2\mu\frac{\partial u_2}{\partial x_2} = -\frac{\partial^2 U}{\partial x_2^2} + \frac{\lambda + 2\mu}{2(\lambda + \mu)}P. \tag{3.4}$$

The function P is a harmonic function, since

$$\Delta P = \Delta\Delta U = 0.$$

Let Q denote a harmonic function conjugated to P, i.e. a function which satisfies the Cauchy-Riemann equations

$$\frac{\partial P}{\partial x_1} = \frac{\partial Q}{\partial x_2}, \qquad \frac{\partial P}{\partial x_2} = -\frac{\partial Q}{\partial x_1}.$$

Then the expression

$$f(z) = P(x_1, x_2) + i\,Q(x_1, x_2)$$

will be a holomorphic function of the complex variable $z = x_1 + i\,x_2$ in a domain S occupied by a body. Let further

$$\varphi(z) = p + i\,q = \frac{1}{4}\int f(z)dz. \tag{3.5}$$

Obviously we have

$$\varphi'(z) = \frac{\partial p}{\partial x_1} + i\frac{\partial q}{\partial x_1} = \frac{1}{4}(P + i\,Q),$$

and by using the Cauchy-Riemann equations

$$\frac{\partial p}{\partial x_1} = \frac{\partial q}{\partial x_2}, \qquad \frac{\partial p}{\partial x_2} = -\frac{\partial q}{\partial x_1},$$

we get

$$\frac{\partial p}{\partial x_1} = \frac{\partial q}{\partial x_2} = \frac{1}{4}P, \qquad \frac{\partial p}{\partial x_2} = -\frac{\partial q}{\partial x_1} = -\frac{1}{4}Q.$$

Thus

$$P = 4\frac{\partial p}{\partial x_1} = 4\frac{\partial q}{\partial x_2},$$

and therefore equations (3.4) can be rewritten as

$$2\mu\frac{\partial u_1}{\partial x_1} = -\frac{\partial^2 U}{\partial x_1^2} + \frac{2(\lambda + 2\mu)}{\lambda + \mu}\frac{\partial p}{\partial x_1},$$

$$2\mu\frac{\partial u_2}{\partial x_2} = -\frac{\partial^2 U}{\partial x_2^2} + \frac{2(\lambda + 2\mu)}{\lambda + \mu}\frac{\partial q}{\partial x_2}.$$

After integration we get

$$2\mu\, u_1 = -\frac{\partial U}{\partial x_1} + \frac{2(\lambda + 2\mu)}{\lambda + \mu}p + f_1(x_2),$$

$$2\mu\, u_2 = -\frac{\partial U}{\partial x_2} + \frac{2(\lambda + 2\mu)}{\lambda + \mu}q + f_2(x_1),$$

where $f_1(x_2)$ and $f_2(x_1)$ are functions depending only on x_2 and x_1 respectively. Substituting these values into third equation of (3.3) and taking into account that

$$\frac{\partial p}{\partial x_2} + \frac{\partial q}{\partial x_1} = 0,$$

we get

$$f_1'(x_2) + f_2'(x_1) = 0,$$

where it follows that functions $f_1(x_2)$ and $f_2(x_1)$ have the form

$$f_1 = 2\mu(-\epsilon x_2 + \alpha), \qquad f_2 = 2\mu(\epsilon x_1 + \beta),$$

where α, β, ϵ are arbitrary constants. Omitting these relations which give only a rigid body motion, we finally get the representations for displacements

$$2\mu\, u_1 = -\frac{\partial U}{\partial x_1} + \frac{2(\lambda + 2\mu)}{\lambda + \mu}p,$$

$$2\mu\, u_2 = -\frac{\partial U}{\partial x_2} + \frac{2(\lambda + 2\mu)}{\lambda + \mu}q.$$

Since the function $\varphi(z)$ defined by (3.5) is holomorphic in the domain S, then displacements u_1 and u_2 are univalent functions in the whole domain. Thus we see that any biharmonic function defines a strain state, which satisfies all of the conditions.

Finally, we recall the theorem which plays a crucial role in application of the complex function theory to problems of linear elasticity.

26

Theorem 3.1 (Goursat's theorem in $\mathbb{C}$). *A function $f \in C^4(\Omega)$ is a solution of $\Delta\Delta U = 0$ $\Leftrightarrow \exists$ two holomorphic functions $\Phi(z)$ and $\Psi(z)$ where*

$$f = \frac{1}{2}\left(\bar{z}\Phi(z) + z\overline{\Phi(z)} + \Psi(z) + \overline{\Psi(z)}\right) = \mathbf{Re}\left(\bar{z}\Phi(z) + \Psi(z)\right)$$

and $z = x_1 + i\,x_2 \in \mathbb{C}$.

We omit the proof of the theorem and give just references. The original proof was constructed in [Goursat 1898]. Later on another proof was introduced by Muskhelishvili in his book [Mußchelischwili 1971], where he had used the conception of holomorphic functions and harmonic conjugates, which we have introduced above.

With the help of the Goursat's theorem and presented formulae, components of stresses and displacement can be also formulated as follows

$$
\begin{aligned}
2\mu(u_1 + i\,u_2) &= \kappa\,\Phi(z) - z\,\overline{\Phi'(z)} - \overline{\Psi(z)}, \\
\sigma_{11} + \sigma_{22} &= 2\left[\Phi'(z) + \overline{\Phi'(z)}\right] = 4\,\mathbf{Re}\left[\Phi'(z)\right], \\
\sigma_{22} - \sigma_{11} + 2i\,\sigma_{12} &= 2[\bar{z}\,\Phi''(z) + \Psi'(z)],
\end{aligned}
\tag{3.6}
$$

where $\Phi(z)$ and $\Psi(z)$ are two holomorphic functions in terms of the complex variable z. The factor κ is Kolosov's constant, which is defined as follows

$$
\kappa = \begin{cases} 3 - 4\nu & \text{for plane strain,} \\ \dfrac{3 - \nu}{1 + \nu} & \text{for plane stress.} \end{cases}
$$

The formulae (3.6) were introduced by G. W. Kolosov [Kolosov 1909], and later on were theoretically justified by N. I. Muskhelishvili [Mußchelischwili 1971]. These formulae are known as the *Kolosov-Muskhelishvili formulae*.

Let us now discuss the question about definiteness of the introduced functions $\Phi(z)$ and $\Psi(z)$. For a given stress state the function $\Phi'(z)$ is defined from the second formula of (3.6) up to an imaginary constant, since the real part of this function is given. Hence, all possible functions are different from $\Phi'(z)$ only by a purely imaginary constant

$$\Phi'_1(z) = \Phi'(z) + C\,i,
\tag{3.7}$$

where $\Phi'_1(z)$ is a possible function and C is a real constant.

By taking into account that

$$
\begin{aligned}
\Phi(z) &= \int \Phi'(z)dz, & \Psi(z) &= \int \Psi'(z)dz, \\
\Phi_1(z) &= \int \Phi'_1(z)dz, & \Psi_1(z) &= \int \Psi'_1(z)dz,
\end{aligned}
$$

it follows

$$\Phi_1(z) = \Phi(z) + C\,i\,z + \gamma,$$

where $\gamma = \alpha + i\,\beta$ is an arbitrary complex constant.

According to (3.7) $\Phi_1''(z) = \Phi''(z)$ from the third formula of (3.6) we get

$$\Psi_1'(z) = \Psi(z),$$

and finally we have

$$\Psi_1(z) = \Psi(z) + \gamma',$$

where γ' is an arbitrary complex constant.

Hence, we have the following result. For a given stress state the function $\Psi'(z)$ is fully determined, the function $\Phi'(z)$ is determined up to the term $C\,i$, the function $\Phi(z)$ is determined up to the term $C\,i\,z + \gamma$, and the function $\Psi(z)$ is defined up to the term γ', where C is real, and γ, γ' are arbitrary complex constants.

The inverse is also correct, i.e. a stress state will not change if we apply the following replacement for functions $\Phi(z)$ and $\Psi(z)$

$$\begin{aligned}\Phi(z) &\rightarrow \Phi(z) + C\,i\,z + \gamma, \\ \Psi(z) &\rightarrow \Psi(z) + \gamma',\end{aligned} \tag{A}$$

where C is real, and γ, γ' are arbitrary complex constants.

Let us now consider the case if components of displacement u_1, u_2 are given. If components of displacement are given, then components of stresses are fully determined. Therefore, in this case we cannot use replacements different from the described above. Let us check how this replacement influences the components of displacement, which are given by

$$2\mu(u_1 + i\,u_2) = \kappa\Phi(z) - z\overline{\Phi'(z)} - \overline{\Psi(z)}.$$

By direct substitution we see, that

$$2\mu(u_1 + i\,u_2) \quad \text{becomes} \quad 2\mu(u_1^* + i\,u_2^*),$$

where

$$2\mu(u_1^* + i\,u_2^*) = 2\mu(u_1 + i\,u_2) + (\kappa + 1)C\,i\,z + \kappa\,\gamma - \bar{\gamma}'.$$

Hence, by assuming $\gamma = \alpha + i\,\beta$, $\gamma' = \alpha' + i\,\beta'$, we have

$$u_1^* = u_1 + u_1^0, \qquad u_2^* = u_2 + u_2^0,$$

where

$$u_1^0 = -\frac{(\kappa + 1)C}{2\mu}x_2 + \frac{\kappa\alpha - \alpha'}{2\mu}, \qquad u_2^0 = \frac{(\kappa + 1)C}{2\mu}x_1 + \frac{\kappa\beta + \beta'}{2\mu}.$$

We see, that additional terms have the form

$$u_1^0 = -\varepsilon\,x_2 + \alpha_0, \qquad u_2^0 = \varepsilon\,x_1 + \beta_0,$$

where

$$\varepsilon = \frac{(\kappa + 1)C}{2\mu}, \qquad \alpha_0 = \frac{\kappa\alpha - \alpha'}{2\mu}, \qquad \beta_0 = \frac{\kappa\beta + \beta'}{2\mu},$$

28

and these terms express just a rigid body motion.

Finally, we have that the replacement (A) can be performed without changing of displacement only in the case if

$$C = 0, \qquad \kappa\gamma - \gamma' = 0.$$

Therefore, for given components of displacement the constants C, γ, γ' can be chosen arbitrarily.

3.1.1 Analytical solution near the crack tip

By using the Kolosov-Muskhelishvili formulae (3.6) we are going to construct now the analytical solution in a field near a crack tip. Later on this analytical solution will be used in the coupling process. Let now $\Omega \subset \mathbb{C}$ be a bounded simply connected domain containing a crack. The crack tip produces a singularity of the solution in the domain Ω. Due to this fact the solution near the crack tip must be handled more carefully, for that reason we will use the methods of the complex function theory. We locate the Cartesian coordinate system at the crack-tip. The crack will be directed along the negative direction of the x_1 axis, and the axis x_2 will be orthogonal to the crack (see Fig. 3.1).
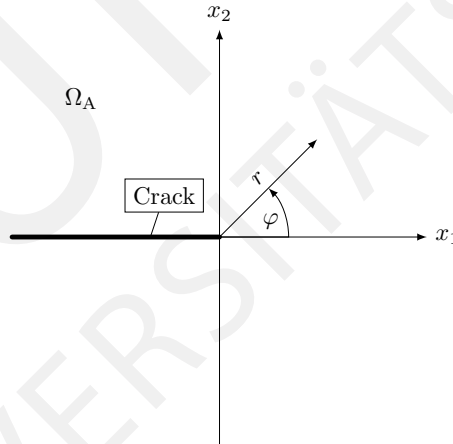
Figure 3.1: Geometrical settings near the crack tip

We are going to switch to the polar coordinate system $x_1 = r\cos\varphi$, $x_2 = r\sin\varphi$, $r \geq 0, -\pi \leq \varphi < \pi$. Corresponding to [Mußchelischwili 1971] the Kolosov-Muskhelishvili formulae in polar coordinates are given by

$$2\mu(u_r + i\,u_\varphi) = e^{-i\varphi}\left(\kappa\,\Phi(z) - z\,\overline{\Phi'(z)} - \overline{\Psi(z)}\right)$$

$$\sigma_{rr} + \sigma_{\varphi\varphi} = 2[\Phi'(z) + \overline{\Phi'(z)}]$$

$$\sigma_{\varphi\varphi} - \sigma_{rr} + 2i\,\sigma_{r\varphi} = 2e^{2i\varphi}[\bar{z}\,\Phi''(z) + \Psi'(z)]$$

29

By adding the last two equations we will get the equation which connects the stresses $\sigma_{\varphi\varphi}$ and $\sigma_{r\varphi}$

$$\sigma_{\varphi\varphi} + i\,\sigma_{r\varphi} = \Phi'(z) + \overline{\Phi'(z)} + e^{2i\,\varphi}[\bar{z}\,\Phi''(z) + \Psi'(z)]. \tag{3.8}$$

We introduce the functions $\Phi(z)$ and $\Psi(z)$ by series expansions in the domain Ω_A

$$\Phi(z) = \sum_{k=0}^{\infty} a_k z^{\lambda_k}, \qquad \Psi(z) = \sum_{k=0}^{\infty} b_k z^{\lambda_k},$$

where a_k and b_k are unknown coefficients, which should be determined through the boundary conditions for the global problem, and the powers λ_k describe the behaviour of the displacements and stresses near the crack tip and should be determined by this asymptotic behaviour and through the boundary conditions on the crack faces.

The crack faces are assumed to be traction free [Liebowitz 1968], i.e. the normal stresses $\sigma_{\varphi\varphi}$ and the shear stresses $\sigma_{r\varphi}$ on the crack faces are equal zero for $\varphi = \pi$ or $\varphi = -\pi$. After substituting functions $\Phi(z)$ and $\Psi(z)$ into (3.8) we get the following equation for the stresses

$$
\begin{aligned}
\sigma_{\varphi\varphi} + i\,\sigma_{r\varphi} &= \sum_{k=0}^{\infty} r^{\lambda_k - 1}\left(\lambda_k a_k e^{i\varphi(\lambda_k - 1)} + \lambda_k \bar{a}_k e^{-i\varphi(\lambda_k - 1)} + \right. \\
&\qquad \left. + a_k \lambda_k(\lambda_k - 1) e^{i\varphi(\lambda_k - 1)} + b_k \lambda_k e^{i\varphi(\lambda_k + 1)}\right),
\end{aligned}
$$

or by using Euler's formula

$$
\begin{aligned}
\sigma_{\varphi\varphi} + i\,\sigma_{r\varphi} &= \sum_{k=0}^{\infty} r^{\lambda_k - 1}\left[\lambda_k a_k \left(\cos\{\varphi(\lambda_k - 1)\} + i\sin\{\varphi(\lambda_k - 1)\}\right) + \right. \\
&\quad + \lambda_k \bar{a}_k \left(\cos\{\varphi(\lambda_k - 1)\} - i\sin\{\varphi(\lambda_k - 1)\}\right) + \\
&\quad + a_k \lambda_k(\lambda_k - 1)\left(\cos\{\varphi(\lambda_k - 1)\} + i\sin\{\varphi(\lambda_k - 1)\}\right) + \\
&\quad \left. + b_k \lambda_k \left(\cos\{\varphi(\lambda_k + 1)\} + i\sin\{\varphi(\lambda_k + 1)\}\right)\right].
\end{aligned}
$$

The boundary conditions on the crack faces lead to the following system

$$
\begin{cases}
-\cos(\pi\lambda_k)\left(\lambda_k a_k + \lambda_k \bar{a}_k + a_k \lambda_k(\lambda_k - 1) + b_k \lambda_k\right) + \\
+i\sin(\pi\lambda_k)\left(\lambda_k a_k - \lambda_k \bar{a}_k + a_k \lambda_k(\lambda_k - 1) + b_k \lambda_k\right) = 0, \\
\\
-\cos(\pi\lambda_k)\left(\lambda_k a_k + \lambda_k \bar{a}_k + a_k \lambda_k(\lambda_k - 1) + b_k \lambda_k\right) - \\
-i\sin(\pi\lambda_k)\left(\lambda_k a_k - \lambda_k \bar{a}_k + a_k \lambda_k(\lambda_k - 1) + b_k \lambda_k\right) = 0.
\end{cases} \tag{3.9}
$$

The homogeneous system (3.9) has non-trivial solutions only in case if its determinant is equals zero. The determinant of this system is given by

$$
\begin{vmatrix}
-\cos(\pi\lambda_k) & i\sin(\pi\lambda_k) \\
-\cos(\pi\lambda_k) & -i\sin(\pi\lambda_k)
\end{vmatrix} = 2i\cos(\pi\lambda_k)\sin(\pi\lambda_k),
$$

30

and the exponents λ_k are given by

$$\sin(2\pi\lambda_k) = 0 \qquad \rightarrow \qquad \lambda_k = \frac{n}{2}, \ n = 0, 1, \ldots. \tag{3.10}$$

The displacement field and components of stress tensor in polar coordinates can be written as

$$2\mu(u_r + i\,u_\varphi) = \sum_{n=1}^{\infty} r^{\frac{n}{2}} \left(\kappa\, a_n e^{i\varphi(\frac{n}{2}-1)} - \frac{n}{2}\bar{a}_n e^{-i\varphi(\frac{n}{2}-1)} - \bar{b}_n e^{-i\varphi(\frac{n}{2}+1)} \right),$$

$$\sigma_{rr} + \sigma_{\varphi\varphi} = \sum_{n=1}^{\infty} r^{\frac{n}{2}-1} \left(n\, a_n e^{i\varphi(\frac{n}{2}-1)} + n\, \bar{a}_n e^{-i\varphi(\frac{n}{2}-1)} \right), \tag{3.11}$$

$$\sigma_{\varphi\varphi} - \sigma_{rr} + 2i\,\sigma_{r\varphi} = \sum_{n=1}^{\infty} r^{\frac{n}{2}-1} \left(n\left(\frac{n}{2}-1\right) a_n e^{i\varphi(\frac{n}{2}-1)} + n\, b_n e^{i\varphi(\frac{n}{2}+1)} \right).$$

After transformation back, the displacement field and components of stress tensor in the Cartesian coordinates are given by the following expression

$$2\mu(u_1 + i\,u_2) = \sum_{n=1}^{\infty} r^{\frac{n}{2}} \left(\kappa\, a_n e^{i\varphi\frac{n}{2}} - \frac{n}{2}\bar{a}_n e^{-i\varphi(\frac{n}{2}-2)} - \bar{b}_n e^{-i\varphi\frac{n}{2}} \right),$$

$$\sigma_{11} + \sigma_{22} = \sum_{n=1}^{\infty} r^{\frac{n}{2}-1} \left(n\, a_n e^{i\varphi(\frac{n}{2}-1)} + n\, \bar{a}_n e^{-i\varphi(\frac{n}{2}-1)} \right), \tag{3.12}$$

$$\sigma_{22} - \sigma_{11} + 2i\,\sigma_{12} = \sum_{n=1}^{\infty} r^{\frac{n}{2}-1} \left(n\left(\frac{n}{2}-1\right) a_n e^{i\varphi(\frac{n}{2}-3)} + n\, b_n e^{i\varphi(\frac{n}{2}-1)} \right).$$

The formulas (3.11) and (3.12) have correct asymptotic behaviour near the crack tip, but the boundary conditions on the crack faces must be still satisfied. To obtain the traction free conditions on the crack faces we substitute known values of λ_k (3.10) into the system (3.9), and we get

$$\begin{cases} -\cos\left(\pi\frac{n}{2}\right)\left(\frac{n}{2}a_k + \frac{n}{2}\bar{a}_k + a_k\frac{n}{2}\left(\frac{n}{2}-1\right) + b_k\frac{n}{2}\right) + \\ \quad + i\sin\left(\pi\frac{n}{2}\right)\left(\frac{n}{2}a_k - \frac{n}{2}\bar{a}_k + a_k\frac{n}{2}\left(\frac{n}{2}-1\right) + b_k\frac{n}{2}\right) = 0, \\[2mm] -\cos\left(\pi\frac{n}{2}\right)\left(\frac{n}{2}a_k + \frac{n}{2}\bar{a}_k + a_k\frac{n}{2}\left(\frac{n}{2}-1\right) + b_k\frac{n}{2}\right) - \\ \quad - i\sin\left(\pi\frac{n}{2}\right)\left(\frac{n}{2}a_k - \frac{n}{2}\bar{a}_k + a_k\frac{n}{2}\left(\frac{n}{2}-1\right) + b_k\frac{n}{2}\right) = 0. \end{cases}$$

Solving this system we have the following relations between the coefficients a_k and b_k

$$\begin{cases} b_n = \bar{a}_n - \dfrac{n}{2}a_n, & n = 1, 3, \ldots, \\[2mm] b_n = -\bar{a}_n - \dfrac{n}{2}a_n, & n = 2, 4, \ldots, \end{cases}$$

31

or in form of real and imaginary parts of the coefficients

$$
\begin{cases}
b_n^{(1)} = a_n^{(1)} \left(1 - \dfrac{n}{2} \right), & n = 1, 3, \ldots, \\[2mm]
b_n^{(1)} = -a_n^{(1)} \left(1 + \dfrac{n}{2} \right), & n = 2, 4, \ldots,
\end{cases}
$$

and

$$
\begin{cases}
b_n^{(2)} = -a_n^{(2)} \left(1 + \dfrac{n}{2} \right), & n = 1, 3, \ldots, \\[2mm]
b_n^{(2)} = a_n^{(2)} \left(1 - \dfrac{n}{2} \right), & n = 2, 4, \ldots.
\end{cases}
$$

Finally we have the following expressions for the polar components of the displacement and the stresses

$$
\begin{aligned}
2\mu(u_r + i\, u_\varphi) &= \sum_{n=1,3}^{\infty} r^{\frac{n}{2}} \left[a_n \left(\kappa\, e^{i\varphi(\frac{n}{2}-1)} - e^{-i\varphi(\frac{n}{2}+1)} \right) + \frac{n}{2} \bar{a}_n \left(e^{-i\varphi(\frac{n}{2}+1)} - e^{-i\varphi(\frac{n}{2}-1)} \right) \right] + \\
&\quad + \sum_{n=2,4}^{\infty} r^{\frac{n}{2}} \left[a_n \left(\kappa\, e^{i\varphi(\frac{n}{2}-1)} + e^{-i\varphi(\frac{n}{2}+1)} \right) + \frac{n}{2} \bar{a}_n \left(e^{-i\varphi(\frac{n}{2}+1)} - e^{-i\varphi(\frac{n}{2}-1)} \right) \right],
\end{aligned}
$$

$$
\sigma_{rr} + \sigma_{\varphi\varphi} = \sum_{n=1}^{\infty} r^{\frac{n}{2}-1} \left(n\, a_n e^{i\varphi(\frac{n}{2}-1)} + n\, \bar{a}_n e^{-i\varphi(\frac{n}{2}-1)} \right),
$$

$$
\begin{aligned}
\sigma_{\varphi\varphi} - \sigma_{rr} + 2i\, \sigma_{r\varphi} &= \sum_{n=1,3}^{\infty} r^{\frac{n}{2}-1} \left[a_n \left(n \left(\frac{n}{2} - 1 \right) e^{i\varphi(\frac{n}{2}-1)} - n\frac{n}{2} e^{i\varphi(\frac{n}{2}+1)} \right) + n\bar{a}_n e^{i\varphi(\frac{n}{2}+1)} \right] + \\
&\quad \sum_{n=2,4}^{\infty} r^{\frac{n}{2}-1} \left[a_n \left(n \left(\frac{n}{2} - 1 \right) e^{i\varphi(\frac{n}{2}-1)} - n\frac{n}{2} e^{i\varphi(\frac{n}{2}+1)} \right) - n\bar{a}_n e^{i\varphi(\frac{n}{2}+1)} \right],
\end{aligned}
$$

and for the Cartesian components

$$
\begin{aligned}
2\mu(u_1 + i\, u_2) &= \sum_{n=1,3}^{\infty} r^{\frac{n}{2}} \left[a_n \left(\kappa\, e^{i\varphi\frac{n}{2}} - e^{-i\varphi\frac{n}{2}} \right) + \frac{n}{2} \bar{a}_n \left(e^{-i\varphi\frac{n}{2}} - e^{-i\varphi(\frac{n}{2}-2)} \right) \right] + \\
&\quad + \sum_{n=2,4}^{\infty} r^{\frac{n}{2}} \left[a_n \left(\kappa\, e^{i\varphi\frac{n}{2}} + e^{-i\varphi\frac{n}{2}} \right) + \frac{n}{2} \bar{a}_n \left(e^{-i\varphi\frac{n}{2}} - e^{-i\varphi(\frac{n}{2}-2)} \right) \right],
\end{aligned}
\tag{3.13}
$$

$$
\sigma_{11} + \sigma_{22} = \sum_{n=1}^{\infty} r^{\frac{n}{2}-1} \left(n\, a_n e^{i\varphi(\frac{n}{2}-1)} + n\, \bar{a}_n e^{-i\varphi(\frac{n}{2}-1)} \right),
$$

$$
\begin{aligned}
\sigma_{22} - \sigma_{11} + 2i\, \sigma_{12} &= \sum_{n=1,3}^{\infty} r^{\frac{n}{2}-1} \left[a_n \left(n \left(\frac{n}{2} - 1 \right) e^{i\varphi(\frac{n}{2}-3)} - n\frac{n}{2} e^{i\varphi(\frac{n}{2}-1)} \right) + n\bar{a}_n e^{i\varphi(\frac{n}{2}-1)} \right] + \\
&\quad \sum_{n=2,4}^{\infty} r^{\frac{n}{2}-1} \left[a_n \left(n \left(\frac{n}{2} - 1 \right) e^{i\varphi(\frac{n}{2}-3)} - n\frac{n}{2} e^{i\varphi(\frac{n}{2}-1)} \right) - n\bar{a}_n e^{i\varphi(\frac{n}{2}-1)} \right].
\end{aligned}
\tag{3.14}
$$

The displacement field (3.13) satisfies all the conditions on the crack faces. The asymptotic behaviour at the crack tip is controlled by half-integer powers. Values $n < 0$ lead to unboundedness of the function (3.13) at the origin, the value $n = 0$ corresponds to a constant displacement field and is usually omitted by mechanical reasons [Anderson 2005]. Because of these reasons the series must begin with $n = 1$.

If we compare this general form of the solution with the classical solutions from [Liebowitz 1968, Anderson 2005] for a crack in an infinite body, we will see that the constructed solution (3.13)-(3.14) contains these well-known solution in first terms, but the coefficients a_n must be determined via the global boundary conditions. The idea to work with an infinite series comes from the fact that we are looking for solutions in bounded domains, therefore non-leading terms in a series could play an important role for a behaviour near the crack tip. This construction doesn't require a prior knowledge about a mode of fracture, and via coupling with a finite element solution we must be able to represent different scenarios near the crack tip dependently on the global boundary conditions. The construction of such a coupling we will describe in Chapter 4.

3.2 Conformal mapping

Another important tool of the complex function theory which helps to solve various applied problems is the conformal mapping. In this section we give only a brief introduction to this topic. Conformal mapping plays a crucial role in mechanical applications. Originally it was introduced based on physical considerations, and only later it was found out that it has also some very important properties from point of view of the complex function theory.

In literature exist several ways of deriving a definition of a conformal mapping: one can introduce at first a whole concept of analytic functions and relate it afterwards to some geometrical properties of these functions, see for example [Bieberbach 1964, Nehari 1952]; or another approach which studies immediately geometrical properties of mapping functions and observing their analyticity afterwards. We will follow the second approach based on ideas from [Lavrentev & Shabat 1987]. Let us assume, that we have a continuous one-to-one mapping of a domain D onto a domain D^*:

$$w = f(z) = u(x, y) + i\, v(x, y). \tag{3.15}$$

Additionally, we assume that functions $u(x, y)$ and $v(x, y)$ are differentiable in this domain. Let us fix an arbitrary point $z_0 \in D$ and in the neighbourhood of this point we change increments of the functions u and v by their differentials. By definition of the differential, the increments can be represented as

$$\left. \begin{array}{rcl} u - u_0 & = & \dfrac{\partial u}{\partial x}\,(x - x_0) + \dfrac{\partial u}{\partial y}\,(y - y_0) + \eta_1 \Delta r, \\[3mm] v - v_0 & = & \dfrac{\partial v}{\partial x}\,(x - x_0) + \dfrac{\partial v}{\partial y}\,(y - y_0) + \eta_2 \Delta r, \end{array} \right\} \tag{3.16}$$

where $\eta_1 \Delta r$ and $\eta_2 \Delta r$ are the terms of higher order with respect to other terms in these formulae, partial derivatives are taken at the point z_0, and $\Delta r = \sqrt{(x - x_0)^2 + (y - y_0)^2}$, and η_1, η_2 tend to zero for $\Delta r \to 0$. The change of the increments by differentials is equivalent to omit in the relations (3.16) the terms $\eta_1 \Delta r$ and $\eta_2 \Delta r$ (we assume, that $\left(\dfrac{\partial u}{\partial x}\right)^2 + \left(\dfrac{\partial u}{\partial y}\right)^2$ and $\left(\dfrac{\partial v}{\partial x}\right)^2 + \left(\dfrac{\partial v}{\partial y}\right)^2$ are different from zero, otherwise representation 3.16 wouldn't be possible).

Geometrically this change is equal to the changing of the mapping $w = f(z)$ by the following mapping

$$
\left.
\begin{aligned}
u - u_0 &= \frac{\partial u}{\partial x}(x - x_0) + \frac{\partial u}{\partial y}(y - y_0), \\[2mm]
v - v_0 &= \frac{\partial v}{\partial x}(x - x_0) + \frac{\partial v}{\partial y}(y - y_0),
\end{aligned}
\right\}
\tag{3.17}
$$

which is called the main linear part of the mapping (3.15). The mapping (3.17) can be rewritten as follows

$$
\left.
\begin{aligned}
u &= ax + by + l, \\
v &= cx + dy + m,
\end{aligned}
\right\}
\tag{3.18}
$$

where the coefficients

$$
a = \frac{\partial u}{\partial x}, \quad b = \frac{\partial u}{\partial y}, \quad c = \frac{\partial v}{\partial x}, \quad d = \frac{\partial v}{\partial y},
$$

$$
l = u_0 - \frac{\partial u}{\partial x}x_0 - \frac{\partial u}{\partial y}y_0, \quad m = v_0 - \frac{\partial v}{\partial x}x_0 - \frac{\partial v}{\partial y}y_0,
\tag{3.19}
$$

independent on x and y. The mapping (3.18) represents the linear transformation of a plane (x, y).

Now we recall some basic properties of linear transformations. Let the linear transformation (3.18) be uniquely defined in a whole plane z, additionally we assume that its determinant

$$
\Delta = ad - bc
$$

is different from zero. Then an inverse mapping of (3.18) is also uniquely defined in a whole plane w, which is given by

$$
\left.
\begin{aligned}
x &= \frac{1}{\Delta}(du - bv - dl + bm), \\[2mm]
y &= \frac{1}{\Delta}(-cu + av + lc - am).
\end{aligned}
\right\}
\tag{3.20}
$$

Thus, for $\Delta \neq 0$ the mapping (3.18) realises a one to one mapping of a whole plane z to a whole plane w.

Let us consider a set of parallel lines with a slope $k = \tan\varphi$, i.e. lines $y = kx + C$. By using formulae (3.20) we observe that this set of lines transforms also to a set of parallel lines $-cu + av + lc - am = k(du - bv - dl + bm) + C\Delta$ with a slope

$$k^* = \tan\theta = \frac{c + kd}{a + kb}.$$

It follows, that the mapping (3.18) transforms squares in a plane z to parallelograms in a plane w.

Let $z_0 = x_0 + iy_0$ and $w_0 = u_0 + iv_0$ be a pair of points corresponding to each other under the mapping (3.18), then we can represent this mapping as follows

$$\left.\begin{array}{rl} u - u_0 &= a(x - x_0) + b(y - y_0), \\ v - v_0 &= c(x - x_0) + d(y - y_0), \end{array}\right\}$$

and its inverse by

$$\left.\begin{array}{rl} x - x_0 &= \dfrac{d}{\Delta}(u - u_0) - \dfrac{b}{\Delta}(v - v_0), \\[2mm] y - y_0 &= -\dfrac{c}{\Delta}(u - u_0) + \dfrac{a}{\Delta}(v - v_0). \end{array}\right\} \tag{3.21}$$

By formulae (3.21) we can say that circles with the center at a point z_0

$$(x - x_0)^2 + (y - y_0)^2 = r^2,$$

transformed under the mapping (3.18) into ellipses with the center at the point w_0

$$(d^2 + c^2)(u - u_0)^2 - 2(bd + ac)(u - u_0)(v - v_0) + (b^2 + a^2)(v - v_0)^2 = \Delta^2 r^2. \tag{3.22}$$

An important question: what should be the conditions for the coefficients in the mapping (3.18) to assure that circles will be transformed to new circles? From (3.22) we get the following equations

$$bd + ac = 0, \qquad a^2 + b^2 = c^2 + d^2. \tag{3.23}$$

First equation gives us $\dfrac{a}{d} = -\dfrac{b}{c} = \lambda$, and consequently by using $a = \lambda d$, $d = -\lambda c$ from the second equation we get $\lambda^2 = 1$. Therefore we need to consider two cases.

The case $\lambda = 1$ leads to the relations

$$a = d, \qquad b = -c, \tag{3.24}$$

and the mapping (3.15) is described by a linear function of a complex variable as follows

$$w = Az + B, \tag{3.25}$$

where

$$A = \sqrt{\Delta}e^{i\alpha}, \qquad B = l + im.$$

Thus under conditions (3.24) the linear transformation (3.18) is reduced to a translation of a plane z on a vector $B = l + im$, and its rotation by an angle $\alpha = \operatorname{Arg} A$ and a proportional dilation with a coefficient $\sqrt{\Delta} = |A|$. Such transformation is called the proper similarity map.

In the case $\lambda = -1$ we have

$$a = -d, \qquad b = c, \tag{3.26}$$

and $\Delta = -a^2 - b^2 < 0$. Therefore the transformation (3.18) can be written in the following form

$$w = \sqrt{-\Delta}\, e^{i\alpha} \bar{z} + B. \tag{3.27}$$

Thus under conditions (3.26) additionally to a rotation and translation we get a symmetry with respect to the real axis by changing z to $\bar{z}$. This transformation is called the improper similarity map.

From the geometrical meaning of mapping (3.25) and (3.27) it becomes clear, that they preserve the similarity of figures, in particular they preserve angles between two lines, and transform squares in the plane z to squares in the plane w. The linear transformations having this property are called the orthogonal transformations. Thus conditions (3.23) are orthogonality conditions.

Finally we have the following definition

Definition 3.1. The one-to-one mapping

$$w = f(z) = u(x, y) + i\, v(x, y)$$

of the domain D onto the domain D^* is called conformal, if in the neighbourhood of any point of D the main linear part of this mapping preserves the angle between lines in D and keeps the orientation.

From that follows two main properties of conformal mappings

1. a conformal mapping transforms infinitesimal circles into circles with accuracy up to infinitesimals of higher order;

2. a conformal mapping preserves angles between curves at the points of their intersection.

By using formulae (3.19) and (3.24) we can write the conditions for conformality of a mapping (3.15) in the following form

$$\frac{\partial u}{\partial x} = \frac{\partial v}{\partial y}, \qquad \frac{\partial u}{\partial y} = -\frac{\partial v}{\partial x},$$

and the following condition should be satisfied

$$\Delta = \left(\frac{\partial u}{\partial x}\right)^2 + \left(\frac{\partial v}{\partial x}\right)^2 = |f'(z_0)^2| \neq 0,$$

otherwise the linear part of a transformation $w = f(z)$ is degenerated, that contradicts to a conformality condition. Thus the conformality conditions coincide with the Cauchy-Riemann conditions for a function $f(z)$ be a holomorphic (analytic) in a domain D, and its derivative $f'(z)$ must be different from zero everywhere in D. Finally we obtain the following definition:

Definition 3.2. A function $w = f(z)$ realises a conformal mapping of a domain D if and only if this function in a domain is 1) one-to-one, 2) holomorphic and 3) everywhere in D the derivative $f'(z)$ is different from zero.

To this short introduction in conformal mapping we recall the main theorem of the theory of conformal mappings, also known as the Riemann mapping theorem [Riemann 1851].

Theorem 3.2. *For any simply connected domains D and D^* (with boundaries that contain more than one point), and for arbitrary defined points $z_0 \in D$ and $w_0 \in D^*$ and a real number α_0, there exists one and only one conformal mapping*

$$w = f(z)$$

of the domain D onto the domain D^* such that

$$f(z_0) = w_0, \qquad \arg f'(z_0) = \alpha_0.$$

By the assertion of the Riemann mapping theorem we can try to simplify practical problems in a two dimensional geometry by mapping them to some simple or canonical domains. But in reality one problem remains open: how to construct a mapping function from one domain to another? One the most canonical methods for construction of a mapping function is the Bergman kernel method [Levin et al. 1978], for an overview on other existing methods we refer to [Gaier 1964]. Unfortunately these methods lead to a boundary value problem for the mapping function, which is usually much more complicated than the original problem. This drawback significantly reduces possible practical applications of the conformal mapping for arbitrary domains. But by research of many mathematicians a lot of mapping functions were already constructed, for an overview we refer to [Kober 1957]. Among these functions a particular interest for applied problems in engineering plays the Schwarz-Christoffel mapping, which allows to map polygonal domains (typical type of domains coming from engineering) to some canonical domains. In the next section we introduce some more details of this mapping.

3.2.1 Schwarz-Christoffel mapping

Many problems of the continuum mechanics are formulated for domains which can be represented by polygons. Such domains can be successfully mapped to one of the canonical domains (unit disk or half plane) by the Schwarz-Christoffel mapping. Following [Driscoll & Trefethen 2002], we introduce basic definitions for application of the Schwarz-Christoffel mapping.

A (generalised) polygon Γ is defined by a collection of vertices $w_1, \ldots, w_n$ and real interior angles $\alpha_1\pi, \ldots, \alpha_n\pi$. It is convenient for indexing purposes to define $w_{n+1} = w_1$ and $w_0 = w_n$. The vertices, which lie in the extended complex plane $\mathbb{C} \cup \{\infty\}$, are given in counterclockwise order according to the orientation of the boundary curve (i.e., locally the polygon is "to the left" as one traverses the side from w_k to w_{k+1}).

The interior angle at vertex k is defined as the angle swept from the outgoing side at w_k to the incoming side. If $|w_k| < \infty$, we have the angle coefficients $\alpha_k \in (0, 2]$. If $\alpha_k = 2$, the sides incident on w_k are collinear, and w_k is the tip of a slit. The definition of the interior angle is applied on the Riemann sphere if $w_k = \infty$. In this case, $\alpha_k \in [-2, 0]$. Specifying α_k is redundant if w_k and its neighbours are finite, but otherwise α_k is needed to determine the polygon uniquely.

In addition to preceding restrictions on the angles α_k, we require that the polygon makes a total turn of 2π. That is,

$$\sum_{k=1}^{n}(1 - \alpha_k) = 2,$$

or, equivalently,

$$\sum_{k=1}^{n}\alpha_k = n - 2.$$

We shall also require the polygon to be simple (forbidden is a self-intersection and thus covering part of the plane more than once). This condition has no elementary expression in terms of the vertices and angles – in a sense, it is artificial.

The following theorem gives the formula for the conformal map from the unit disk E.

Theorem 3.3. *Let P be the interior of a polygon Γ having vertices $w_1, \ldots, w_n$ and interior angles $\alpha_1\pi, \ldots, \alpha_n\pi$ in counterclockwise order. Let ω be any conformal map from the unit disk E to P. Then the Schwarz-Christoffel formula for a disk has the form*

$$\omega(z) = A + C \int_{z_0}^{z} \prod_{k=1}^{n}\left(1 - \frac{\zeta}{z_k}\right)^{\alpha_k - 1} d\zeta, \tag{3.28}$$

for some complex constants A and C, where $w_k = \omega(z_k)$ for $k = 1, \ldots, n$.

The exponents in the integrand induce the correct angles in the image of the unit disk, regardless of where the prevertices lie on the unit circle. However, the locations of the prevertices determine the side lengths of the resulting image. In order to map to a given target, then, we must determine the locations of the prevertices by enforcing conditions involving the side length.

The three degrees of freedom in the map may be determined by specifying $z_{n-2} = -1$, $z_{n-1} = -i$, and $z_n = 1$. We need still to determine $n - 3$ real quantities – the arguments

of the remaining prevertices. For a bounded polygon, this accomplished by the $n-3$ real conditions, the so-called, parameter problem

$$\frac{\left| \int\limits_{z_j}^{z_{j+1}} \omega'(\zeta) d\zeta \right|}{\left| \int\limits_{z_1}^{z_2} \omega'(\zeta) d\zeta \right|} = \frac{|w_{j+1} - w_j|}{|w_2 - w_1|}, \quad j = 2, \ldots, n-2, \tag{3.29}$$

where ω' comes from (3.28). The following theorem explains why vertex w_n does not explicitly appear in these conditions.

Theorem 3.4. *Assume that $\alpha_n \neq 1$ and $\alpha_n \neq 2$. A bounded polygon is uniquely determined, up to scaling, rotation, and translation, by its angles and the $n-3$ side-length ratios appearing on the right-hand sides of (3.29).*

3.2.2 Kolosov-Muskhelishvili formulae under a conformal mapping

Let us consider an arbitrary simply connected domain $\Omega \subset \mathbb{C}$ with boundary $\Gamma = \Gamma_0 \cup \Gamma_1$, which is represented by a polygon (see Fig. 3.2). We also allow that the domain Ω can have a slit or several slits, but the simply connectedness of Ω has not to be disturbed by these slits.

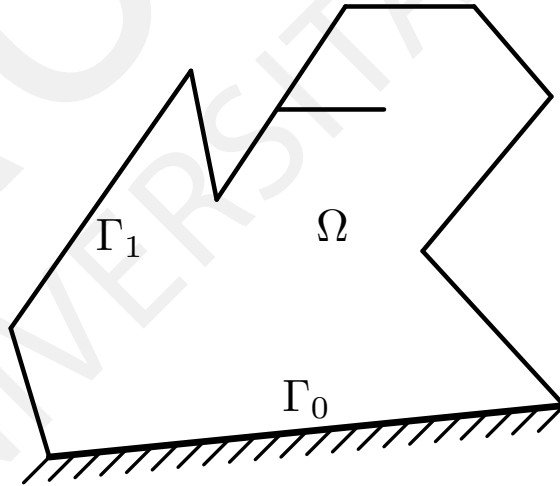Figure 3.2: Polygonal simply connected domain

We will solve a boundary value problem for the Lamé equation (2.18) in Ω. As we have discussed above, an exact solution to a linear elasticity problem can be constructed by the Kolosov-Muskhelishvili formulae (3.6), but due to polygonal shape of the domain Ω, in general, it is a non trivial task to construct an exact solution to a boundary value

problem in the original geometry. But by applying a conformal mapping (3.15), which is defined by the Schwarz-Christoffel mapping (3.28) we can transfer the original problem to one of the canonical domains.

Under a conformal mapping $\omega(\zeta)$ from the original domain to the unit disk, the Kolosov-Muskhelishvili formulae are written as follows [Mußchelischwili 1971]

$$2\mu|\omega'(\zeta)|(u_r + i\,u_\varphi) = \frac{\bar{\zeta}}{r}\overline{\omega'(\zeta)}\left[\kappa\,\Phi(\zeta) - \frac{\omega(\zeta)}{\overline{\omega'(\zeta)}}\overline{\Phi'(\zeta)} - \overline{\Psi(\zeta)}\right],$$

$$\sigma_{rr} + \sigma_{\varphi\varphi} = 2\left[\Phi'(\zeta) + \overline{\Phi'(\zeta)}\right], \tag{3.30}$$

$$\sigma_{\varphi\varphi} - \sigma_{rr} + 2i\,\sigma_{r\varphi} = \frac{2\zeta^2}{r^2\overline{\omega'(\zeta)}}\left[\overline{f(\zeta)}\,\Phi''(\zeta) + \omega'(\zeta)\Psi'(\zeta)\right].$$

The mapping function $\omega(\zeta)$ in formulae (3.30) represents a mapping from original geometry to the unit disk, i.e. for the case of a polygonal domain from Fig. 3.2 it implies a calculation of the inverse of the Schwarz-Christoffel mapping (3.28). Fig. 3.3 shows a Schwarz-Christoffel mapping $\omega(z)$ from the unit disk E to a polygon P, and its inverse mapping $\omega^{-1}(\zeta)$. Under a conformal mapping each part of original boundary is mapped on to a respective part of the unit circle.
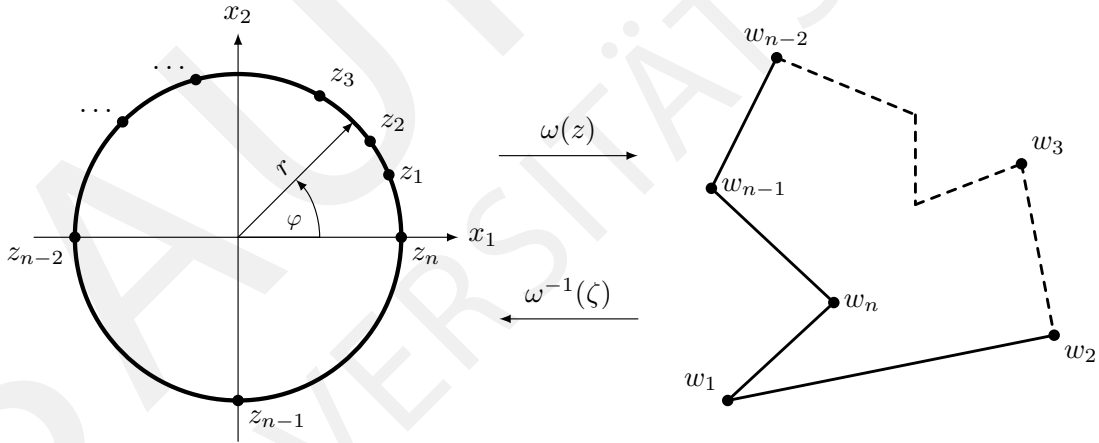
Figure 3.3: Mapping of the unit disk to a polygon

Formulae (3.30) together with the Schwarz-Christoffel formulae (3.28) allow us to handle linear elasticity problems for realistic geometries. In practical calculations it leads to a mixed boundary value problem in the unit disk, which can be efficiently solved by using the method of analytic continuation, i.e. by solving a Riemann-Hilbert boundary value problem for a holomorphic function. The solution of a Riemann-Hilbert boundary value problem in a context of elasticity theory was firstly discussed in [Mußchelischwili 1971].

For practical purposes it's important to mention that the conformal mapping allows to map curved cracks to straight cracks, which are well studied in the literature.

3.3 Solution of three dimensional problems by the Papkovich-Neuber approach

Since not all problems which are coming from real applications can be satisfactory reduced to plane problems, it's significantly important to have methods which allow to construct a solution of spatial problems. In the beginning of the 1930s Papkovich [Papkovich 1932], and Neuber [Neuber 1934] simultaneously have proposed a method for solution of three dimensional problems of linear elasticity, which is nowadays known as the Papkovich-Neuber approach. This approach will play also a crucial role in a generalisation of the Kolosov-Muskhelishvili formulae to three dimensions, which we will introduce in next sections.

The main idea of this approach is to solve a homogeneous system of equations (2.18) by using a spatial stress function which could be represented by four harmonic functions. Thus a general solution according the Papkovich-Neuber approach has the following form

$$2\mu\,u_1 = -\frac{\partial F}{\partial x_1} + C\Phi_1,$$

$$2\mu\,u_2 = -\frac{\partial F}{\partial x_2} + C\Phi_2, \tag{3.31}$$

$$2\mu\,u_3 = -\frac{\partial F}{\partial x_3} + C\Phi_3,$$

where Φ_1, Φ_2, Φ_3 are harmonic functions, and F is a stress function.

By substitution (3.31) into equations (2.18) we get after some calculations

$$-\frac{\partial}{\partial x_1}\left[\frac{2\mu}{1-2\nu}\vartheta - \Delta\,F\right] = 0,$$

$$-\frac{\partial}{\partial x_2}\left[\frac{2\mu}{1-2\nu}\vartheta - \Delta\,F\right] = 0,$$

$$-\frac{\partial}{\partial x_3}\left[\frac{2\mu}{1-2\nu}\vartheta - \Delta\,F\right] = 0.$$

As we can see the expression in brackets doesn't depend on coordinates and therefore we get

$$2\mu\vartheta - (1-2\nu)\Delta\,F = C,$$

where C is a constant corresponding to a rigid body motion, and we assign it to zero, i.e. we get

$$2\mu\vartheta = (1-2\nu)\Delta\,F.$$

By substituting (3.31) into (2.19) we obtain

$$2\mu\vartheta = -\Delta\,F + C\left(\frac{\partial\Phi_1}{\partial x_1} + \frac{\partial\Phi_2}{\partial x_2} + \frac{\partial\Phi_3}{\partial x_3}\right).$$

By comparing the last two equation we get the following relation

$$2(1-\nu)\Delta F = C\left(\frac{\partial\Phi_1}{\partial x_1} + \frac{\partial\Phi_2}{\partial x_2} + \frac{\partial\Phi_3}{\partial x_3}\right), \qquad (3.32)$$

which implies that the stress function F should contain a homogeneous part $\Phi_0 \in \ker\Delta$ and an inhomogeneous part satisfying equation (3.32), and finally we have

$$F = \Phi_0 + x_1\Phi_1 + x_2\Phi_2 + x_3\Phi_3, \qquad (3.33)$$

where $\Phi_i, i = 0, 1, 2, 3$ are harmonic functions. The application of the Laplace operator Δ on the equation (3.33) leads to

$$\Delta F = 2\left(\frac{\partial\Phi_1}{\partial x_1} + \frac{\partial\Phi_2}{\partial x_2} + \frac{\partial\Phi_3}{\partial x_3}\right),$$

and by comparing the result with (3.32) we see that

$$C = (1-\nu).$$

Finally we obtain that a spatial stress function F satisfies the biharmonic equation

$$\Delta\Delta F = 0,$$

as we have seen it previously in the case of plane problems.

The Papkovich-Neuber approach allows us to construct an exact solution to spatial problems of linear elasticity if we choose four harmonic functions. The question of reducing a number of functions arises in applications. Because an exact solution with four harmonic functions is only possible for very simple geometry, and in a case of numerical calculations such a variability in a choice could lead to instability of a system of linear equations coming from boundary conditions.

Another problem with the Papkovich-Neuber approach is that representation of solutions three dimensional elasticity is complete, but introduces many linear dependent functions which can lead to numerical stability problems. This disadvantage was observed by Bauch in [Bauch 1981] where it was shown that if classical spherical harmonics are used in the Papkovich-Neuber representation then $8n + 4$ polynomial solutions are generated, but the dimension of the subspace of polynomial solutions of degree n is only $6n+3$. To fix the linear dependent functions is a very difficult task, but one can overcome these difficulties by working with a hypercomplex function theory which we introduce in the next section.

3.4 Methods of hypercomplex function theory for three dimensional problems

As we have shown in section 3.1 the complex function theory is a very powerful tool for solving two dimensional problems of linear elasticity, but it's not restricted only to

42

elasticity problems and can be easily applied to various problems of mathematical physics. Due to a wide range of applications of the complex function theory it's naturally to ask about its suitable generalisation to higher dimensions.

In 1843 W.R. Hamilton has introduced the algebra of the real quaternions as a generalisation of complex numbers to $\mathbb{R}^4$, and in 1878 W.K. Clifford has proposed the real Clifford algebra which generalises complex numbers to higher dimensions. But only around 1930 a hypercomplex analysis in the algebra of real quaternions and in the real Clifford algebra appeared as a special topic in works of R. Fueter [Fueter 1935], G.C. Moisil and N. Théodoresco [Moisil & Théodoresco 1931]. A generalisation of the complex analysis to higher dimensions was introduced in the late sixties by a group of Belgian mathematicians, and it was called the Clifford analysis. Their results were published later in the book [Brackx et al. 1982]. A way from the classical complex analysis to its higher dimensional generalisation is fully presented in [Gürlebeck et al. 2008].

After developing the theoretical basis of a higher dimensional analysis a question of applications of the new theory was posted by several mathematicians. For an overview of richness of the hypercomplex analysis in various fields of mathematical physics we refer to [Gürlebeck & Sprößig 1989, Kravchenko & Shapiro 1996, Gürlebeck & Sprößig 1997, Kravchenko 2003] and the references therein. A direct application of the hypercomplex function theory to linear elasticity problems was presented in [Bock & Gürlebeck 2009] by introduction of a three dimensional generalisation of the Kolosov-Muskhelishvili formulae (3.6). These, so-called, generalised Kolosov-Muskhekishvili formulae describe the physical state of a solid body in terms of two monogenic functions, and make it possible to construct exact solutions to such problems. Construction and proofs related to these formulae were described in the PhD thesis [Bock 2009], and in [Bock & Gürlebeck 2009] where a polynomial basis which is generated by these formulae was studied. Another example of application to three-dimensional elasticity problems could be found in [Patrault et al. 2014].

In this section we introduce some basic ideas of the hypercomplex analysis, and we will end up with the generalised Kolosov-Muskhelishvili formulae.

3.4.1 Basics of the hypercomplex analysis

Let $\mathbf{e}_0, \mathbf{e}_1, \mathbf{e}_2, \mathbf{e}_3$ be an orthonormal basis of the Euclidean vector space $\mathbb{R}^4$. We introduce an associative multiplication of the basis vectors $\mathbf{e}_j$ subject to the multiplication rules:

$$\begin{aligned}
\mathbf{e}_i\mathbf{e}_j + \mathbf{e}_j\mathbf{e}_i &= -2\delta_{ij}\mathbf{e}_0 & i,j &= 1,2,3, \\
\mathbf{e}_0\mathbf{e}_i &= \mathbf{e}_i\mathbf{e}_0 = \mathbf{e}_i, & i &= 0,1,2,3, \\
\mathbf{e}_1\mathbf{e}_2\mathbf{e}_3 &= -\mathbf{e}_0.
\end{aligned}$$

Extended by $\mathbb{R}$-linearity to $\mathbb{R}^4$ this non-commutative product generates the algebra of real quaternions denoted by $\mathbb{H}$. The real vector space $\mathbb{R}^4$ will be embedded in $\mathbb{H}$ by identifying the element $\mathbf{a} = (a_0, a_1, a_2, a_3) \in \mathbb{R}^4$ with the element

$$\mathbf{a} = a_0\mathbf{e}_0 + a_1\mathbf{e}_1 + a_2\mathbf{e}_2 + a_3\mathbf{e}_3 \in \mathbb{H}.$$

Note that $\mathbf{e}_0 = (1, 0, 0, 0)^{\mathrm{T}}$ is the multiplicative unit element of $\mathbb{H}$. As usual we will identify $\mathbf{e}_0$ with 1 if there is no reason for misunderstandings.

The real number $\mathbf{Sc}\,\mathbf{a} := a_0$ is called the scalar part of $\mathbf{a}$ and $\mathbf{Vec}\,\mathbf{a} := a_1\mathbf{e}_1 + a_2\mathbf{e}_2 + a_3\mathbf{e}_3$ is the vector part of $\mathbf{a}$. Analogous to the complex case, the conjugate of $\mathbf{a} := a_0 + a_1\mathbf{e}_1 + a_2\mathbf{e}_2 + a_3\mathbf{e}_3 \in \mathbb{H}$ is the quaternion $\bar{\mathbf{a}} := a_0 - a_1\mathbf{e}_1 - a_2\mathbf{e}_2 - a_3\mathbf{e}_3$. The norm of $\mathbf{a}$ is given by $|\mathbf{a}| = \sqrt{\mathbf{a}\bar{\mathbf{a}}}$ and coincides with the corresponding Euclidean norm of $\mathbf{a}$, as a vector in $\mathbb{R}^4$. Since we will solve a boundary value problem from spatial linear fracture mechanics, let us consider the subset

$$\mathcal{A} := \mathrm{span}_{\mathbb{R}}\{1, \mathbf{e}_1, \mathbf{e}_2\}$$

of $\mathbb{H}$. The real vector space $\mathbb{R}^3$ can be embedded in $\mathcal{A}$ by the identification of each element $\mathbf{x} = (x_1, x_2, x_3)^{\mathrm{T}} \in \mathbb{R}^3$ with the reduced quaternion

$$\mathbf{x} = x_1 + x_2\mathbf{e}_1 + x_3\mathbf{e}_2 \in \mathcal{A}.$$

As a consequence, we will often use the same symbol $\mathbf{x}$ to represent a point in $\mathbb{R}^3$ as well as to represent the corresponding reduced quaternion. Note that the set $\mathcal{A}$ is only a real vector space but not a sub-algebra of $\mathbb{H}$. For the coordinate axes x, y, z we will use the notation x_1, x_2, x_3. Moreover, we introduce the Fueter variables [Fueter 1935]

$$\mathbf{z}_1 \quad = \quad -\tfrac{1}{2}(\mathbf{e}_1\mathbf{x} + \mathbf{x}\mathbf{e}_1) \quad = \quad x_2 - x_1\mathbf{e}_1,$$

$$\mathbf{z}_2 \quad = \quad -\tfrac{1}{2}(\mathbf{e}_2\mathbf{x} + \mathbf{x}\mathbf{e}_2) \quad = \quad x_3 - x_1\mathbf{e}_2,$$

and we have

$$(\mathbf{z}_1, \mathbf{z}_2) : \mathbf{z}_1 = x_2 - x_1\mathbf{e}_1, \mathbf{z}_2 = x_3 - x_1\mathbf{e}_2 \cong \mathbb{R}^3 \cong \mathcal{A}.$$

Let Ω be an open subset of $\mathbb{R}^3$ with a piecewise smooth boundary. An $\mathbb{H}$-valued function is a mapping

$$f : \Omega \to \mathbb{H}$$

such that

$$f(\mathbf{x}) = \sum_{i=0}^{3} f^i(\mathbf{x})\mathbf{e}_i, \quad \mathbf{x} \in \Omega.$$

The coordinates f^i are real-valued functions defined in Ω, i.e.

$$f^i : \Omega \to \mathbb{R}, \quad i = 0, 1, 2, 3.$$

Continuity, differentiability or integrability of f are defined coordinate-wisely. For continuously real-differentiable functions $f : \Omega \subset \mathbb{R}^3 \to \mathbb{H}$, which we will denote for simplicity by $f \in C^1(\Omega, \mathbb{H})$, the operator

$$\bar{\partial} = \frac{\partial}{\partial x_1} + \mathbf{e}_1\frac{\partial}{\partial x_2} + \mathbf{e}_2\frac{\partial}{\partial x_3} \tag{3.34}$$

44

is called generalized Cauchy-Riemann operator. The corresponding conjugate generalized Cauchy-Riemann operator is defined as

$$\partial = \frac{\partial}{\partial x_1} - \mathbf{e}_1 \frac{\partial}{\partial x_2} - \mathbf{e}_2 \frac{\partial}{\partial x_3}. \tag{3.35}$$

We define and denote the Cauchy-Riemann operators completely analogous to the complex one dimensional case. Here, we follow the notation used in [Gürlebeck et al. 2008], which is opposed to the commonly used notation in the Clifford analysis, but analogues to complex function theory.

Definition 3.3. A function $f \in C^1(\Omega, \mathbb{H})$ is called left (resp. right) monogenic in Ω if

$$\bar{\partial} f = 0 \quad \text{in} \quad \Omega \quad (\text{resp.}, f \bar{\partial} = 0 \quad \text{in} \quad \Omega).$$

We point out that in general left (resp. right) monogenic functions are not right (resp. left) monogenic. From now on we use only left monogenic functions that, for simplicity, we call monogenic and sometimes denote by $f \in \ker \bar{\partial}$.

Definition 3.4. Using the generalized Cauchy-Riemann operator (3.34) and its conjugate (3.35) we define the differential operators

$$\overline{\partial_i} = \frac{1}{2} \overline{\partial \mathbf{e}_i} = \frac{1}{2} \overline{\mathbf{e}_i} \left(\frac{\partial}{\partial x_1} + \mathbf{e}_1 \frac{\partial}{\partial x_2} + \mathbf{e}_2 \frac{\partial}{\partial x_3} \right)$$

and the associated conjugate differential operator

$$\partial_i = \frac{1}{2} \partial \mathbf{e}_i = \frac{1}{2} \left(\frac{\partial}{\partial x_1} - \mathbf{e}_1 \frac{\partial}{\partial x_2} - \mathbf{e}_2 \frac{\partial}{\partial x_3} \right) \mathbf{e}_i$$

with $i = 0, 1, 2$.

3.4.2 Generalised Kolosov-Muskhelishvili formulae

Analogously to the plane case, first we introduce a generalisation of the theorem of Goursat. For all proofs in this section we refer to [Bock & Gürlebeck 2009] and [Bock 2009].

Theorem 3.5. *Let Ω be a star-shaped domain and $F \in C^4(\Omega, \mathbb{R})$ be a solution of the biharmonic equation $\Delta\Delta F = 0$. Then there exist two monogenic functions Φ, Ψ in Ω, with*

$$F(\mathbf{x}) = \frac{1}{2} \left[\bar{\mathbf{x}} \Phi(\mathbf{x}) + \overline{\Phi(\mathbf{x})} \mathbf{x} + \Psi(\mathbf{x}) + \overline{\Psi(\mathbf{x})} \right] = \mathbf{Sc} \left(\bar{\mathbf{x}} \Phi(\mathbf{x}) + \Psi(\mathbf{x}) \right).$$

By applying this generalised theorem of Goursat and by using the Papkovich-Neuber approach, the so-called, generalised Kolosov-Muskhelishvili formulae were introduced in the previous study [Bock & Gürlebeck 2009]. For complete derivation we refer again to [Bock 2009], and here we only recall them.

$$\begin{aligned}
2\mu(u_1 + u_2 \mathbf{e}_1 + u_3 \mathbf{e}_2) &= (\overline{\partial_1 \Phi}) \mathbf{z}_1 + (\overline{\partial_2 \Phi}) \mathbf{z}_2 - \bar{x}(\overline{\partial_0 \bar{\Phi}}) - \overline{\partial_0 \Psi} - \overline{\partial_0 \bar{\Psi}} + \\
&\quad + \frac{2\alpha - 1}{2}(\Phi - \mathbf{e}_3 \bar{\Phi} \mathbf{e}_3),
\end{aligned} \tag{3.36}$$

$$\sigma_{11} + \sigma_{22} + \sigma_{33} = (4-\alpha)(\partial_0\Phi + \overline{\partial_0\Phi}) = 2(4-\alpha)\mathbf{Sc}[\partial_0\Phi], \qquad (3.37)$$

$$\begin{aligned}
-\sigma_{11} + \sigma_{22} + \sigma_{33}+ &= 2\left[(\partial_0\overline{\partial_0\Phi})\mathbf{x} - \bar{\mathbf{z}}_1(\partial_0\partial_1\Phi) - \bar{\mathbf{z}}_2(\partial_0\partial_2\Phi) + \partial_0\partial_0\Psi + \partial_0\overline{\partial_0\Psi}\right] + \\
+2\sigma_{12}\mathbf{e}_1 + 2\sigma_{13}\mathbf{e}_2 &\quad +(2-\alpha)(\partial_0\Phi + \overline{\partial_0\Phi}) + (1-\alpha)(\partial_0\bar\Phi + \mathbf{e}_3(\partial_0\bar\Phi)\mathbf{e}_3),
\end{aligned}$$
$$(3.38)$$

$$\begin{aligned}
\sigma_{11} - \sigma_{22} + \sigma_{33}- &= 2\mathbf{e}_1\left[(\partial_0\overline{\partial_1\Phi})\mathbf{x} - \bar{\mathbf{z}}_1(\partial_1\partial_1\Phi) - \bar{\mathbf{z}}_2(\partial_1\partial_2\Phi) + \partial_0\partial_1\Psi + \partial_0\overline{\partial_1\Psi}\right] - \\
-2\sigma_{12}\mathbf{e}_1 + 2\sigma_{23}\mathbf{e}_3 &\quad -\mathbf{e}_1(\partial_1\Phi + (\alpha-2)\overline{\partial_1\Phi}) + 2\mathbf{e}_1(\partial_0\bar\Phi)\mathbf{e}_1 - \alpha\mathbf{e}_1(\partial_2\Phi - \overline{\partial_2\Phi})\mathbf{e}_3+ \\
&\quad +(\alpha-1)\mathbf{e}_2(\overline{\partial_1\bar\Phi})\mathbf{e}_3,
\end{aligned}$$
$$(3.39)$$

$$\begin{aligned}
\sigma_{11} + \sigma_{22} - \sigma_{33}- &= 2\mathbf{e}_2\left[(\partial_0\overline{\partial_2\Phi})\mathbf{x} - \bar{\mathbf{z}}_1(\partial_1\partial_2\Phi) - \bar{\mathbf{z}}_2(\partial_2\partial_2\Phi) + \partial_0\partial_2\Psi + \partial_0\overline{\partial_2\Psi}\right] - \\
-2\sigma_{13}\mathbf{e}_2 - 2\sigma_{23}\mathbf{e}_3 &\quad -\mathbf{e}_2(\partial_2\Phi + (\alpha-2)\overline{\partial_2\Phi}) + 2\mathbf{e}_2(\partial_0\bar\Phi)\mathbf{e}_2 + \alpha\mathbf{e}_2(\partial_1\Phi - \overline{\partial_1\Phi})\mathbf{e}_3+ \\
&\quad +(1-\alpha)\mathbf{e}_1(\overline{\partial_2\bar\Phi})\mathbf{e}_3,
\end{aligned}$$
$$(3.40)$$

where Φ, Ψ are two monogenic functions, μ and $\alpha = 2(1-\nu)$ are material parameters.

The formulae (3.36)-(3.40) represent all of the components of the displacement vector $\mathbf{u}$ and the stress tensor $\tilde{\boldsymbol{\sigma}}$ in terms of only two monogenic functions, and thus we can construct exact solutions to three-dimensional elasticity problems by choosing appropriate functions Φ and Ψ. But unfortunately in practice a choice or a construction of these monogenic functions is not a trivial task.

One of the first monogenic polynomial system was introduced in [Malonek 1990]. The constructed monogenic system was based on a permutational product, which requires high computational costs for higher order polynomials. To reduce computational costs several other monogenic polynomial systems were introduced in many works, we refer to [Bock & Gürlebeck 2010], [Caçao et al. 2001], [Caçao et al. 2004], [Morais & Le 2010], and the references therein. These systems were based on spherical harmonics and were constructed to provide the Appell property. Such Appell systems are very efficient in numerical calculation. But for real applications in three-dimensional elasticity theory, which are given in an arbitrary geometry, it's a very difficult task to find coefficients of monogenic systems from the given boundary conditions. This task, in general, cannot be solved for an arbitrary geometry. Therefore it's important to propose a method which uses advantages of the hypercomplex function theory and combines them with a well-know numerical method. Such a coupled method we will introduce during the next chapters. Due to the complexity of a construction in higher dimensions we will start from a complex plane, and we will discuss and proof as much as we can for that case.

Chapter 4

Realisation of coupling

Often in practice we face problems which cannot be efficiently solved by single standard methods, like for instance singular problems, or coupled problems which connect different fields of mathematical physics. The solution of such problems by standard numerical methods, like the finite element method [Zienkiewicz 1971], or the boundary element method [Brebbia & Dominguez 1992], can be very costly and inaccurate. Therefore already in the late seventies an approach which combines together the finite element and the boundary element method was proposed by Zienkiwicz in [Zienkiewicz et al. 1977]. This approach has shown a good performance by utilising advantages of both methods. In particular such a coupling makes sense in a case of interface problems, problems in unbounded domain, multiphysics problems, problems with a singularity, for details we refer to [Costabel & Stephan 1990], [Hsiao et al. 2000], [Bermúdez et al. 2007] and references therein.

Another coupled method which is mainly motivated by handling complicated geometries is the Schwarz alternating method. This method was proposed by Schwarz [Schwarz 1890] as an iterative procedure for constructing a harmonic function in a nontrivial domain by decomposition the domain into two subdomains and solving corresponding "coupling" boundary value problems. After more than one hundred years this method was brought to the engineers by works of Lions [Lions 1988, Lions 1989, Lions 1990], and became a basis for the domain decomposition method [Smith et al. 1996]. The idea of this method is a decomposition of an original domain into several subdomains. This idea is of a significant importance in nowadays since computer clusters and parallel computations are becoming more common things. By the domain decomposition method one can handle the computation with the finite element method which contains millions degrees of freedom in reasonable time.

The FEM-BEM coupling and the domain decomposition method are very powerful numerical tools for handling complicated problems, but they are also not free of drawbacks, for instance, in a case of BEM one has to solve numerically a boundary integral equation, which could lead to additional refinement in a coupling region. In the case of the domain decomposition method a resulting system of equations could contain millions of unknowns, and thus cannot be handled on a normal computer.

An alternative could be an idea of such a coupled method which will lead to lower computational costs without loosing the accuracy of a solution. To insure the accuracy one can start with a construction of an analytical solution in a certain region of interest, and couple it after this with a well-established numerical method, such as the finite element method, in the remaining part of a domain. The idea of such coupling was introduced in a series of works of R. Piltner [Piltner 1982, Piltner 1985, Piltner 2003, Piltner 2008], where he has introduced a special element containing an exact solution for a crack problem, and coupled it with the standard FEM via nodes at the boundary of the special element. In his approach the coupling was realised only by values at the nodes, and a global solution between nodes has a jump.

In previous studies a new method for a coupling of an analytical and finite element solution was proposed, see for instance [Bock et al. 2012, Bock et al. 2012, Bock et al. 2013, Gürlebeck & Legatiuk 2014]. The main idea of this approach is to get the global continuity of the solution through the whole interaction interface between two solutions. To obtain that continuity we introduce a special element containing an exact solution to a singular problem, in our case to a crack tip problem, and couple it with a finite element solution by, so-called, coupling elements. The requirement for these coupling elements is to insure C^0 continuity for displacements. For that reason a special interpolation operator has been constructed that preserves the analytical solution on the coupling interface, couples it continuously with special elements which have a polynomial connection to the standard elements. In this chapter we introduce step by step this concept.

In [Bock et al. 2013] following P. G. Ciarlet [Ciarlet 1978] some basic steps for convergence analysis of the proposed method have been performed. In this theory one of the most important roles is played by the unisolvence property of the interpolation operator that is used for the finite element approximation. In [Bock et al. 2012] it has been shown that for a given special distribution of interpolation nodes the corresponding interpolation problem is uniquely solvable. In this chapter the generalised results for an arbitrary number of nodes will be presented. This is the necessary result to define the basis functions for the interpolation operator which permit an arbitrary refinement of the mesh and makes the method practically applicable. Based on this result the convergence and error estimates of the proposed scheme will be proved in Chapter 5.

4.1 Problem of coupling

Let now $\Omega \subset \mathbb{C}$ be a bounded simply connected domain containing a crack. We introduce a triangulation $\mathcal{F}_h$ over Ω as follow

$$\Omega = \bigcup_{T \in \mathcal{F}_h} T \bigcup_{\Omega_{\mathrm{SE}} \in \mathcal{F}_h} \Omega_{\mathrm{SE}}, \tag{4.1}$$

where T are triangular finite elements, and Ω_{SE} are special elements, which serve to describe the behaviour of the continuum near a crack tip. The special elements are always located at the crack tip (see Fig. 4.1).
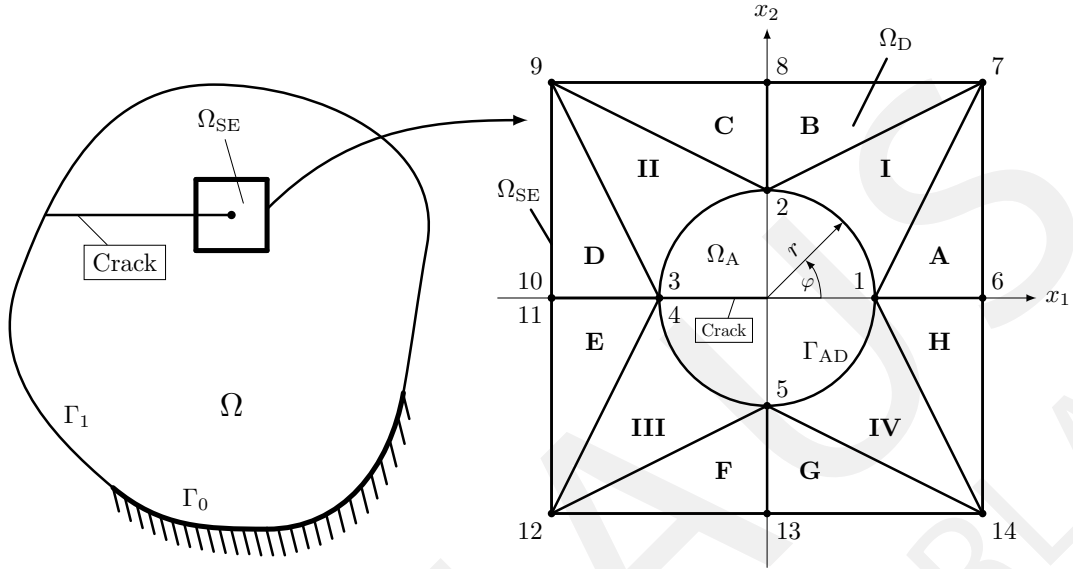
Figure 4.1: Geometrical settings of the special element

The domain Ω_{SE} is decomposed in the two sub-domains $\Omega_{\mathrm{SE}} = \Omega_{\mathrm{A}} \cup \Omega_{\mathrm{D}}$ separated by the fictitious joint interface $\Gamma_{\mathrm{AD}} = \overline{\Omega}_{\mathrm{A}} \cap \overline{\Omega}_{\mathrm{D}}$. The discrete "numerical" domain, denoted by Ω_{D}, is modelled by two different kinds of elements: the constant strain triangles (CST-elements) with C^0 continuity (elements $A - H$ in the Fig. 4.1) and the coupling elements with C^0 continuity to the CST-elements, and with C^∞ continuity on the interface Γ_{AD} (elements I-IV in the Fig. 4.1), which couple the "numerical" domain Ω_{D} with the "analytical" domain Ω_{A}. The C^∞ continuity on the interface Γ_{AD} should be understood in a sense, that the interpolation functions are infinitely differentiable on the interface. But, this does not mean automatically that the connection between elements will be better than $C^0(\Omega)$. For that we would need to introduce additional conditions.

A crack is modelled as a mathematical cut, and the nodes $3, 10$ and $4, 11$ belong to the upper and lower crack faces, respectively. We call the sub-domain Ω_{A} analytical in that sense, that the constructed solutions are exact solutions to the differential equation in Ω_{A}. Analogously, the numerical sub-domain Ω_{D} means, that the constructed solutions are based on the finite element approximation. The idea behind this special element is to get a continuous connection through the whole interaction interface Γ_{AD} by introducing new shape functions over the curved triangles I-IV.

Fig. 4.1 shows only an example of possible triangulation inside the special element Ω_{SE}. For practical reasons we can increase the number of coupling elements on the interface Γ_{AD}, we will illustrate this option in convergence analysis and numerical examples in the next chapters.

In the domain Ω we solve the following boundary value problem for the Lamé equa-

49

tion (2.18)

$$
\begin{cases}
-\mu \, \Delta \mathbf{u} - (\lambda + \mu) \mathrm{grad} \, \mathrm{div} \, \mathbf{u} = \mathbf{f} & \text{in} \quad \Omega, \\
\mathbf{u} = 0 \quad \text{on} \quad \Gamma_0, \\
\displaystyle\sum_{j=1}^{2} \sigma_{ij}(\mathbf{u}) n_j = g_i \quad \text{on} \quad \Gamma_1, \quad 1 \le i \le 2.
\end{cases}
$$

The basic idea of coupling consists in construction of a strong solution to the Lamé equation in Ω_A, and couple it with a weak solution which is obtained by finite element method. The details of weak formulation and finite element method we will discuss in Chapter 5. The strong solution to the crack tip problem was constructed in Chapter 3 and it's given by formula (3.13) for displacements, for completeness of explanations we repeat this formula here

$$
\begin{aligned}
2\mu(u_1 + i\,u_2) \;=\; & \sum_{n=1,3}^{\infty} r^{\frac{n}{2}} \left[a_n \left(\kappa\, e^{i\varphi \frac{n}{2}} - e^{-i\varphi \frac{n}{2}} \right) + \frac{n}{2} \bar{a}_n \left(e^{-i\varphi \frac{n}{2}} - e^{-i\varphi(\frac{n}{2}-2)} \right) \right] + \\
& + \sum_{n=2,4}^{\infty} r^{\frac{n}{2}} \left[a_n \left(\kappa\, e^{i\varphi \frac{n}{2}} + e^{-i\varphi \frac{n}{2}} \right) + \frac{n}{2} \bar{a}_n \left(e^{-i\varphi \frac{n}{2}} - e^{-i\varphi(\frac{n}{2}-2)} \right) \right].
\end{aligned}
$$

4.2 Main interpolation theorem

After construction of the analytical solution we need to solve the problem of coupling on the interface Γ_{AD}. Let us consider n nodes on the interface Γ_{AD} belonging to the interval $[-\pi, \pi]$ (see Fig. 4.2). To define the unknown coefficients a_n in (3.13) we introduce a special interpolation operator and solve an interpolation problem on the interface Γ_{AD}. The idea is to get C^0 continuity through the joint interface Γ_{AD}. This can be reached if the corresponding interpolation problem is always solvable and the interpolation operator is preserving the analytical solution on Γ_{AD}. For connection with standard finite elements we will use a linear interpolator.

As the interpolation function $f_n(\varphi)$ we use partial sums of the analytical solution (3.13) restricted to the interface Γ_{AD} (i.e. $r = r_A$). Additionally, to be able to represent by this interpolation function all polynomials up to a certain degree, we add a constant to our ansatz. As it was mentioned in Chapter 3, typically the constant part in the analytical solution for an infinite plane is excluded by mechanical reasons: the constant means a rigid motion of the infinite plane. But in bounded domains situation is different, because boundary conditions play the most important role. In this case the coefficients in the analytical solution are controlled by the boundary conditions, i.e. if the boundary conditions do not allow a rigid body motion, then the constant part would be removed during construction of the solution. Thus the adding of a constant to the ansatz doesn't influence the mechanical behaviour.
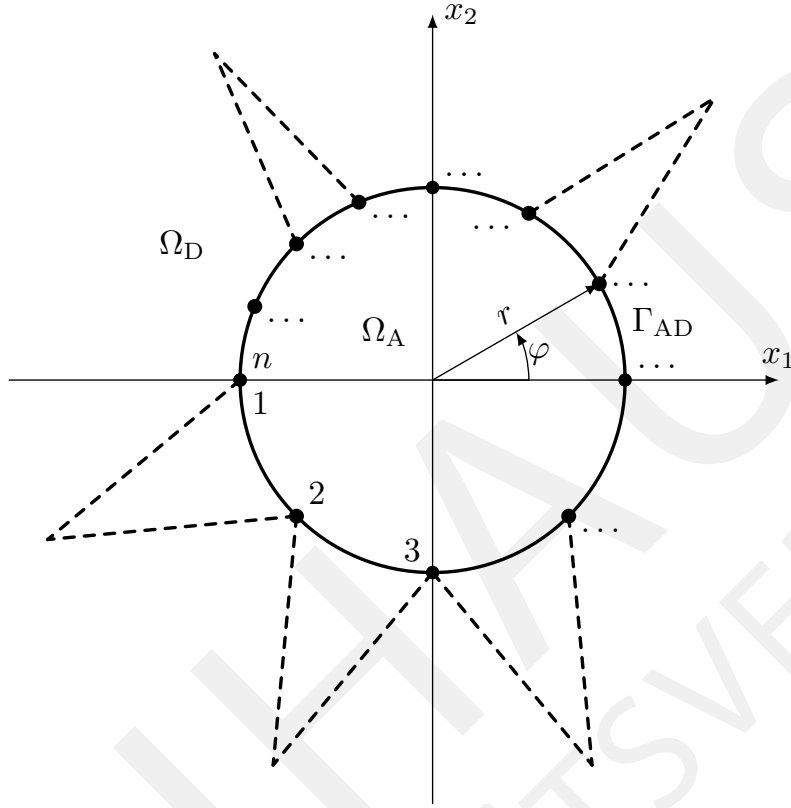
Figure 4.2: The coupling problem

We obtain the following interpolation function on the interface Γ_{AD}

$$
\begin{aligned}
f_n(\varphi) \;=\; & \sum_{k=0,2,\ldots}^{N_1} r_{\mathrm{A}}^{\frac{k}{2}} \left[a_k \left(\kappa\, e^{i\varphi\frac{k}{2}} + e^{-i\varphi\frac{k}{2}} \right) + \frac{k}{2}\bar{a}_k \left(e^{-i\varphi\frac{k}{2}} - e^{-i\varphi(\frac{k}{2}-2)} \right) \right] + \\[2mm]
& + \sum_{k=1,3,\ldots}^{N_2} r_{\mathrm{A}}^{\frac{k}{2}} \left[a_k \left(\kappa\, e^{i\varphi\frac{k}{2}} - e^{-i\varphi\frac{k}{2}} \right) + \frac{k}{2}\bar{a}_k \left(e^{-i\varphi\frac{k}{2}} - e^{-i\varphi(\frac{k}{2}-2)} \right) \right],
\end{aligned}
\tag{4.2}
$$

where the numbers of basis functions are related to n as follows:

$$
N_1 = n - m, \quad \text{with} \quad \left\{ \begin{array}{ll} m = 2 & \text{for even } n, \\ m = 1 & \text{for odd } n, \end{array} \right.
$$

$$
N_2 = n - m, \quad \text{whith} \quad \left\{ \begin{array}{ll} m = 1 & \text{for even } n, \\ m = 2 & \text{for odd } n. \end{array} \right.
$$

In [Bock et al. 2012] it is shown that for $n = 5$ the corresponding interpolation problem at the interface can be solved for arbitrary data. To have a basis for the convergence

51

of the coupled FE-method we need the solvability for arbitrary number and location of nodes. Main problems are the occurrence of the half integer powers in the set of ansatz functions and the fact that the coefficients a_k and $\bar{a}_k$ are not independent.

Now we formulate the following theorem:

Theorem 4.1. *For n given arbitrary nodes $\varphi_0, \varphi_1, \ldots, \varphi_{n-1}$ basis functions of the form (4.2) exist, satisfying the canonical interpolation problem*

$$f_n^{<i>}(\varphi_k) = \delta_{(i-1)k}, \quad k = 0, \ldots, n-1, \tag{4.3}$$

where $i = 1, \ldots, n$ is the number of the canonical problem.

Proof. Without loss of generality we will consider here the first canonical problem for $f_n^{<1>}$. In all upcoming calculations we take $r_A = 1$. We start our proof by introducing the new variable

$$t = e^{i\frac{\varphi}{2}}, \qquad |t| = 1.$$

The function (4.2) can then be rewritten as

$$
\begin{aligned}
f_n(t) &= \sum_{k=0,2,\ldots}^{N_1} \left[a_k \kappa\, t^k + a_k \kappa\, t^{-k} + \frac{k}{2}\bar{a}_k\, t^{-k} - \frac{k}{2}\bar{a}_k\, t^{-k+4} \right] + \\
&\quad + \sum_{k=1,3,\ldots}^{N_2} \left[a_k \kappa\, t^k - a_k \kappa\, t^{-k} + \frac{k}{2}\bar{a}_k\, t^{-k} - \frac{k}{2}\bar{a}_k\, t^{-k+4} \right].
\end{aligned}
\tag{4.4}
$$

Depending on the number n of nodes on the interface Γ_{AD} we have a different number of functions from the even and odd parts of the basis. For the case of an even number of nodes we have $N_2 = N_1 + 1$ and in the case of an odd number of nodes we have $N_1 = N_2 + 1$. This fact must be taken into account during the proof.

Let us consider at first the case when the number of nodes n is **even**. In this case we can write the interpolation function (4.4) as one finite sum

$$
\begin{aligned}
f_n(t) &= \sum_{k=0}^{\frac{1}{2}n-1} \left[\frac{2k+1}{2}\bar{a}_{2k+1}\, t^{-2k-1} + a_{2k}\kappa\, t^{-2k} + k\bar{a}_{2k}\, t^{-2k} - \right. \\
&\quad - k\bar{a}_{2k}\, t^{-2k+4} + a_{2k+1}\kappa\, t^{2k+1} - a_{2k+1}\kappa\, t^{-2k-1} + \\
&\quad \left. + a_{2k}\kappa\, t^{2k} - \frac{2k+1}{2}\bar{a}_{2k+1}\, t^{-2k+3} \right].
\end{aligned}
\tag{4.5}
$$

The interpolation problem (4.3) reads as follows:

$$f_n(t_j) = \delta_{0j}, \qquad j = 0, \ldots, n-1.$$

52

Analysing equation (4.5) we observe that the lowest degree is $-n+1$. Therefore, to obtain a polynomial we multiply both sides of (4.5) by t^{n-1} and we get at the nodes

$$\sum_{k=0}^{\frac{1}{2}n-1} \left[\frac{2k+1}{2}\bar{a}_{2k+1}\, t_j^{n-2k-2} + a_{2k}\kappa\, t_j^{n-2k-1} + k\bar{a}_{2k}\, t_j^{n-2k-1} - \right.$$

$$-k\bar{a}_{2k}\, t_j^{n-2k+3} + a_{2k+1}\kappa\, t_j^{n+2k} - a_{2k+1}\kappa\, t_j^{n-2k-2} +$$

$$\left. +a_{2k}\kappa\, t_j^{n+2k-1} - \frac{2k+1}{2}\bar{a}_{2k+1}\, t_j^{n-2k+2} \right] = \delta_{0j}\, t_j^{n-1}.$$

Now, we introduce a new right hand side

$$w_j := \delta_{0j}\, t_j^{n-1}, \qquad j = 0, \ldots, n-1.$$

Collecting all summands with the same degree we can write the polynomial with new coefficients α_l

$$\sum_{l=0}^{2n-2} \alpha_l t^l \quad := \quad \sum_{k=0}^{\frac{1}{2}n-1} \left[\frac{2k+1}{2}\bar{a}_{2k+1}\, t^{n-2k-2} + a_{2k}\kappa\, t^{n-2k-1} + \right.$$

$$+k\bar{a}_{2k}\, t^{n-2k-1} - k\bar{a}_{2k}\, t^{n-2k+3} +$$

$$+a_{2k+1}\kappa\, t^{n+2k} - a_{2k+1}\kappa\, t^{n-2k-2} + \tag{4.6}$$

$$\left. +a_{2k}\kappa\, t^{n+2k-1} - \frac{2k+1}{2}\bar{a}_{2k+1}\, t^{n-2k+2} \right].$$

Thus we get the following equivalent interpolation problem

$$\sum_{l=0}^{2n-2} \alpha_l t_j^l = w_j, \qquad j = 0, \ldots, n-1. \tag{4.7}$$

Due to the fact that the polynomial (4.6) contains also shifted powers t^{n-2k+3} and t^{n-2k+2}, the equations relating the new coefficients α_l with the original coefficients a_k will change the form with the increasing number of nodes. We will consider here only the case $n > 6$, because then these relating equations take their general form and the proof applies for all $n > 6$. The remaining three cases $n = 2$, $n = 4$, and $n = 6$ can be easily obtained directly from (4.7) and will not influence the generality of the proof.

For $n > 6$ we can separate the following four groups of equations between α_l and a_k:

$$
\text{(I)} \quad
\begin{cases}
\alpha_{2j} = \dfrac{n-1-2j}{2}\bar{a}_{n-1-2j} - \kappa\, a_{n-1-2j}, \\[4mm]
\alpha_{2j+1} = \kappa\, a_{n-2-2j} + \left(\dfrac{n}{2} - 1 - j\right)\bar{a}_{n-2-2j},
\end{cases}
\quad j = 0, 1,
$$

$$
\text{(II)} \quad
\begin{cases}
\alpha_{2j} = \dfrac{n-1-2j}{2}\bar{a}_{n-1-2j} - \kappa\, a_{n-1-2j} - \dfrac{n+3-2j}{2}\bar{a}_{n+3-2j}, \\[4mm]
\qquad\quad j = 2, \ldots, \dfrac{n-2}{2}, \\[4mm]
\alpha_{2j+1} = \kappa\, a_{n-2-2j} + \left(\dfrac{n}{2} - 1 - j\right)\bar{a}_{n-2-2j} - \left(\dfrac{n}{2} + 1 - j\right)a_{n+2-2j}, \\[4mm]
\qquad\quad j = 2, \ldots, \dfrac{n-4}{2},
\end{cases}
\tag{4.8}
$$

$$
\text{(III)} \quad
\begin{cases}
\alpha_{2j} = \kappa\, a_{2j-n+1} + \dfrac{2j-n-3}{2}\bar{a}_{n+3-2j}, \\[4mm]
\alpha_{2j-1} = \left(\dfrac{n}{2} - j + 2\right)\kappa\, a_{2j-n} - \left(\dfrac{n}{2} - j + 2\right)\bar{a}_{2j-n},
\end{cases}
\quad j = \dfrac{n}{2}, \dfrac{n+2}{2},
$$

$$
\text{(IV)} \quad
\begin{cases}
\alpha_{2j} = \kappa\, a_{2j+1-n}, \\[4mm]
\alpha_{2j-1} = \kappa\, a_{2j-n},
\end{cases}
\quad j = \dfrac{n+4}{2}, \ldots, n-1.
$$

From the equations (4.8) we can calculate explicitly all of the original coefficients a_l. The group (IV) leads to the following equations:

$$
\begin{cases}
a_{2j-n} = \dfrac{\alpha_{2j-1}}{\kappa}, \\[4mm]
a_{2j+1-n} = \dfrac{\alpha_{2j}}{\kappa},
\end{cases}
\quad j = \dfrac{n}{2} + 2, \ldots, n-1.
\tag{4.9}
$$

This group of equations includes all of the coefficients a_l for $l = 4, \ldots, n-1$. Therefore we need only to add equations for the four remaining coefficients. We can calculate the coefficients a_0, a_1, a_3 from group (III) of equations (4.8). The coefficient a_2 can be obtained from the sum of the third equation in group (III) and equation $n-6$ from group (II).

These coefficients are given by

$$
\begin{cases}
a_0 &= \dfrac{\alpha_{n-1}}{2\kappa} + \dfrac{\bar{\alpha}_{n+3}}{\kappa^2}, \\[2mm]
a_1 &= \left[\dfrac{\alpha_n}{\kappa} + \dfrac{3\bar{\alpha}_{n+2}}{2\kappa^2} \right]\left(1 - \dfrac{3}{4\kappa^2} \right)^{-1}, \\[2mm]
a_2 &= \dfrac{\alpha_{n-3} + \alpha_{n+1}}{2\kappa} + \dfrac{3\bar{\alpha}_{n+5}}{2\kappa^2}, \\[2mm]
a_3 &= \dfrac{\alpha_{n+2}}{\kappa} + \dfrac{1}{2\kappa}\left[\dfrac{\bar{\alpha}_n}{\kappa} + \dfrac{3\alpha_{n+2}}{2\kappa^2} \right]\left(1 - \dfrac{3}{4\kappa^2} \right)^{-1}.
\end{cases}
\tag{4.10}
$$

The interpolation problem (4.7) contains $2n-1$ unknown coefficients α_l, but from the interpolation nodes we can get only n equations. Therefore, we formulate $n-1$ additional equations to determine all coefficients α_l. For that reason we extend (4.6) to the whole complex plane and add $n-1$ Hermite-type interpolation conditions

$$
\sum_{l=0,1}^{2n-2} \alpha_l \left(\frac{\partial^j t^l}{\partial t^j} \right)_{t=t_*} = w_j^*, \qquad j = 0, \ldots, 2n-2,
\tag{4.11}
$$

where for simplicity we take the additional node t_* at 0 and the values w_j^* are defined as follows:

$$
w_j^* = \begin{cases}
0, & j = 0, \ldots, n-5, \\
\beta_j, & j = n-4, \ldots, n-2,
\end{cases}
\tag{4.12}
$$

with arbitrary complex numbers β_j.

The obtained "extended" interpolation problem (4.3), (4.11) is always solvable (for more details, see for instance [Davis 1975]). The solution of this interpolation problem will give us all coefficients α_l, which are needed to define the original coefficients a_k.

To insure that the coefficients a_k satisfy the original interpolation problem (4.3) we need to satisfy compatibility conditions for the coefficients α_k. By using formulae (4.9)-(4.10) we obtain these conditions from the groups (I) and (II) of equations (4.8). The first group gives the following four equations

$$
\begin{aligned}
\alpha_{2j} + \alpha_{2n-2-2j} - (n-2j-1)\frac{\bar{\alpha}_{2n-2-2j}}{2\kappa} &= 0, \\[2mm]
\alpha_{2j+1} - \alpha_{2n-3-2j} - \left(\frac{n-2}{2} - j \right)\frac{\bar{\alpha}_{2n-3-2j}}{\kappa} &= 0,
\end{aligned}
\tag{4.13}
$$

for $j = 0, 1$. The second group leads to the remaining $n-5$ equations

$$
\begin{aligned}
\alpha_{2j} + \alpha_{2n-2-2j} - (n-2j-1)\frac{\bar{\alpha}_{2n-2-2j}}{2\kappa} + (n-2j+3)\frac{\bar{\alpha}_{2n-2(j-1)}}{2\kappa} &= 0, \\[2mm]
\alpha_{2j+1} - \alpha_{2n-3-2j} - \left(\frac{n-2}{2} - j \right)\frac{\bar{\alpha}_{2n-3-2j}}{\kappa} + \left(\frac{n-2}{2} + 2 - j \right)\frac{\bar{\alpha}_{2n-2j+1}}{\kappa} &= 0,
\end{aligned}
\tag{4.14}
$$

for $j = 2, \ldots, \frac{n-6}{2}$.

$$\alpha_{n+2} + \frac{1}{2}\left[\frac{\bar{\alpha}_n}{\kappa} + \frac{3\alpha_{n+2}}{2\kappa^2}\right]\left(1 - \frac{3}{4\kappa^2}\right)^{-1} + \alpha_{n-4} + \frac{7\bar{\alpha}_{n+6}}{2\kappa} - $$

$$\hspace{3cm} (4.15)$$

$$-\frac{3\bar{\alpha}_{n+2}}{2\kappa} - \frac{3}{4\kappa}\left[\frac{\alpha_n}{\kappa} + \frac{3\bar{\alpha}_{n+2}}{2\kappa^2}\right]\left(1 - \frac{3}{4\kappa^2}\right)^{-1} \hspace{1cm} = \hspace{0.3cm} 0,$$

$$\alpha_{n-3} - \frac{\alpha_{n-3} + \alpha_{n+1}}{2} - \frac{3\bar{\alpha}_{n+5}}{2\kappa} - \frac{\bar{\alpha}_{n-3} + \bar{\alpha}_{n+1}}{2\kappa} - \frac{3\alpha_{n+5}}{2\kappa^2} + \frac{3\bar{\alpha}_{n+5}}{\kappa} = 0, \hspace{0.5cm} (4.16)$$

$$\kappa\left[\frac{\alpha_n}{\kappa} + \frac{3\bar{\alpha}_{n+2}}{2\kappa^2}\right]\left(1 - \frac{3}{4\kappa^2}\right)^{-1} + \alpha_{n-2} + \frac{5\bar{\alpha}_{n+4}}{2\kappa} - $$

$$\hspace{3cm} (4.17)$$

$$-\frac{1}{2}\left[\frac{\bar{\alpha}_n}{\kappa} + \frac{3\alpha_{n+2}}{2\kappa^2}\right]\left(1 - \frac{3}{4\kappa^2}\right)^{-1} \hspace{1cm} = \hspace{0.3cm} 0.$$

Our goal is to show that there exists a set of complex numbers β_j such that the compatibility conditions (4.13)-(4.17) are satisfied. Considering the first $n-4$ equations of (4.11) with the values (4.12) we get immediately that

$$\alpha_l = 0, \qquad i = 0, \ldots, n-5.$$

Applying these results to first $n-4$ compatibility conditions (4.13)-(4.14) we obtain

$$\alpha_l = 0, \qquad i = n+3, \ldots, 2n-2.$$

Therefore first $n-4$ compatibility conditions are satisfied, and we need to check the remaining three equations (4.15)-(4.17). Taking into account the remaining three values of w_j^* we get the following equations

$$\alpha_{n+2} + \frac{1}{2}\left[\frac{\bar{\alpha}_n}{\kappa} + \frac{3\alpha_{n+2}}{2\kappa^2}\right]\left(1 - \frac{3}{4\kappa^2}\right)^{-1} + \beta_{n-4} - \frac{3\bar{\alpha}_{n+2}}{2\kappa} - $$

$$-\frac{3}{4\kappa}\left[\frac{\alpha_n}{\kappa} + \frac{3\bar{\alpha}_{n+2}}{2\kappa^2}\right]\left(1 - \frac{3}{4\kappa^2}\right)^{-1} = 0,$$

$$\beta_{n-3} - \frac{\beta_{n-3} + \alpha_{n+1}}{2} - \frac{\bar{\beta}_{n-3} + \bar{\alpha}_{n+1}}{2\kappa} = 0,$$

$$\kappa\left[\frac{\alpha_n}{\kappa} + \frac{3\bar{\alpha}_{n+2}}{2\kappa^2}\right]\left(1 - \frac{3}{4\kappa^2}\right)^{-1} + \beta_{n-2} - \frac{1}{2}\left[\frac{\bar{\alpha}_n}{\kappa} + \frac{3\alpha_{n+2}}{2\kappa^2}\right]\left(1 - \frac{3}{4\kappa^2}\right)^{-1} = 0.$$

The second equation can be satisfied only if $\alpha_{n+1} = \beta_{n-3} = 0$. The solution of the two

other equations is given by

$$
\begin{aligned}
\alpha_n \quad &= \quad -\frac{4\kappa^2 \,\Re\left[\hat{\beta}_{n-2}\right]}{(4\kappa^2-3)\left(1-\frac{1}{2\kappa}\right)} + \frac{6\kappa \,\Re\left[\hat{\beta}_{n-4}\right]}{(4\kappa^2-3)\left(1-\frac{3}{2\kappa}\right)} - \frac{4i\,\kappa^2\,\Im\left[\hat{\beta}_{n-2}\right]}{(4\kappa^2-3)\left(1+\frac{1}{2\kappa}\right)} - \\
&\qquad -\frac{6i\,\kappa\,\Im\left[\hat{\beta}_{n-4}\right]}{(4\kappa^2-3)\left(1+\frac{3}{2\kappa}\right)}, \\[2ex]
\alpha_{n+2} \quad &= \quad -\frac{4\kappa^2 \,\Re\left[\hat{\beta}_{n-4}\right]}{(4\kappa^2-3)\left(1-\frac{3}{2\kappa}\right)} + \frac{2\kappa \,\Re\left[\hat{\beta}_{n-2}\right]}{(4\kappa^2-3)\left(1-\frac{1}{2\kappa}\right)} - \frac{4i\,\kappa^2\,\Im\left[\hat{\beta}_{n-4}\right]}{(4\kappa^2-3)\left(1+\frac{3}{2\kappa}\right)} - \\
&\qquad -\frac{2i\,\kappa\,\Im\left[\hat{\beta}_{n-2}\right]}{(4\kappa^2-3)\left(1+\frac{1}{2\kappa}\right)},
\end{aligned}
$$

where

$$
\hat{\beta}_{n-2} \quad := \quad \beta_{n-2}\left(1-\frac{3}{4\kappa^2}\right),
$$

$$
\hat{\beta}_{n-4} \quad := \quad \beta_{n-4}\left(1-\frac{3}{4\kappa^2}\right).
$$

Finally, we obtained that all compatibility conditions are satisfied. Thus we have shown, that such set of complex numbers β_j exists, and the statement of the theorem is true for the case of even number of nodes.

Now we will complete the proof by considering the case when the number of nodes n is **odd**. We will omit some details which are similar to the even case. In the case of an odd number of nodes we need to keep the structure of the interpolation function (4.4) with two separate sums

$$
\begin{aligned}
f_n(t) \quad = \quad & \sum_{k=0,1}^{\frac{n-1}{2}} \left[a_{2k}\kappa\, t^{2k} + a_{2k}\kappa\, t^{-2k} + k\bar{a}_{2k}\, t^{-2k} - k\bar{a}_{2k}\, t^{-2k+4} \right] + \\
& + \sum_{k=1,2}^{\frac{n-1}{2}} \left[a_{2k-1}\kappa\, t^{2k-1} - a_k\kappa\, t^{-2k+1} + \frac{2k-1}{2}\bar{a}_{2k-1}\, t^{-2k+1} - \frac{2k-1}{2}\bar{a}_{2k-1}\, t^{-2k+5} \right].
\end{aligned}
$$

To simplify the above function we extract the term for $k=0$ from the first sum, collect

common terms and get

$$f_n(t) = 2a_0\kappa + \sum_{k}^{\frac{n-1}{2}} \Big[t^{-2k}(a_{2k}\kappa + k\,\bar{a}_{2k}) +$$

$$+ t^{-2k+1}\left(\frac{2k-1}{2}\bar{a}_{2k-1} - a_{2k-1}\kappa\right) - k\,\bar{a}_{2k}t^{-2k+4} -$$

$$- \frac{2k-1}{2}\bar{a}_{2k-1}t^{-2k+5} + a_{2k-1}\kappa\,t^{2k-1} + a_{2k}\kappa\,t^{2k} \Big].$$

The lowest degree is $-n+1$. Therefore, as in the previous case we multiply both sides of the interpolation problem by t^{n-1}, and we get the following equivalent interpolation problem

$$\sum_{l=0}^{2n-2} \alpha_l t_j^l = w_j,$$

for $j = 0, \ldots, n-1$.

Since the polynomial basis contains also shifted powers t^{n-2k+3} and t^{n-2k+4} the equations relating the new coefficients α_l with the original coefficients a_k will change with increasing n and take their general form for $n > 7$. We will consider only this case. The remaining three cases $n = 3$, $n = 5$, and $n = 7$ can be easily obtained directly from the interpolation problem and will not influence the generality of the proof.

Similar to the even case, for $n > 7$ we can get four groups of equations between α_k and a_k

$$\text{(I)} \quad \begin{cases} \alpha_{2j} = \kappa\,a_{n-1-2j} + \left(\dfrac{n-1}{2} - j\right)\bar{a}_{n-1-2j}, \\[3mm] \hspace{5cm} j = 0, 1, \\[3mm] \alpha_{2j+1} = \dfrac{n-2-2j}{2}\bar{a}_{n-2-2j} - \kappa\,a_{n-2-2j}, \end{cases}$$

$$\text{(II)} \quad \begin{cases} \alpha_{2j} = \kappa\,a_{n-1-2j} + \left(\dfrac{n-1}{2} - j\right)\bar{a}_{n-1-2j} - \left(\dfrac{n+3}{2} - j\right)a_{n+3-2j}, \\[3mm] \alpha_{2j+1} = \dfrac{n-2-2j}{2}\bar{a}_{n-2-2j} - \kappa\,a_{n-2-2j} - \dfrac{n+2-2j}{2}\bar{a}_{n+2-2j}, \\[2mm] \hspace{1cm} j = 2, \ldots, \frac{n-3}{2}, \end{cases}$$

$$\text{(III)} \quad \begin{cases} \alpha_{2j} = \left(\dfrac{n-1}{2} - j + 2\right)\kappa\,a_{2j-n+1} - \dfrac{n+3-2j}{2}\bar{a}_{n+3-2j}, \\[3mm] \alpha_{2j-1} = \kappa\,a_{2j-n+2} + \dfrac{2j-n-2}{2}\bar{a}_{n+2-2j}, \\[2mm] \hspace{1cm} j = \frac{n-1}{2}, \frac{n+1}{2}, \end{cases}$$

$$(4.18)$$

$$\text{(IV)} \quad \begin{cases} \alpha_{2j} &= \kappa\, a_{2j-n+1}, \\[2mm] \alpha_{2j-1} &= \kappa\, a_{2j-n+2}, \end{cases} \quad j = \tfrac{n+3}{2}, \dots, n-1. \tag{4.19}$$

Analogously to the even case, from equations (4.18)-(4.19) we get the explicit formulae for the coefficients a_k. From group (IV) we get the following equations for a_k for $k = 4, \dots, n-1$

$$\begin{cases} a_{2j-n+1} &= \dfrac{\alpha_{2j}}{\kappa}, \\[3mm] a_{2j-n+2} &= \dfrac{\alpha_{2j-1}}{\kappa}, \end{cases} \quad j = \dfrac{n+3}{2}, \dots, n-1.$$

Formulae for the remaining coefficients a_0, a_1, a_2, a_3 are completely the same as in the even case, and they are given by (4.10).

Applying the same ideas as in the case of even number of nodes we introduce some additional Hermite-type conditions (4.11). The remaining task is to prove the compatibility conditions for the case of an odd number of nodes. From the first group we get the following equations

$$\begin{cases} \alpha_{2j} - \alpha_{2n-2-2j} - \left(\dfrac{n-1}{2} - j\right)\dfrac{\bar{\alpha}_{2n-2-2j}}{\kappa} &= 0, \\[3mm] \alpha_{2j+1} + \alpha_{2n-3-2j} - (n-2j-2)\dfrac{\bar{\alpha}_{2n-3-2j}}{2\kappa} &= 0, \end{cases} \quad j = 0, 1.$$

The second group leads to the following $n-5$ equations:

$$\begin{cases} \alpha_{2j} - \alpha_{2n-2j-2} - \left(\dfrac{n-1}{2} - j\right)\dfrac{\bar{\alpha}_{2n-2-2j}}{\kappa} + \\[3mm] \quad + \left(\dfrac{n-1}{2} - j + 2\right)\dfrac{\bar{\alpha}_{2n-2(j-1)}}{\kappa} = 0, \quad j = 2, \dots, \dfrac{n-5}{2}, \\[4mm] \alpha_{2j+1} - \alpha_{2n-2j-3} - (n-2j-2)\dfrac{\bar{\alpha}_{2n-3-2j}}{2\kappa} + \\[3mm] \quad + (n-2j+2)\dfrac{\bar{\alpha}_{2n-2j+1}}{2\kappa} = 0, \quad j = 2, \dots, \dfrac{n-7}{2}, \\[4mm] \alpha_{n+2} + \dfrac{1}{2}\left[\dfrac{\bar{\alpha}_n}{\kappa} + \dfrac{3\alpha_{n+2}}{2\kappa^2}\right]\left(1 - \dfrac{3}{4\kappa^2}\right)^{-1} + \alpha_{n-4} + \dfrac{7\bar{\alpha}_{n+6}}{2\kappa} - \\[4mm] \quad - \dfrac{3\bar{\alpha}_{n+2}}{2\kappa} - \dfrac{3}{4\kappa}\left[\dfrac{\alpha_n}{\kappa} + \dfrac{3\bar{\alpha}_{n+2}}{2\kappa^2}\right]\left(1 - \dfrac{3}{4\kappa^2}\right)^{-1} = 0, \\[4mm] \alpha_{n-3} - \dfrac{\alpha_{n-3} + \alpha_{n+1}}{2} - \dfrac{3\bar{\alpha}_{n+5}}{2\kappa} - \dfrac{\bar{\alpha}_{n-3} + \bar{\alpha}_{n+1}}{2\kappa} - \dfrac{3\alpha_{n+5}}{2\kappa^2} + \dfrac{3\bar{\alpha}_{n+5}}{\kappa} = 0, \end{cases}$$

$$\begin{cases} \kappa \left[\dfrac{\alpha_n}{\kappa} + \dfrac{3\bar{\alpha}_{n+2}}{2\kappa^2} \right] \left(1 - \dfrac{3}{4\kappa^2} \right)^{-1} + \alpha_{n-2} + \dfrac{5\bar{\alpha}_{n+4}}{2\kappa} - \\[3mm] -\dfrac{1}{2} \left[\dfrac{\bar{\alpha}_n}{\kappa} + \dfrac{3\alpha_{n+2}}{2\kappa^2} \right] \left(1 - \dfrac{3}{4\kappa^2} \right)^{-1} = 0. \end{cases}$$

In a similar way as for the case of an even number of nodes it can be shown, that there exists a set of complex numbers β_j such that the compatibility conditions are satisfied and the statement of the theorem is true for the case of an odd number of nodes.

$\square$

The proved theorem plays a crucial role in the theory of convergence of the proposed method, which we will discuss in Chapter 5.

4.3   Construction of the shape functions

After constructing the general proof of the main interpolation theorem we can apply these results for practical calculations and construction of shape functions for finite element approximation. To perform that construction we consider the following interpolation problem

$$f_n(\varphi_k) = y_k, \tag{4.20}$$

where y_k are arbitrary complex numbers, $\varphi_k \in [-\pi, \pi]$ are interpolation nodes, for simplicity we assume, that they are equidistant

$$\varphi_{k+1} = \varphi_1 + \frac{2\pi k}{n-1}, \qquad k = 0, \ldots, n-1,$$

where n is total number of nodes on Γ_{AD}.

The right hand side in (4.20) can be associated with the unknown displacements $\mathrm{U}_1, \ldots, \mathrm{U}_n$ at the nodes on the joint interface Γ_{AD}, which are written in a complex form. Due to this fact, after solution of the interpolation problem we will get the unknown coefficients a_k as functions of the unknown displacements U_k. Since the coefficients a_k and $\bar{a}_k$ are connected by complex conjugation it's necessary to decompose them into real and imaginary parts

$$a_k = a_k^{(1)} + i\, a_k^{(2)}, \qquad \bar{a}_k = a_k^{(1)} - i\, a_k^{(2)}, \tag{4.21}$$

and we can do the same for the right hand side

$$\mathrm{U}_k = \mathrm{U}_k^{(1)} + i\, \mathrm{U}_k^{(2)}.$$

Finally, by applying Euler's formula we get the following representation of the interpolation function (4.2)

$$
\begin{aligned}
f_n(\varphi) \;=\; & \sum_{k=0,2}^{N_1} r_A^{\frac{k}{2}} \left[a_k^{(1)} \left(\cos\varphi \frac{k}{2} \left(\kappa + \frac{1}{2}(k+2) \right) - \frac{k}{2}\cos\left\{ \varphi\left(\frac{k}{2}-2\right)\right\}\right) - \right. \\
& - a_k^{(2)} \left(\sin\varphi \frac{k}{2} \left(\kappa + \frac{1}{2}(k-2) \right) - \frac{k}{2}\sin\left\{ \varphi\left(\frac{k}{2}-2\right)\right\}\right) + \\
& + i\, a_k^{(1)} \left(\sin\varphi \frac{k}{2} \left(\kappa - \frac{1}{2}(k+2) \right) + \frac{k}{2}\sin\left\{ \varphi\left(\frac{k}{2}-2\right)\right\}\right) + \\
& \left. + i\, a_k^{(2)} \left(\cos\varphi \frac{k}{2} \left(\kappa - \frac{1}{2}(k-2) \right) + \frac{k}{2}\cos\left\{ \varphi\left(\frac{k}{2}-2\right)\right\}\right) \right] + \\
& + \sum_{k=1,3}^{N_2} r_A^{\frac{k}{2}} \left[a_k^{(1)} \left(\cos\varphi \frac{k}{2} \left(\kappa + \frac{1}{2}(k-2) \right) - \frac{k}{2}\cos\left\{ \varphi\left(\frac{k}{2}-2\right)\right\}\right) - \right. \\
& - a_k^{(2)} \left(\sin\varphi \frac{k}{2} \left(\kappa + \frac{1}{2}(k+2) \right) - \frac{k}{2}\sin\left\{ \varphi\left(\frac{k}{2}-2\right)\right\}\right) + \\
& + i\, a_k^{(1)} \left(\sin\varphi \frac{k}{2} \left(\kappa - \frac{1}{2}(k-2) \right) + \frac{k}{2}\sin\left\{ \varphi\left(\frac{k}{2}-2\right)\right\}\right) + \\
& \left. + i\, a_k^{(2)} \left(\cos\varphi \frac{k}{2} \left(\kappa - \frac{1}{2}(k+2) \right) + \frac{k}{2}\cos\left\{ \varphi\left(\frac{k}{2}-2\right)\right\}\right) \right].
\end{aligned}
$$

Now the interpolation problem (4.20) can be written as

$$
f_n^{(1)}(\varphi_k) + i\, f_n^{(2)}(\varphi_k) = \mathrm{U}_k^{(1)} + i\,\mathrm{U}_k^{(2)},
$$

or in system notation

$$
\mathbf{F}\,\mathbf{A} = \mathbf{U}, \tag{4.22}
$$

where $\mathbf{F}$ is the interpolation matrix $\dim(\mathbf{F}) = 2n \times 2n$, $\mathbf{A}$ is the vector of unknown coefficients and $\mathbf{U}$ is the vector of unknown displacements.

After solving the system (4.22) and taking into account (4.21), we obtain the unknown coefficients a_k parametrically depending on the unknown displacement U_k, $k = 1, \ldots, n$,

and thus the displacement field in Ω_A can be written as follows

$$
\mathbf{u}(r, \varphi, \mathbf{U}_i) = \sum_{k=0,2,\ldots}^{N_1} r^{\frac{k}{2}} \left[a_k(\mathbf{U}_i) \left(\kappa\, e^{i\varphi\frac{k}{2}} + e^{-i\varphi\frac{k}{2}} \right) + \frac{k}{2} \bar{a}_k(\mathbf{U}_i) \left(e^{-i\varphi\frac{k}{2}} - e^{-i\varphi(\frac{k}{2}-2)} \right) \right] +
$$

$$
+ \sum_{k=1,3,\ldots}^{N_2} r^{\frac{k}{2}} \left[a_k(\mathbf{U}_i) \left(\kappa\, e^{i\varphi\frac{k}{2}} - e^{-i\varphi\frac{k}{2}} \right) + \frac{k}{2} \bar{a}_k(\mathbf{U}_i) \left(e^{-i\varphi\frac{k}{2}} - e^{-i\varphi(\frac{k}{2}-2)} \right) \right].
$$

$$(4.23)$$

To obtain shape functions N_i^A for the analytical element defined over Ω_A we substitute into (4.23) the following relations

$$
\mathbf{U}_k = \delta_{ki},
$$

where $k = 1, \ldots, n$, and $i = 1, \ldots, n$ is a number of the shape function N_i^A. Thus we obtain

$$
N_1^A \;\; := \;\; \mathbf{u}(r, \varphi, 1, 0, \ldots, 0),
$$

$$
N_2^A \;\; := \;\; \mathbf{u}(r, \varphi, 0, 1, \ldots, 0),
$$
$$
\vdots
$$
$$
N_n^A \;\; := \;\; \mathbf{u}(r, \varphi, 0, 0, \ldots, 1).
$$

Finally we obtain the following representation of the displacement in Ω_A

$$
\mathbf{u}(r, \varphi, \mathrm{U}_1, \ldots, \mathrm{U}_n) = \sum_{k=1}^{n} N_k^A(r, \varphi) \mathrm{U}_k
$$

The functions $N_k^A(r, \varphi)$ represent the basis for finite element approximation in the analytical element over Ω_A. These functions build the partition of unity for an arbitrary number of nodes. Fig. 4.3 and 4.4 illustrate these basis function at the interface Γ_{AD} in case of 5 and 9 equidistantly distributed nodes, respectively.
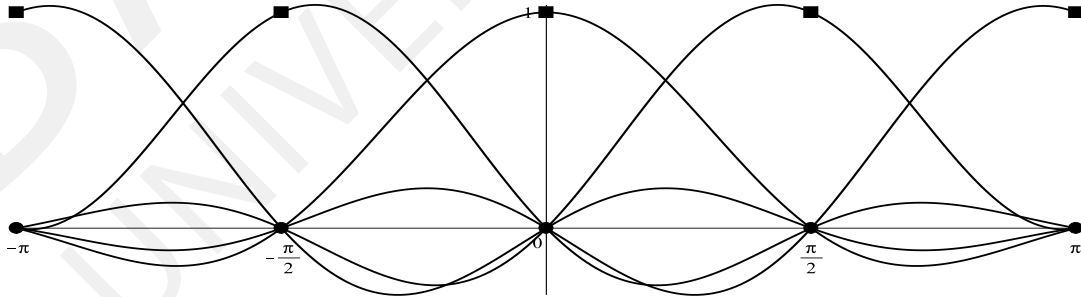

Figure 4.3: Shape functions of the analytical element at the interface Γ_{AD} for $n = 5$
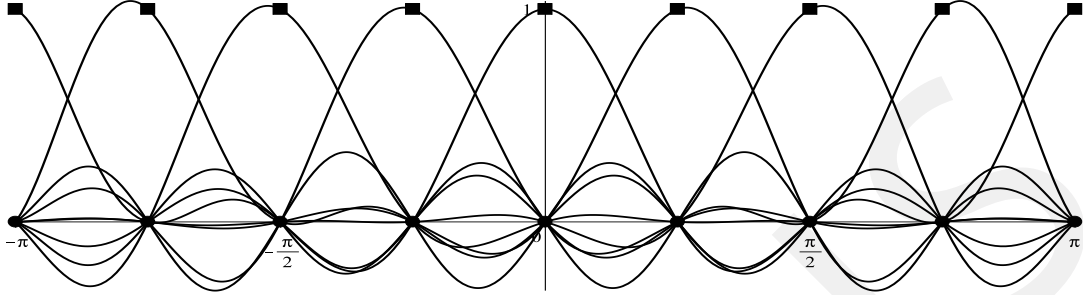
Figure 4.4: Shape functions of the analytical element at the interface Γ_{AD} for $n = 9$

As we can see from these figures the shape functions $N_k^A(r, \varphi)$ satisfy the interpolation conditions at the nodes, and the interpolation nodes are given by

$$\varphi_k = \left\{ -\pi, -\frac{\pi}{2}, 0, \frac{\pi}{2}, \pi \right\} \quad \text{for} \quad n = 5,$$

$$\varphi_k = \left\{ -\pi, -\frac{3\pi}{4}, -\frac{\pi}{2}, \frac{\pi}{4}, 0, \frac{\pi}{4}, \frac{\pi}{2}, \frac{3\pi}{4}, \pi \right\} \quad \text{for} \quad n = 9.$$

We remark that Fig. 4.3 and 4.4 show only two particular cases of nodes distribution, which we have chosen by practical reasons to obtain a symmetric mesh in a domain Ω. But according to the theorem 4.1 the corresponding interpolation problem is uniquely solvable for an arbitrary nodes distribution and for an arbitrary number of nodes n.

Fig. 4.5 shows the shape functions in the analytical element for five interpolation nodes. The shape functions are discontinuous during passing the crack faces, but they all are continuous at the crack tip. This fact completely coincides with expectations from the mechanical model, because displacement field (3.13) must be continuous in the whole domain, but passing the crack faces it has a jump. Thus the constructed shape functions can be used for finite element approximation. As we can see from the Fig. 4.5f these functions build a partition of unity in the whole domain Ω_{A}.

By choosing different numbers N_1 and N_2 we can play with the basis functions in (4.2) to obtain different combinations of polynomials and half integers, for instance Fig. 4.6 shows the case of $N_1 = 6$ and $N_2 = 0$, which corresponds to the classical polynomial interpolation.

Thus the proposed procedure for construction of the shape functions gives us a flexibility in applications. Depending from case to case one can choose to have more half-integer powers in a series, like for the case of small cracked bodies where we cannot be sure that a fracture can be represented only by a leading coefficient, or if we know that a considered problem has no singularity we can take only a polynomial part of the basis. In this case it is not an overkilling to work with the proposed method, because we can easily reduce computational costs by avoiding refinement.
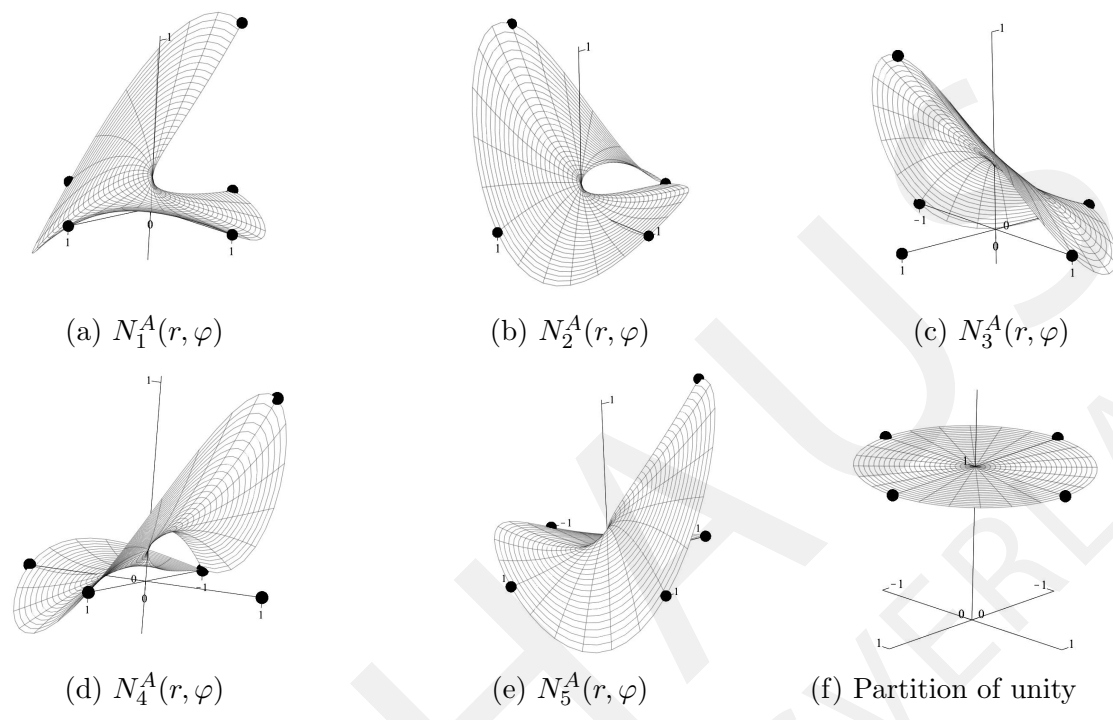
(a) $N_1^A(r, \varphi)$

(b) $N_2^A(r, \varphi)$

(c) $N_3^A(r, \varphi)$

(d) $N_4^A(r, \varphi)$

(e) $N_5^A(r, \varphi)$

(f) Partition of unity

Figure 4.5: Shape functions over the analytical element for $n = 5$

(a) $N_1^A(r, \varphi)$

(b) $N_2^A(r, \varphi)$

(c) $N_3^A(r, \varphi)$
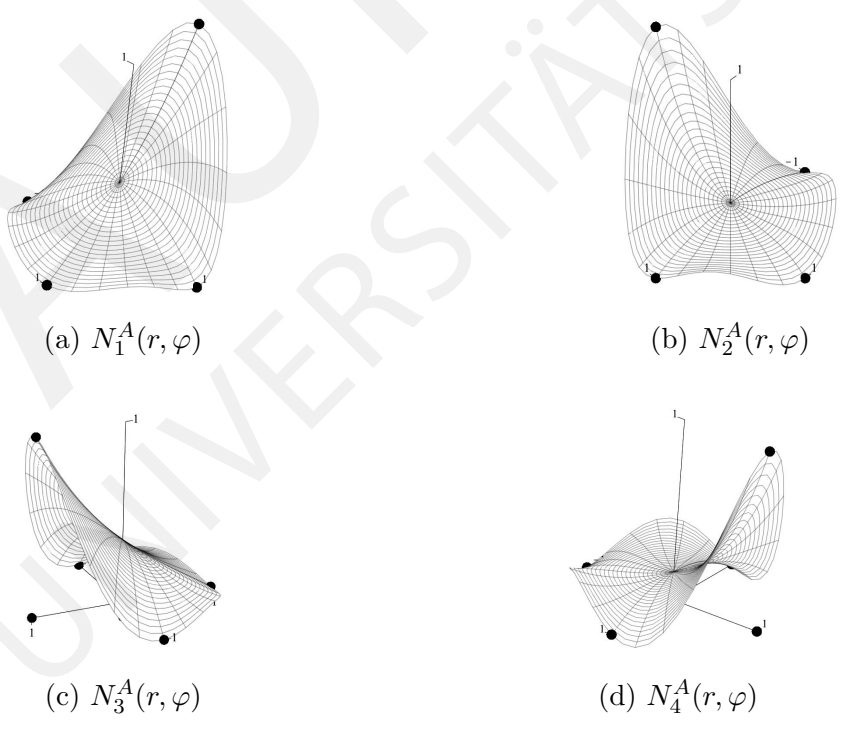
(d) $N_4^A(r, \varphi)$

Figure 4.6: Shape functions over the analytical element for $n = 4$, $N_1 = 6$, $N_2 = 0$

4.4 Geometrical properties of a triangulation with the special element

After solving the interpolation problem at the interface Γ_{AD} and constructing the basis functions for the analytical element, we can start with a construction of coupling elements. Coupling elements together with the analytical element and some CST elements will build a special element, which is introduced into a triangulation (4.1). Since we introduce new elements into finite element mesh we have to discuss their geometrical properties and criteria for a refinement. For our settings we can underline three possible strategies for a refinement:

(i) we refine a whole finite element mesh by a scaling factor without changing a number of coupling elements;

(ii) we refine a whole finite element mesh by a scaling factor with changing a number of coupling elements;

(iii) we fix the radius r_{A} of the analytical domain and increase a number of coupling elements, and refine the standard elements around.

In this section we present some ideas according to these strategies, particularly we will be more focused on the cases of increasing number of coupling elements. To control the size of the coupling element we will apply a classical criterion for checking a shape parameter.

4.4.1 Basic definitions

Following [Schumaker 2007] we will introduce at first some facts about triangles and their important properties. Let us consider three points v_1, v_2, v_3 in $\mathbb{R}^2$ not belonging to one line. Then the convex hull of these points form a triangle which we write as $T\colon = \langle v_1, v_2, v_3 \rangle$. We call the points $v_i\colon = (x_i, y_i), i = 1, 2, 3$ the vertices of T, and denote the three edges of T by $\langle v_1, v_2 \rangle$, $\langle v_2, v_3 \rangle$ and $\langle v_3, v_1 \rangle$. The area of T is given by

$$A_T = \frac{1}{2}\det(M),$$

where

$$M = \begin{pmatrix} 1 & 1 & 1 \\ x_1 & x_2 & x_3 \\ y_1 & y_2 & y_3 \end{pmatrix}.$$

The area of a triangle is positive if the vertices of T are listed in counterclockwise order, and it is negative in clockwise order.

We now introduce some ways to measure the size and shape of a triangle.

Definition 4.1. Given a triangle T, we write $|T|$ for the length of its longest edge, and ρ_T for the radius of the largest disk that can be inscribed in T. The center of this disk is called the **incenter** of T, and ρ_T is called the **inradius** of T. We call the ratio $\kappa_T := \dfrac{|T|}{\rho_T}$ the **shape parameter** of T.

For an equilateral triangle, $\kappa_{TE} = 2\sqrt{3}$. Any other triangle has a larger shape parameter. Another way to measure the shape of a triangle is in terms of its angles. Let θ_T be the smallest angle in T. The size of θ_T can be used to bound the shape parameter κ_T by the following lemma:

Lemma 4.1. *For any triangle T,*

$$\frac{1}{\tan\left(\dfrac{\theta_T}{2}\right)} \leq \kappa_T \leq \frac{2}{\tan\left(\dfrac{\theta_T}{2}\right)} \leq \frac{2}{\sin\left(\dfrac{\theta_T}{2}\right)}. \tag{4.24}$$

Proof. [Schumaker 2007] Let v be a vertex with angle θ_T, and let e be an attached edge. The line connecting the incenter of T to v must bisect the angle at that vertex. Thus, $\frac{\rho_T}{|e|} \leq \tan\left(\frac{\theta_T}{2}\right)$, which immediately implies the first inequality. The second inequality can be obtained by applying elementary trigonometry. $\qquad\square$

To avoid too small angles in the coupling elements we will use a simple condition to bound the shape parameter κ_T.

Definition 4.2. For any coupling element $\mathbb{T}$ the shape parameter $\kappa_{\mathbb{T}}$ must be not bigger than the doubled shape parameter of an equilateral triangle κ_{TE}, i.e

$$\kappa_{\mathbb{T}} \leq 2\,\kappa_{TE}. \tag{4.25}$$

If this condition fails, then we should change the geometrical parameters of the coupling element.

4.4.2 Geometrical parameters of the coupling element

To discuss some geometrical details of the construction of the triangulation, let us consider first only a part of the special element - one coupling element (see Fig. 4.7). Note that from point of view of the construction of basis functions for the coupling element, the structure of this element is much more complicated than just three vertices v_1, v_2, v_3 and part of a circle $\langle v_3, v_1 \rangle$. But this sophisticated construction will not influence the geometry of the coupling element and strategy for refinement.

To apply bounds (4.25) for $\kappa_{\mathbb{T}}$ of the coupling elements we should perform some simple geometrical calculations. Fig. 4.8 shows all geometrical quantities, which are needed for direct application of (4.25).
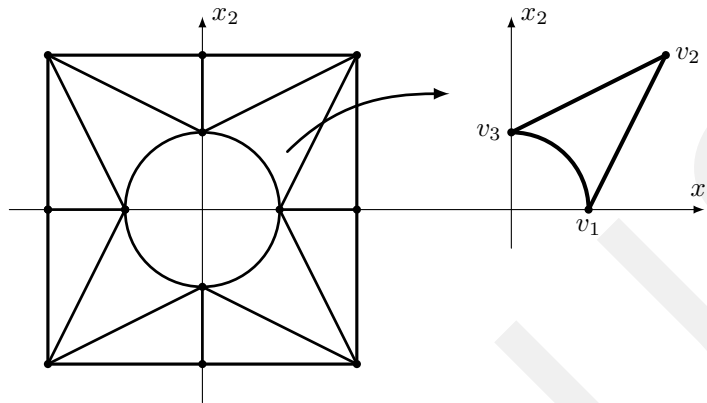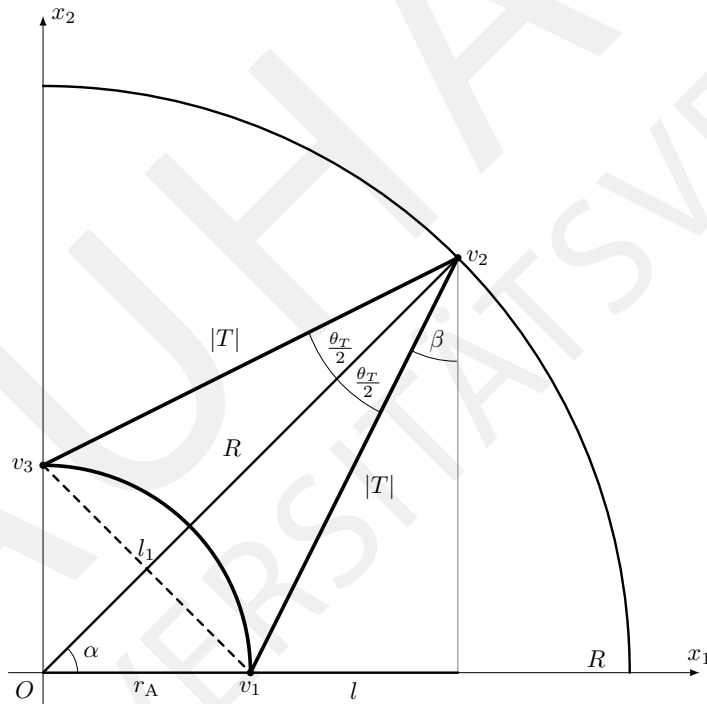
Figure 4.7: One coupling element $\mathbb{T}$

Figure 4.8: Geometry of a coupling element

By straight-forward calculations we have:

$$
\begin{aligned}
\rho_{\mathbb{T}} &= \sqrt{\frac{(p-|T|)^2(p-l_1)}{p}}, \\
|T| &= \sqrt{(r_A + l)^2 \tan^2 \alpha + l^2},
\end{aligned}
\tag{4.26}
$$

67

where

$$p = \frac{2\sqrt{(r_A + l)^2 \tan^2 \alpha + l^2} + 2\, r_A \sin \alpha}{2},$$

$$l_1 = 2\, r_A \sin \alpha,$$

and the angle α is defined as follows

$$\alpha = \frac{\varphi_3 - \varphi_1}{2}, \tag{4.27}$$

where φ_3 and φ_1 are angular coordinates of the vertices v_3 and v_1 respectively.

The smallest angle of the coupling element is given by

$$\frac{\theta_{\mathbb{T}}}{2} = \frac{\pi}{2} - \alpha - \arcsin\left(\frac{l}{\sqrt{(r_A + l)^2 \tan^2 \alpha + l^2}}\right), \tag{4.28}$$

and now we can apply the bounds (4.24) to control the quality of refinement of the special element, and r_A represents the radius of the analytical domain.

Finally, the radius R of the greater circle is defined by

$$R = \frac{r_A + l}{\cos \alpha}. \tag{4.29}$$

This radius represents the circle on which lay all vertices of the coupling elements not belonging to the curved edge $\langle v_3, v_1 \rangle$.

Remark 2. In fact, because of curved edge $\langle v_3, v_1 \rangle$ the inradius ρ_T of the coupling element is in reality smaller than calculated. But with increasing number of vertices at the circle we will have better and better approximation of the curved edge $\langle v_3, v_1 \rangle$ by straight edge $\langle v_3^*, v_1^* \rangle$ (dashed line in Fig. 4.8). And moreover, as we can see from Fig. 4.8, the smallest angle is always belonging to the vertex v_2, i.e. existing of a smaller inradius due to curved edge doesn't effect the smallest angle.

The formulae (4.26)-(4.29) give general geometrical properties of the coupling element. For a greater number of coupling elements these formulae must be applied separately for each of the elements. Now we are ready to discuss a refinement of the special element for different number of the coupling elements.

4.4.3 Local coordinates of the coupling element

The coupling elements $\mathbb{T}$ are described by local coordinates ξ and η. Due to the geometrical shape of the coupling element it is natural to introduce two coordinates: angular coordinate ξ and linear coordinate η. The angular coordinate ξ serves to get a continuous coupling through the whole interaction interface Γ_{AD}. The second coordinate η is used as a linear interpolator to connect the coupling elements with the CST-elements.

For purpose of calculations we need to relate the local coordinates ξ, η with Cartesian coordinates x_1, x_2. The goal of this subsection is to construct a mapping from Cartesian

coordinate system to non orthogonal coordinate system of the coupling element. In Fig. 4.9 we denote by x_1, x_2 the standard Cartesian coordinates, and by r, φ we denote the classical polar coordinates. The orientation of axes ξ, η is chosen to have a right-handed coordinate system.
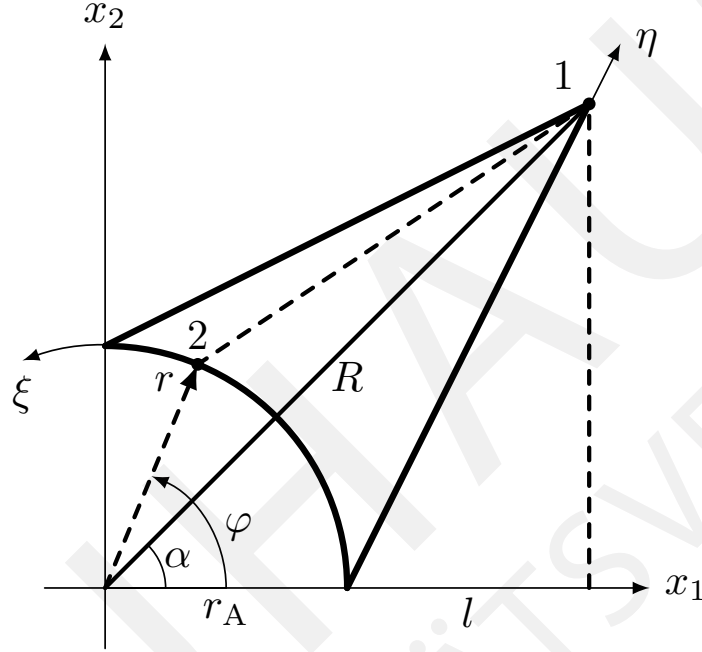

Figure 4.9: Local coordinates (ξ, η) of a coupling element $\mathbb{T}$

We start our construction with the classical definition of a line by two points

$$\frac{x_1 - x_1^{(1)}}{x_1^{(2)} - x_1^{(1)}} = \frac{x_2 - x_2^{(1)}}{x_2^{(2)} - x_2^{(1)}} \Rightarrow x_2 = \frac{x_1 - x_1^{(1)}}{x_1^{(2)} - x_1^{(1)}} \left(x_2^{(2)} - x_2^{(1)} \right) + x_2^{(1)}. \qquad (4.30)$$

By using this definition we will express the equation of a line between points 1 and 2 in Fig. 4.9. The coordinates $\left(x_1^{(1)}, x_2^{(1)} \right)$ of point 1 can be related with radius R and angle α as follows

$$\begin{cases} x_1^{(1)} = R \cos(k\,\alpha), \\ \\ x_2^{(1)} = R \sin(k\,\alpha), \end{cases} \qquad (4.31)$$

where R is given by

$$R = \frac{r_{\mathrm{A}} + l}{\cos \alpha},$$

and $k = 1, 3, \ldots, 2N - 1$ with N describing a number of coupling elements. The formulae (4.31) gives a general rule how to calculate the location of the vertex of the coupling element not belonging to the curved edge.

69

The coordinates $\left(x_1^{(2)}, x_2^{(2)}\right)$ of point 2 are given by definition of the polar coordinate system:

$$\begin{cases} x_1^{(2)} = r_\text{A} \cos \varphi, \\[2mm] x_2^{(2)} = r_\text{A} \sin \varphi, \end{cases} \tag{4.32}$$

in these formulae we took into account, that the radial coordinate r at the circle is equal to the radius of the analytical domain r_A.

After substitution formulae (4.31)-(4.32) into (4.30) we have

$$x_2^{(1)} = \frac{x_1 - R \cos(k\,\alpha)}{r_\text{A} \cos \varphi - R \cos(k\,\alpha)} \left(r_\text{A} \sin \varphi - R \sin(k\,\alpha)\right) + R \sin(k\,\alpha),$$

$$x_1 \in [r_\text{A} \cos \varphi, R \cos(k\,\alpha)].$$

The coordinate $\eta \in [0,1]$ can be related with Cartesian coordinate x_1 by linear mapping with conditions $x_1(0) = r_\text{A} \cos \varphi$ and $x_1(1) = R \cos(k\,\alpha)$ as follows

$$x_1(\eta) = r_\text{A} \cos \varphi + (R \cos(k\,\alpha) - r_\text{A} \cos \varphi)\eta.$$

Now we can replace the angular coordinate φ by ξ. And finally we have the following mapping between Cartesian coordinates and coordinates of the coupling element

$$\begin{cases} x_1 = r_\text{A} \cos \xi + (R \cos(k\,\alpha) - r_\text{A} \cos \xi)\eta, & \eta \in [0,1], \\[3mm] x_2 = \dfrac{x_1 - R \cos(k\,\alpha)}{r_\text{A} \cos \xi - R \cos(k\,\alpha)}(r_\text{A} \sin \xi - R \sin(k\,\alpha)) + R \sin(k\,\alpha), & \xi \in [-\pi, \pi]. \end{cases} \tag{4.33}$$

The inverse transformation can be explicitly calculated from above relations.

4.4.4 Global refinement with a special element

In this section we consider a way how to refine a triangulation with a special element in a case of an increasing number of coupling elements. In all refinements we will use equidistant distribution of vertices at the interface Γ_AD to preserve the symmetry of the triangulation. Without loss of generality for all examples we let $r_\text{A} = 1$. Since we are considering a fixed radius r_A, there are only two parameters remain which will influence a shape of triangulation: the length l and the angle α. The angle can be expressed in terms on number of nodes n on the arc $[0, \frac{\pi}{2}]$, as follows

$$\alpha = \frac{\pi}{4(n+1)},$$

this formula comes from the fact, that we always have the nodes at $\varphi = 0$ and $\varphi = \frac{\pi}{2}$, and from the definition of angle α according to Fig. 4.8.

To start an investigation of triangulation, let us use the length $l = r_A$, and this relation can be changed if condition (4.25) fails. According to formulae (4.26)-(4.29) the geometrical parameters for $n = 0$ are

$$
\begin{aligned}
\alpha &= \frac{\pi}{4} & l_1 &= \sqrt{2} \\[2mm]
|T| &= \sqrt{5} & R &= 2\sqrt{2} \\[2mm]
\rho_{\mathbb{T}} &= \frac{3}{2\sqrt{5} + \sqrt{2}} & \kappa_{\mathbb{T}} &= \frac{\sqrt{5}}{3}(2\sqrt{5} + \sqrt{2}) \approx 4.3874 \\[2mm]
\frac{\theta_{\mathbb{T}}}{2} &= \frac{\pi}{4} - \arcsin\left(\frac{\sqrt{5}}{5}\right) \approx 18.435°
\end{aligned} \tag{4.34}
$$

and condition (4.25) is satisfied

$$
\kappa_{\mathbb{T}} \le 4\sqrt{3} \approx 6.9282,
$$

and the triangulation (Fig. 4.10) with such geometrical parameters can be applied for calculation. The total number of elements in the special element in such triangulation is 13: 1 analytical element, 4 coupling elements and 8 CST.

Let us increase the number of nodes on the circle and consider now $n = 1$. The geometrical parameters of such triangulation are

$$
\begin{aligned}
\alpha &= \frac{\pi}{8} & l_1 &= 2\sin\left(\frac{\pi}{8}\right) \\[2mm]
|T| &= \sqrt{4\tan\left(\frac{\pi}{8}\right)^2 + 1} & R &= \frac{2}{\cos\left(\frac{\pi}{8}\right)} \\[2mm]
\rho_{\mathbb{T}} &\approx 0.2824 & \kappa_{\mathbb{T}} &\approx 4.5975 \\[2mm]
\frac{\theta_{\mathbb{T}}}{2} &\approx 17.1392°
\end{aligned} \tag{4.35}
$$

and condition (4.25) is satisfied

$$
\kappa_{\mathbb{T}} \le 4\sqrt{3} \approx 6.9282,
$$

and the triangulation (Fig. 4.11) with such geometrical parameters can be applied for calculation. The total number of elements in the special element in such triangulation is 22: 1 analytical element, 8 coupling elements and 13 CST. As we can see from Fig. 4.11 only the special element and the first layer of ordinary triangles around the special element must be handled with special refinement. The rest part of the triangulation can be treated as usual.
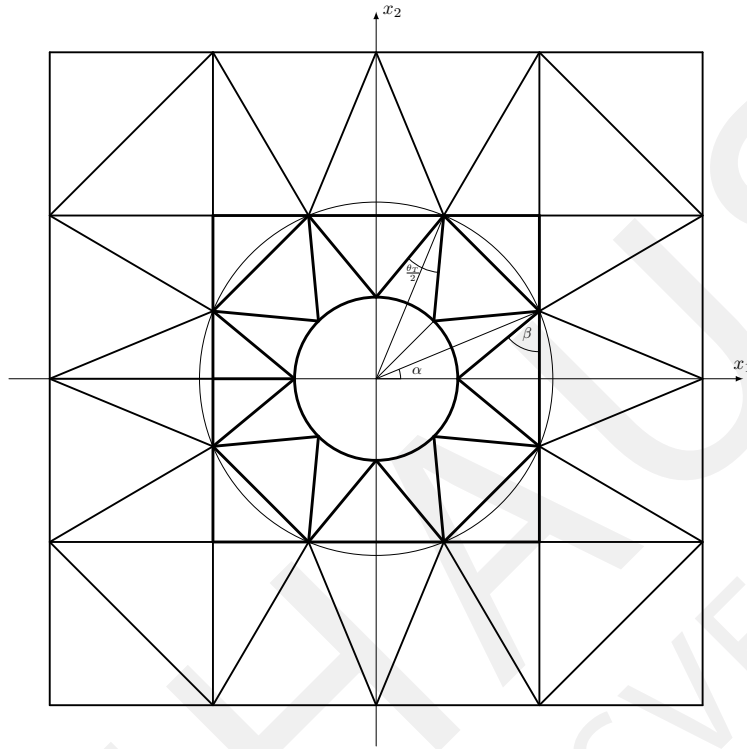
Figure 4.10: Four coupling elements

After adding one more node, i.e. now $n = 2$, we have

$$
\begin{aligned}
\alpha &= \frac{\pi}{12} & l_1 &= 2\sin\left(\frac{\pi}{12}\right) \\[2mm]
|T| &= \sqrt{4\tan\left(\frac{\pi}{12}\right)^2 + 1} & R &= \frac{2}{\cos\left(\frac{\pi}{12}\right)} \\[2mm]
\rho_{\mathbb{T}} &\approx 0.2052 & \kappa_{\mathbb{T}} &\approx 5.5293 \\[2mm]
\frac{\theta_{\mathbb{T}}}{2} &\approx 13.1867^\circ
\end{aligned}
\tag{4.36}
$$

and condition (4.25) is satisfied

$$
\kappa_{\mathbb{T}} \leq 4\sqrt{3} \approx 6.9282,
$$

and the triangulation (Fig. 4.12) with such geometrical parameters can be applied for calculation. The total number of elements in the special element in such triangulation is 34: 1 analytical element, 12 coupling elements and 21 CST. By increasing a number of coupling elements, like in Fig. 4.12, we can follow to two strategies:

- perform a refinement of the triangulation in the bigger area around the special element;

72

Figure 4.11: Eight coupling elements

- perform a refinement only in few normal triangles and come to certain "uniform size" of triangles;

In this study we will follow the second strategy.

After adding one more node, i.e. now $n = 3$, we have

$$
\begin{array}{rclcrcl}
\alpha & = & \dfrac{\pi}{16} & & l_1 & = & 2\sin\left(\dfrac{\pi}{16}\right) \\[3mm]
|T| & = & \sqrt{4\tan\left(\dfrac{\pi}{16}\right)^2 + 1} & R & = & \dfrac{2}{\cos\left(\frac{\pi}{16}\right)} \\[3mm]
\rho_{\mathbb{T}} & \approx & 0.1624 & & \kappa_{\mathbb{T}} & \approx & 6.6263 \\[3mm]
\dfrac{\theta_{\mathbb{T}}}{2} & \approx & 10.4438° & &
\end{array}
\tag{4.37}
$$

and condition (4.25) is satisfied

$$
\kappa_{\mathbb{T}} \le 4\sqrt{3} \approx 6.9282,
$$

and the triangulation (Fig. 4.13) with such geometrical parameters can be applied for calculation. The total number of elements in the special element in such triangulation is 46: 1 analytical element, 16 coupling elements and 29 CST.

73
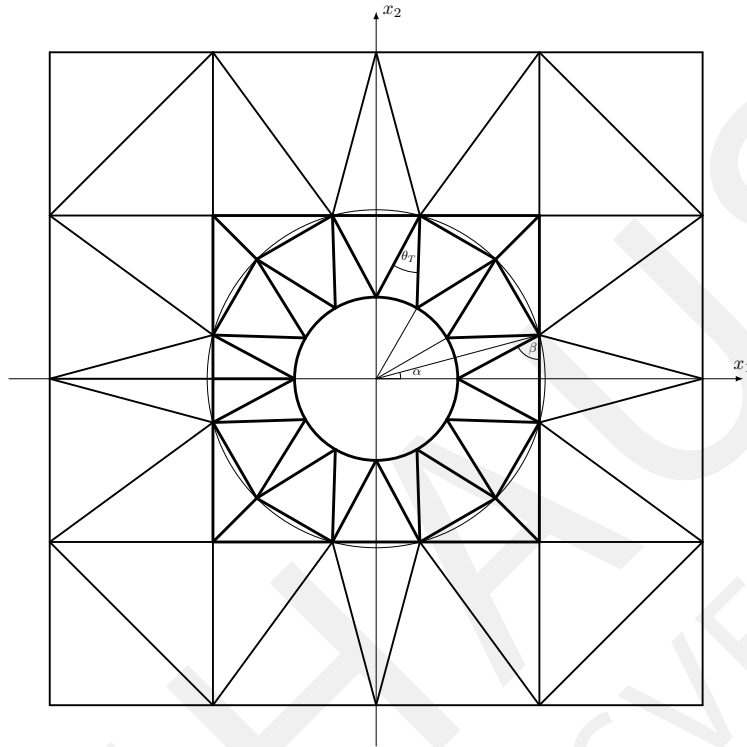
Figure 4.12: Twelve coupling elements

For $n = 4$, we have

$$
\begin{aligned}
\alpha &= \frac{\pi}{20} & l_1 &= 2\sin\left(\frac{\pi}{20}\right) \\[2mm]
|T| &= \sqrt{4\tan\left(\frac{\pi}{20}\right)^2 + 1} & R &= \frac{2}{\cos\left(\frac{\pi}{20}\right)} \\[2mm]
\rho_{\mathbb{T}} &\approx 0.1346 & \kappa_{\mathbb{T}} &\approx 7.7926 \\[2mm]
\frac{\theta_{\mathbb{T}}}{2} &\approx 8.5765°
\end{aligned}
\tag{4.38}
$$

and now condition (4.25) fails

$$
\kappa_T > 4\sqrt{3} \approx 6.9282,
$$

and the triangulation with such geometrical parameters cannot be applied for calculation. To overcome this problem we will change the length l. For the next calculations we take

74
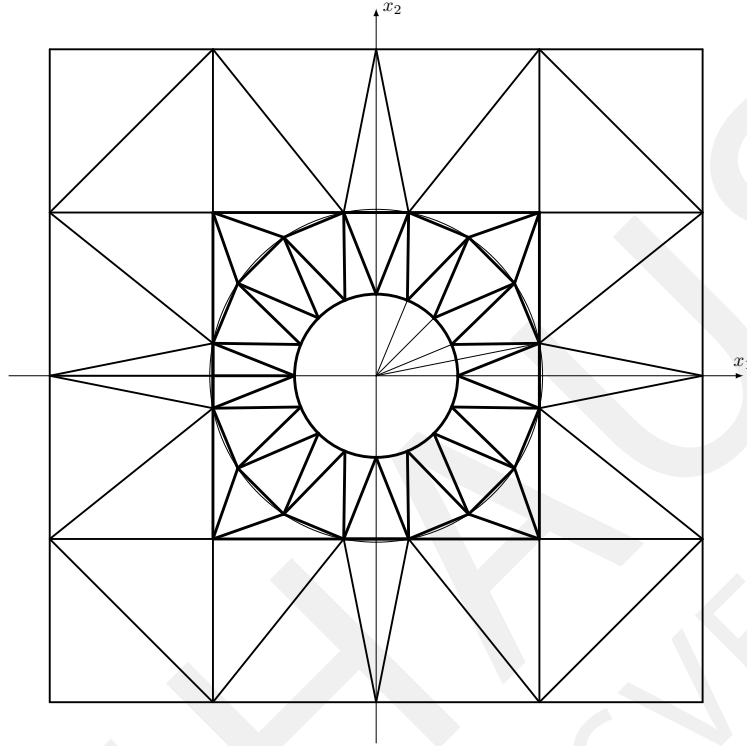
Figure 4.13: Sixteen coupling elements

$l = \frac{1}{2} r_{\mathrm{A}}$, and now for $n = 4$, we have

$$
\begin{aligned}
\alpha &= \frac{\pi}{20} & l_1 &= 2\sin\left(\frac{\pi}{20}\right) \\[2mm]
|T| &= \sqrt{9\tan\left(\frac{\pi}{20}\right)^2 + 1} & R &= \frac{3}{2\cos\left(\frac{\pi}{20}\right)} \\[2mm]
\rho_{\mathbb{T}} &\approx 0.1169 & \kappa_{\mathbb{T}} &\approx 4.7315 \\[2mm]
\frac{\theta_{\mathbb{T}}}{2} &\approx 16.4148° &&
\end{aligned}
\tag{4.39}
$$

and condition (4.25) is satisfied now

$$
\kappa_{\mathbb{T}} \le 4\sqrt{3} \approx 6.9282,
$$

and the triangulation (Fig. 4.14) with such geometrical parameters can be applied for calculation. The total number of elements in the special element in such triangulation is 79: 1 analytical element, 20 coupling elements and 58 CST.

Additional nodes at the boundary of the special element (bold square in Fig. 4.14) are placed equidistantly with step size equal to r_{A}, and can be easily calculated.
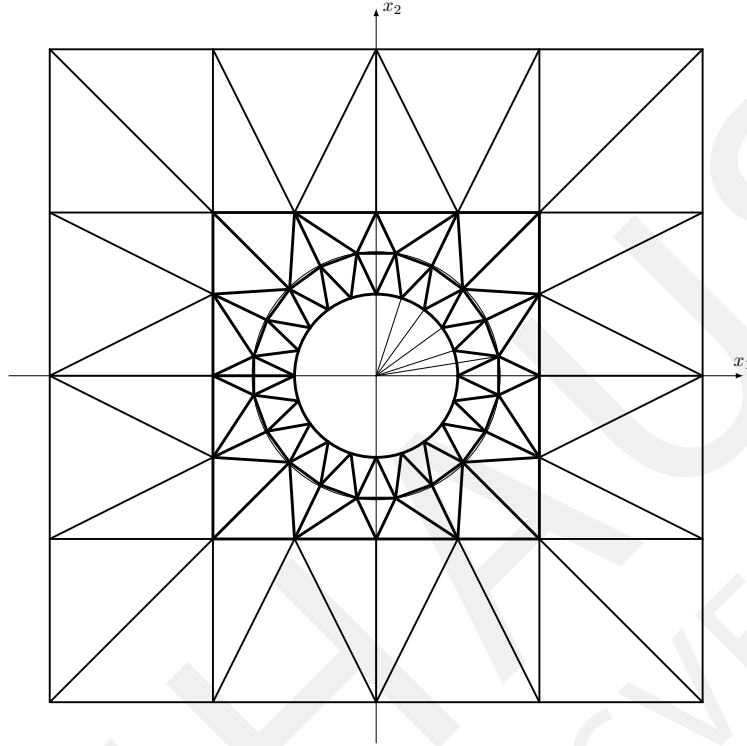
75

Figure 4.14: Twenty coupling elements

For $n = 5$, we have

$$
\begin{aligned}
\alpha &= \frac{\pi}{24} & l_1 &= 2\sin\left(\frac{\pi}{24}\right) \\[2mm]
|T| &= \sqrt{9\tan\left(\frac{\pi}{24}\right)^2 + 1} & R &= \frac{3}{2\cos\left(\frac{\pi}{24}\right)} \\[2mm]
\rho_{\mathbb{T}} &\approx 0.1018 & \kappa_{\mathbb{T}} &\approx 5.2765 \\[2mm]
\frac{\theta_{\mathbb{T}}}{2} &\approx 14.0519°
\end{aligned}
\tag{4.40}
$$

and condition (4.25) is satisfied

$$
\kappa_{\mathbb{T}} \le 4\sqrt{3} \approx 6.9282,
$$

and the triangulation (Fig. 4.15) with such geometrical parameters can be applied for calculation. The total number of elements in the special element in such triangulation is 107: 1 analytical element, 24 coupling elements and 82 CST.

Additional nodes at the boundary of the special element (bold square in Fig. 4.15) are placed with step size related to r_A. For instance, the upper bound of the special element has additional nodes at: $-r_A, -\frac{r_A}{2}, 0, \frac{r_A}{2}, r_A$ and vertical coordinate is taken equal $2\,r_A$.
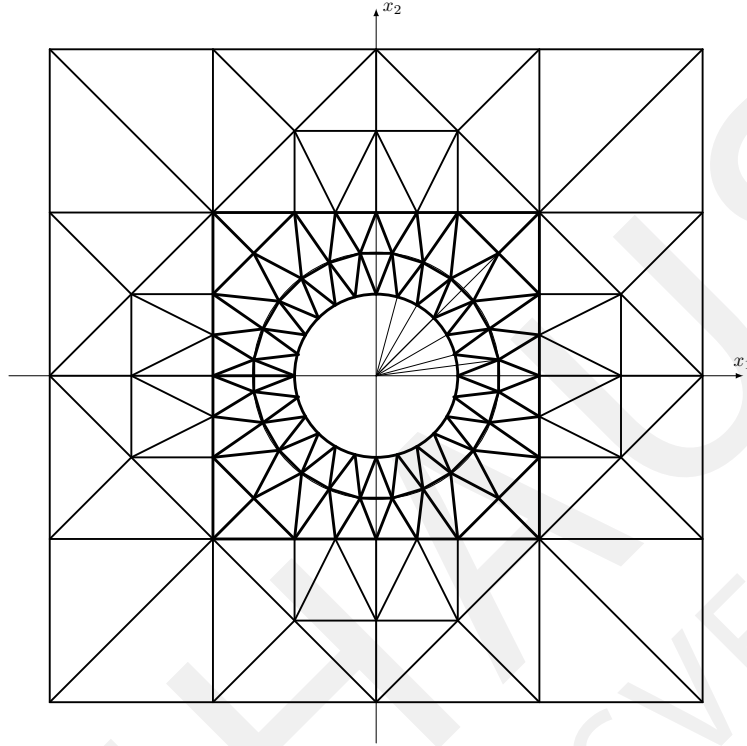
Figure 4.15: Twenty four coupling elements

For $n = 6$, we have

$$
\begin{aligned}
\alpha &= \frac{\pi}{28} & l_1 &= 2\sin\left(\frac{\pi}{28}\right) \\
|T| &= \frac{1}{2}\sqrt{9\tan\left(\frac{\pi}{28}\right)^2 + 1} & R &= \frac{3}{2\cos\left(\frac{\pi}{28}\right)} \\
\rho_{\mathbb{T}} &\approx 0.0903 & \kappa_{\mathbb{T}} &\approx 5.8470 \\
\frac{\theta_{\mathbb{T}}}{2} &\approx 14.0519°
\end{aligned}
\tag{4.41}
$$

and condition (4.25) is satisfied

$$
\kappa_{\mathbb{T}} \leq 4\sqrt{3} \approx 6.9282,
$$

and the triangulation (Fig. 4.16) with such geometrical parameters can be applied for calculation. The total number of elements in the special element in such triangulation is 119: 1 analytical element, 28 coupling elements and 89 CST.

Additional nodes at the boundary of the special element (bold square in Fig. 4.16) are placed equidistantly with step size related to $\frac{r_A}{2}$.
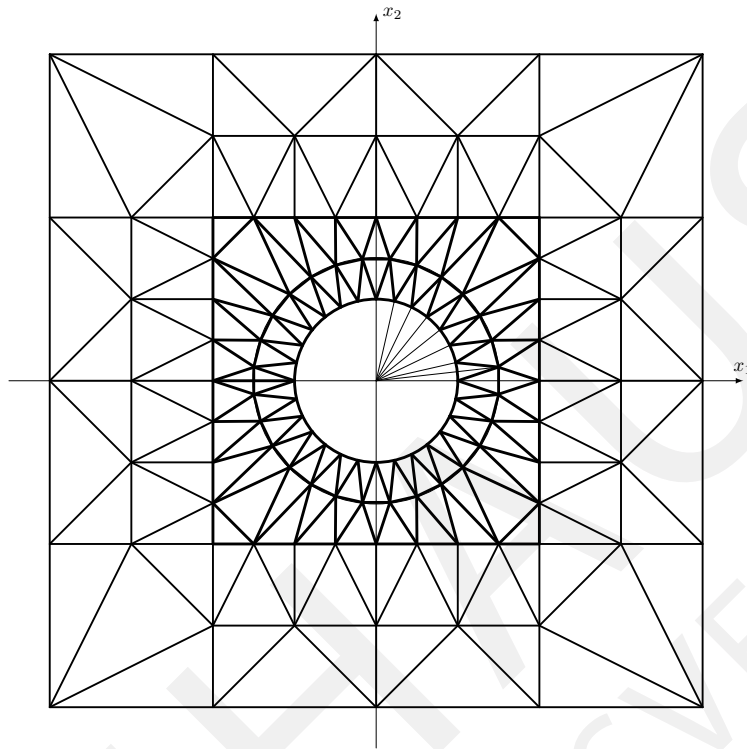
77

Figure 4.16: Twenty eight coupling elements

Fig. 4.17 shows an increase of the number of elements in the special element with respect to a total number of nodes at the circle.
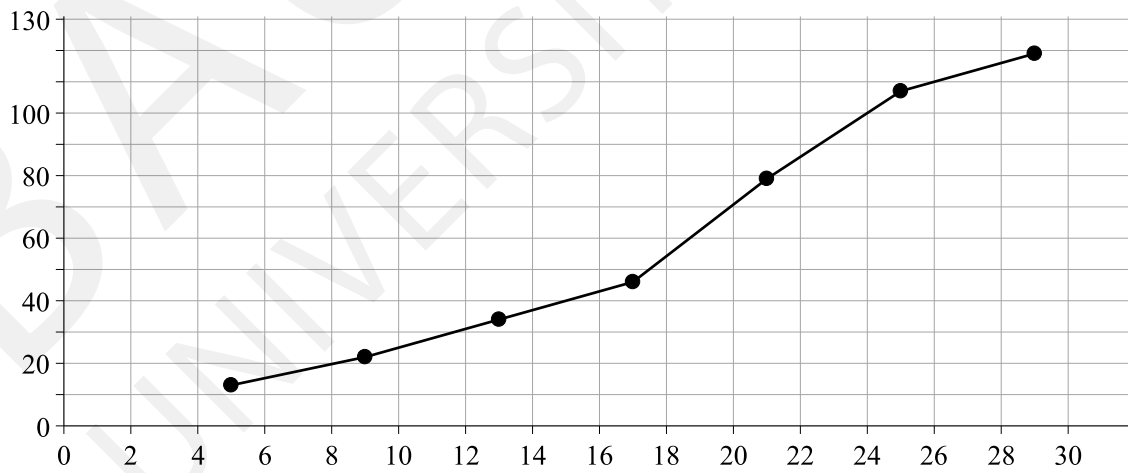

Figure 4.17: Increase of elements in the special element

As we can see, the increase goes close to linear law: for six times more nodes we have almost ten times more elements. Of course, computational costs for the special element are usually higher than for ordinary finite elements, but these computations must be done

78

only in one element and not for all problems we should use very dense triangulation in the special element. Additionally, all of the refinements which we have shown in this section can be used together with scaling of the whole triangulation.

Finally we introduce the following inequalities

$$\left[\tan\left(\frac{\pi}{2} - \frac{\pi}{4(n+1)} - \arcsin\left(\frac{l}{\sqrt{(r_A + l)^2 \tan^2 \frac{\pi}{4(n+1)} + l^2}} \right) \right) \right]^{-1} \le \kappa_{\mathbb{T}},$$

$$\kappa_{\mathbb{T}} \le 2 \left[\tan\left(\frac{\pi}{2} - \frac{\pi}{4(n+1)} - \arcsin\left(\frac{l}{\sqrt{(r_A + l)^2 \tan^2 \frac{\pi}{4(n+1)} + l^2}} \right) \right) \right]^{-1},$$

where the bounds for the shape parameter $\kappa_{\mathbb{T}}$ are expressed in terms of the number of nodes n, the radius r_A, and length l.

4.4.5 Numbering of vertices

Another important aspect of the finite element procedure is a numbering of nodes in a finite element mesh. The goal of numbering is to obtain elements with smallest possible difference in numbers of its vertices. Such a numbering will lead to a smaller band in a global stiffness matrix. Another important problem which is related to the numbering is the condition number of the global stiffness matrix, which is on of the key aspect of stability. By choosing different strategies for the numbering one can obtain very different condition numbers.

At the moment we are interested in studying the quality of the proposed method, but not in the smallest possible computational costs. Therefore we consider the following strategy for numbering:

1. we create a triangulation for a cracked domain with a special element located at the origin of a coordinate system;

2. we start our numbering from the special element.

For normal triangles T_j we go around its boundary in counterclockwise order starting from one arbitrary vertex. After we get the list with vertices for each triangle in the triangulation. The lists for analytical elements and for coupling elements have a more complicated structure.

To illustrate this strategy let us consider the triangulation with eight coupling elements shown in Fig. 4.11. We start the numbering procedure with the vertex at $(r_A, 0)$, and we continue counterclockwise.

In this example we continue with counterclockwise numbering even after the special element. Such strategy gives advantages in the structure of a global stiffness matrix, but it works, of course, only for rectangular domains. For more complicated shape we will use
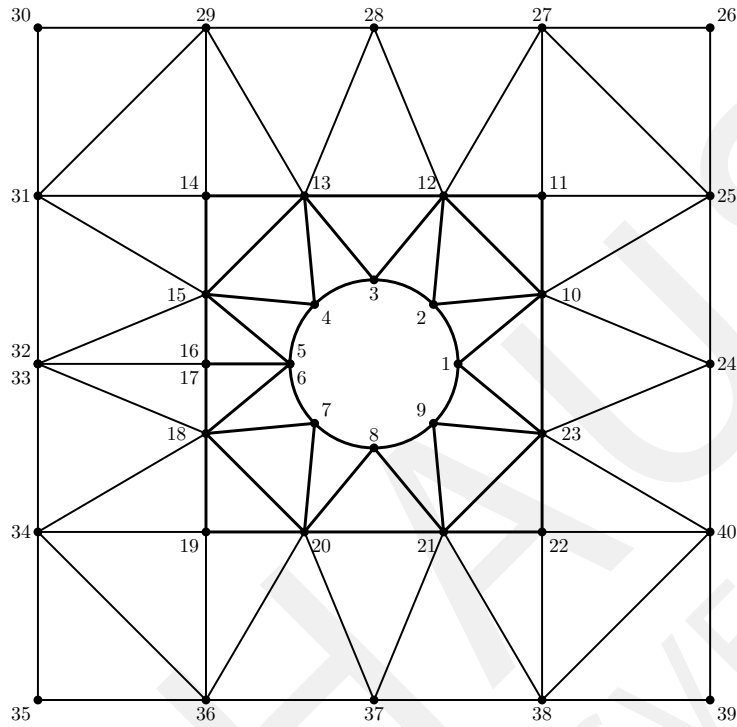
Figure 4.18: An example of numbering of a triangulation with the special element

counterclockwise numbering in the special element, and after we will continue with the left lower node of a body (Fig. 4.19). In this case we have some disturbance in structure of the matrix, but it will occur only in connection with few triangles around the special element.

According to Fig. 4.19 we can create a list with triangles and their vertices for the special element (see the left Table 4.1). A list for all other normal triangles can be done in the same manner, but starting from the left lower corner. Additionally to the list of normal triangles we should create and store the list of coupling and analytical elements (see the right Table 4.1). A big number of vertices belonging to each of special and analytical elements are explained by a complicated construction of the interpolation functions for these elements. For our consideration here it is important to pay attention to this fact and store separately a list for normal triangles and for the modified elements, or with some addition markers for the modified elements.

Remark 3. The strategy with numbering starting from the special element fails in a case of several special elements in a triangulation. In that case one can start from a arbitrary vertex in a triangulation (typically a lower left node of a body), but numbering of each special element must be done continuously to avoid disturbance in a global stiffness matrix. We illustrate this case in Fig. 4.20, but we will not go into details.
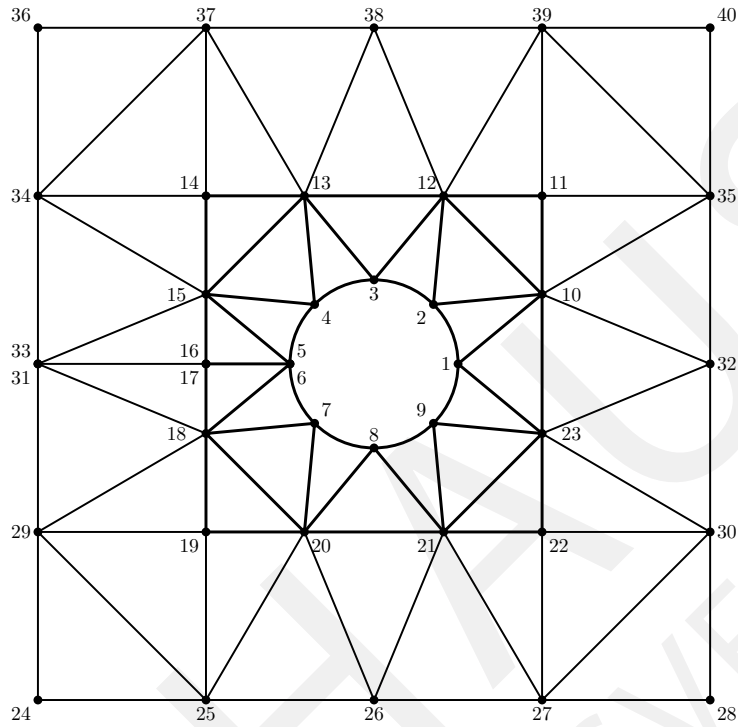
80

Figure 4.19: Another example of numbering of a triangulation with the special element

T_i	**Vertices**
1	1,23,10
2	2,10,12
3	10,11,12
4	3,12,13
5	4,13,15
6	13,14,15
7	5,15,16
8	6,17,18
9	7,18,20
10	18,19,20
11	8,20,21
12	9,21,23
13	21,22,23

T	**Vertices**
$\mathbb{A}$	1,2,3,4,5,6,7,8,9
$\mathbb{T}_1$	1,2,3,4,5,6,7,8,9,10
$\mathbb{T}_2$	1,2,3,4,5,6,7,8,9,12
$\mathbb{T}_3$	1,2,3,4,5,6,7,8,9,13
$\mathbb{T}_4$	1,2,3,4,5,6,7,8,9,15
$\mathbb{T}_5$	1,2,3,4,5,6,7,8,9,18
$\mathbb{T}_6$	1,2,3,4,5,6,7,8,9,20
$\mathbb{T}_7$	1,2,3,4,5,6,7,8,9,21
$\mathbb{T}_8$	1,2,3,4,5,6,7,8,9,23

Table 4.1: List for the special element: normal triangles (left), coupling and analytical elements (right)
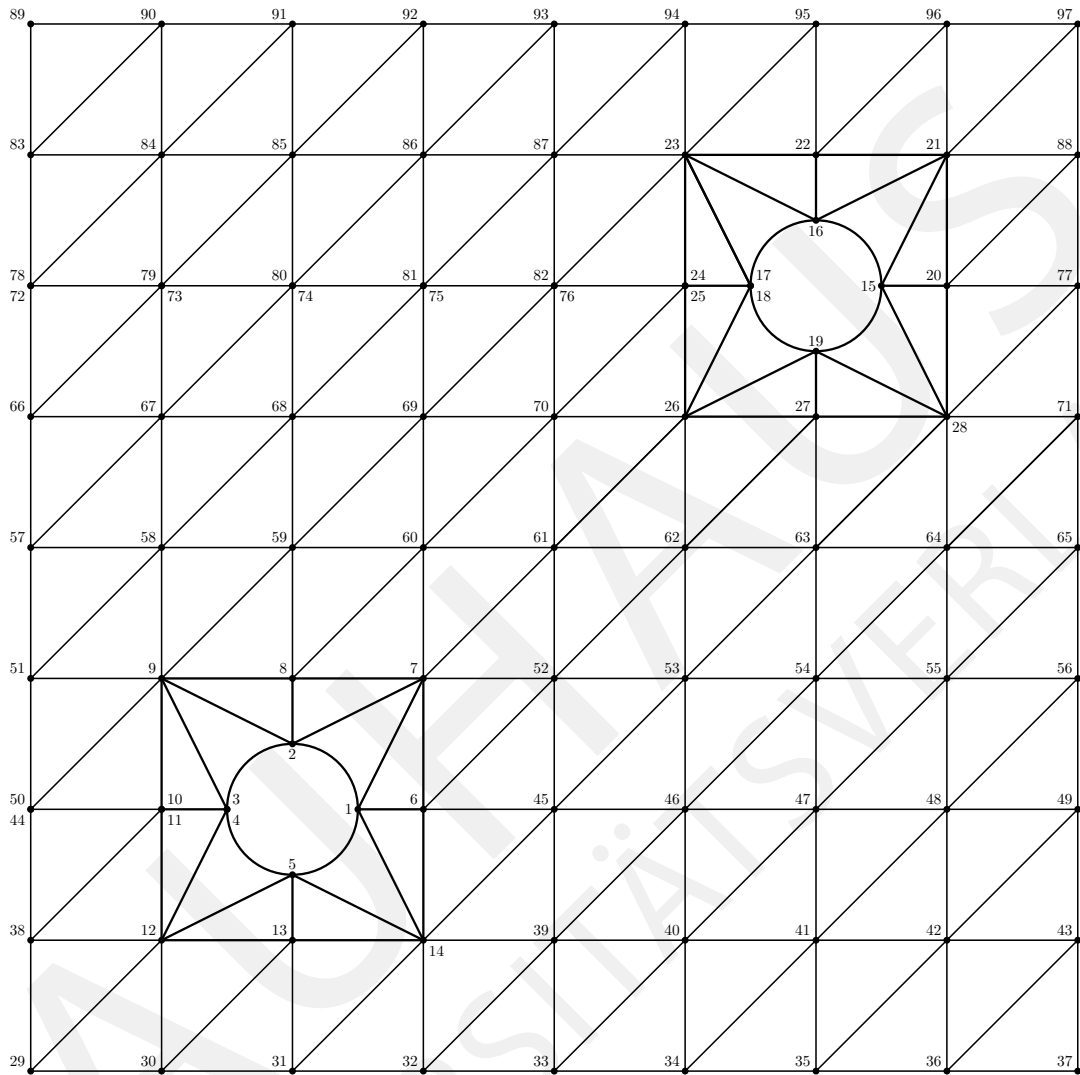
81

Figure 4.20: Example of numbering with several special elements

4.4.6 Algorithm for triangulation

Now we can shortly summarise our considerations from this section as a draft of an algorithm for construction of a triangulation with the special element:

1. define radius r_A;

2. decide how many coupling element we want to have;

3. make an assumption about the length l;

4. check the shape parameter $\kappa_{\mathbb{T}}$;

5. calculate coordinates of vertices in the special element;

6. perform the numbering of the special element;

7. create a triangulation of the rest part of domain.

4.5 Shape functions for coupling elements

The construction of shape functions for coupling elements is realised in several steps, at first we restrict the shape functions of an analytical element to the interface Γ_{AD} and replacing the coordinate φ by the coordinate ξ, i.e. we have

$$
\begin{aligned}
\hat{N}_1^{\mathbb{T}} &:= N_1^A(r_{\mathrm{A}}, \xi), \\
\hat{N}_2^{\mathbb{T}} &:= N_2^A(r_{\mathrm{A}}, \xi), \\
&\vdots \\
\hat{N}_n^{\mathbb{T}} &:= N_n^A(r_{\mathrm{A}}, \xi).
\end{aligned}
$$

In the second step we multiply each of the functions $\hat{N}_k^{\mathbb{T}}, k = 1, \ldots, n$ by a linear interpolator $\eta \in [0, 1]$ as we have introduced it previously, and add one more linear function to a basis. Finally we obtain

$$
\begin{aligned}
N_1^{\mathbb{T}} &:= N_1^A(r_{\mathrm{A}}, \xi)(1 - \eta), \\
N_2^{\mathbb{T}} &:= N_2^A(r_{\mathrm{A}}, \xi)(1 - \eta), \\
&\vdots \\
N_n^{\mathbb{T}} &:= N_n^A(r_{\mathrm{A}}, \xi)(1 - \eta), \\
N_{n+1}^{\mathbb{T}} &:= \eta.
\end{aligned}
$$

The obtained shape functions are presented in Fig. 4.21 for the case of five nodes at the interface Γ_{AD}. As we can see by the proposed construction we obtain the desired continuity, since the shape functions are continuous through the whole interaction interface between the analytical and the finite element solution, and they are linearly connected to the standard elements.

Fig. 4.21g shows that the constructed shape functions built a partition of unity over the coupling elements. Thus the proposed procedure for coupling assures the desired continuity, and the constructed shape functions $N_k^A, k = 1, \ldots, n$ and $N_i^{\mathbb{T}}, i = 1, \ldots, n+1$ satisfy all the requirements for shape functions in the finite element method.

Remark 4. We would like to underline, that the proposed construction is only an example of possible ways how to obtain a global C^0 continuity of solution. A proposed scheme for the refinement is a possible idea which can be easily realised in practice, but of course in real application one can find out that we need a more elegant method for the refinement. Moreover, by this construction it's possible to ask for higher order continuity between two solutions, but this task is out of scope of this thesis.
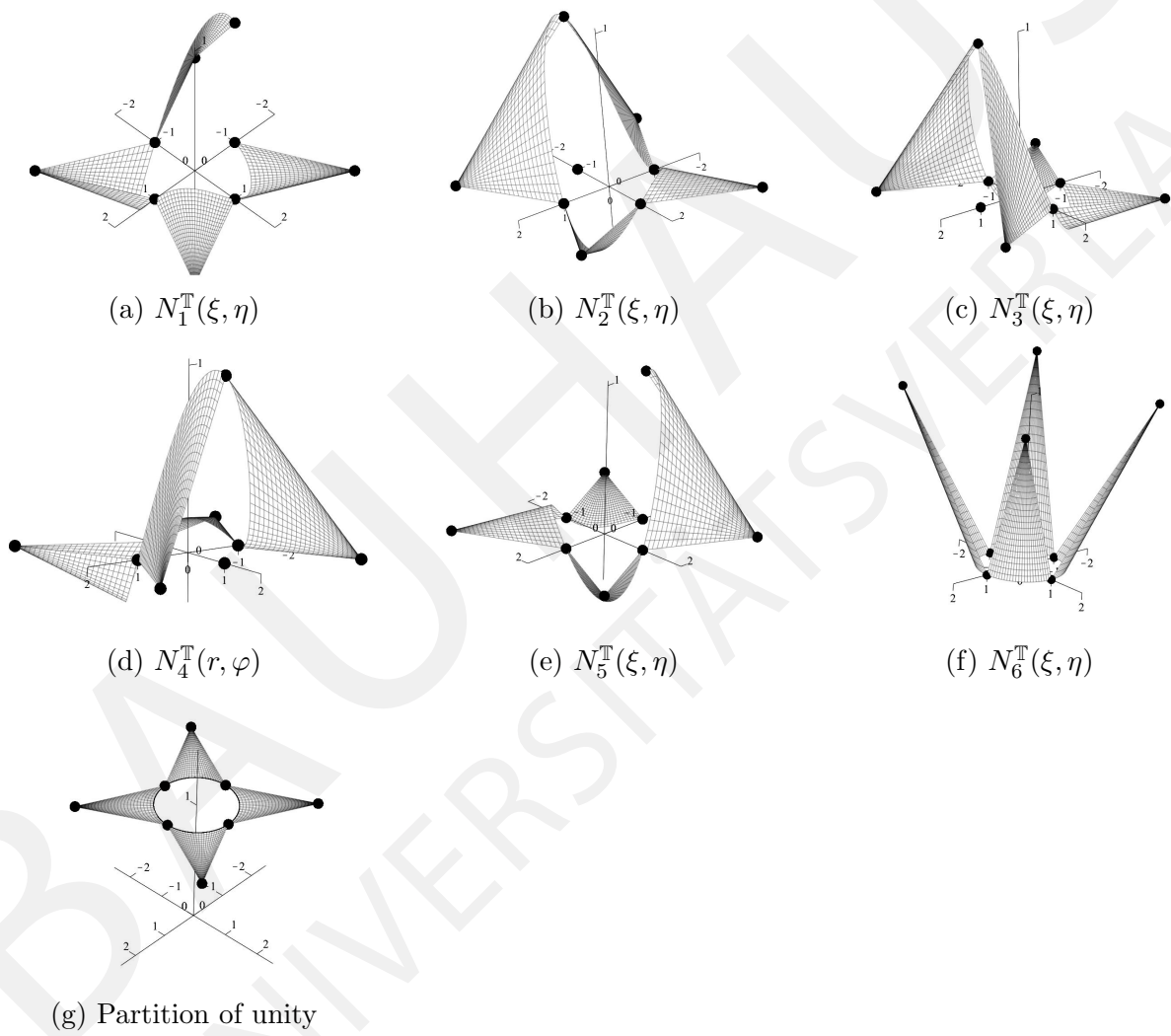
(a) $N_1^{\mathbb{T}}(\xi, \eta)$

(b) $N_2^{\mathbb{T}}(\xi, \eta)$

(c) $N_3^{\mathbb{T}}(\xi, \eta)$

(d) $N_4^{\mathbb{T}}(r, \varphi)$

(e) $N_5^{\mathbb{T}}(\xi, \eta)$

(f) $N_6^{\mathbb{T}}(\xi, \eta)$

(g) Partition of unity

Figure 4.21: Shape functions over the coupling elements for $n = 5$

Chapter 5

Numerical analysis of the coupled method

The problems of linear elasticity, which we have introduced in Chapter 2, are described by system of partial differential equations (2.18). Following the book of Michlin [Michlin 1970] we introduce in this section some basics ideas of direct and variational methods of mathematical physics. In applications our goal is to calculate (at least approximately) the physical quantities of interest, which are unknown displacements for the linear elasticity problems. For many problems the best choice could be the so-called direct methods. According to Sobolev [Sobolev 1988] direct methods are the methods of approximate solution for partial differential equations or integral equations, which reduce these problems to finite systems of algebraic equations.

In many cases of applications of direct methods the problem of integration of a differential equation can be successfully replaced by a problem of finding a function which gives a minimal value to a certain integral. The problems of such types are called variational problems. Thus in many cases the original problem of integration of a differential equation, or so-called a strong problem, can be replaced by a variational or so-called the weak problem. Methods which are based on this replacement are called variational methods. The most important method from the scope of variational methods is the method known in engineering literature as the energetic method.

Many of the direct methods can be applied more efficiently not directly to a differential equation, but to an equivalent variational problem. For example it can be applied to the well-known Ritz method, which is a method to approximate the solutions of variational problems. This fact shows a close connection between direct and variational methods.

Another motivation for the variational methods comes from boundary value problems with singularities. Because in this case can happen that the strong solution of a differential equation doesn't exist, like for example in the case of an interface problem: if we consider an interface between two material, then the stresses have jump at the interface.

Historically the first variational method was formulated as the so-called "Dirichlet principle". According to this principle among all functions, which have a given value at the boundary of a domain Ω, the function which gives a minimal value to the "Dirichlet

integral"

$$\iint\limits_{\Omega} \left[\left(\frac{\partial u}{\partial x} \right)^2 + \left(\frac{\partial u}{\partial y} \right)^2 \right] dxdy$$

is a harmonic function in Ω.

The Dirichlet principle was widely used by Riemann in his work on complex function theory. In the eyes of Riemann the fact of existence of a function which minimizes the Dirichlet integral was obvious. But later Weierstraß has given a critical remark, and on a simple example he has shown that the minimal value of the integral not always can be reached. Some time later Hadamard has shown another example of a function, which is a solution of the Dirichlet problem in Ω (in the classical sense), but the Dirichlet integral for that function is divergent.

Because of these examples the Dirichlet principle was forgotten for a long time, and appears again only in works of Hilbert. Hilbert has shown, that problems of the Dirichlet principle are not related to "a small incorrectness" in its formulation, but in much deeper condition, which is called now by completeness of a metric space.

The next outstanding event was the creation of the Ritz method by a German engineer in 1909 [Ritz 1909]. This method was particularly interesting for people from applied sciences, because it offers a suitable tool, which was not available before. In that time a lot of papers with applications of the Ritz method to problems of mathematical physics were published. Due to its simplicity the Ritz method became the basic method for direct variational methods. Even the finite element method is a particular case of the Ritz method for a certain choose of a basis.

Another very important direct method is the Bubnov-Galerkin method, which was proposed by Bubnov [Bubnov 1913], and later extended by Galerkin [Galerkin 1915]. Bubnov has shown that ideas of the Ritz method can be applied directly to a differential equation, and it's not necessary to write at first an energy functional. For linear problems the resulting system of the Galerkin method is equal to a system which can be obtained by the Ritz method. The finite element method can be obtained by choosing a certain basis from both of these methods.

Due its more general formulation the Galerkin method is usually considered as the basis for the finite element method. The finite element method is the most popular numerical method for solving boundary value problems in the computational mechanics. Among the other numerical methods, like for instance boundary element method, finite difference method, etc., the finite element method historically became very popular among engineers in applied fields of science.

Originally it was introduced by Courant in his paper [Courant 1943], but at that time the importance of his results was ignored by other scientists. Later, in the fifties the method was re-invented by engineers related to the names of Argyris [Argyris 1954-1955], Turner, Clough, Martin and Topp [Turner et al. 1956]. The name "finite element method" was proposed by Clough [Clough 1960]. After works of Oden [Oden 1972], and Zienkiewicz [Zienkiewicz 1971] in the seventies, the finite element method finally became the most popular numerical method for applied problems.

In this chapter we introduce the important foundation of the Galerkin method, and the finite element method. We start from some necessary tools of functional analysis, which are important for a further discussion about the convergence of the proposed method. In the end of this chapter we describe the finite element with holomorphic functions, which is a consequence of the ideas for coupling, which we have introduced in Chapter 3.

5.1   Preliminaries from functional analysis

In the theory of the finite element method Sobolev spaces play a very important role. Therefore in this section we will give some basic information about them. According to the purpose of this section we will list only a few definitions, and for more information we refer to [Adams 1975], [Adams & Fournier 2003], [Hunter & Nachtergaele 2001]. Throughout this thesis we will work only with real functional spaces.

Sobolev spaces are Banach spaces of functions whose weak derivatives belong to L^p spaces. We define Sobolev spaces of functions whose domain is an open subset Ω of $\mathbb{R}^n$, equipped with n-dimensional Lebesgue measure. $L^p(\Omega)$ denotes the space of Lebesgue measurable functions $f : \Omega \to \mathbb{R}$ whose pth power are integrable.

Definition 5.1. A test function $\varphi : \Omega \to \mathbb{R}$ on an open subset Ω of $\mathbb{R}^n$ is a function with continuous partial derivatives of all orders whose support is a compact subset of Ω. We denote the set of test functions on Ω by $C_0^\infty(\Omega)$.

Definition 5.2. Let m be a positive integer, $1 \leq p \leq \infty$, and Ω an open subset of $\mathbb{R}^n$. The Sobolev space $W^{m,p}(\Omega)$ consists of all functions $f : \Omega \to \mathbb{R}$ such that $\partial^\alpha f \in L^p(\Omega)$ for all weak partial derivatives of order $0 \leq |\alpha| \leq m$. We define a norm on $W^{m,p}(\Omega)$ by

$$\|f\|_{m,p,\Omega} = \left(\sum_{0 \leq |\alpha| \leq m} \int_\Omega |\partial^\alpha f(x)|^p dx \right)^{\frac{1}{p}}$$

when $1 \leq p < \infty$, and by

$$\|f\|_{m,\infty,\Omega} = \max_{0 \leq |\alpha| \leq m} \left\{ \operatorname*{ess.\,sup}_{x \in \Omega} |\partial^\alpha f(x)| \right\}$$

when $p = \infty$.

For $p = 2$, corresponding to the case of square integrable functions it's common to write $W^{m,2}(\Omega) = H^m(\Omega)$, but in this thesis we will always use the classical notation $W^{m,p}(\Omega)$ for all values of p. The space $W^{m,p}(\Omega)$ is a Banach space, and $W^{m,2}(\Omega)$ is a Hilbert space.

We will also use the semi-norms

$$|f|_{m,p,\Omega} = \left(\sum_{|\alpha|=m} \int_\Omega |\partial^\alpha f(x)|^p dx \right)^{\frac{1}{p}}$$

when $1 \le p < \infty$, and by

$$|f|_{m,\infty,\Omega} = \max_{|\alpha|=m} \left\{ \underset{x\in\Omega}{\mathrm{ess.\,sup}} \, |\partial^\alpha f(x)| \right\}$$

when $p = \infty$.

Next, we define a Sobolev space of functions which "vanish on the boundary of Ω".

Definition 5.3. The closure of $C_0^\infty(\Omega)$ in $W^{m,p}(\Omega)$ is denoted by

$$W_0^{m,p}(\Omega) = \overline{C_0^\infty(\Omega)}.$$

Informally, we can think of $W_0^{m,p}(\Omega)$ as the $W^{m,p}(\Omega)$-functions whose derivatives of an order less than or equal $m-1$ vanish on the boundary $\partial\Omega$ of Ω. Compactly supported functions are dense in $W^{m,p}(\mathbb{R}^n)$, so that $W_0^{m,p}(\mathbb{R}^n) = W^{m,p}(\mathbb{R}^n)$.

5.2 Abstract variational problems

In this section following [Ciarlet 1978] we introduce a basic information about abstract variational problems and some theory around them. In the end we give a variational formulation of the Lamé equation (2.18), which we have introduced in Chapter 2.

Let there be given a normed vector space V with norm $\|\cdot\|$, a continuous bilinear functional $a(\cdot,\cdot): V \times V \to \mathbb{R}$, a continuous linear functional $f: V \to \mathbb{R}$ and a non empty subset U of the space V. With these data we associate an abstract minimization problem: Find an element u such that

$$u \in U \qquad \text{and} \qquad J(u) = \inf_{v\in U} J(v), \tag{5.1}$$

where the functional $J: V \to \mathbb{R}$ is defined by

$$J: v \in V \to J(v) = \frac{1}{2}a(v,v) - f(v).$$

The next theorem sets up the existence and uniqueness properties of the solution of this problem. We will leave this theorem without proof, for more details we refer again to [Ciarlet 1978].

Theorem 5.1. *Let there be given a normed vector space V with norm $\|\cdot\|$, a continuous bilinear functional $a(\cdot,\cdot): V \times V \to \mathbb{R}$, a continuous linear functional $f: V \to \mathbb{R}$ and a non empty subset U of the space V. Additionally, we assume that*

(i) the space V is complete,

(ii) U is a closed convex subset of V,

(iii) the bilinear functional $a(\cdot,\cdot)$ is symmetric and V-elliptic, in the sense that

$$\exists \alpha > 0, \quad \alpha\|v\|^2 \le a(v,v), \quad \forall v \in V.$$

Then the abstract minimization problem (5.1) has one and only one solution.

By this theorem, each problem has one and only one solution if the space V is complete, the subset U of V is closed and convex, and the bilinear form is V-elliptic, continuous, and symmetric.

Let us now give equivalent formulations of the problem (5.1).

Theorem 5.2. *An element u is the solution of the abstract minimization problem (5.1) if and only if it satisfies the relations*

$$a(u, v - u) \geq f(v - u), \qquad u \in U \quad and \quad \forall\, v \in U,$$

in the general case, or

$$a(u, v) \geq f(v), \quad a(u, u) = f(u), \qquad u \in U \quad and \quad \forall\, v \in U,$$

if U is a closed convex cone with vertex 0, or

$$a(u, v) = f(v), \qquad \in U \quad and \quad \forall\, v \in U, \tag{5.2}$$

if U is a closed subspace.

Now we introduce a variational formulation of a linear elasticity problem. Let Ω be a bounded open connected subset of $\mathbb{R}^3$ with a Lipschitz-continuous boundary Γ. We define the space

$$\mathbf{V} = \mathbf{U} = \left\{ \mathbf{v} = (v_1, v_2, v_3) \in \left(W^{1,2}(\Omega) \right)^3; \quad v_i = 0, \text{ on } \Gamma_0, 1 \leq i \leq 3 \right\}, \tag{5.3}$$

where Γ_0 is a $d\gamma$-measurable subset of Γ, with a strictly positive $d\gamma$-measure. The space $\mathbf{V}$ is equipped with the norm

$$\mathbf{v} = (v_1, v_2, v_3) \rightarrow \|\mathbf{v}\|_{1,2,\Omega} = \left(\sum_{i=1}^{3} \|v_i\|_{1,2,\Omega}^2 \right)^{\frac{1}{2}}.$$

For any $\mathbf{v} = (v_1, v_2, v_3) \in (W^{1,2}(\Omega))^3$ let

$$\varepsilon_{ij}(\mathbf{v}) = \varepsilon_{ji}(\mathbf{v}) = \frac{1}{2} \left(\partial_j v_i + \partial_i v_j \right), \quad 1 \leq i, j \leq 3,$$

and

$$\sigma_{ij}(\mathbf{v}) = \sigma_{ji}(\mathbf{v}) = \lambda \left(\sum_{k=1}^{3} \varepsilon_{kk}(\mathbf{v}) \right) \delta_{ij} + 2\mu\, \varepsilon_{ij}(\mathbf{v}), \quad 1 \leq i, j \leq 3, \tag{5.4}$$

where δ_{ij} is the Kronecker's symbol, and λ and μ are two constants which are assumed to satisfy $\lambda > 0$, $\mu > 0$. We define the bilinear functional as follows

$$a(\mathbf{u}, \mathbf{v}) = \int_{\Omega} \sum_{i,j=1}^{3} \sigma_{ij}(\mathbf{u})\varepsilon_{ij}(\mathbf{v})dx = \int_{\Omega} \left\{ \lambda \operatorname{div} \mathbf{u} \operatorname{div} \mathbf{v} + 2\mu \sum_{i,j=1}^{3} \varepsilon_{ij}(\mathbf{u})\varepsilon_{ij}(\mathbf{v}) \right\} dx, \tag{5.5}$$

and the linear functional

$$q(\mathbf{v}) = \int\limits_{\Omega} \mathbf{f} \cdot \mathbf{v} dx + \int\limits_{\Gamma_1} \mathbf{g} \cdot \mathbf{v} d\gamma = \int\limits_{\Omega} \sum_{i=1}^{3} f_i v_i dx + \int\limits_{\Gamma_1} \sum_{i=1}^{3} g_i v_i d\gamma, \qquad (5.6)$$

where $\mathbf{f} = (f_1, f_2, f_3) \in (L^2(\Omega))^3$ and $\mathbf{g} = (g_1, g_2, g_3) \in (L^2(\Gamma_1))^3$, with $\Gamma_1 = \Gamma \setminus \Gamma_0$ are given functions.

These bilinear and linear functionals are continuous over the space $\mathbf{V}$. The $\mathbf{V}$-ellipticity can be proved by using Korn's inequality. Thus we conclude that there exists a unique function $\mathbf{u} \in \mathbf{V}$ which minimizes the functional

$$J(\mathbf{v}) = \frac{1}{2} \int\limits_{\Omega} \left\{ \lambda \left(\operatorname{div} \mathbf{v} \right)^2 + 2\mu \sum_{i,j=1}^{3} \left(\varepsilon_{ij}(\mathbf{v}) \right)^2 \right\} dx - \left(\int\limits_{\Omega} \mathbf{f} \cdot \mathbf{v} dx + \int\limits_{\Gamma_1} \mathbf{g} \cdot \mathbf{v} d\gamma \right) \qquad (5.7)$$

over the space $\mathbf{V}$, or equivalently, which is such that

$$\int\limits_{\Omega} \sum_{i,j=1}^{3} \sigma_{ij}(\mathbf{u}) \varepsilon_{ij}(\mathbf{v}) dx = \int\limits_{\Omega} \mathbf{f} \cdot \mathbf{v} dx + \int\limits_{\Gamma_1} \mathbf{g} \cdot \mathbf{v} d\gamma \quad \forall \mathbf{v} \in \mathbf{V}. \qquad (5.8)$$

Equations (5.3), (5.5) and (5.6) represent the variational problem which is associated with the Lamé equation (2.18). The body $\hat{\Omega}$ cannot move along Γ_0, and along Γ_1, surface forces of density $\mathbf{g}$ are given. In addition, a volume force, of density $\mathbf{f}$, is prescribed inside the body $\hat{\Omega}$.

The strain tensor is defined by $\varepsilon(\mathbf{u})$, and the stress tensor is defined by $\sigma(\mathbf{u})$, which we have introduced in Chapter 2. Hooke's law (2.11) is represented now by the linear equation (5.4). The constants λ and μ are still Lamé constants.

Variational equation (5.8) represents the principle of virtual work, valid for all kinematically admissible displacements $\mathbf{v}$, i.e. which satisfy the boundary condition $\mathbf{v} = 0$ on Γ_0.

The functional J of (5.7) is the total energy of the body. It is the sum of the strain energy:

$$\frac{1}{2} \int\limits_{\Omega} \left\{ \lambda \left(\operatorname{div} \mathbf{v} \right)^2 + 2\mu \sum_{i,j=1}^{3} \left(\varepsilon_{ij}(\mathbf{v}) \right)^2 \right\} dx,$$

and of the potential energy of the exterior forces:

$$-\left(\int\limits_{\Omega} \mathbf{f} \cdot \mathbf{v} dx + \int\limits_{\Gamma_1} \mathbf{g} \cdot \mathbf{v} d\gamma \right).$$

5.3 Fundamentals of the finite element method

Since the finite element method is a special case of the Galerkin method, we start this section with a short reminder on the general idea of application of the Galerkin method to abstract variational problems given by equation (5.2). The method consists in formulation of such problems in finite dimensional subspaces of the space V. For each finite dimensional subspace V_h of the space V we define the discrete problem: Find $u_h \in V_h$ such that

$$a(u_h, v_h) = f(v_h), \qquad \forall v_h \in V_h. \tag{5.9}$$

By the Lax-Milgram lemma (see, for example [Ciarlet 1978]) each of these discrete problems has a unique solution u_h, which is called a discrete solution.

Let the set of functions $\varphi_1, \varphi_2, \ldots, \varphi_n$ be a basis in the space V_h. Then the function

$$u_h^{(n)} = \sum_{k=1}^{n} a_k^{(n)} \varphi_k$$

is a solution of the discrete problem (5.9), and the coefficients a_k must be determined through the orthogonality condition, which leads to the following linear system of equations

$$\sum_{k=1}^{n} (a\varphi_k, \varphi_j) \, a_k = (f, \varphi_j), \qquad j = 1, 2, \ldots, n,$$

whose matrix is always invertible, since the bilinear functional, being assumed to be V-elliptic, is a priori V_h-elliptic. For the elasticity problems, the matrix $(a\varphi_k, \varphi_j)$ and the vector (f, φ_j) are called the stiffness matrix and the load vector, respectively.

According to (5.5) the coefficients $(a\varphi_k, \varphi_j)$ are integrals of the form

$$(a\varphi_k, \varphi_j) = \int_{\Omega} \left\{ \lambda \operatorname{div} \varphi_k \operatorname{div} \varphi_j + 2\mu \sum_{i,j=1}^{3} \varepsilon_{ij}(\varphi_k)\varepsilon_{ij}(\varphi_j) \right\} dx,$$

and these coefficients are zero if the measure of the intersection of supports of the basis functions φ_k and φ_j is zero.

During next subsections we introduce shortly the basic ideas of the finite element method. In this thesis we work with the most classical version of the finite element method, therefore all general ideas will be remained according to [Ciarlet 1978] with certain extension to our settings. The choice of the classical version of the finite element method is based on two facts: on one hand the method is well-established for purposes of practical use, and on another hand a serious theoretical basis has been developed.

5.3.1 Three basic aspects of the finite element method

The finite element method, in its simplest form, is a specific process of constructing subspaces V_h, which are called finite element spaces. Let us recall three basic aspects of this construction.

(FEM 1) The first aspect is that a triangulation $\mathcal{F}_h$ is established over the set $\bar{\Omega}$, i.e. the set $\bar{\Omega}$ is subdivided into a finite number of subsets $\mathbf{K}$, called finite elements, in such a way that the following properties are satisfied:

(i) $\bar{\Omega} = \underset{\mathbf{K} \in \mathcal{F}_h}{\cup} \mathbf{K}$.

(ii) For each $\mathbf{K} \in \mathcal{F}_h$ the subset $\mathbf{K}$ is closed and the interior $\mathring{\mathbf{K}}$ is non-empty.

(iii) For each distinct $\mathbf{K}_1, \mathbf{K}_2 \in \mathcal{F}_h$, one has $\mathring{\mathbf{K}}_1 \cap \mathring{\mathbf{K}}_2 = \emptyset$.

(iv) For each $\mathbf{K} \in \mathcal{F}_h$ the boundary $\partial \mathbf{K}$ is Lipschitz-continuous.

(v) Any face of a finite element $\mathbf{K}_1$ is either a face of another finite element $\mathbf{K}_2$, in which case the finite elements $\mathbf{K}_1$ and $\mathbf{K}_2$ are said to be adjacent, or a portion of the boundary Γ of the set Ω.

Once such a triangulation $\mathcal{F}_h$ is established over the set $\bar{\Omega}$, one defines a finite element space $\mathbf{X}_h$, which is a finite-dimensional space of functions defined over the set $\bar{\Omega}$. Let v_h be a set of all basis functions defined over the set $\bar{\Omega}$. We define the local spaces $\mathbf{P_K}$ of the basis functions over the finite elements $\mathbf{K} \in \mathcal{F}_h$ by the restrictions $v_{h|\mathbf{K}}$ of the functions $v_h \in \mathbf{X}_h$ as follows

$$\mathbf{P_K} = \left\{ v_{h|\mathbf{K}} : v_h \in \mathbf{X}_h \right\}.$$

(FEM 2) The second basic aspect of the finite element method is that the spaces $\mathbf{P_K}$, $\mathbf{K} \in \mathcal{F}_h$ contain functions which provide a unisolvence property over $\mathbf{K}$. We will provide in the next section the meaning of the unisolvence property.

(FEM 3) The third basic aspect of the finite element method is that there exists at least one "canonical" basis in the space V_h whose corresponding basis functions have supports which are as "small" as possible.

Remark 5. The (FEM 2) was originally formulated by [Ciarlet 1978] in a bit more restrictive way as follows:

- The second basic aspect of the finite element method is that the spaces $\mathbf{P_K}$, $\mathbf{K} \in \mathcal{F}_h$ contain polynomials, or, at least, contain functions which are "close to" polynomials.

We have introduced it in more general way based on the "close to" remark, and as we will see later on, the more general second aspect allows us to extend results of P.G. Ciarlet to the case of functions different from polynomial by studying properties which have to be satisfied by these functions.

Finally we will call the finite element method which is introduced according to (FEM 1) – (FEM 2) the conforming finite element method.

5.3.2 General properties of finite elements and finite element spaces

In (FEM 1) we have introduced the definition of finite elements from geometrical point of view. Let us now introduce a more general definition of a finite element in $\mathbb{R}^n$ as a triple $(\mathbf{K}, P, \Sigma)$ where:

(i) $\mathbf{K}$ is a closed subset of $\mathbb{R}^n$ with a non empty interior and a Lipschitz-continuous boundary;

(ii) P is a space of real-valued functions defined over the set $\mathbf{K}$;

(iii) Σ is a finite set of linearly independent continuous linear functionals $\varphi_i, 1 \leq i \leq N$, defined over the space P.

By definition, it is assumed that the set Σ is P-unisolvent in the following sense: given any real scalars $\alpha_i, 1 \leq i \leq N$, there exists a unique function $p \in P$ which satisfies

$$\varphi_i(p) = \alpha_i, \qquad 1 \leq i \leq N.$$

Consequently, there exist functions $p_i \in P, 1 \leq i \leq N$, which satisfy

$$\varphi_i(p_i) = \delta_{ij}, \qquad 1 \leq j \leq N.$$

Since we have

$$p = \sum_{i=1}^{N} \varphi_i(p) p_i, \qquad \forall p \in P.$$

This implies that the space P is finite-dimensional and that $\dim P = N$.

The linear functionals $\varphi_i, 1 \leq i \leq N$, are called the degrees of freedom of the finite element, and the functions $p_i, 1 \leq i \leq N$, are called the basis functions of the finite element.

Remark 6. The P-unisolvence of the set Σ is equivalent to the fact that the N continuous linear functionals φ_i form a basis in the dual space of P. As a consequence, one may view the bases $(\varphi_i)_i^N$ and $(p_i)_i^N$ as being dual bases, in the algebraic sense.

Since our main interest are applications to linear elasticity, the degrees of freedom for these problems typically of the following types:

$$
\begin{aligned}
p &\rightarrow p(a_i^0), \\
p &\rightarrow (D\,p)(a_i^1)\xi_{ik}^1, \\
p &\rightarrow (D^2 p)(a_i^2)(\xi_{ik}^2, \xi_{il}^2),
\end{aligned}
\tag{5.10}
$$

where the points $a_i^r, r = 0, 1, 2$, belong to the finite element, and the (non-zero) vectors $\xi_{ik}^1, \xi_{ik}^2, \xi_{il}^2$ are either constructed from a geometry of the finite element or fixed vectors of $\mathbb{R}^n$. The points $a_i^r, r = 0, 1, 2$, are called the nodes of the finite element.

Given a finite element $(\mathbf{K}, P, \Sigma)$, and given a function $v = \mathbf{K} \to \mathbb{R}$, sufficiently smooth so that the degrees of freedom $\varphi_i(v), 1 \le i \le N$, are well defined, let

$$\Pi v = \sum_{i=1}^{N} \varphi_i(v) p_i$$

denote the P-interpolant of the function v, which is unambiguously defined since the set Σ is P-unisolvent. Indeed, the P-interpolant, also denoted $\Pi_{\mathbf{K}} v$, is equivalently characterized by the conditions

$$\Pi v \in P, \quad \text{and} \quad \varphi_i(\Pi v) = \varphi_i(v), \quad 1 \le i \le N.$$

Whenever the degrees of freedom are of the form (5.10), let s denote the maximal order of derivatives occurring in the definition of the set Σ. Then, for all elements which we will use here, the inclusion $P \subset C^s(\mathbf{K})$ holds. Consequently, the domain $\operatorname{dom}\Pi$ of the P-interpolation operator Π is the space

$$\operatorname{dom}\Pi = C^s(\mathbf{K}).$$

It follows immediately that over the space $P \subset \operatorname{dom}\Pi$, the interpolation operator reduces to the identity, i.e.

$$\Pi p = p, \quad \forall\, p \in P.$$

Next important step in the finite element methods is a description of a given family $(\mathbf{K}, P_{\mathbf{K}}, \Sigma_{\mathbf{K}})$ of finite elements. For practical purposes it's very beneficial if one can describe a family of finite elements by using a certain reference element from the family. This idea leads to affine families of finite elements. We give here only the definition, and for all of the details we again refer to [Ciarlet 1978].

Definition 5.4. Two finite elements $(\hat{K}, \hat{P}, \hat{\Sigma})$ and (K, P, Σ), with degrees of freedom of the form (5.10), are said to be affine-equivalent if there exists an invertible affine mapping:

$$F : \hat{x} \in \mathbb{R}^n \to F(\hat{x}) = B\,\hat{x} + b \in \mathbb{R},$$

such that the following relations hold:

$$K \;=\; F(\hat{K}),$$

$$P \;=\; \left\{ p : K \to \mathbb{R}; \quad p = \hat{p} \cdot F^{-1}, \quad \hat{p} \in \hat{P} \right\},$$

$$a_i^r \;=\; F(\hat{a}_i^r), \quad r = 0, 1, 2,$$

$$\xi_{ik}^1 \;=\; B\,\hat{\xi}_{ik}^1, \quad \xi_{ik}^2 = B\,\hat{\xi}_{ik}^2, \quad \xi_{il}^2 = B\,\hat{\xi}_{il}^2,$$

whenever the nodes a_i^r, resp. $\hat{a}_i^r$, and vectors $\xi_{ik}^1, \xi_{ik}^2, \xi_{il}^2$, resp. $\hat{\xi}_{ik}^1, \hat{\xi}_{ik}^2, \hat{\xi}_{il}^2$, occur in the definition of the set Σ, resp. $\hat{\Sigma}$.

The next step is a description of the construction of a finite element space from the data of finite elements $(\mathbf{K}, P_{\mathbf{K}}, \Sigma_{\mathbf{K}})$. For the sake of simplicity we restrict ourselves to the case where the boundary of the domain $\bar{\Omega}$ is polygonal, or can be approximated with arbitrary accuracy by polygonal elements $\mathbf{K}$. From the conditions (FEM 1) we can state that the sets of degrees of freedom of adjacent finite elements have to be related as follows: whenever $(\mathbf{K}_l, P_{\mathbf{K}_l}, \Sigma_{\mathbf{K}_l})$ with $\Sigma_{\mathbf{K}_l} = \left\{ p(a_i^l), 1 \le i \le N_l \right\}, l = 1, 2$ are two adjacent finite elements, then

$$\left(\bigcup_{i=1}^{N_1} \{a_i^1\} \right) \bigcap \mathbf{K}_2 = \left(\bigcup_{i=1}^{N_2} \{a_i^2\} \right) \bigcap \mathbf{K}_1.$$

We define the set

$$\mathcal{N}_h = \bigcup_{\mathbf{K} \in \mathcal{F}_h} \mathcal{N}_{\mathbf{K}},$$

where, for each finite element $\mathbf{K} \in \mathcal{F}_h$, $\mathcal{N}_{\mathbf{K}}$ denotes the set of nodes. For each $b \in \mathcal{N}_h$, we let $\mathbf{K}_\lambda, \lambda \in \Lambda(b)$, denote all those finite elements to which belongs the node b, $\Lambda(b)$ is the set of polygons with a common vertex b. Then the associated finite element space X_h is the subspace of the product space $\prod\limits_{\mathbf{K} \in C_h^s} P_{\mathbf{K}}$, defined by

$$X_h = \left\{ v = v(\mathbf{K})_{\mathbf{K} \in \mathcal{F}_h} \in \prod_{\mathbf{K} \in \mathcal{F}_h}; \quad \forall b \in \mathcal{N}_h, \forall \lambda, \mu \in \Lambda(b), \quad v_{\mathbf{K}_\lambda}(b) = v_{\mathbf{K}_\mu}(b) \right\}.$$

Therefore a function in the space X_h is uniquely determined by the set of functional values at the vertices of the triangulation

$$\Theta_h = \{v(b), \quad b \in \mathcal{N}_h\},$$

which is called the set of degrees of freedom of the finite element space.

When the degrees of freedom of all finite elements are of some of the types (5.10), the degree of freedom of the finite element space are of some of the following types:

$$\begin{aligned} v &\rightarrow v(b_j^0), \\ v &\rightarrow (D\,v)(b_j^1)\eta_{jk}^1, \\ v &\rightarrow (D^2\,v)(b_j^2)\left(\eta_{jk}^2, \eta_{jl}^2\right), \end{aligned} \qquad (5.11)$$

where the points $b_j^r, r = 0, 1, 2$, called the nodes of the finite element space, make up a set which is generally denoted $\mathcal{N}_h$.

If we write the set Σ_h as

$$\Sigma_h = \{\varphi_{j,h}, \quad 1 \le j \le M\}, \qquad (5.12)$$

then the basis functions $w_j, 1 \le j \le M$, of the finite element space are defined by the relations

$$w_j \in X_h, \quad \text{and} \quad \varphi_{i,h}(w_j) = \delta_{ij}, \quad 1 \le i \le M. \qquad (5.13)$$

The basis functions of the finite element space are derived from the basis functions of the finite elements, as follows: Let $\varphi_h \in \Sigma_h$ be of the form (5.11), let b be the associated node, and let $\mathbf{K}_\lambda, \lambda \in \Lambda(b)$, denote all the finite elements of $\mathcal{F}_h$ for which b is a node. For each $\lambda \in \Lambda(b)$, let p_λ denote the basis function of the finite element $\mathbf{K}_\lambda$ associated with the restriction of φ_h to $\mathbf{K}_\lambda$. Then the function $w \in X_h$ defined by

$$w = \begin{cases} p_\lambda & \text{over } \mathbf{K}_\lambda, \quad \lambda \in \Lambda(b), \\ 0 & \text{elsewhere,} \end{cases}$$

is the basis function of the space X_h associated with the degree of freedom φ_h.

Let there be given a finite element space X_h with a set of degrees of freedom of the form (5.12). Then with any function $v : \bar{\Omega} \to \mathbb{R}$ sufficiently smooth so that the degrees of freedom $\varphi_{j,h}, 1 \le j \le M$ are well defined, we associate the function

$$\Pi_h v = \sum_{j=1}^M \varphi_{j,h}(v) w_j,$$

where the functions w_j are the basis functions defined in (5.13). The function $\Pi_h v$, called the X_h-interpolant of the function v, is equivalently characterized by the conditions

$$\Pi_h v \in X_h \quad \text{and} \quad \varphi_{j,h}(\Pi_h v) = \varphi_{j,h}(v), \quad 1 \le j \le M.$$

Let s denote the maximal order of directional derivatives occurring in the finite elements $(\mathbf{K}, P_\mathbf{K}, \Sigma_\mathbf{K}), \mathbf{K} \in \mathcal{F}_h$, we will usually consider, that the domain $\operatorname{dom} \Pi_h$ of the X_h-interpolation operator Π_h is the space

$$\operatorname{dom} \Pi_h = C^s(\Omega).$$

The next theorem states a relationship between the "global" interpolation operator Π_h and the "local" interpolation operators $\Pi_\mathbf{K}$.

Theorem 5.3. *Let v be an arbitrary function in the space $\operatorname{dom} \Pi$. Then the restriction $v|_\mathbf{K}$ belongs to the space $\operatorname{dom} \Pi$, and we have*

$$(\Pi v)|_\mathbf{K} = \Pi_\mathbf{K} v|_\mathbf{K}, \qquad \forall \mathbf{K} \in \mathcal{F}_h.$$

Additionally to the definition 5.4 of the affine-equivalent finite elements we will need a more general definition of the affine-equivalent sets:

Definition 5.5. Two open subsets Ω and $\hat{\Omega}$ of $\mathbb{R}^n$ are called affine-equivalent if there exists an invertible affine mapping

$$F : \hat{x} \in \mathbb{R}^n \to F(\hat{x}) = B\hat{x} + b \in \mathbb{R}^n \tag{5.14}$$

such that $\Omega = F(\hat{\Omega})$. The correspondences

$$\hat{x} \in \hat{\Omega} \to x = F(\hat{x}) \in \Omega, \tag{5.15}$$

$$(\hat{v} : \hat{\Omega} \to \mathbb{R}) \to (v = \hat{v}F^{-1} : \Omega \to \mathbb{R}), \tag{5.16}$$

hold between the points $\hat{x} \in \hat{\Omega}$ and $x \in \Omega$, and between functions defined over the set $\hat{\Omega}$ and the set Ω. We have $\hat{v}(\hat{x}) = v(x)$ for all points $\hat{x}$ and x in the correspondence (5.15) and all functions $\hat{v}, v$ in the correspondence (5.16).

5.3.3 Remarks for the coupling method

We denote in the sequel by $\mathcal{P}_k$ a k-dimensional space of functions, which satisfy a differential equation in Ω. Additionally to that we define a special interpolation operator $\hat{\Pi}$ based on the analytical solution, which is given in (4.2). Since we are working with C^0-continuity of the finite element solution in Ω, we define the domain of definition of $\hat{\Pi}$ as the space $\mathrm{dom}\,\hat{\Pi} = C^0(\Omega)$. But we would like to mention that one can ask also for higher order continuity, i.e. in that case $\mathrm{dom}\,\hat{\Pi} = C^s(\Omega)$, where s denotes the highest order derivative appearing in the definition of degrees of freedom for the special element. The interpolation operator $\hat{\Pi}$, as it was proved in Chapter 4, has the following invariance property

$$\hat{\Pi}\hat{p} = \hat{p}, \qquad \forall\, \hat{p} \in \mathcal{P}_k(\Omega). \tag{5.17}$$

To proceed further with the convergence analysis of the proposed scheme we need to make an important remark. In the classical theory of the finite elements method the convergence analysis is based on the definition of affine-equivalent sets (see again [Ciarlet 1978]). All estimates in this classical case are derived for a reference element, and then transferred to an element in the existing triangulation by an affine mapping. The quality of these estimates depends on the regularity of basis functions, and on the characteristic size of an element in the triangulation. This theory cannot be applied directly to our setting, because additionally to the standard elements T (which are fully covered by the classical theory), we have the coupling elements $\mathbb{T}$ and the analytical elements $\mathbb{A}$. The difficulties with elements $\mathbb{T}$ and $\mathbb{A}$ are coming from several aspects:

(i) the regularity of basis function is restricted by a singular term in the analytical solution (3.13);

(ii) the coupling elements are not affine-equivalent to each other, because the interpolation operator $\hat{\Pi}$ is constructed in a way, that instead of several separated coupling elements, in fact, we have one coupled element.

To overcome these difficulties we need to consider two possible strategies. First strategy is that we consider a coupled element $\mathbb{T}\mathbb{A} = \mathbb{A} \cup \mathbb{T}$ in Ω_{SE} as one element in the triangulation, and this element can be considered as an affine-equivalent to a reference coupled element. The second strategy is to consider all elements separately, particularly this strategy is significantly important in the case when we fix the radius of Ω_{A}. The idea of fixing the radius r_{A} is coming from practical experience, because if r_{A} goes to zero we the influence of the correct approximation of the singular solution is also going to zero. In opposite to it from fixed radius and greater number of the coupling elements one can expect "better" approximation of the boundary values for the analytical solution, which could lead to a higher quality of results near the singularity.

We will perform the convergence analysis for both of these strategies separately during next sections.

5.4 Convergence with the coupled element $\mathbb{TA}$

At first we consider the convergence analysis with the coupled element $\mathbb{TA}$, which is a union of the coupling elements $\mathbb{T}$ and the analytical element $\mathbb{A}$ inside of the each special element (see Fig. 5.1). The idea behind of this construction is to get an element which will belong to the affine-equivalent family of finite elements. This is possible due to the fact, that we have constructed the continuous interpolation operator $\hat{\Pi}$ between $\mathbb{A}$ and $\mathbb{T}$, i.e. $\operatorname{dom}\hat{\Pi} = C^0(\mathbb{TA})$.
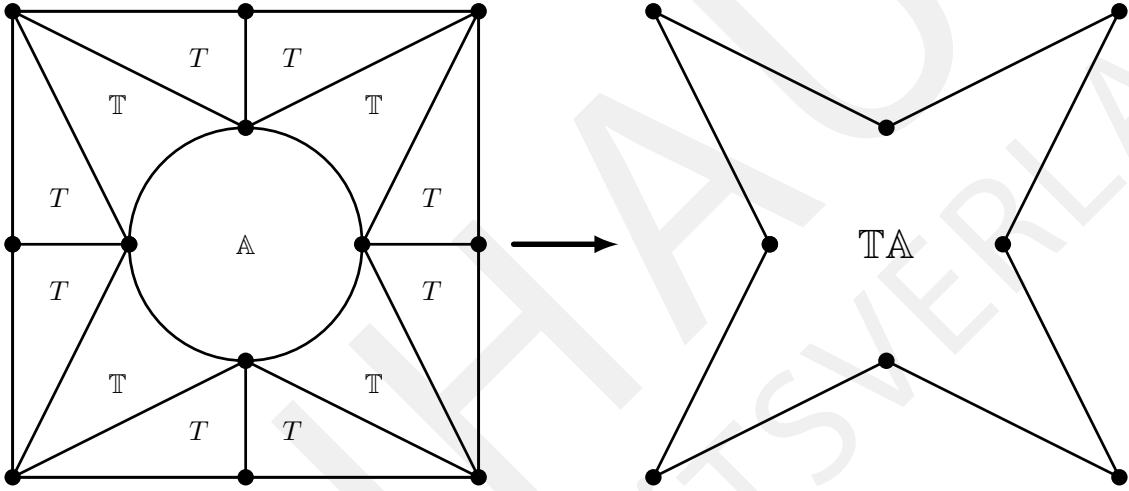
Figure 5.1: The coupled element $\mathbb{TA} = \mathbb{A} \cup \mathbb{T}$ in Ω_{SE}

To complete the definition of the coupled element $\mathbb{TA}$ we introduce:

(i) Ξ is the set of degrees of freedom of the coupled element $\mathbb{TA}$, which is defined as follows

$$\Xi_k = \Sigma_{\mathbb{T}_i} \cup \Sigma_{\mathbb{A}},$$

where $\mathbb{T}_i$ denotes the coupling elements belonging to the special element $\Omega_{\mathrm{SE}}^{(k)}$ in the triangulation $\mathcal{F}_h$;

(ii) $\mathcal{P}_{\mathbb{TA}}$ is the set of the basis functions of the coupled element $\mathbb{TA}$, which is defined as follows

$$\mathcal{P}_k(\mathbb{TA}) = \mathcal{P}_{\mathbb{T}_i} \cup \mathcal{P}_k,$$

where $\mathcal{P}_{\mathbb{T}_i}$ denotes the set of the basis function of the coupling elements belonging to the special element $\Omega_{\mathrm{SE}}^{(k)}$ in the triangulation $\mathcal{F}_h$.

Thus we defined the coupled element $(\mathbb{TA}, \mathcal{P}_k, \Xi)$ as an element from the affine-equivalent family of finite elements in the sense of the definition 5.4.

Our goal here is to get a classical error estimate in $W^{1,p}(\mathbb{TA})$. To construct this estimate we need to assure that the Sobolev embedding theorems are satisfied for the singular functions (3.13) and (4.2). Since the analytical solution has a singularity of order

$\frac{1}{2}$, the desired embeddings can be satisfied for the value of $p \in \left(1, \frac{4}{3}\right)$. Therefore we can formulate the following theorem:

Theorem 5.4. *Let* $\left(\hat{\mathbb{TA}}, \hat{\mathcal{P}}_k, \hat{\Xi}\right)$ *be a coupled element, where we denote by* $\hat{\Xi}$ *the set of its degrees of freedom. If for some numbers* $p \leq q \leq \infty$ *that are chosen based on the analytical solution the following continuous embeddings hold*

$$W^{2,p}(\hat{\mathbb{TA}}) \hookrightarrow C^0(\hat{\mathbb{TA}}), \tag{5.18}$$

$$W^{2,p}(\hat{\mathbb{TA}}) \hookrightarrow W^{1,q}(\hat{\mathbb{TA}}), \tag{5.19}$$

$$\mathcal{P}_k(\hat{\mathbb{TA}}) \subset W^{1,q}(\hat{\mathbb{TA}}), \tag{5.20}$$

then there exists a constant $C\left(\hat{\mathbb{TA}}, \hat{\mathcal{P}}_k, \hat{\Xi}\right)$ *such that for all affine-equivalent elements* $(\mathbb{TA}, \mathcal{P}_k, \Xi)$, *and all functions* $v \in W^{2,p}(\mathbb{TA})$ *we have*

$$|v - \Pi_{\mathbb{TA}}v|_{1,q,\mathbb{TA}} \leq C\left(\hat{\mathbb{TA}}, \hat{\mathcal{P}}_k, \hat{\Xi}\right) \{\mathrm{meas}(\mathbb{TA})\}^{\frac{1}{q}-\frac{1}{p}} \frac{h_{\mathbb{TA}}^2}{\rho_{\mathbb{TA}}} |v|_{2,p,\mathbb{TA}}, \tag{5.21}$$

where $\Pi_{\mathbb{TA}}$ *denotes the* $\mathcal{P}_{\mathbb{TA}}$-*interpolant of the function* v, *and*

$$\begin{cases} \mathrm{meas}(\mathbb{TA}) = dx & - \quad \textit{measure of } \mathbb{TA}, \\ h_{\mathbb{TA}} = \mathrm{diam}(\mathbb{TA}), \\ \rho_{\mathbb{TA}} = \sup\{\mathrm{diam}(S); \quad S \textit{ is a ball contained in } \mathbb{TA}\}. \end{cases}$$

Proof. The proof of this theorem is completely analogous to the proof in [Ciarlet 1978] for polynomial preserving operators. A straightforward adaptation to our setting is possible by considering a wider class of operators, which preserve not only polynomials, but also half-integer terms, which could appear in the analytical solution, i.e. we use the invariance property (5.17). Another important condition is the domain of definition of the operator $\hat{\Pi}$ that is defined over $\mathbb{TA}$. As it was proved in the main interpolation theorem in Chapter 4 we can construct the operator $\hat{\Pi}$ for an arbitrary number of nodes, and thus obtain the continuity for the basis functions inside of the coupled element $\mathbb{TA}$, therefore the standard proof can be adapted here. $\square$

Remark 7. The quality of the estimate (5.21) strongly depends on the value of q, since the value of $\{\mathrm{meas}(\mathbb{TA})\}^{\frac{1}{q}-\frac{1}{p}}$ can vary with q. To give more information about it we express the factor $\mathrm{meas}(\mathbb{TA})$ in terms of $h_{\mathbb{TA}}$ and $\rho_{\mathbb{TA}}$ by using the following inequality

$$\sigma_2 \rho_{\mathbb{TA}}^2 \leq \mathrm{meas}(\mathbb{TA}) \leq \sigma_2 h_{\mathbb{TA}}^2,$$

where σ_2 denotes the dx-measure of a unit sphere in $\mathbb{R}^2$. If the difference $\frac{1}{q} - \frac{1}{p}$ is negative, then we need to use the left inequality to get an estimate, and the right inequality in the opposite case. Moreover the left inequality should be taking for all values $q > p$, and right inequality can be used only in the case $q = p$. By using these inequalities we avoid an increase of error in $\mathbb{TA}$.

We work with regular finite elements $\mathbb{TA}$ in the following sense:

(i) there exists a constant C such that

$$\frac{h_{\mathbb{TA}}}{\rho_{\mathbb{TA}}} \leq C \quad \forall\, \mathbb{TA}\text{-elements}.$$

(ii) the diameters $h_{\mathbb{TA}}$ approach zero.

For such elements we can get the following estimation for the norm:

Theorem 5.5. *Let* $(\mathbb{TA}, \mathcal{P}_{\mathbb{TA}}, \Xi_{\mathbb{TA}})$ *be a given regular affine family of coupled elements, whose reference element* $\left(\hat{\mathbb{TA}}, \hat{\mathcal{P}}_k, \hat{\Xi}\right)$ *satisfies assumptions (5.18), (5.19) and (5.20). Then there exists a constant* $C\left(\hat{\mathbb{TA}}, \hat{\mathcal{P}}_k, \hat{\Xi}\right)$ *such that for all coupled elements* $\mathbb{TA}$ *in the family, and all functions* $v \in W^{2,p}(\mathbb{TA})$ *we have*

$$\|v - \Pi_{\mathbb{TA}} v\|_{1,q,\mathbb{TA}} \leq C\left(\hat{\mathbb{TA}}, \hat{\mathcal{P}}_k, \hat{\Xi}\right) \{\mathrm{meas}(\mathbb{TA})\}^{\frac{1}{q} - \frac{1}{p}} h_{\mathbb{TA}} |v|_{2,p,\mathbb{TA}}. \tag{5.22}$$

Remark 8. The quality of the estimate (5.22) can be still improved by working with the difference $v - \Pi_{\mathbb{TA}} v$ in the analytical element. Because if the leading coefficient in front of the singular term can be calculated exactly, then this difference will belong to a better Sobolev space. But to investigate this question is not a purpose of this work at the moment.

To come from the local error estimate (5.22) to the global error estimate over Ω we use the theorem 5.3 which relates the local and the global interpolation operator. To end up discussion in this subsection we will show a global error estimate in Ω, which is made by summing up the local errors element-by-element. We have the following estimate for the norm:

$$\|v - v_h\|_{1,p,\Omega}^2 \leq \sum_{T \in \mathcal{F}_h} \|v - v_h\|_{1,p,T}^2 + \sum_{\mathbb{TA} \in \mathcal{F}_h} \|v - v_h\|_{1,p_1,\mathbb{TA}}^2,$$

where the parameter p_1 depends on regularity of the analytical solution, and must be chosen to satisfy the embedding (5.18).

To investigate the convergence rate for the proposed method we apply the scaling parameters h_1 and h_2 (refinement parameters) to the affine mappings (5.14) for the standard element T and for the coupled elements $\mathbb{TA}$, respectively. Additionally we restrict the diameters ρ_1, ρ_2 to be proportional to h_1, h_2, and for $p = q$ and $p_1 = q_1$ we get

$$\|v - v_h\|_{1,q,\Omega} \leq C_1 h_1 |v|_{2,p,T} + C_2 h_2 |v|_{2,p_1,\mathbb{TA}}. \tag{5.23}$$

Finally we set the scaling parameters h_1 and h_2 to be equal to h, and thus we obtain

$$\|v - v_h\|_{1,q,\Omega} \leq C\, h\left(|v|_{2,p,T} + |v|_{2,p_1,\mathbb{TA}}\right). \tag{5.24}$$

The estimates (5.23)-(5.24) are sharper than in the case of using the norms instead of the semi-norms. Because in the current case we can get a zero error for the special types of boundary conditions: for instance, for the boundary conditions which lead to a solution represented by a linear function.

5.5 Convergence with a fixed radius

In this section we show convergence results for the second strategy in the case of a fixed radius of the analytical domain Ω_A. Due to the fixed radius a global refinement by a scaling factor is not an appropriate choice in this case. Instead of such a global refinement we can increase the number of the coupling elements around, i.e. we increase the number of the interpolation nodes in the corresponding interpolation problem at the interface Γ_{AD}. This approach can lead to lower computational costs since a local refinement near the singularity is not necessary, but of course with the increasing number of the nodes we need to perform some adaptation of the mesh around the special element to avoid a big change in the area of neighbour elements. Thus, one of the goals of this strategy is to try to reduce the number of elements in the triangulation $\mathcal{F}_h$.

Remark 9. We would like to underline that the idea of the fixed size of a finite element cannot be covered by the classical theory. As we have seen in the previous section, the estimate for the norm is based on the condition that the diameters h_K have to approach zero, which is obviously not true for a fixed size of $\mathbb{A}$. Therefore we have to introduce new ideas of the error estimation.

In this case we consider each type of elements separately: T, $\mathbb{T}$ and $\mathbb{A}$. For the coupling elements $\mathbb{T}$ we define by $\mathcal{P}_{\mathbb{T}}$ a set of its basis functions. The singularity in (3.13) comes from the leading term $r^{\frac{1}{2}}$, but since the basis functions for the coupling elements $\mathbb{T}$ are based on the interpolation function (4.2) defined on the interface Γ_{AD}, i.e. for $r = r_A$, the set $\mathcal{P}_{\mathbb{T}}$ has no singular function. Due to the fact that the elements $\mathbb{T}$ are constructed in a way to get C^0 continuity between the elements, we can apply directly results from [Ciarlet 1978], and we formulate the following theorem:

Theorem 5.6. *Let $(\mathbb{T}, \mathcal{P}_k, \Xi_{\mathbb{T}})$ be a coupling element from a given triangulation $\mathcal{F}_h$, where we denote by $\Xi_{\mathbb{T}}$ the set of its degrees of freedom. If for some numbers $p, q \in [1, \infty)$ and for some integers m, k the following continuous embeddings hold*

$$W^{k+1,p}(\mathbb{T}) \hookrightarrow C^0(\mathbb{T}),$$

$$W^{k+1,p}(\mathbb{T}) \hookrightarrow W^{m,q}(\mathbb{T}),$$

$$\mathcal{P}_k(\mathbb{T}) \subset W^{m,q}(\mathbb{T}),$$

then there exists a constant $C(\mathbb{T}, \mathcal{P}_k, \Xi_{\mathbb{T}})$ such that for all functions $v \in W^{k+1,p}(\mathbb{T})$ we have

$$|v - \Pi_{\mathbb{T}} v|_{m,q,\mathbb{T}} \leq C(\mathbb{T}, \mathcal{P}_k, \Xi_{\mathbb{T}}) \{\text{meas}(\mathbb{T})\}^{\frac{1}{q} - \frac{1}{p}} \frac{h_{\mathbb{T}}^{k+1}}{\rho_{\mathbb{T}}^m} |v|_{k+1,p,\mathbb{T}},$$

where $\Pi_{\mathbb{T}}$ denotes the $\mathcal{P}_{\mathbb{T}}$-interpolant of the function v, and

$$\begin{cases} \text{meas}(\mathbb{T}) = dx & - \quad \text{measure of } \mathbb{T}, \\ h_{\mathbb{T}} = \text{diam}(\mathbb{T}), \\ \rho_{\mathbb{T}} = \sup\{\text{diam}(S); \quad S \text{ is a ball contained in } \mathbb{T}\}. \end{cases}$$

The construction of the error estimate in $\mathbb{A}$ requires a more advanced technique, since the radius of Ω_A is fixed and cannot approach zero. Instead, we consider the task of approximation by interpolation in our settings: what is the quality of the approximation of $\mathbf{u}(z)$ defined by (3.13) by $f_n(z)$ with an increasing number of the coupling elements, i.e. with an increasing number of the interpolation nodes?

Let us take a closer look on the interpolation problem (4.20)

$$f_n(\varphi_j) = \mathbf{U}_j, \quad j = 0, \ldots, n-1, \tag{5.25}$$

where $\varphi_j \in [-\pi, \pi]$ are interpolation nodes, which can be arbitrary but all different, $\mathbf{U}_j$ are unknown displacements at the interpolation nodes. The displacements $\mathbf{U}_j$ are determined through the solution of a global boundary value problem in Ω, it means that they are approximated by the finite element solution, therefore we have the following interpolation problem instead

$$f_n(\varphi_j) = \tilde{\mathbf{U}}_j, \quad j = 0, \ldots, n-1, \tag{5.26}$$

where $\tilde{\mathbf{U}}_j$ denotes the approximated values of displacements. We will call in the sequel the interpolation problem (5.25) the "exact" interpolation problem, and the interpolation problem (5.26) the "approximated" interpolation problem. Correspondingly, we will denote by $f_n(\varphi)$ and $\tilde{f}_n(\varphi)$ the "exact" and the "approximated" interpolation functions. Our goal here is to estimate the error between the exact solution and the "approximated" interpolation function, i.e.

$$|\mathbf{u}(r_A, \varphi) - \tilde{f}_n(\varphi)|,$$

where $\mathbf{u}(r_A, \varphi)$ is the exact solution in Ω_A restricted to the interface Γ_{AD}. Let us rewrite this error as follows

$$
\begin{aligned}
|\mathbf{u}(r_A, \varphi) - \tilde{f}_n(\varphi)| &\leq |\mathbf{u}(r_A, \varphi) - f_n(\varphi) + f_n(\varphi) - \tilde{f}_n(\varphi)| \leq \\
&\leq |\mathbf{u}(r_A, \varphi) - f_n(\varphi)| + |f_n(\varphi) - \tilde{f}_n(\varphi)|,
\end{aligned}
$$

where $|\mathbf{u}(r_A, \varphi) - f_n(\varphi)|$ is the error of the "exact" interpolation, and $|f_n(\varphi) - \tilde{f}_n(\varphi)|$ is the coupling error. The coupling error represents the difference between the "exact" interpolation and the "approximated" interpolation which we have in reality. We will consider these errors separately.

5.5.1 Error of the exact interpolation

We consider the "exact" interpolation problem (5.25). Since in this case the right hand side is given by the exact displacements, which are defined by the exact solution $\mathbf{u}(r_A, \varphi_j)$ on the interface Γ_{AD}. Thus we have the following interpolation problem

$$f_n(\varphi_j) = \mathbf{u}(r_A, \varphi_j), \quad j = 0, \ldots, n-1.$$

This problem corresponds to the classical question of approximation of an analytic function $f(z)$ by its interpolation polynomial $p_n(z)$. Results related to the approximation by

interpolation can be found in [Davis 1975, Gaier 1987]. The main idea is based on the Hermitian representation of an analytic function $f(z)$, see for example [Markushevich 1967].

Let us consider an analytic function $f(z)$ and a set of points $z_1, z_2, \ldots, z_m$ in a domain G. The Hermitian representation of the function $f(z)$ is given by

$$f(z) = \Pi(z) + R(z),$$

where $\Pi(z)$ is the interpolating polynomial of function $f(z)$ satisfying the interpolation conditions at points $z_1, z_2, \ldots, z_m$, and $R(z)$ is the interpolation error. Functions $\Pi(z)$ and $R(z)$ can be represented as the Cauchy-type integrals

$$\Pi(z) = \frac{1}{2\pi i} \int\limits_{\gamma} \frac{f(\zeta)}{\omega(\zeta)} \frac{\omega(\zeta) - \omega(z)}{\zeta - z} d\zeta,$$

$$R(z) = \frac{1}{2\pi i} \int\limits_{\gamma} \frac{f(\zeta)}{\zeta - z} \frac{\omega(z)}{\omega(\zeta)} d\zeta,$$

where γ is a closed rectifiable Jordan curve lying in G and containing the points $z_1, \ldots, z_m$, and $\omega(z)$ is the polynomial defined by

$$\omega(z) = (z - z_1) \cdots (z - z_m).$$

Based on the Hermitian representation the following theorem can be proved:

Theorem 5.7. *[Davis 1975] Let E, S, and G be bounded simply connected regions, $E \subset S \subset G$, whose boundaries are C_E, C_S, and C_G, respectively. C_G is a simple, closed, rectifiable curve, and C_S and C_G are assumed to be disjoint.*

Let $\delta =$ minimum distance from C_G to C_E, $\Delta =$ maximum distance from C_S to C_E and assume that $\frac{\Delta}{\delta} < 1$.

Let the interpolation points lie in R and let $f(z)$ be analytic in and on C_G. Then the interpolation polynomial $p_n(f; z)$ converges to $f(z)$ uniformly in S.

To be able to apply this theorem to our setting we have to perform some intermediate steps, because the interpolation function (4.2) is not a polynomial due to the presence of half-integer powers. To overcome this difficulties we will use the ideas from the proof of the main interpolation theorem 4.1. We introduce the new variable

$$t = e^{i\frac{\varphi}{2}}, \qquad |t| = 1.$$

As we have shown, the interpolation function (4.2) for the case of an even number of nodes can be written as follows

$$f_n(t) = \sum_{k=0}^{\frac{1}{2}n-1} \left[\frac{2k+1}{2} \bar{a}_{2k+1} t^{-2k-1} + a_{2k}\kappa t^{-2k} + k\bar{a}_{2k} t^{-2k} - \right.$$

$$- k\bar{a}_{2k} t^{-2k+4} + a_{2k+1}\kappa t^{2k+1} - a_{2k+1}\kappa t^{-2k-1} +$$

$$\left. + a_{2k}\kappa t^{2k} - \frac{2k+1}{2} \bar{a}_{2k+1} t^{-2k+3} \right],$$

and for the case of an odd number

$$f_n(t) = 2a_0\kappa + \sum_{k=1,2}^{\frac{n-1}{2}} \left[t^{-2k}(a_{2k}\kappa + k\,\bar{a}_{2k}) - k\,\bar{a}_{2k}t^{-2k+4} - \frac{2k-1}{2}\bar{a}_{2k-1}t^{-2k+5} + \right.$$

$$\left. + t^{-2k+1}\left(\frac{2k-1}{2}\bar{a}_{2k-1} - a_{2k-1}\kappa\right) + a_{2k-1}\kappa\,t^{2k-1} + a_{2k}\kappa\,t^{2k} \right].$$

In the both cases the interpolation problem (5.25) can be reformulated in the form

$$P(t_j) = t_j^{n-1}\mathbf{u}(r_A, t_j), \quad j = 0, \dots, n-1,$$

where $P(t)$ is a polynomial of the form

$$P(t) := \sum_{l=0}^{2n-2} \alpha_l t^l.$$

According to the theorem 5.7 we consider a bounded simply connected region E containing all interpolation nodes t_j, and a greater bounded simply connected region G covering E where the function $\mathbf{u}(r,t)$ is analytic, and its boundary is a Jordan curve. Additionally we consider a bounded simply connected region S, such that $E \subset S \subset G$, and the boundaries of these regions are denoted by C_E, C_S, C_G, and C_E and C_S are disjoint.

By using the integral representation of the interpolation error we have

$$R(t) := \mathbf{u}(r_A, t) - P(t) = \frac{1}{2\pi i} \int_{C_G} \frac{(t - t_1)\cdots(t - t_n)\mathbf{u}(r_A, \xi)\,d\xi}{(\xi - t_1)\cdots(\xi - t_n)(\xi - t)}. \tag{5.27}$$

If we denote by $M = \max_{\xi \in C_G} |\mathbf{u}(r_A, \xi)|$, $d = \min_{\xi \in C_G} |\xi - t|$ for $t \in S$, $L(C_G) =$ length of C_G, then with the assumption that the function $\mathbf{u}(r,t)$ is analytic in and on C_G, the interpolation error (5.27) can be estimated as follows

$$|R(t)| \leq \frac{ML(C_G)}{2\pi d}\left(\frac{\Delta}{\delta}\right)^{n+1}, \tag{5.28}$$

where δ is the minimum distance from C_G to C_E, Δ is the maximum distance from C_S to C_E.

To adapt the estimate (5.28) to our settings we need to consider the general properties of the domain Ω and of the triangulation $\mathcal{F}_h$. According to Fig. 5.2 we define C_G as follows

$$C_G = \sup\left(\mathbf{B}_k(\Omega)\right),$$

where $\mathbf{B}_k(\Omega)$ are balls contained in Ω. Since the interpolation nodes are located on the boundary Γ_{AD}, which is represented by a circle of a radius r_A, it seems to be natural to consider C_E, C_S and C_G as circles of greater radii. In this case the estimate will be also true in a domain after a transformation by the new variable t.
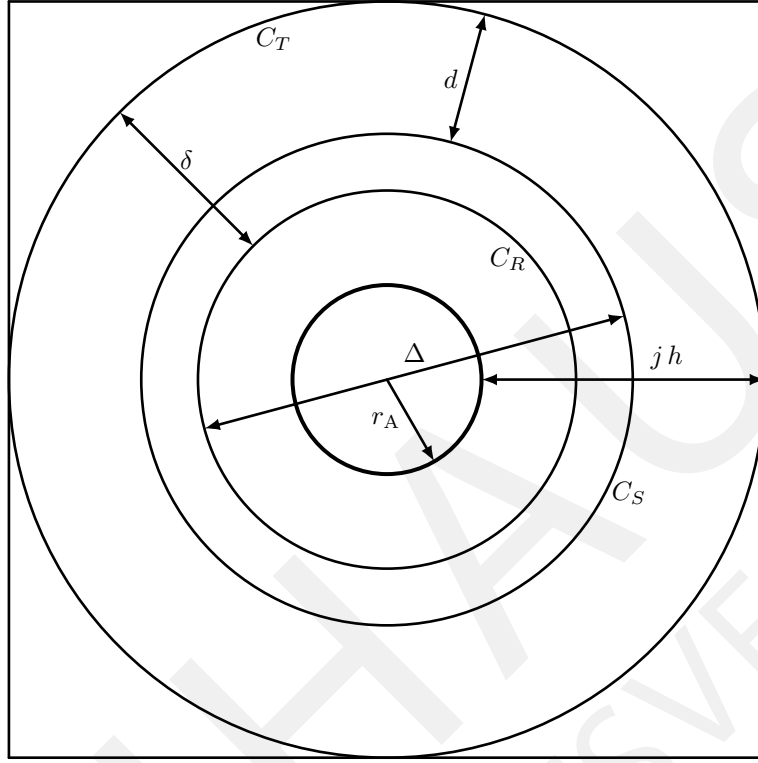
Figure 5.2: Geometrical parameters for the estimate $|R(t)|$

Since we construct the triangulation $\mathcal{F}_h$ with a characteristic size of the standard elements h, and the distance between Ω_A and any boundary of Ω can be expressed by $j\,h$, where $j > 1$. Finally we define the distances from the crack tip O to the boundaries of E, S and G as follows

$$|C_E - O| = r_A + \varepsilon, \quad |C_S - O| = r_A + 2\varepsilon, \quad |C_G - O| = r_A + j\,h,$$

for $\varepsilon > 0$, and the parameters in the estimate (5.28) can be expressed as follows

$$d = j\,h - 2\varepsilon, \quad \delta = j\,h - \varepsilon, \quad \Delta = 2r_A + \varepsilon, \quad L(C_G) = 2\pi(r_A + j\,h).$$

Finally we get the following estimate for our settings

$$|R(t)| \leq \frac{M2\pi(r_A + j\,h)}{2\pi(j\,h - 2\varepsilon)} \left(\frac{2r_A + \varepsilon}{j\,h - \varepsilon}\right)^{n+1} \leq \frac{M(r_A + j\,h)}{j\,h - 2\varepsilon} \left(\frac{2r_A}{j\,h}\right)^{n+1}, \tag{5.29}$$

for $\varepsilon > 0$. From the estimate (5.29) we see that the uniform convergence takes place only if $2r_A < j\,h$, i.e. the diameter of Ω_A must be smaller then the distance from Ω_A to the closest boundary of Ω. Moreover, we can express the fixed radius r_A in terms of the characteristic size h, by using a varying scaling factor $j_1 < j$, which varies with a

105

refinement of the standard mesh around Ω_{SE}. Additionally we say that $\varepsilon = h$, and we get the following estimate

$$|R(t)| \leq \frac{M(j_1 + 2j)}{2j - 4} \left(\frac{j_1}{j}\right)^{n+1},$$

(5.30)

which give us an exponential convergence for the exact boundary data. The quality of the estimate depends on the distance between Ω_{A} to the closest boundary of Ω, since in the case of a greater distance one can take a finer mesh around the special element which leads to a greater number of interpolation nodes.

Remark 10. Let us now for simplicity denote by L_1 the distance from the analytical domain Ω_{A} to the closest boundary of Ω, and let $\varepsilon = \frac{L_1}{4}$. Then the error estimate (5.29) reads as follows

$$|R(t)| \leq \frac{2M(r_A + L_1)}{L_1} \left(\frac{2r_A}{L_1}\right)^{n+1},$$

and the error can be controlled by choosing the optimal ratio $\frac{r_A}{L_1}$ for a given domain Ω.

Thus the estimate (5.30) gives us the desired estimate for the "exact" interpolation problem (5.25). In the next step we will present an alternative proof of the main interpolation theorem, which will play a significant role in the estimation of the coupling error $|f_n(\varphi) - \tilde{f}_n(\varphi)|$.

5.5.2 Alternative proof of the main interpolation theorem

In Chapter 4 we have proved the main interpolation theorem 4.1. But in this subsection we will give an alternative proof for the interpolation theorem. The requirement for the alternative proof comes from the error estimation of the coupling. As we will see in the sequel by using the alternative proof we will be able to obtain the desired error estimate in an elegant way. Let us consider the following theorem:

Theorem 5.8. *For given n arbitrary interpolation nodes $\varphi_j \in [-\pi, \pi]$ and n arbitrary complex numbers y_j there exists a unique function (4.2), such that*

$$f_n(\varphi_j) = y_j, \quad j = 0, \ldots, n-1.$$

(5.31)

Proof. At first we rewrite the interpolation function (4.2) as follows

$$f_n(\varphi) = \sum_{k=0,2}^{N_1} r_{\mathrm{A}}^{\frac{k}{2}} b_k e^{i\varphi\frac{k}{2}} + \sum_{k=0,2}^{N_1} r_{\mathrm{A}}^{\frac{k}{2}} d_k e^{-i\varphi\frac{k}{2}} - \sum_{k=0,2}^{N_1} r_{\mathrm{A}}^{\frac{k}{2}} c_k e^{-i\varphi\left(\frac{k}{2}-2\right)} +$$

$$+ \sum_{k=1,3}^{N_2} r_{\mathrm{A}}^{\frac{k}{2}} b_k e^{i\varphi\frac{k}{2}} - \sum_{k=1,3}^{N_2} r_{\mathrm{A}}^{\frac{k}{2}} f_k e^{-i\varphi\frac{k}{2}} - \sum_{k=1,3}^{N_2} r_{\mathrm{A}}^{\frac{k}{2}} c_k e^{-i\varphi\left(\frac{k}{2}-2\right)},$$

where the new coefficients $b_k, c_k, d_k,$ and f_k are connected with the old coefficients a_k by the following equations

$$b_k = a_k \kappa, \quad c_k = \frac{k}{2}\bar{a}_k, \quad d_k = \frac{b_k}{\kappa} + c_k, \quad f_k = \frac{b_k}{\kappa} - c_k.$$

(5.32)

106

Notice that the coefficients in front of $e^{-i\varphi\left(\frac{k}{2}-2\right)}$ for different values of k belong to, either $e^{i\varphi\frac{k}{2}}$ or to $e^{-i\varphi\frac{k}{2}}$, we can simplify the expression for (4.2) to the following form

$$f_n(\varphi) = \sum_{\substack{k=-N_1, \\ -N_1+2,\dots}}^{N_1} A_k\, e^{i\varphi\frac{k}{2}} + \sum_{\substack{k=-N_2, \\ -N_2+2,\dots}}^{N_2} B_k\, e^{i\varphi\frac{k}{2}}, \tag{5.33}$$

where the coefficients A_k and B_k with help of (5.32) can be related to the original coefficients a_k and $\bar{a}_k$ as follows

$$A_k = \begin{cases} r_{\mathrm{A}}^{\frac{|k|}{2}}\, a_{|k|} + \dfrac{|k|}{2} r_{\mathrm{A}}^{\frac{|k|}{2}}\, \bar{a}_{|k|}, & \text{for } -N_1 \le k < -N_1 + 4, \\[2ex] r_{\mathrm{A}}^{\frac{|k|}{2}}\, a_{|k|} + \dfrac{|k|}{2} r_{\mathrm{A}}^{\frac{|k|}{2}}\, \bar{a}_{|k|} - \dfrac{|k|+4}{2} r_{\mathrm{A}}^{\frac{|k|+4}{2}}\, \bar{a}_{|k|+4}, & \text{for } -N_1 + 4 \le k \le -2, \\[2ex] a_0(\kappa+1) - 2\, r_{\mathrm{A}}^2 \bar{a}_4, & \text{for } k = 0, \\[2ex] \kappa\, r_{\mathrm{A}}\, a_2 - r_{\mathrm{A}}\bar{a}_2, & \text{for } k = 2, \\[2ex] r_{\mathrm{A}}^{\frac{k}{2}}\, \kappa\, a_k, & \text{for } 4 \le k \le N_1, \end{cases} \tag{5.34}$$

and

$$B_k = \begin{cases} -r_{\mathrm{A}}^{\frac{|k|}{2}}\, a_{|k|} + \dfrac{|k|}{2} r_{\mathrm{A}}^{\frac{|k|}{2}}\, \bar{a}_{|k|}, & \text{for } -N_2 \le k < -N_2 + 4, \\[2ex] \dfrac{|k|}{2} r_{\mathrm{A}}^{\frac{|k|}{2}}\, \bar{a}_{|k|} - r_{\mathrm{A}}^{\frac{|k|}{2}}\, a_{|k|} - \dfrac{|k|+4}{2} r_{\mathrm{A}}^{\frac{|k|+4}{2}}\, \bar{a}_{|k|+4}, & \text{for } -N_2 + 4 \le k \le -1, \\[2ex] \kappa\, r_{\mathrm{A}}^{\frac{1}{2}}\, a_1 - \dfrac{3}{2}\, r_{\mathrm{A}}^{\frac{3}{2}}\bar{a}_3, & \text{for } k = 1, \\[2ex] \kappa\, r_{\mathrm{A}}^{\frac{3}{2}}\, a_3 - \dfrac{1}{2}\, r_{\mathrm{A}}^{\frac{1}{2}}\bar{a}_1, & \text{for } k = 3, \\[2ex] \kappa\, r_{\mathrm{A}}^{\frac{k}{2}}\, a_k, & \text{for } 5 \le k \le N_2. \end{cases} \tag{5.35}$$

The interpolation function (5.33) contains $2n - 1$ coefficients, but we have only n interpolation nodes, therefore we have to find $n - 1$ additional relations which should help us to identify uniquely the coefficients A_k and B_k. This problem can be overcome by studying equations (5.34)-(5.35). One can observe that the coefficients $A_{-|k|}$ and $B_{-|k|}$ can be expressed in terms of the coefficients $A_{|k|}$ and $B_{|k|}$, respectively. We get the following

equations

$$
A_{-|k|} = \begin{cases} \kappa^{-1} A_{|k|} + \dfrac{|k|}{2}\kappa^{-1}\bar{A}_{|k|}, & \text{for } -N_1 \le k < -N_1 + 4, \\[2ex] \kappa^{-1} A_{|k|} + \dfrac{|k|}{2}\kappa^{-1}\bar{A}_{|k|} - \dfrac{|k|+4}{2}\kappa^{-1}\bar{A}_{|k|+4}, & \text{for } -N_1 + 4 \le k \le -4, \\[2ex] (\kappa-1)^{-1}\left[A_2 + \kappa^{-1}\bar{A}_2\right] + (\kappa-1)^{-1}\left[\bar{A}_2 + \kappa^{-1} A_2\right] - \\ -3\kappa^{-1}\bar{A}_6, & \text{for } k = -2, \end{cases} \tag{5.36}
$$

and

$$
B_{-|k|} = \begin{cases} -\kappa^{-1} B_{|k|} + \dfrac{|k|}{2}\kappa^{-1}\bar{B}_{|k|}, \text{ for } -N_2 \le k < -5, \\[2ex] -r_{\mathrm{A}}^{\frac{3}{2}}\left(\kappa B_3 + \dfrac{1}{2}\bar{B}_1\right)\left(\kappa^2 r_{\mathrm{A}}^{\frac{3}{2}} - \dfrac{3}{4}r_{\mathrm{A}}^{\frac{3}{2}}\right)^{-1} + \\[2ex] +\dfrac{3}{2}r_{\mathrm{A}}^{\frac{3}{2}}\left(\kappa\bar{B}_3 + \dfrac{1}{2}B_1\right)\left(\kappa^2 r_{\mathrm{A}}^{\frac{3}{2}} - \dfrac{3}{4}r_{\mathrm{A}}^{\frac{3}{2}}\right)^{-1} - \dfrac{7}{2}\kappa^{-1}\bar{B}_7, \text{ for } k = -3, \\[2ex] -\dfrac{1}{2}\kappa^{-1} B_1 - \dfrac{3}{2}\kappa^{-1}r_{\mathrm{A}}^{\frac{3}{2}}\left(\kappa\bar{B}_3 + \dfrac{1}{2}B_1\right)\left(\kappa^2 r_{\mathrm{A}}^{\frac{3}{2}} - \dfrac{3}{4}r_{\mathrm{A}}^{\frac{3}{2}}\right)^{-1} + \\[2ex] +\dfrac{3}{4}r_{\mathrm{A}}^{\frac{3}{2}}\left(\kappa B_3 + \dfrac{1}{2}\bar{B}_1\right)\left(\kappa^2 r_{\mathrm{A}}^{\frac{3}{2}} - \dfrac{3}{4}r_{\mathrm{A}}^{\frac{3}{2}}\right)^{-1} - \dfrac{5}{2}\kappa^{-1}\bar{B}_5, \text{ for } k = -1. \end{cases} \tag{5.37}
$$

Finally we combine two sums in (5.33) into one sum

$$
f_n(\varphi) = \sum_{k=0}^{n-1} c_k\, e^{i\varphi\frac{k}{2}},
$$

with the coefficients c_k defined by

$$
c_k = \begin{cases} A_k, & \text{if } k \text{ is even,} \\ B_k, & \text{if } k \text{ is odd.} \end{cases}
$$

Thus we have obtained an equivalent interpolation problem

$$
\sum_{k=0}^{n-1} c_k\, e^{i\varphi_j\frac{k}{2}} = y_j, \quad j = 0,\ldots,n-1, \tag{5.38}
$$

with exactly n unknown coefficients c_k. The matrix of the equivalent interpolation problem is a Vandermonde matrix, and its determinant is given by

$$
\mathbf{det}(F) = \prod_{1 \le j < k \le n} (e^{i\frac{1}{2}\varphi_k} - e^{i\frac{1}{2}\varphi_j}) \ne 0,
$$

where by F we denote the interpolation matrix. The product in this determinant is not equal to zero due to the assumption on the interpolation nodes.

Thus the interpolation problem (5.38) is uniquely solvable for an arbitrary number of nodes, and for an arbitrary right hand side, i.e. we can uniquely identify the coefficients c_k, and consequently A_k and B_k for all values of k.

The next step in this proof is to show that from the coefficients A_k and B_k we can uniquely calculate the original coefficients a_k and $\bar{a}_k$. The important point here is that the coefficients a_k and $\bar{a}_k$ are connected by the complex conjugation, and therefore the transformation must preserve these dependencies. To overcome this problem we decompose all of the coefficients into real and imaginary parts as follows

$$
\begin{aligned}
a_k &= a_k^{(1)} + i a_k^{(2)}, \quad \bar{a}_k = a_k^{(1)} - i a_k^{(2)}, \\[4pt]
A_k &= A_k^{(1)} + i A_k^{(2)}, \quad \bar{A}_k = A_k^{(1)} - i A_k^{(2)}, \\[4pt]
B_k &= B_k^{(1)} + i B_k^{(2)}, \quad \bar{B}_k = B_k^{(1)} - i B_k^{(2)}.
\end{aligned}
$$

After that the formulae (5.34)-(5.35) can be rewritten as follows

$$
A_k^{(1)} = \begin{cases}
a_{|k|}^{(1)} \, r_{\mathrm{A}}^{\frac{|k|}{2}} \left(1 + \dfrac{|k|}{2} \right), & \text{for } -N_1 \le k < -N_1 + 4, \\[10pt]
a_{|k|}^{(1)} \, r_{\mathrm{A}}^{\frac{|k|}{2}} \left(1 + \dfrac{|k|}{2} \right) - \dfrac{|k|+4}{2} r_{\mathrm{A}}^{\frac{|k|+4}{2}} a_{|k|+4}^{(1)}, & \text{for } -N_1 + 4 \le k \le -2, \\[10pt]
a_0^{(1)}(\kappa + 1) - 2\, r_{\mathrm{A}}^2 \bar{a}_4^{(1)}, & \text{for } k = 0, \\[10pt]
r_{\mathrm{A}}\, a_2^{(1)}(\kappa - 1), & \text{for } k = 2, \\[10pt]
r_{\mathrm{A}}^{\frac{k}{2}} \kappa\, a_k^{(1)}, & \text{for } 4 \le k \le N_1,
\end{cases}
$$

$$
A_k^{(2)} = \begin{cases}
a_{|k|}^{(2)} \, r_{\mathrm{A}}^{\frac{|k|}{2}} \left(1 - \dfrac{|k|}{2} \right), & \text{for } -N_1 \le k < -N_1 + 4, \\[10pt]
a_{|k|}^{(2)} \, r_{\mathrm{A}}^{\frac{|k|}{2}} \left(1 - \dfrac{|k|}{2} \right) + \dfrac{|k|+4}{2} r_{\mathrm{A}}^{\frac{|k|+4}{2}} a_{|k|+4}^{(2)}, & \text{for } -N_1 + 4 \le k \le -2, \\[10pt]
a_0^{(2)}(\kappa + 1) + 2\, r_{\mathrm{A}}^2 \bar{a}_4^{(2)}, & \text{for } k = 0, \\[10pt]
r_{\mathrm{A}}\, a_2^{(2)}(\kappa + 1), & \text{for } k = 2, \\[10pt]
r_{\mathrm{A}}^{\frac{k}{2}} \kappa\, a_k^{(2)}, & \text{for } 4 \le k \le N_1,
\end{cases}
$$

$$
B_k^{(1)} = \begin{cases}
r_{\mathrm{A}}^{\frac{|k|}{2}}\, a_{|k|}^{(1)} \left(\dfrac{|k|}{2} - 1 \right), & \text{for } -N_2 \le k < -N_2 + 4, \\[3mm]
r_{\mathrm{A}}^{\frac{|k|}{2}}\, a_{|k|}^{(1)} \left(\dfrac{|k|}{2} - 1 \right) - \dfrac{|k|+4}{2}\, r_{\mathrm{A}}^{\frac{|k|+4}{2}} a_{|k|+4}^{(1)}, & \text{for } -N_2 + 4 \le k \le -1, \\[3mm]
\kappa\, r_{\mathrm{A}}^{\frac{1}{2}}\, a_1^{(1)} - \dfrac{3}{2}\, r_{\mathrm{A}}^{\frac{3}{2}}\, a_3^{(1)}, & \text{for } k = 1, \\[3mm]
\kappa\, r_{\mathrm{A}}^{\frac{3}{2}}\, a_3^{(1)} - \dfrac{1}{2}\, r_{\mathrm{A}}^{\frac{1}{2}} a_1^{(1)}, & \text{for } k = 3, \\[3mm]
\kappa\, r_{\mathrm{A}}^{\frac{k}{2}}\, a_k^{(1)}, & \text{for } 5 \le k \le N_2,
\end{cases}
$$

$$
B_k^{(2)} = \begin{cases}
-r_{\mathrm{A}}^{\frac{|k|}{2}}\, a_{|k|}^{(2)} \left(\dfrac{|k|}{2} + 1 \right), & \text{for } -N_2 \le k < -N_2 + 4, \\[3mm]
r_{\mathrm{A}}^{\frac{|k|}{2}}\, a_{|k|}^{(2)} \left(\dfrac{|k|}{2} + 1 \right) + \dfrac{|k|+4}{2}\, r_{\mathrm{A}}^{\frac{|k|+4}{2}} a_{|k|+4}^{(2)}, & \text{for } -N_2 + 4 \le k \le -1, \\[3mm]
\kappa\, r_{\mathrm{A}}^{\frac{1}{2}}\, a_1^{(2)} + \dfrac{3}{2}\, r_{\mathrm{A}}^{\frac{3}{2}}\, a_3^{(2)}, & \text{for } k = 1, \\[3mm]
\kappa\, r_{\mathrm{A}}^{\frac{3}{2}}\, a_3^{(2)} + \dfrac{1}{2}\, r_{\mathrm{A}}^{\frac{1}{2}} a_1^{(2)}, & \text{for } k = 3, \\[3mm]
\kappa\, r_{\mathrm{A}}^{\frac{k}{2}}\, a_k^{(2)}, & \text{for } 5 \le k \le N_2.
\end{cases}
$$

By using the relations (5.36)-(5.37) we get all of the coefficients A_k, B_k for $k < 0$ in terms of combinations of the coefficients for $k > 0$. Therefore we get the transformation from

$a_k, \bar{a}_k$ to A_k, B_k in a matrix form as follows

$$
\begin{pmatrix}
A_0^{(1)} \\
A_0^{(2)} \\
B_1^{(1)} \\
B_1^{(2)} \\
\vdots \\
B_{N_2}^{(1)} \\
B_{N_2}^{(2)} \\
A_{N_1}^{(1)} \\
A_{N_1}^{(2)}
\end{pmatrix}
= M
\begin{pmatrix}
a_0^{(1)} \\
a_0^{(2)} \\
a_1^{(1)} \\
a_1^{(2)} \\
\vdots \\
a_{N_2}^{(1)} \\
a_{N_2}^{(2)} \\
a_{N_1}^{(1)} \\
a_{N_1}^{(2)}
\end{pmatrix},
$$

where the matrix M has the following structure

$$
M =
\begin{pmatrix}
\kappa+1 & 0 & 0 & 0 & 0 & 0 & 0 & 0 & \dots & 0 & 0 & 0 & 0 \\
0 & \kappa+1 & 0 & 0 & 0 & 0 & 0 & 0 & \dots & 0 & 0 & 0 & 0 \\
0 & 0 & \kappa\, r_{\mathrm{A}}^{\frac{1}{2}} & 0 & 0 & 0 & -\frac{3}{2} r_{\mathrm{A}}^{\frac{1}{2}} & 0 & \dots & 0 & 0 & 0 & 0 \\
0 & 0 & 0 & \kappa\, r_{\mathrm{A}}^{\frac{1}{2}} & 0 & 0 & 0 & \frac{3}{2} r_{\mathrm{A}}^{\frac{1}{2}} & \dots & 0 & 0 & 0 & 0 \\
0 & 0 & 0 & 0 & r_{\mathrm{A}}(\kappa-1) & 0 & 0 & 0 & \dots & 0 & 0 & 0 & 0 \\
0 & 0 & 0 & 0 & 0 & r_{\mathrm{A}}(\kappa+1) & 0 & 0 & \dots & 0 & 0 & 0 & 0 \\
0 & 0 & -\frac{1}{2} r_{\mathrm{A}}^{\frac{1}{2}} & 0 & 0 & 0 & \kappa\, r_{\mathrm{A}}^{\frac{3}{2}} & 0 & \dots & 0 & 0 & 0 & 0 \\
0 & 0 & 0 & \frac{1}{2} r_{\mathrm{A}}^{\frac{1}{2}} & 0 & 0 & 0 & \kappa\, r_{\mathrm{A}}^{\frac{3}{2}} & \dots & 0 & 0 & 0 & 0 \\
\vdots & \vdots & \vdots & \vdots & \vdots & \vdots & \vdots & \vdots & \ddots & \vdots & \vdots & \vdots & \vdots \\
0 & 0 & 0 & 0 & 0 & 0 & 0 & 0 & \dots & \kappa\, r_{\mathrm{A}}^{\frac{N_2}{2}} & 0 & 0 & 0 \\
0 & 0 & 0 & 0 & 0 & 0 & 0 & 0 & \dots & 0 & \kappa\, r_{\mathrm{A}}^{\frac{N_2}{2}} & 0 & 0 \\
0 & 0 & 0 & 0 & 0 & 0 & 0 & 0 & \dots & 0 & 0 & \kappa\, r_{\mathrm{A}}^{\frac{N_1}{2}} & 0 \\
0 & 0 & 0 & 0 & 0 & 0 & 0 & 0 & \dots & 0 & 0 & 0 & \kappa\, r_{\mathrm{A}}^{\frac{N_1}{2}}
\end{pmatrix}.
$$

The dimension of the transformation matrix M is $\dim(M) = 2n \times 2n$, depending on even or odd number of the interpolation nodes we will have either the coefficients corresponding to $A_{N_1}^{(1)}, A_{N_1}^{(2)}$ or $B_{N_2}^{(1)}, B_{N_2}^{(2)}$ in the last row of the matrix M. Now we will show that the transformation matrix has a non-zero determinant. If we rearrange the rows and columns of the matrix M in order to have at first equations corresponding to the coefficients $B_1^{(1)}, B_1^{(2)}, B_3^{(1)}, B_3^{(2)}$, we see that the determinant $\mathbf{det}(M)$ can be decomposed

by the rows $5, \ldots, 2n$, and we obtain

$$\mathbf{det}(M) = \left(\prod_{i=5}^{2n} M_{ii} \right) \cdot |M_4|,$$

where the matrix M_4 is given by

$$M_4 = \begin{pmatrix} \kappa\, r_{\mathrm{A}}^{\frac{1}{2}} & 0 & -\frac{3}{2} r_{\mathrm{A}}^{\frac{3}{2}} & 0 \\ 0 & \kappa\, r_{\mathrm{A}}^{\frac{1}{2}} & 0 & -\frac{3}{2} r_{\mathrm{A}}^{\frac{3}{2}} \\ -\frac{1}{2} r_{\mathrm{A}}^{\frac{1}{2}} & 0 & \kappa\, r_{\mathrm{A}}^{\frac{3}{2}} & 0 \\ 0 & \frac{1}{2} r_{\mathrm{A}}^{\frac{1}{2}} & 0 & \kappa\, r_{\mathrm{A}}^{\frac{3}{2}} \end{pmatrix}.$$

The determinant of this matrix can be calculated explicitly

$$|M_4| = \frac{1}{16} r_{\mathrm{A}}^4 (4\kappa - 3)^2.$$

Finally we obtain the following expression for the determinant

$$\mathbf{det}(M) = \frac{1}{16} r_{\mathrm{A}}^4 (4\kappa - 3)^2 \prod_{i=5}^{2n} M_{ii}. \tag{5.39}$$

Looking at the structure of the transformation M we see, that the entries M_{ij}, and particularly M_{ii}, depend only on parameters N_1, N_2, r_{A}, and κ, which by their definition are all positive. Therefore the product in (5.39) cannot be equal to zero.

The remaining part is to discuss the determinant $|M_4|$, which contains $(4\kappa - 3)^2$. The parameter κ is a material constant, which is related to the Poisson's ratio ν as follows

$$\kappa = \begin{cases} 3 - 4\nu & \text{for plane strain,} \\ \dfrac{3 - \nu}{1 + \nu} & \text{for plane stress.} \end{cases}$$

Taking into account that $\nu \in (0, \frac{1}{2})$ one can easily see that $\kappa \in (1, 3)$, and therefore

$$(4\kappa - 3)^2 \neq 0.$$

Thus we have shown, that the determinant $\mathbf{det}(M)$ is not equal to zero, and therefore the transformation matrix has an inverse for an odd number of nodes. The case of an even number of nodes is analogous.

Finally we have proved that interpolation problem (5.31) is uniquely solvable for an arbitrary number of interpolation nodes and for an arbitrary right hand side. $\qquad\square$

5.5.3 The coupling error

Our interest now is to estimate the difference $|f_n(\varphi) - \tilde{f}_n(\varphi)|$ between the "approximated" and the "exact" interpolation function. Let us denote by $\boldsymbol{\Phi} = \{\Phi_1, \Phi_2, \ldots, \Phi_n\}$ a vector of the basis functions corresponding to (4.2), then the "approximated" and the "exact" interpolation functions are given by

$$f_n(\varphi) = [a]^T \boldsymbol{\Phi}, \qquad \tilde{f}_n(\varphi) = [\tilde{a}]^T \boldsymbol{\Phi},$$

where $[a]$ and $[\tilde{a}]$ are the vectors of unknown coefficients corresponding to the interpolation problems (5.25)-(5.26), respectively. These vectors of the unknown coefficients can be expressed as follows

$$a = [\Phi_k(\varphi_j)]^{-1} \mathbf{U}, \qquad \tilde{a} = [\Phi_k(\varphi_j)]^{-1} \tilde{\mathbf{U}},$$

where $\mathbf{U}$ and $\tilde{\mathbf{U}}$ are vectors of the "exact" and the "approximated" displacements. Let us introduce the following notation

$$\mathbf{G} = [\mathrm{G}]_{kj} = [\Phi_k(\varphi_j)]^{-1}$$

for the inverse of the interpolation matrix. Now we can write

$$|f_n(\varphi) - \tilde{f}_n(\varphi)| = |[a]^T \boldsymbol{\Phi} - [\tilde{a}]^T \boldsymbol{\Phi}| = \left|[\mathbf{G}\,\mathbf{U}]^T \boldsymbol{\Phi} - \left[\mathbf{G}\,\tilde{\mathbf{U}}\right]^T \boldsymbol{\Phi}\right| =$$

$$= \left|\mathbf{U}^T \mathbf{G}^T \boldsymbol{\Phi} - \tilde{\mathbf{U}}^T \mathbf{G}^T \boldsymbol{\Phi}\right| = \left|\left(\mathbf{U}^T - \tilde{\mathbf{U}}^T\right) \mathbf{G}^T \boldsymbol{\Phi}\right|.$$

Let us introduce the constant δ^* as follows

$$|\mathbf{U}_j - \tilde{\mathbf{U}}_j| \leq \delta^*, \quad j = 0, \ldots, n-1,$$

this inequality implies, that the coupling error explicitly depends only on the quality of approximation for the displacements at the interface Γ_{AD}, which is seems to be a natural assumption. We have

$$|f_n(\varphi) - \tilde{f}_n(\varphi)| \leq \delta^* \left|\mathbf{G}^T \boldsymbol{\Phi}\right|, \tag{5.40}$$

thus we need to estimate the transposed inverse of interpolation matrix $\mathbf{G}^T$ and the vector of the basis functions $\boldsymbol{\Phi}$.

We start the construction of the coupling estimate by considering the matrix $[\mathrm{G}]_{kj}$. As an estimate we will use the spectral norm of the matrix, which is defined as follows, see for instance [Gantmacher 1966, Phillips & Taylor 1996]:

Definition 5.6. The spectral norm of a matrix A is defined by

$$\|A\|_2 = \sqrt{\rho(A\,A^*)},$$

where $\rho(A\,A^*)$ is the spectral radius of $A\,A^*$ defined as follows

$$\rho(A\,A^*) = \max_{1 \leq i \leq n} |\lambda_i|,$$

where $\lambda_1, \lambda_2, \ldots, \lambda_n$ are the eigenvalues of $A\,A^*$.

Bounds for the eigenvalues are given by the Gerschgorin's theorems:

Theorem 5.9. *[Gerschgorin 1931, Phillips & Taylor 1996] The eigenvalues of an $n \times n$ matrix A lie within the union of n (Gerschgorin) disks D_i in the complex plane with centre a_{ii} and radius*

$$\Lambda_i = \sum_{\substack{j=1, \\ j \neq i}}^{n} |a_{ij}|, \quad i = 1, 2, \ldots, n.$$

Thus D_i is the set of points $z \in \mathbb{C}$ given by

$$|z - a_{ii}| \leq \Lambda_i, \quad i = 1, 2, \ldots, n.$$

Theorem 5.10. *[Gerschgorin 1931, Phillips & Taylor 1996] If s of the Gerschgorin disks in the complex plane form a connected domain which is isolated from the remaining $n - s$ disks, then there are precisely s eigenvalues of A within this connected domain.*

The matrix $[\Phi_k(\varphi_j)]^{-1}$ obtained from the basis function in the form (4.2) is not diagonally dominant, and therefore its Gerschgorin disks will not give us the isolated regions for the eigenvalues. To make the estimates more precise we will work with the transformation matrix M and with the Vandermonde matrix F which were introduced in the alternative proof of the main interpolation theorem. In this case the coefficients a_k and $\tilde{a}_k$ can be calculated as follows

$$a = M^{-1} F^{-1} \mathbf{U}, \qquad \tilde{a} = M^{-1} F^{-1} \tilde{\mathbf{U}},$$

and the estimate (5.40) has the following form

$$|f_n(\varphi) - \tilde{f}_n(\varphi)| \leq \delta^* \left| M^{-1} F^{-1} \mathbf{\Phi} \right| \leq \delta^* \left\| M^{-1} \right\|_2 \left\| F^{-1} \right\|_2 \left\| \mathbf{\Phi} \right\|_2, \tag{5.41}$$

and the remaining task is to estimate the spectral norms of M^{-1} and F^{-1}, and the norm of $\mathbf{\Phi}$.

Let us at first study the matrix M. The spectral norm of the inverse matrix can be calculated as follows

$$\|M^{-1}\|_2 = \sqrt{\rho \left([M^{-1}]^T M^{-1} \right)} = \sqrt{\rho \left([M M^T]^{-1} \right)} = \sqrt{\left(\min_{1 \leq i \leq n} |\lambda_i| \right)^{-1}},$$

where $\lambda_1, \lambda_2, \ldots, \lambda_n$ are the eigenvalues of $M M^T$.

Taking into account the structure of the matrix M one can verify by straightforward calculations, that the matrix $M M^T$ has the following form

$$\left[M M^T \right]_{ij} = \begin{cases} (M_{ii})^2 & \text{for} \quad i = j = 1, 2, 11, 12, \ldots, 2\,n, \\ m_{ij} & \text{for} \quad i, j = 3, \ldots, 10, \end{cases}$$

114

and the submatrix m is explicitly given by

$$m = \begin{pmatrix}
\frac{1}{4}r_{\mathrm{A}}(4\kappa^2+9r_{\mathrm{A}}^2) & 0 & 0 & 0 & \dots \\
0 & \frac{1}{4}r_{\mathrm{A}}(4\kappa^2+9r_{\mathrm{A}}^2) & 0 & 0 & \dots \\
0 & 0 & r_{\mathrm{A}}^2(\kappa^2-2\kappa+1+4r_{\mathrm{A}}^2) & 0 & \dots \\
0 & 0 & 0 & r_{\mathrm{A}}^2(\kappa^2+2\kappa+1+4r_{\mathrm{A}}^2) & \dots \\
-\frac{1}{2}\kappa\,r_{\mathrm{A}}(1+3r_{\mathrm{A}}^2) & 0 & 0 & 0 & \dots \\
0 & \frac{1}{2}\kappa\,r_{\mathrm{A}}(1+3r_{\mathrm{A}}^2) & 0 & 0 & \dots \\
0 & 0 & -2r_{\mathrm{A}}^4\,\kappa & 0 & \dots \\
0 & 0 & 0 & 2r_{\mathrm{A}}^4\,\kappa & \dots
\end{pmatrix} \tag{5.42}$$

$$\begin{pmatrix}
\dots & -\frac{1}{2}\kappa\,r_{\mathrm{A}}(1+3r_{\mathrm{A}}^2) & 0 & 0 & 0 \\
\dots & 0 & \frac{1}{2}\kappa\,r_{\mathrm{A}}(1+3r_{\mathrm{A}}^2) & 0 & 0 \\
\dots & 0 & 0 & -2r_{\mathrm{A}}^4\,\kappa & 0 \\
\dots & 0 & 0 & 0 & 2r_{\mathrm{A}}^4\,\kappa \\
\dots & \frac{1}{4}r_{\mathrm{A}}(1+4\kappa^2\,r_{\mathrm{A}}^2) & 0 & 0 & 0 \\
\dots & 0 & \frac{1}{4}r_{\mathrm{A}}(1+4\kappa^2\,r_{\mathrm{A}}^2) & 0 & 0 \\
\dots & 0 & 0 & r_{\mathrm{A}}^4\,\kappa^2 & 0 \\
\dots & 0 & 0 & 0 & r_{\mathrm{A}}^4\,\kappa^2
\end{pmatrix} \tag{5.43}$$

Thus the $2n - 8$ eigenvalues of the matrix $M\,M^T$ are given by

$$\lambda_i = (M_{ii})^2, \, i = 1, 2, 11, 12, \dots, 2\,n,$$

or by taking into account the form of elements M_{ii}

$$\lambda_{1,2} = (\kappa + 1)^2,$$

$$\lambda_i = \begin{cases} \kappa^2\,r_{\mathrm{A}}^{\frac{i-1}{2}}, & \text{if } i \text{ is odd,} \\[2mm] \kappa^2\,r_{\mathrm{A}}^{\frac{i-2}{2}}, & \text{if } i \text{ is even,} \end{cases} \quad i = 11, \dots, 2\,n.$$

The remaining eight eigenvalues are the eigenvalues of the matrix (5.42)-(5.43), which are

explicitly given by

$$\lambda_3 = \frac{1}{2}r_\mathrm{A}^2 \left(\kappa^2 r_\mathrm{A}^2 + \kappa^2 + 2\kappa + 1 + 4r_\mathrm{A}^2 + \left(\kappa^2 - 2\kappa^2 r_\mathrm{A} + \kappa^2 r_\mathrm{A}^2 + 2\kappa + 1 - 2\kappa\, r_\mathrm{A} + 4r_\mathrm{A}^2 \right)^{\frac{1}{2}} \right.$$
$$\left. \left(\kappa^2 + 2\kappa^2 r_\mathrm{A} + \kappa^2 r_\mathrm{A}^2 + 2\kappa + 1 + 2\kappa\, r_\mathrm{A} + 4r_\mathrm{A}^2 \right)^{\frac{1}{2}} \right),$$

$$\lambda_4 = \frac{1}{2}r_\mathrm{A}^2 \left(\kappa^2 r_\mathrm{A}^2 + \kappa^2 + 2\kappa + 1 + 4r_\mathrm{A}^2 - \left(\kappa^2 - 2\kappa^2 r_\mathrm{A} + \kappa^2 r_\mathrm{A}^2 + 2\kappa + 1 - 2\kappa\, r_\mathrm{A} + 4r_\mathrm{A}^2 \right)^{\frac{1}{2}} \right.$$
$$\left. \left(\kappa^2 + 2\kappa^2 r_\mathrm{A} + \kappa^2 r_\mathrm{A}^2 + 2\kappa + 1 + 2\kappa\, r_\mathrm{A} + 4r_\mathrm{A}^2 \right)^{\frac{1}{2}} \right),$$

$$\lambda_5 = \frac{1}{2}r_\mathrm{A}^2 \left(\kappa^2 r_\mathrm{A}^2 + \kappa^2 - 2\kappa + 1 + 4r_\mathrm{A}^2 + \left(\kappa^2 - 2\kappa^2 r_\mathrm{A} + \kappa^2 r_\mathrm{A}^2 - 2\kappa + 1 + 2\kappa\, r_\mathrm{A} + 4r_\mathrm{A}^2 \right)^{\frac{1}{2}} \right.$$
$$\left. \left(\kappa^2 + 2\kappa^2 r_\mathrm{A} + \kappa^2 r_\mathrm{A}^2 - 2\kappa + 1 - 2\kappa\, r_\mathrm{A} + 4r_\mathrm{A}^2 \right)^{\frac{1}{2}} \right),$$

$$\lambda_6 = \frac{1}{2}r_\mathrm{A}^2 \left(\kappa^2 r_\mathrm{A}^2 + \kappa^2 - 2\kappa + 1 + 4r_\mathrm{A}^2 - \left(\kappa^2 - 2\kappa^2 r_\mathrm{A} + \kappa^2 r_\mathrm{A}^2 - 2\kappa + 1 + 2\kappa\, r_\mathrm{A} + 4r_\mathrm{A}^2 \right)^{\frac{1}{2}} \right.$$
$$\left. \left(\kappa^2 + 2\kappa^2 r_\mathrm{A} + \kappa^2 r_\mathrm{A}^2 - 2\kappa + 1 - 2\kappa\, r_\mathrm{A} + 4r_\mathrm{A}^2 \right)^{\frac{1}{2}} \right),$$

$$\lambda_{7,9} = \frac{1}{8}r_\mathrm{A} \left(9r_\mathrm{A}^2 + 4\kappa^2 r_\mathrm{A}^2 + 1 + 4\kappa^2 + \left(4\kappa^2 - 8\kappa^2 r_\mathrm{A} + 4\kappa^2 r_\mathrm{A}^2 + 1 + 6r_\mathrm{A} + 9r_\mathrm{A}^2 \right)^{\frac{1}{2}} \right.$$
$$\left. \left(4\kappa^2 + 8\kappa^2 r_\mathrm{A} + 4\kappa^2 r_\mathrm{A}^2 + 1 - 6r_\mathrm{A} + 9r_\mathrm{A}^2 \right)^{\frac{1}{2}} \right),$$

$$\lambda_{8,10} = \frac{1}{8}r_\mathrm{A} \left(9r_\mathrm{A}^2 + 4\kappa^2 r_\mathrm{A}^2 + 1 + 4\kappa^2 - \left(4\kappa^2 - 8\kappa^2 r_\mathrm{A} + 4\kappa^2 r_\mathrm{A}^2 + 1 + 6r_\mathrm{A} + 9r_\mathrm{A}^2 \right)^{\frac{1}{2}} \right.$$
$$\left. \left(4\kappa^2 + 8\kappa^2 r_\mathrm{A} + 4\kappa^2 r_\mathrm{A}^2 + 1 - 6r_\mathrm{A} + 9r_\mathrm{A}^2 \right)^{\frac{1}{2}} \right).$$

As we see the eigenvalues $\lambda_i, i = 1, \ldots, 2\,n$ depend on the only two parameters r_A and κ. Since the parameter r_A is the radius of the analytical domain Ω_A, for practical calculations we can always use a normalised radius, i.e. $r_\mathrm{A} = 1$. For the normalised radius all possible

eigenvalues have the following form

$$\lambda_{1,2} = (\kappa + 1)^2,$$

$$\lambda_3 = \kappa^2 + \kappa + \frac{5}{2} + \frac{1}{2}\sqrt{20\kappa^2 + 20\kappa + 25},$$

$$\lambda_4 = \kappa^2 + \kappa + \frac{5}{2} - \frac{1}{2}\sqrt{20\kappa^2 + 20\kappa + 25},$$

$$\lambda_5 = \kappa^2 - \kappa + \frac{5}{2} + \frac{1}{2}\sqrt{20\kappa^2 - 20\kappa + 25},$$

$$\lambda_6 = \kappa^2 - \kappa + \frac{5}{2} - \frac{1}{2}\sqrt{20\kappa^2 - 20\kappa + 25},$$

$$\lambda_{7,9} = \frac{5}{4} + \kappa^2 + \frac{1}{8}\sqrt{256\kappa^2 + 64},$$

$$\lambda_{8,10} = \frac{5}{4} + \kappa^2 - \frac{1}{8}\sqrt{256\kappa^2 + 64},$$

$$\lambda_i = \kappa^2, \quad i = 11, \ldots, 2\, n.$$

It's easy to check that these eigenvalues are ordered as follows

$$\lambda_6 < \lambda_{8,10} < \lambda_4 < \lambda_i < \lambda_{1,2,5,7,9} < \lambda_3,$$

therefore the smallest eigenvalue for $\kappa \in (1,3)$ is λ_6. Thus the spectral norm of M^{-1} is given by

$$\|M^{-1}\|_2 = \sqrt{\lambda_6^{-1}} = \frac{1}{\sqrt{\kappa^2 - \kappa + \frac{5}{2} - \frac{1}{2}\sqrt{20\kappa^2 - 20\kappa + 25}}}. \tag{5.44}$$

The obtained estimate for the spectral norm of M^{-1} is uniform, i.e. it's independent on the number of interpolation nodes n for $n > 3$.

Now we will construct the estimate for the spectral norm of F^{-1}, where the matrix F is a Vandermonde matrix. Let us consider arbitrary interpolation nodes $j_l \in [-\pi, \pi]$, then the entries of the matrix F can be written as

$$F_{j_l k} = e^{\frac{1}{2}i\frac{2\pi}{n-1}j_l k}, \qquad l = -\frac{n-1}{2}, \ldots, \frac{n-1}{2}, \quad k = 0, \ldots, n-1.$$

In the construction of the estimate we will work with the conjugate of the interpolation matrix, and additionally we rescale the entries of the matrix as follows

$$T_{lk} := \frac{1}{\sqrt{n}}e^{-\frac{1}{2}i\frac{2\pi}{n-1}j_l k}.$$

117

This matrix is also a Vandermonde matrix, and it can be considered as a Fourier matrix for a signal x. Let $\hat{x}$ be its Fourier transform, defined by $\hat{x} = T x$. We will use this relation to the Discrete Fourier Transform later on in the construction of the estimate.

Our goal here is to get estimates for the eigenvalues of the matrix $T T^H$, so we have

$$\left(T T^H\right)_{ab} = \sum_{k=0}^{n-1} F_{j_a k} F^*_{k j_b} = \frac{1}{n} \sum_{k=0}^{n-1} \omega^{\frac{1}{2}(j_a - j_b)k},$$

where

$$\omega = e^{-i \frac{2\pi}{n-1}}.$$

Following [Ferreira 1999] we rewrite the matrix $T T^H$ as follows

$$N = [N_{pq}]_{p,q=0}^{n-1} = [s(j_p - j_q)]_{p,q=0}^{n-1},$$

where

$$s(x) = \frac{1}{n} \sum_{k=0}^{n-1} \omega^{\frac{1}{2}k x}.$$

The introduced matrix N is not diagonally dominant, therefore its Gerschgorin disks are not suitable for getting the estimates. To overcome this problem we introduce additionally to the matrix N and function $s(x)$ two functions $s^+(x)$ and $s^-(x)$, such that their Discrete Fourier Transforms $\hat{s}^+(x), \hat{s}^-(x)$ have to satisfy the following conditions

$$\hat{s}^-(x) \in \mathbb{R}, \qquad \hat{s}^+(x) \in \mathbb{R},$$

$$0 \le \hat{s}^-(x) \le \hat{s}(x) \le \hat{s}^+(x). \tag{5.45}$$

The matrices corresponding to $\hat{s}^-(x)$ and $\hat{s}^+(x)$ are defined by

$$N^+ = \left[N^+_{pq}\right]_{p,q=0}^{n-1} = [s^+(j_p - j_q)]_{p,q=0}^{n-1},$$

$$N^- = \left[N^-_{pq}\right]_{p,q=0}^{n-1} = [s^-(j_p - j_q)]_{p,q=0}^{n-1}.$$

The matrices N^-, N, and N^+ are positive semi-definite, and they can be ordered as follows

$$0 \le N^- \le N \le N^+.$$

Similar we can get estimates for the greatest and the smallest eigenvalues of the matrix N

$$\lambda_{\max}(N^-) \le \lambda_{\max}(N) \le \lambda_{\max}(N^+),$$
$$\lambda_{\min}(N^-) \le \lambda_{\min}(N) \le \lambda_{\min}(N^+). \tag{5.46}$$

The Gerschgorin discs of the matrix N are given by

$$D_i = \left\{z \in \mathbb{C} : |z - N_{ii}| \le R_i(N)\right\},$$

where
$$N_{ii} = s(0) = n,$$
$$R_i(N) = \sum_{\substack{j=0, \\ j\neq i}}^{n-1} |N_{ij}|.$$

As we have mentioned above the matrix N is not diagonally dominant, therefore instead of working with its Gerschgorin disk we will work with the Gerschgorin disks of N^- and N^+. Using the bounds (5.46) we can estimate
$$\lambda_{\max}(N) \leq \lambda_{\max}(N^+) \leq s^+(0) + \max_i R_i(N^+),$$

$$\lambda_{\min}(N) \geq \lambda_{\min}(N^-) \geq s^-(0) - \max_i R_i(N^-).$$

An important task now is to choose two functions $s^+(x)$ and $s^-(x)$ such that the conditions (5.45) are satisfied. Following [Ferreira 1999] we introduce a family of signals $V(k; a, b, l)$, periodic in k with period n, whose discrete Fourier transforms $\hat{V}(k; a, b, l)$ are real and trapezoidal

$$\hat{V}(k; a, b, l) = \begin{cases} \dfrac{k - a + l}{l}, & k \in [a - l + 1, a - l], \\[2mm] 1, & k \in [a, b], \\[2mm] \dfrac{l - k + b}{l}, & k \in [b + 1, b + l - 1]. \end{cases} \qquad (5.47)$$

The inverse discrete Fourier transform of the trapezoidal function (5.47) is given by the expression

$$V(k; a, b, l) = \frac{1}{\sqrt{n}} \sum_{j=-\frac{n-1}{2}}^{\frac{n-1}{2}} \hat{V}(j; a, b, l)\, e^{\frac{1}{2} i \frac{2\pi}{n-1} jk} =$$

$$= e^{i\frac{\pi k}{2(n-1)}(a+b)} \frac{\sin\left(\frac{\pi k l}{2(n-1)}\right) \sin\left(\frac{\pi k}{2(n-1)}(b - a + l)\right)}{l\sqrt{n}\sin^2\left(\frac{\pi k}{2(n-1)}\right)}.$$

As functions $s^+(k)$ and $s^-(k)$ we choose the following functions

$$s^+(k) = \frac{1}{\sqrt{n}} V\left(k; -\frac{n-1}{2}, \frac{n-1}{2}, l\right) = \frac{\sin\left(\frac{\pi k l}{2(n-1)}\right) \sin\left(\frac{\pi k}{2(n-1)}(n - 1 + l)\right)}{l\, n\, \sin^2\left(\frac{\pi k}{2(n-1)}\right)},$$

$$s^-(k) = \frac{1}{\sqrt{n}} V\left(k; -\frac{n-1}{2} + l, \frac{n-1}{2} - l, l\right) = \frac{\sin\left(\frac{\pi k l}{2(n-1)}\right) \sin\left(\frac{\pi k}{2(n-1)}(n - 1 - l)\right)}{l\, n\, \sin^2\left(\frac{\pi k}{2(n-1)}\right)},$$

119

and

$$s^+(0) = \frac{n-1+l}{n}, \quad s^-(0) = \frac{n-1-l}{n}.$$

Let us denote by D the maximum distance between two j_l, and by d the minimum distance, i.e.

$$d \le |j_p - j_q| \le D.$$

Now we want to get the Gerschgorin disks for the matrix associated with the function $V(k; a, b, l)$, and we get

$$\sum_{\substack{p=0,\\p\ne q}}^{n-1} \frac{1}{\sqrt{n}} |V(j_p - j_q; a, b, l)| = \sum_{\substack{p=0,\\p\ne q}}^{n-1} \left| e^{i\frac{\pi k}{2(n-1)}(a+b)} \frac{\sin\left(\frac{\pi(j_p-j_q)l}{2(n-1)}\right) \sin\left(\frac{\pi(j_p-j_q)}{2(n-1)}(b-a+l)\right)}{l\, n\, \sin^2\left(\frac{\pi(j_p-j_q)}{2(n-1)}\right)} \right| \le$$

$$\le \sum_{\substack{p=0,\\p\ne q}}^{n-1} \left| \frac{\sin\left(\frac{\pi(j_p-j_q)l}{2(n-1)}\right) \sin\left(\frac{\pi(j_p-j_q)}{2(n-1)}(b-a+l)\right)}{l\, n\, \sin^2\left(\frac{\pi(j_p-j_q)}{2(n-1)}\right)} \right| =$$

$$= \sum_{\substack{p=0,\\p\ne q}}^{n-1} \left| \frac{\frac{1}{2}\left(\cos\left[\frac{\pi(j_p-j_q)}{2(n-1)}(b-a)\right] - \cos\left[\frac{\pi(j_p-j_q)}{2(n-1)}(b-a+2l)\right]\right)}{l\, n\, \sin^2\left(\frac{\pi(j_p-j_q)}{2(n-1)}\right)} \right|.$$

We expand the numerator in the last fraction into its Taylor series omitting the higher order terms which are small for an increasing value of n, thus we get

$$\frac{1}{2}\left(\cos\left[\frac{\pi(j_p-j_q)}{2(n-1)}(b-a)\right] - \cos\left[\frac{\pi(j_p-j_q)}{2(n-1)}(b-a+2l)\right]\right) =$$

$$= \frac{1}{2}\left(1 - \frac{1}{2}\left[\frac{\pi(j_p-j_q)}{2(n-1)}(b-a)\right]^2 - 1 + \frac{1}{2}\left[\frac{\pi(j_p-j_q)}{2(n-1)}(b-a+2l)\right]^2\right) =$$

$$= \frac{1}{4}\left(\frac{\pi(j_p-j_q)}{2(n-1)}\right)^2 \left((b-a+2l)^2 - (b-a)^2\right) = l\left(\frac{\pi(j_p-j_q)}{2(n-1)}\right)^2 (b-a+l).$$

Thus we obtain the following estimate

$$\sum_{\substack{p=0,\\p\ne q}}^{n-1} \left| \frac{\frac{1}{2}\left(\cos\left[\frac{\pi(j_p-j_q)}{2(n-1)}(b-a)\right] - \cos\left[\frac{\pi(j_p-j_q)}{2(n-1)}(b-a+2l)\right]\right)}{l\, n\, \sin^2\left(\frac{\pi(j_p-j_q)}{2(n-1)}\right)} \right| \le \sum_{\substack{p=0,\\p\ne q}}^{n-1} \left| \frac{l\left(\frac{\pi(j_p-j_q)}{2(n-1)}\right)^2 (b-a+l)}{l\, n\, \sin^2\left(\frac{\pi(j_p-j_q)}{2(n-1)}\right)} \right|,$$

and finally we have

$$\sum_{\substack{p=0,\\p\ne q}}^{n-1} \frac{1}{\sqrt{n}} |V(j_p - j_q; a, b, l)| \le \frac{d^2\, \alpha^2 (b-a+l)}{n\, D^2 \sin^2(\alpha)},$$

120

where $\alpha = \frac{\pi D}{2(n-1)}$. Finally we obtain the following estimates for the eigenvalues

$$\lambda_{\max}(N) \leq \frac{n-1+l}{n} + \frac{d^2 \alpha^2 (n-1+l)}{n D^2 \sin^2(\alpha)},$$

$$\lambda_{\min}(N) \geq \frac{n-1-l}{n} - \frac{d^2 \alpha^2 (n-1-l)}{n D^2 \sin^2(\alpha)}.$$

Minimizing the first expression or maximizing the second with respect to l we get

$$\lambda_{\max}(N) \leq \frac{n-1}{n} + \frac{d^2 \alpha^2 (n-1)}{n D^2 \sin^2(\alpha)},$$

$$\lambda_{\min}(N) \geq \frac{n-1}{n} - \frac{d^2 \alpha^2 (n-1)}{n D^2 \sin^2(\alpha)}.$$

Studying the asymptotic behaviour of the estimate for the smallest eigenvalue $\lambda_{\min}(N)$ we see that

$$\lim_{n \to \infty} \left[\frac{n-1}{n} \left(1 - \frac{d^2 \alpha^2}{D^2 \sin^2(\alpha)} \right) \right] = \frac{D^2 - d^2}{D^2}. \tag{5.48}$$

It follows that for the case of non-equidistant nodes, i.e. $D > d$, one has more specified estimate for the smallest eigenvalue. In the case of the equidistant nodes, i.e. $D = d$, the estimates tells only that the smallest eigenvalue is greater or equal to zero, which is true by the definition of a semi-positive definite matrix. Therefore for the case of the equidistant nodes the estimates has to be improved, but in any case the estimate doesn't lead to a contradiction.

Coming back to the original matrix F^{-1} we get the following estimate:

$$\|F^{-1}\|_2 = \sqrt{\lambda_{min}(N)^{-1}} \leq \sqrt{\frac{n D^2 \sin^2(\alpha)}{(n-1)(D^2 \sin^2(\alpha) - d^2 \alpha^2)}}.$$

Finally, the estimate (5.41) has the form

$$|f_n(\varphi) - \tilde{f}_n(\varphi)| \leq$$

$$\leq \delta^* \sqrt{\frac{n D^2 \sin^2(\alpha)}{(n-1)(D^2 \sin^2(\alpha) - d^2 \alpha^2) \left(\kappa^2 - \kappa + \frac{5}{2} - \frac{1}{2}\sqrt{20\kappa^2 - 20\kappa + 25} \right)}} \, \|\mathbf{\Phi}\|_2 .$$

The remaining part is to estimate the norm of the vector of the basis functions Φ_k. Taking into account that they are of the form

$$\Phi_k(x) = e^{\frac{1}{2} i k x},$$

121

we get

$$|f_n(\varphi) - \tilde{f}_n(\varphi)| \leq$$

$$\leq \sqrt{n}\,\delta^* \sqrt{\frac{n\,D^2\sin^2(\alpha)}{(n-1)(D^2\sin^2(\alpha) - d^2\alpha^2)\left(\kappa^2 - \kappa + \frac{5}{2} - \frac{1}{2}\sqrt{20\kappa^2 - 20\kappa + 25}\right)}}.$$

To obtain the final estimate we need to notice that the error δ^* comes from the finite element approximation, and this error depends on a characteristic size h of the elements (see Fig. 5.3). For our purpose we express this characteristic size in terms of the number of interpolation nodes n as follows

$$h = \tan\left(\frac{\pi}{n-1}\right)(r_A + l), \tag{5.49}$$

where r_A is the radius of the analytical domain and can be normalised to 1, and l is one of the geometric parameters of the coupling elements going to zero with the increasing number of nodes.
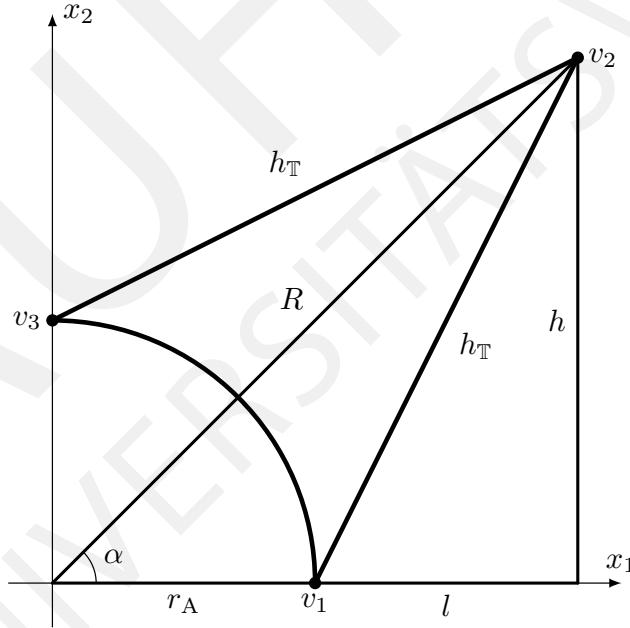
Figure 5.3: Geometry of the coupling element with characteristic sizes

Since we have made the rescaling of the interpolation nodes by $\frac{1}{\sqrt{n}}$ during estimation of the spectral norm for the matrix F^{-1}, we need also to apply this rescaling to the characteristic size of the finite element mesh (5.49), so we obtain

$$h = \frac{1}{\sqrt{n}}\tan\left(\frac{\pi}{n-1}\right)(r_A + l).$$

Finally we get the following coupling error

$$|f_n(\varphi) - \tilde{f}_n(\varphi)| \leq$$

$$\leq \sqrt{\frac{n^2 D^2 \sin^2(\alpha) \left(\frac{1}{\sqrt{n}} \tan\left(\frac{\pi}{n-1}\right)(r_A + l)\right)^2}{(n-1)(D^2 \sin^2(\alpha) - d^2\alpha^2)\left(\kappa^2 - \kappa + \frac{5}{2} - \frac{1}{2}\sqrt{20\kappa^2 - 20\kappa + 25}\right)}}.$$

Since we assume for the spectral norm (5.44) the normalised radius $r_A = 1$ and take into account that the parameter l is decreasing inversely proportional to n, we obtain the following estimate

$$|f_n(\varphi) - \tilde{f}_n(\varphi)| \leq$$

$$\leq \sqrt{\frac{n D^2 \sin^2(\alpha)\left(\tan\left(\frac{\pi}{n-1}\right)\left(1 + \frac{l}{n}\right)\right)^2}{(n-1)(D^2 \sin^2(\alpha) - d^2\alpha^2)\left(\kappa^2 - \kappa + \frac{5}{2} - \frac{1}{2}\sqrt{20\kappa^2 - 20\kappa + 25}\right)}} =: R_C(n).$$

Studying the asymptotic behaviour of this estimate we see that

$$\lim_{n \to \infty}\left[\sqrt{\frac{n D^2 \sin^2(\alpha)\left(\tan\left(\frac{\pi}{n-1}\right)\left(1 + \frac{l}{n}\right)\right)^2}{(n-1)(D^2 \sin^2(\alpha) - d^2\alpha^2)\left(\kappa^2 - \kappa + \frac{5}{2} - \frac{1}{2}\sqrt{20\kappa^2 - 20\kappa + 25}\right)}}\right] = 0.$$

We see that the constructed estimate for the coupling error asymptotically converges to zero independently on the distribution of nodes on the interaction interface Γ_{AD}.

5.5.4 Final estimate

Finally we can combine the obtained error estimates: the error of the "exact" interpolation, the coupling error, the error over the coupling elements, and the error over the standard elements. Finally we can introduce a global error estimate in Ω by the following estimate for the norm:

$$\|v - v_h\|_{1,2,\Omega}^2 \leq \sum_{T \in \mathcal{F}_h} \|v - v_h\|_{1,2,T}^2 + \sum_{\mathbb{T} \in \mathcal{F}_h} \|v - v_h\|_{1,2,\mathbb{T}}^2 + |R(t;n)| + |R_C(n)|,$$

where $R_C(n)$ represents the coupling error.

To investigate the global rate of convergence for this strategy we introduce a scaling factor h for the elements T defined in (5.49). An analogous construction cannot be applied to the elements $\mathbb{T}$, since they are not belonging to an affine family, therefore we use a characteristic size $h_{\mathbb{T}}$ defined as follows

$$h_{\mathbb{T}} = \sqrt{(r_A + l)^2 \tan^2\left(\frac{\pi}{n-1}\right) + l^2}.$$

Making the normalisation of the radius r_A and l, and applying the rescaling as in previous subsection, we obtain

$$h_{\mathbb{T}} = \frac{1}{\sqrt{n}}\sqrt{\left(1+\frac{l}{n}\right)^2 \tan^2\left(\frac{\pi}{n-1}\right) + \left(\frac{l}{n}\right)^2}.$$

Finally, we get

$$\|v - v_h\|_{1,q,\Omega} \le C_1 h(n)|v|_{2,p,T} + C_2 h_{\mathbb{T}}(n)|v|_{2,p,\mathbb{T}} + |R(t;n)| + |R_C(n)|,$$

or, if we replace h by (5.49)

$$\|v - v_h\|_{1,q,\Omega} \le C_1 \tan\left(\frac{\pi}{n-1}\right)\left(1+\frac{l}{n}\right)|v|_{2,p,T} +$$

$$+ C_2 h_{\mathbb{T}}(n)|v|_{2,p,\mathbb{T}} + |R(t;n)| + |R_C(n)|,$$

and thus we get an estimate which includes the information about a fixed radius r_A and the most essential is the number of interpolation nodes.

Chapter 6

Numerical experiments

After the theoretical results for the method of coupling of the analytical and the finite element solution, which we have introduced during the previous chapters, we show in this chapter some basic results of simulations with the proposed method. We will show results for two examples:

(i) The first example is a trivial problem with a known exact solution. For this purpose we will use the classical solution from the fracture mechanics given for a crack in an infinite plane. The exact solution in this case is known, and can be found almost in any books on fracture mechanics, see for example [Anderson 2005, Liebowitz 1968].

(ii) The second example is a more advanced applied example coming from engineering practice. We consider a concrete hinge, which is a part of a bridge column, containing a single crack in the throat region.

The idea of considering such two examples comes from the fact that we are interested in real application of the proposed method. The first, trivial, example serves to show that the convergence of the method takes place not only in the theory, but also in practice. For that reason we consider a problem with a well-known exact solution. In the considered example the exact solution is a first term of the analytical solution for a crack tip problem constructed in Chapter 3. In this case it's particularly interesting to study the behaviour of the method, because by the construction of the special element we need to use the analytical solution with more than one term.

The second example of a concrete hinge shows applicability of the proposed method in engineering practice. Due to the fact that we have proved the convergence of the proposed method in the case of a global refinement, we can expect that the approximated solution for a hinge will converges to a true solution with a refinement. The reason for that expectation is the fact, that the boundary value problem associated with a hinge is completely covered by the proposed theory.

We would like to underline, that this chapter presents only few results of simulations which mostly serve to explore the possible next steps for a theoretical investigation of the method. The task of an efficient computer implementation of the proposed method was

put out of the scope of these simulations. All simulation were performed by a computer program written in the Maple software. All calculation were done on a personal laptop with the following characteristics: Inter Core i7-4500U CPU 1.80 GHz, 8.00 GB RAM, Windows 8 64 bit.

6.1 Test example

As we have mentioned above, that at first we consider a trivial example with known exact solution. Let us consider an infinite plane containing a single crack of a length $2a$, which is inclined by the angle α, with constant stresses $\mathbf{p}$ applied at infinity (see the Fig. 6.1).
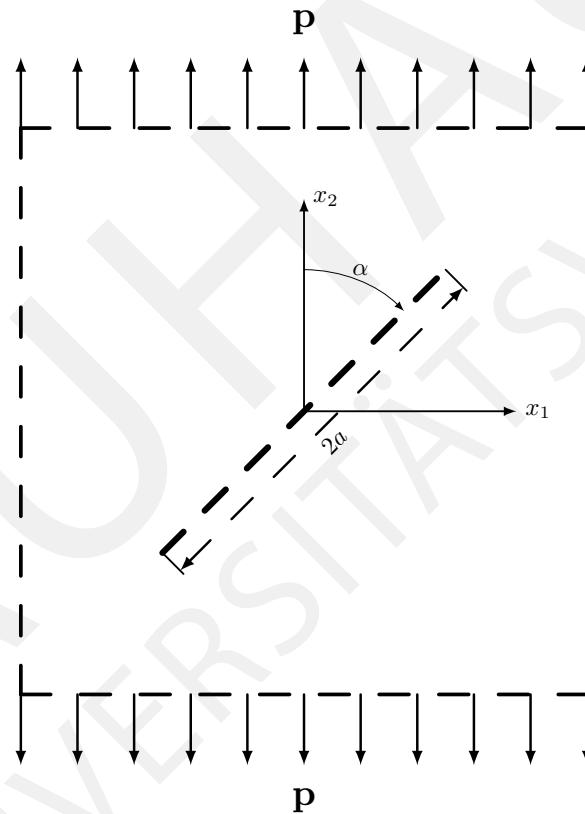
Figure 6.1: The inclined crack in an infinite plane

The exact solution for this problem is given by the following formulae (see again [Liebowitz 1968]) for the displacements

$$
\begin{aligned}
u_1 &= \frac{k_1\sqrt{2r}}{8\mu}\left[(2\kappa-1)\cos\left(\frac{\varphi}{2}\right)-\cos\left(\frac{3\varphi}{2}\right)\right]+\ldots, \\
u_2 &= \frac{k_1\sqrt{2r}}{8\mu}\left[(2\kappa+1)\sin\left(\frac{\varphi}{2}\right)-\sin\left(\frac{3\varphi}{2}\right)\right]+\ldots,
\end{aligned}
\tag{6.1}
$$

126

and for the stresses

$$
\sigma_{11} = \frac{k_1}{\sqrt{2r}} \cos\left(\frac{\varphi}{2}\right) \left[1 - \sin\left(\frac{\varphi}{2}\right) \sin\left(\frac{3\varphi}{2}\right) \right] + \dots,
$$

$$
\sigma_{22} = \frac{k_1}{\sqrt{2r}} \cos\left(\frac{\varphi}{2}\right) \left[1 + \sin\left(\frac{\varphi}{2}\right) \sin\left(\frac{3\varphi}{2}\right) \right] + \dots, \qquad (6.2)
$$

$$
\sigma_{12} = \frac{k_1}{\sqrt{2r}} \cos\left(\frac{\varphi}{2}\right) \sin\left(\frac{\varphi}{2}\right) \cos\left(\frac{3\varphi}{2}\right) + \dots,
$$

where r, φ are polar coordinates, κ and μ are material parameters, and the parameter k_1 is the stress intensity factor for a straight crack corresponding to a normal loading (Mode I), which is defined as follows

$$
k_1 = p \sqrt{a} \sin^2 \alpha,
$$

where p is the value of stresses applied at infinity, a is the half length of the crack. Another important type of fracture is the Mode II, which corresponds to in-plane shear loading and tends to slide one crack face with respect to the other. The stress factor k_2 corresponding to the Mode II is given by

$$
k_2 = p \sqrt{a} \sin \alpha \, \cos \alpha.
$$

For all calculations in this chapter we will consider $\alpha = \frac{\pi}{2}$, thus the stress intensity factors are given by

$$
k_1 = p \sqrt{a}, \qquad k_2 = 0. \qquad (6.3)
$$

One can see that the exact solution (6.1) is nothing more than the term corresponding to $k = 1$ in (3.13) with known coefficient a_1. As it was shown in [Liebowitz 1968], that the stress intensity factors can be related with the real and the imaginary part of the coefficient a_1 as follows

$$
a_1^{(1)} + i \, a_1^{(2)} = \frac{1}{\sqrt{2}} (k_1 - k_2).
$$

As a drawback of such a trivial example we mention that the exact solution (6.1)-(6.2) is represented by only the leading terms in the infinite series (3.13). For many applications such a simplification shows acceptable results, see for example [Anderson 2005], but in practice we often have to deal with cracked bodies which are bounded, and a crack is located in a very narrow part, like for instance in a concrete hinge, for such bodies it is not really clear that one cannot omit all higher order terms. This question requires a more detailed consideration and more sophisticated examples. In our first numerical experiments we will try to deal with this problem by considering different types of the interpolation function (4.2): we will vary the number of the singular terms (half-integer powers) and the number of the regular terms (integer powers).

For simulations we consider a square domain of length L located around one of the crack tips according to the Fig. 6.2.
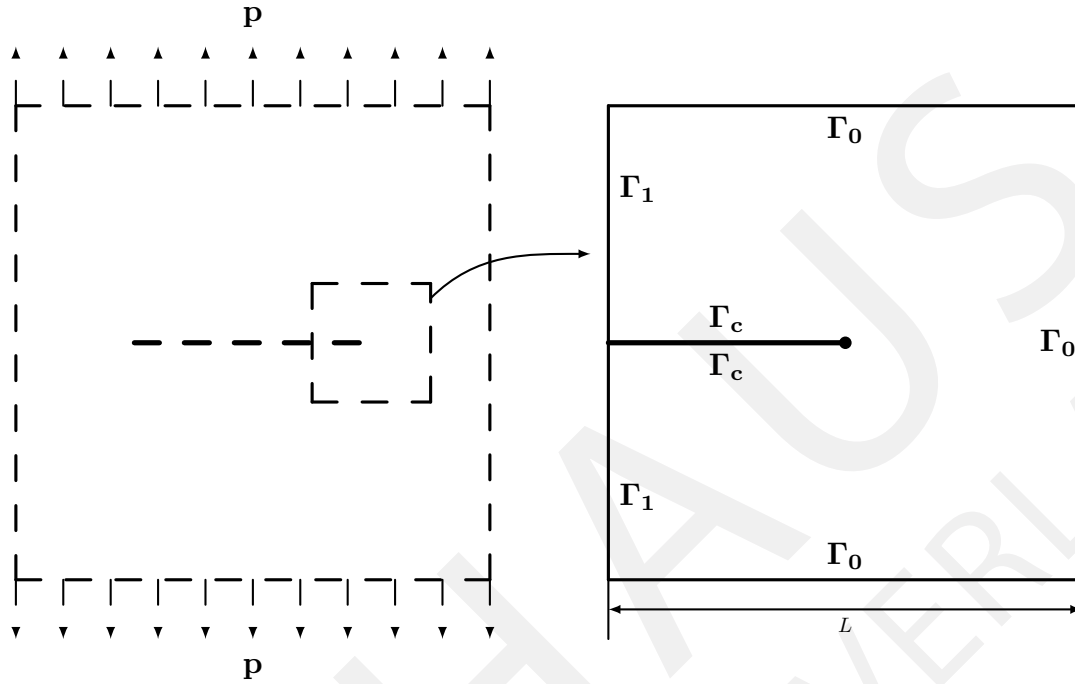
Figure 6.2: Boundary value problem for the test example

Since we know the exact solution for an infinite plane we can take any combination of Dirichlet and Neumann boundary conditions. For the calculation we consider the following boundary conditions, which are common in literature:

$$\begin{cases} \mathbf{u} = u_1 + i\,u_2, & \text{on} \quad \Gamma_0, \\ \sigma_n = \mathbf{n} \cdot \tilde{\boldsymbol{\sigma}}, & \text{on} \quad \Gamma_1, \\ \sigma_n = 0, & \text{on} \quad \Gamma_c, \end{cases} \tag{6.4}$$

where $\mathbf{n}$ is a unit normal vector, $\tilde{\boldsymbol{\sigma}}$ is the stress tensor with components defined by (6.2), and the components u_1 and u_2 are given by (6.1). We will perform calculations with the following material parameters

$$E = 38.9 \cdot 10^9 \text{ N/m}^2, \quad \nu = 0.2.$$

These parameters correspond to the concrete **C**60 which will be used later for a concrete hinge. The parameters μ and κ from (6.1) are defined then by

$$\mu = \frac{E}{2(1+\nu)}, \qquad \kappa = 3 - 4\nu,$$

where κ is chosen for the case of a plane strain. We perform all calculations for the following parameters

$$a = 50 \text{ mm}, \quad L = 10 \text{ mm}, \quad p = 10^4 \text{ N/m}^2.$$

128

To show first numerical results for the test example we will work with relative error in $L^2(\Omega)$ in a percentage form defined as follows

$$\epsilon = \frac{\|\mathbf{u} - \mathbf{u}_h\|_{L^2}}{\|\mathbf{u}\|_{L^2}} \cdot 100\%, \tag{6.5}$$

where $\mathbf{u}_h$ is the approximated solution constructed by the coupling method, and $\mathbf{u}$ is the exact solution (6.1).

Since we would like to test the proposed numerical scheme, we will choose the different number of the basis functions in (4.2) corresponding to half-integer and integer powers. All calculations will be performed according to the first strategy, i.e. by using a global refinement by a scaling parameter. We will show here only results related to four and eight coupling elements. Cases of greater number of coupling element and the second strategy we leave open for future work.

Let us consider at first the case of 5 interpolation nodes at the interface Γ_{AD} corresponding to four coupling elements. We will use in all figures the following notations for lines

—— represents the case of $N_1 = 1$ and $N_2 = 6$. In this case the half-integer powers are represented only by the leading term $r^{\frac{1}{2}}$, and the rest part of the basis is given by integer powers;

- - - represents the case of $N_1 = 3$ and $N_2 = 4$. In this case the half-integer powers are represented the terms $r^{\frac{1}{2}}$, $r^{\frac{3}{2}}$, and the rest part of the basis is given by integer powers;

······ represents the case of $N_1 = 5$ and $N_2 = 2$. In this case the half-integer powers are represented the terms $r^{\frac{1}{2}}$, $r^{\frac{3}{2}}$, $r^{\frac{5}{2}}$, and the rest part of the basis is given by integer powers;

-·-·· represents the case of $N_1 = 7$ and $N_2 = 0$. In this case the half-integer powers are represented the terms $r^{\frac{1}{2}}$, $r^{\frac{3}{2}}$, $r^{\frac{5}{2}}$, $r^{\frac{7}{2}}$, and the only one integer power r^0 is presented in the basis.

The idea of considering different combinations of the basis functions comes from the fact that in real applications for a bounded domain it can be necessary to consider not only the leading terms, but some higher order terms. According to the test example one can expect that the combination $N_1 = 1$ and $N_2 = 6$ will give the lowest error due to the fact that the exact solution (6.1) contains only the leading term.

Let us at first present all figures related to the results for four coupling elements. Fig. 6.3-6.6 show the relative error for the displacements $\mathbf{u}$ in the analytical domain Ω_{A}, in the coupling elements $\mathbb{T}$, in the CST elements, and in the whole domain Ω. For each case we present two figures for the relative error – with respect to the global characteristic size of a finite element mesh, and with respect to the total number of degrees of freedom in the domain Ω.
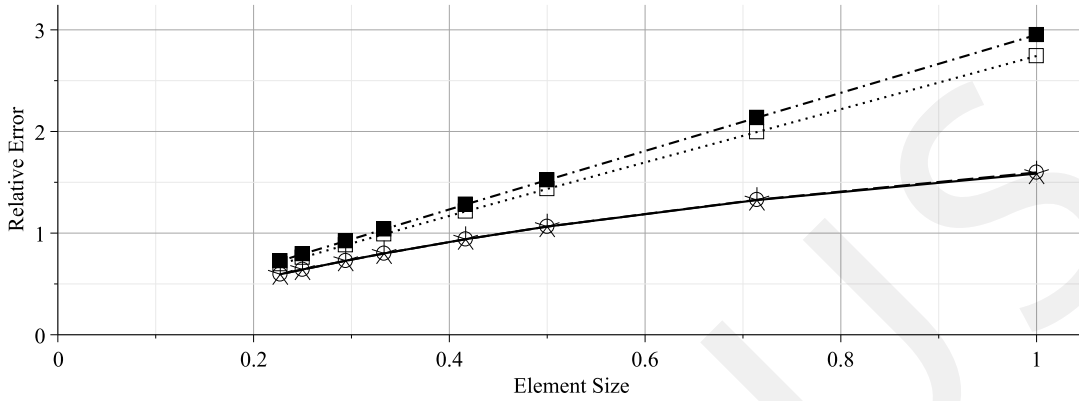
129

(a) With respect to the characteristic size of the finite element mesh
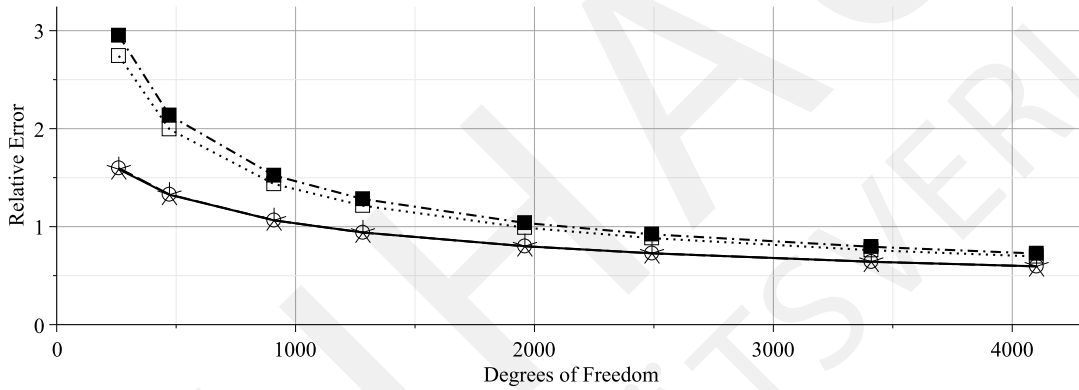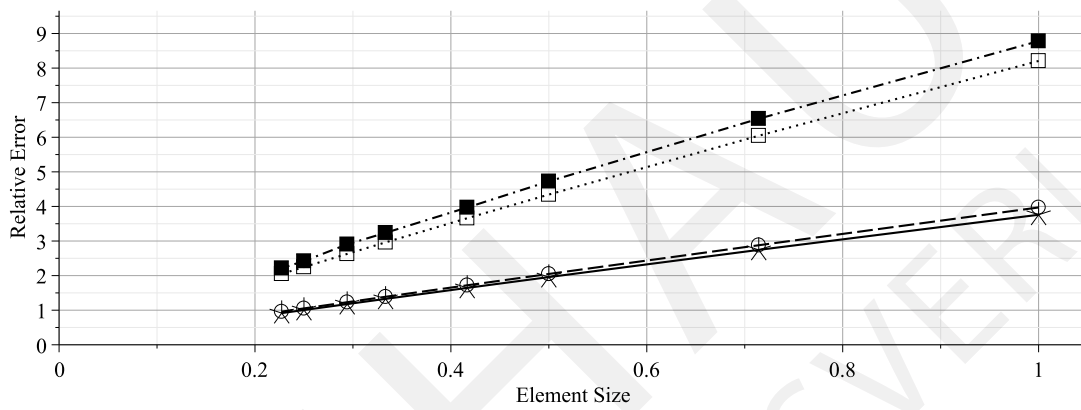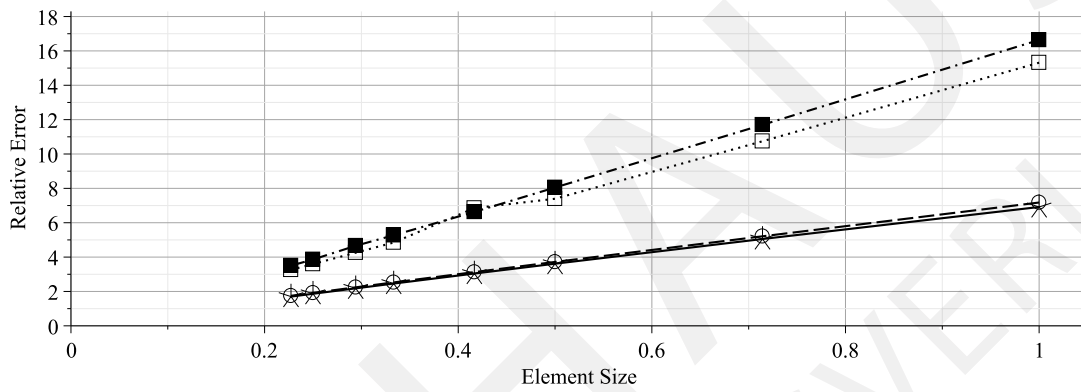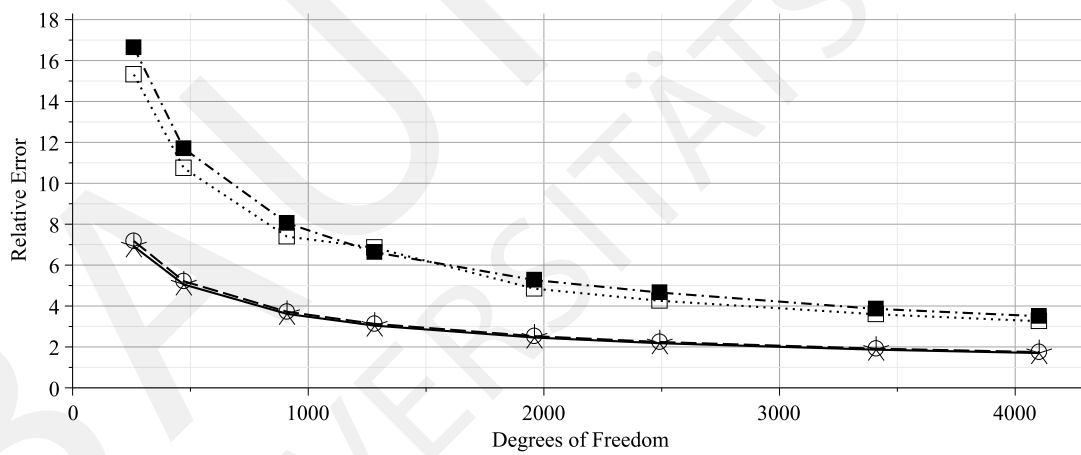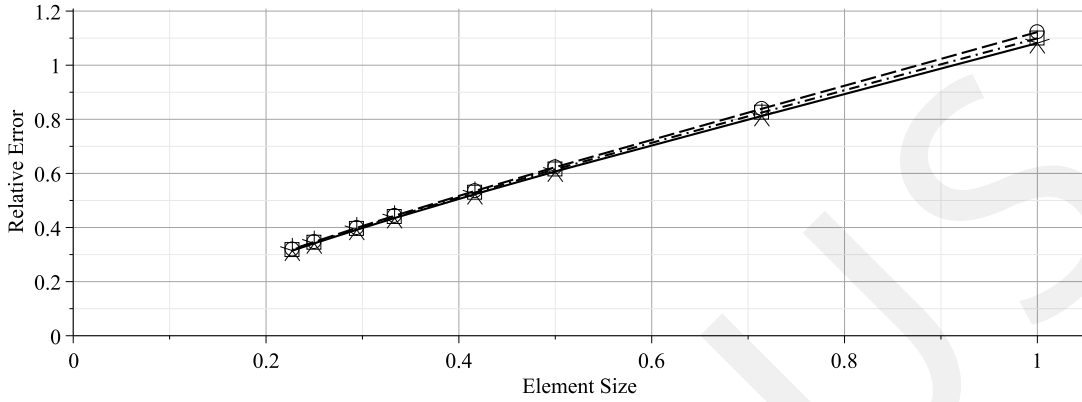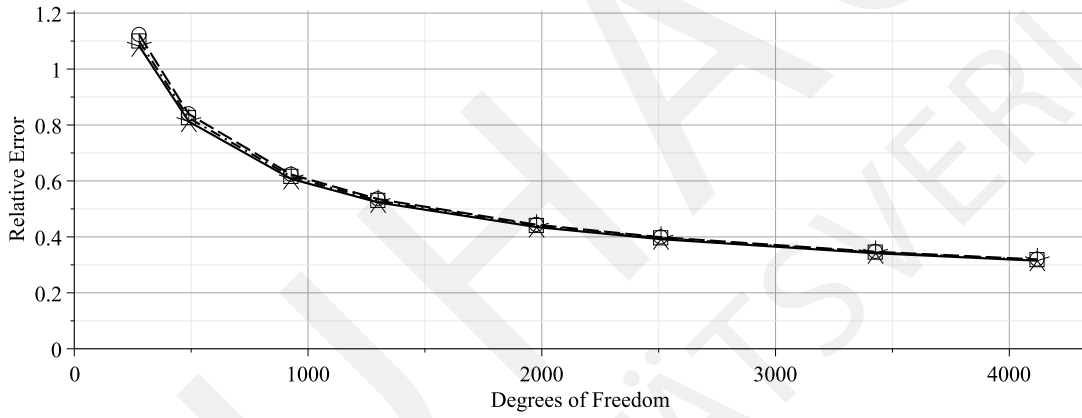

(b) With respect to the number of degrees of freedom

Figure 6.3: Relative error in the analytical domain for different number of basis functions for four coupling elements

As we can see from Fig. 6.3-6.6 the considered case of different combinations of the basis functions can be divided into two groups. First group is presented by $N_1 = 1$, $N_2 = 6$ and $N_1 = 3$, $N_2 = 4$ which leads to almost the same level of error. The second group is given by $N_1 = 5$, $N_2 = 2$ and $N_1 = 7$, $N_2 = 0$ which are also near to each other but not so close as the first group. This observation coincides with the expectations about the method:

- the method converges globally for all possible combinations of the basis functions for the chosen number of coupling elements;

- the convergence rate in the whole domain is not affected by the proposed construction;

- the total error depends on the quality of the approximation near the singularity, which we can see in Fig. 6.6.

The second point is explained by the fact that the proposed construction is local, and therefore one cannot expect better results in the whole domain. The third point is related
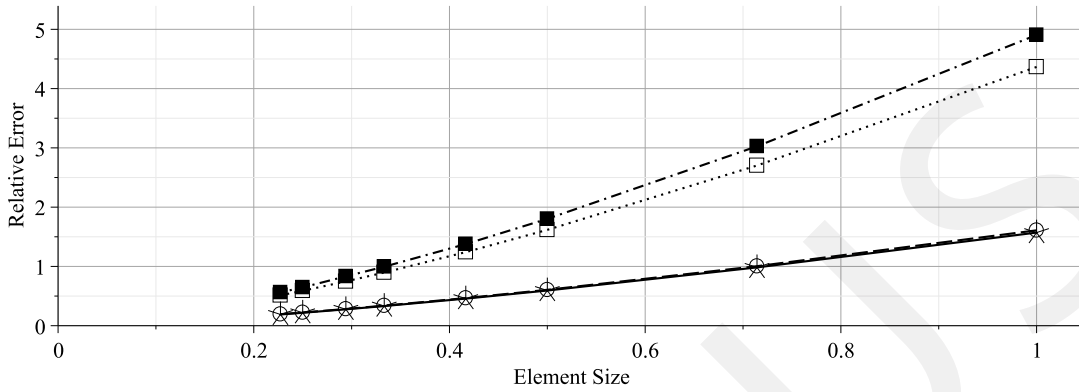
130

(a) With respect to the characteristic size of the finite element mesh
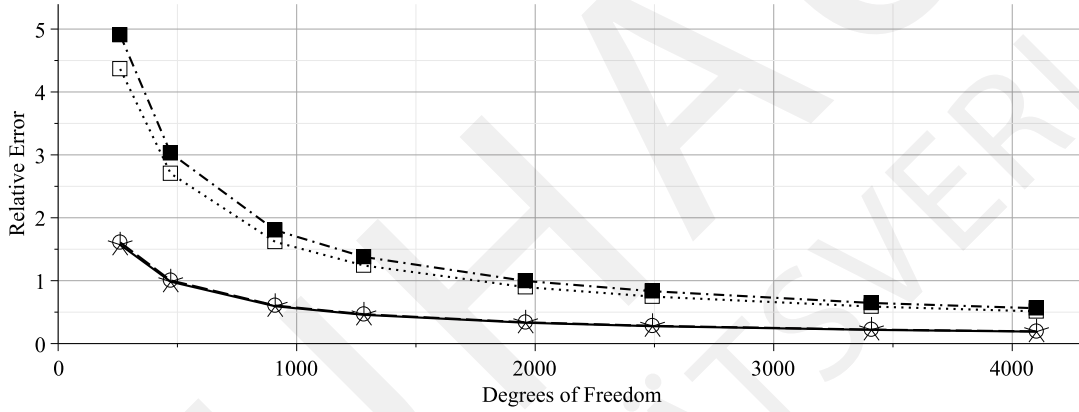
(b) With respect to the number of degrees of freedom

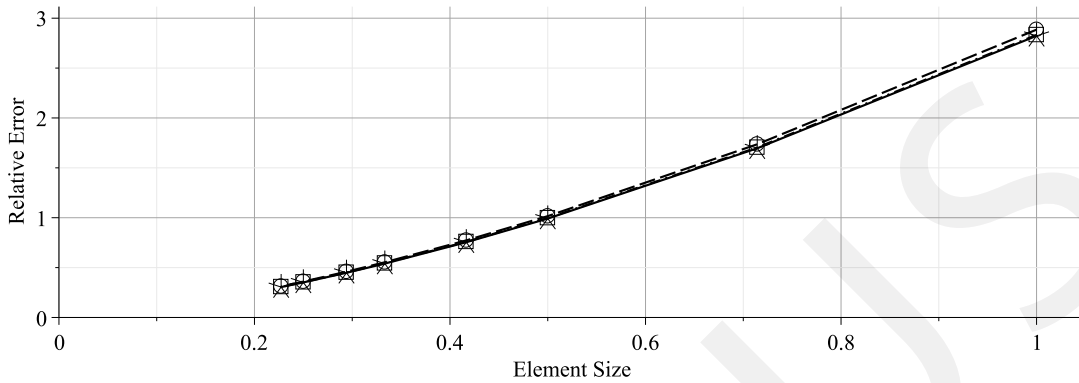Figure 6.4: Relative error in all four coupling elements for different number of basis functions

to theoretical studied of singular problems. As we have mentioned in the end of Chapter 2 the results of Maz'ya, Grisvard, and Costabel show that the exact solution of a singular problem can be decomposed into a regular and a singular part. This fact is clearly reflected by the proposed method: by taking more half-integer powers one improves the quality of approximation of the singular part of exact solution. But in the considered example the exact solution has only one singular terms, therefore the combinations with minimal number of the singular terms give us the best results.

Let us now increase the number of the interpolation nodes to 9, which corresponds to the case of eight coupling elements. Fig. 6.7 shows the relative error in the analytical element for different number of basis functions.

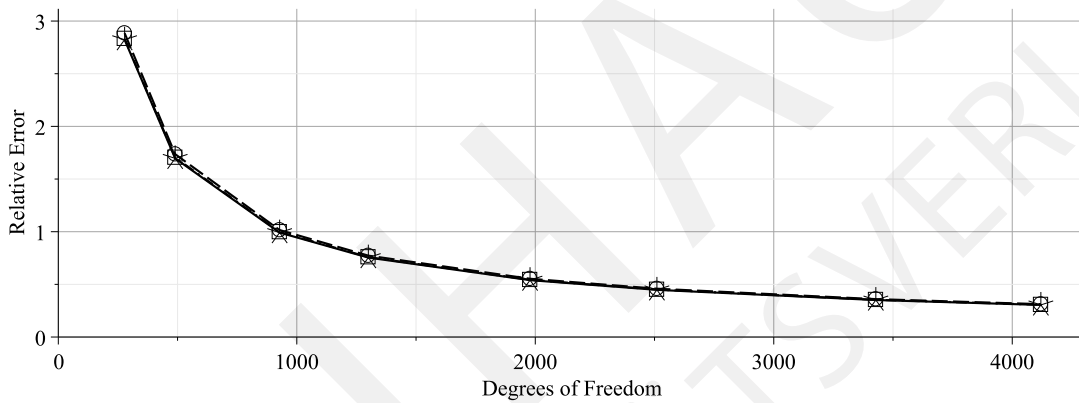Similar to the previous case we use in all figures the following notations for lines

— represents the case of $N_1 = 1$ and $N_2 = 14$. In this case the half-integer powers are represented only by the leading term $r^{\frac{1}{2}}$, and the rest part of the basis is given by integer powers;

131

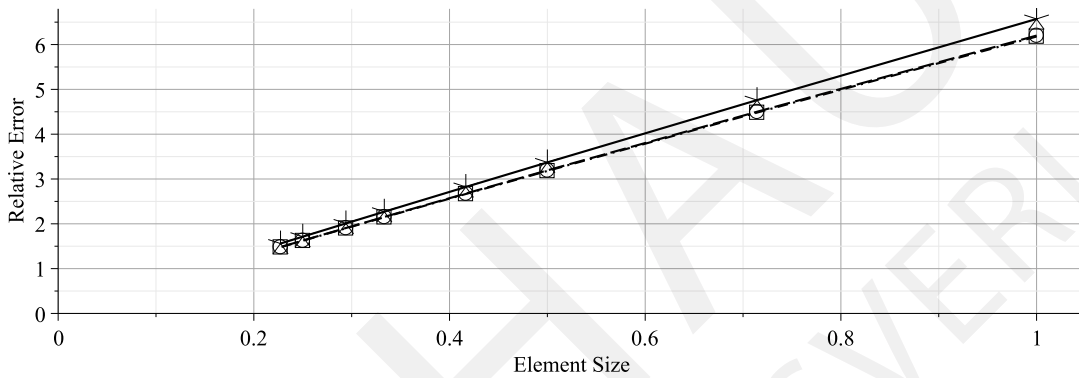(a) With respect to the characteristic size of the finite element mesh
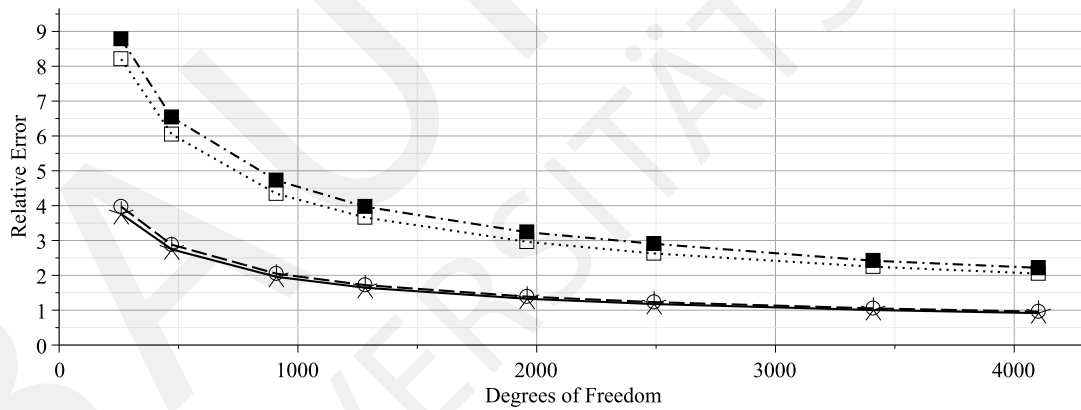
(b) With respect to the number of degrees of freedom

Figure 6.5: Relative error in all CST elements for different number of basis functions

132

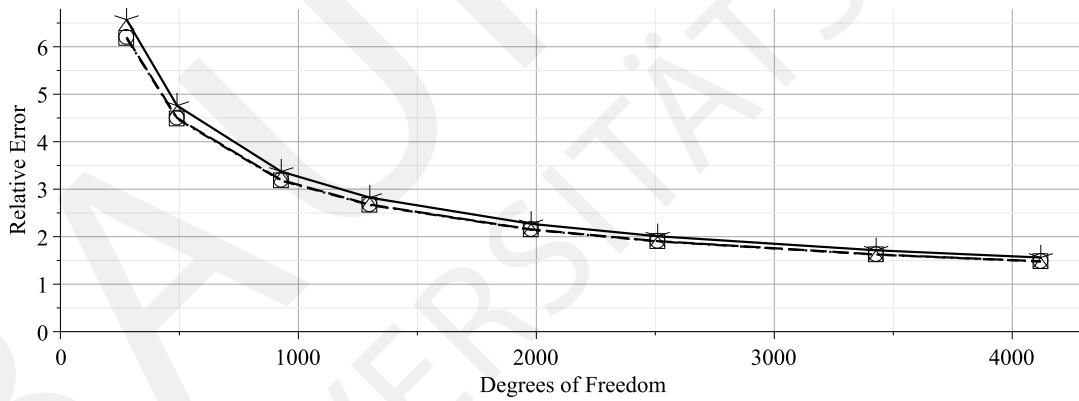(a) With respect to the characteristic size of the finite element mesh

(b) With respect to the number of degrees of freedom

Figure 6.6: Relative error in the whole domain Ω for different number of basis functions

(a) With respect to the characteristic size of the finite element mesh

(b) With respect to the number of degrees of freedom

Figure 6.7: The relative error in the analytical domain for different number of basis functions for eight coupling elements

- - - represents the case of $N_1 = 7$ and $N_2 = 8$. In this case the half-integer powers are represented the terms $r^{\frac{1}{2}}$, $r^{\frac{3}{2}}$, $r^{\frac{5}{2}}$, $r^{\frac{7}{2}}$, and the rest part of the basis is given by integer powers;

- · - · represents the case of $N_1 = 3$ and $N_2 = 12$. In this case the half-integer powers are represented the terms $r^{\frac{1}{2}}$, $r^{\frac{3}{2}}$, and the rest part of the basis is given by integer powers.

The choice of the proposed combinations between half-integer and integer powers is based on results from the simulations with four coupling elements. As we have observed in this case the best accuracy is obtained by taking only the leading term or in the case when $N_2 - N_1 = 1$. But since for $n = 9$ exist more possible combinations we add the case of $N_1 = 3$ and $N_2 = 12$ to consideration.

As we can see from Fig. 6.7-6.10 the relative errors for all considered combinations are almost equal. This fact coincides with the expectation from previous simulation for $n = 5$, that such combinations of the basis function will lead to the best accuracy.
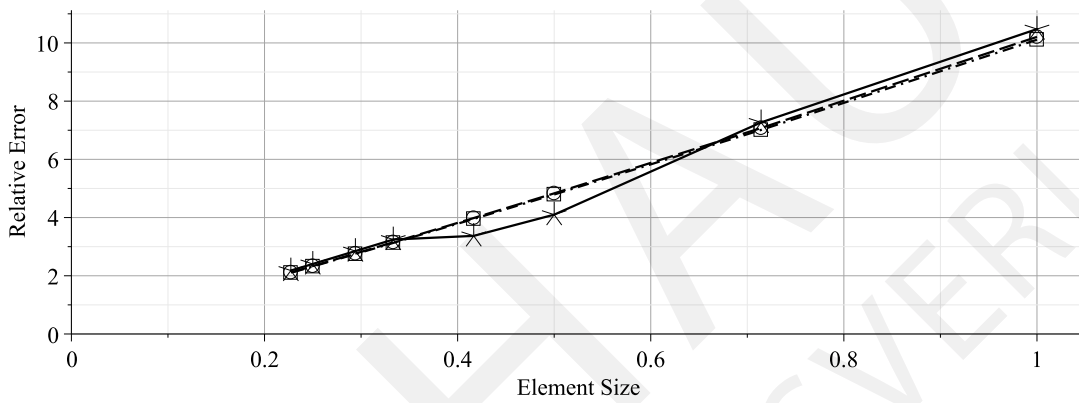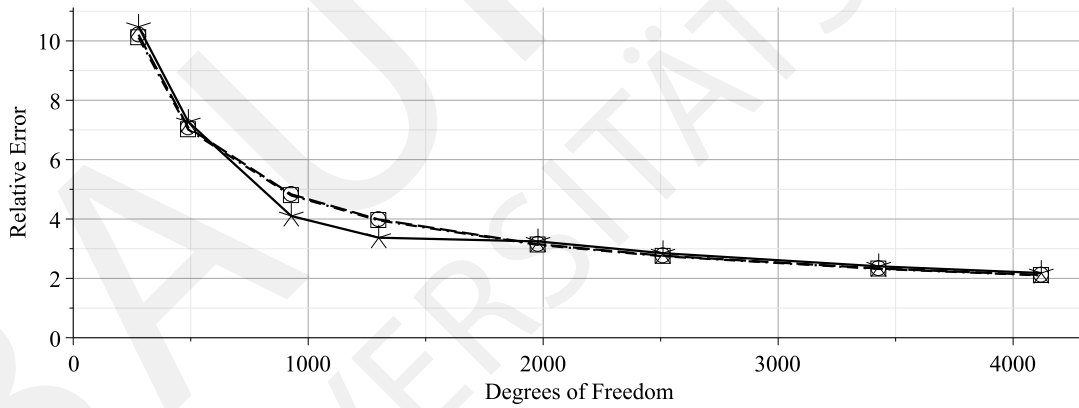
134

(a) With respect to the characteristic size of the finite element mesh

(b) With respect to the number of degrees of freedom

Figure 6.8: Relative error in all eight coupling elements for different number of basis functions

Finally, to conclude experiments with the test example we show results for comparisons of the relative errors with respect to the characteristic size of the finite element mesh between considered two cases. We take for that comparison the two best combinations from the case of four coupling elements and all three considered combinations from the case of eight coupling elements.

Similar to the previous cases we use in all figures the following notations for lines

— represents the case of $N_1 = 1$ and $N_2 = 6$ for four coupling elements;

- - - represents the case of $N_1 = 3$ and $N_2 = 4$ for four coupling elements;

— represents the case of $N_1 = 1$ and $N_2 = 14$ for eight coupling elements;

- - - represents the case of $N_1 = 7$ and $N_2 = 8$ for eight coupling elements;

-·-· represents the case of $N_1 = 3$ and $N_2 = 12$ for eight coupling elements.

135

(a) With respect to the characteristic size of the finite element mesh

(b) With respect to the number of degrees of freedom

Figure 6.9: Relative error in all CST elements for different number of basis functions

136

(a) With respect to the characteristic size of the finite element mesh

(b) With respect to the number of degrees of freedom

Figure 6.10: Relative error in the whole domain Ω for different number of basis functions

Fig. 6.11 shows the relative error in the analytical element. As we can see the case of eight coupling elements lead to lower relative error. This decreased error comes from the fact, that in order to keep the same characteristic size of the finite element mesh for both cases we need to make smaller the radius of Ω_{A}. Therefore we get lower error for eight coupling elements.
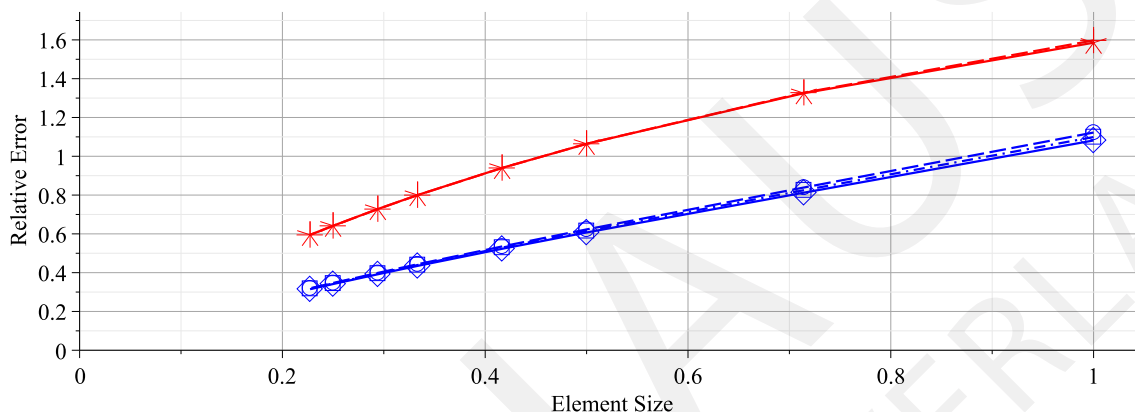
Figure 6.11: Comparison of the relative error in the analytical element

As we can see from Fig. 6.12-6.14 the relatives errors for eight coupling elements
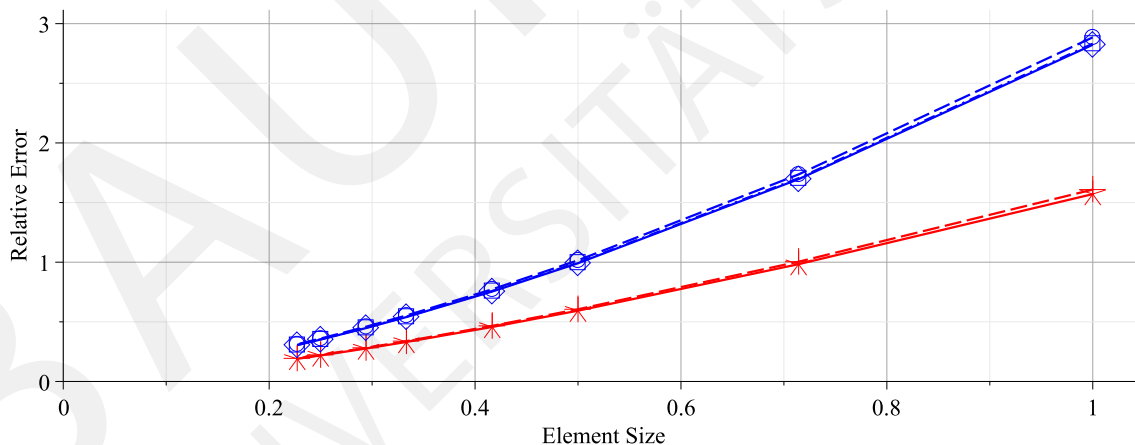
Figure 6.12: Comparison of the relative error in the coupling elements

are greater than in the case of four coupling elements. But the convergence rate is higher for the eight coupling elements, and after the final refinement the relative errors in the whole domain Ω are very near to each other. But due to a smaller radius of the analytical element, the local error is lower for eight coupling elements.

The obtained results show necessity to continue research in the direction of the optimal number of coupling elements and the optimal combination between half-integer and integer powers. This conclusion is based on the fact that with higher number of coupling elements
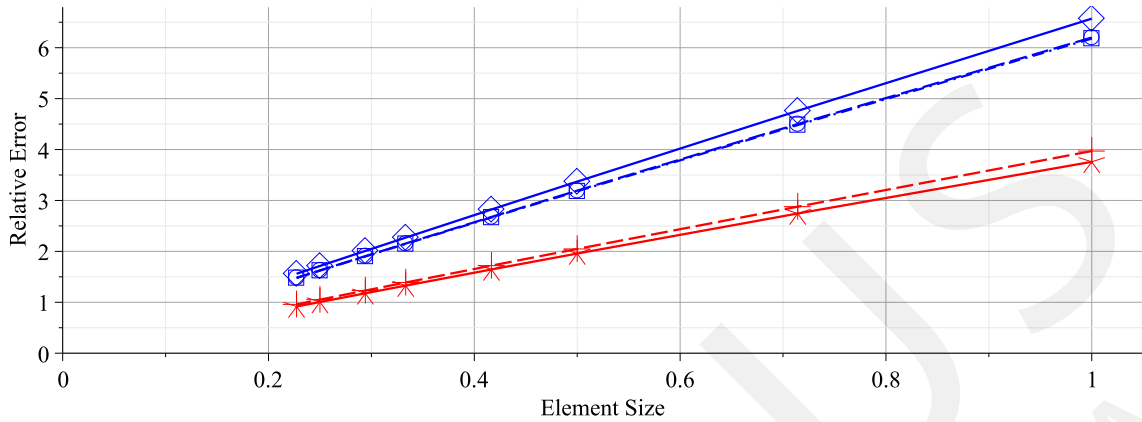
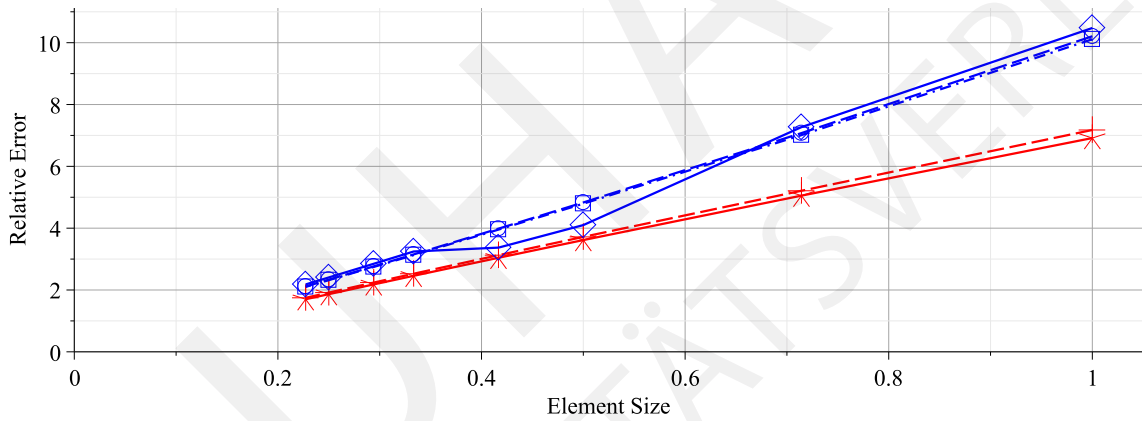Figure 6.13: Comparison of the relative error in the CST elements

Figure 6.14: Comparison of the relative error in the whole domain Ω

we obtained higher rate of convergence for the same number degrees of freedom, and we obtained almost the same accuracy.

6.2 Application to a concrete hinge

Concrete hinges are common and very important construction elements in bridge engineering. Since more than hundred years a lot of bridges were constructed applying concrete hinges. Concrete hinges have been introduced by Eugéne Freyssinet in the end of the nineteenth century, for more details we refer to [Marx & Schacht 2010]. The development of the basic theoretical results according to practical applications of concrete hinges was done later on by Fritz Leonhardt [Leonhardt 1986], in [Leonhardt & Reimann 1965] the full scale was described. In the recent years concrete hinges become again a popular tool for structural engineers during construction of integral bridges.

Due to different factors (moving of bridge, temperature deformations of concrete, dynamic loads, etc.) a crack can be observed in the hinge throat region. Because of

high risks in a case of damage of the hinge it is very important to have a precise model of the hinge itself and of the throat region particularly. The different types of load cases and the structural behaviour of hinges from the engineering point of view were studied in [Morgenthal & Olney 2014]. But not so many models for concrete hinges were investigated so far, and in practice, the methods based on empirical observations from Leonhardt are still actively used by the engineers. The first attempt to the modelling of a concrete hinge by the coupling of an analytical solution and a finite element solution was done in [Legatiuk et al. 2013]. In this section we will present further applications of the proposed method to a real practical problem in a non-trivial geometry. Fig. 6.15 shows schematically important geometrical parameters of a concrete hinge.
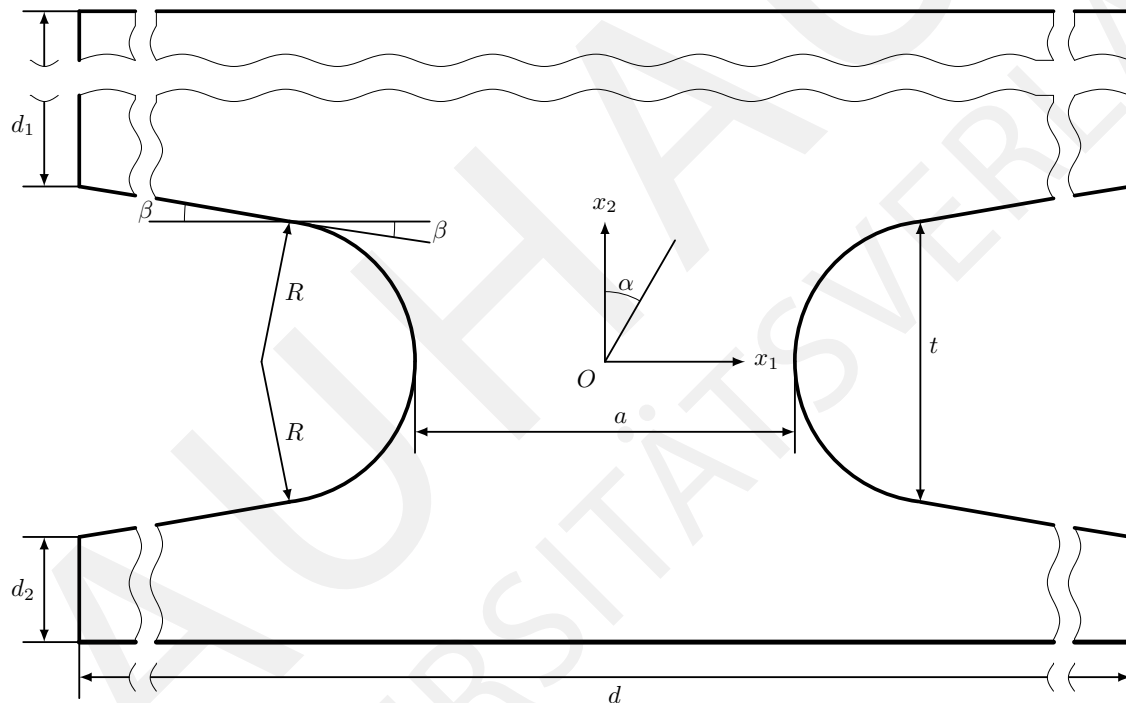

Figure 6.15: Geometrical parameters of a concrete hinge

Leonhardt made the following suggestions for the geometrical parameters

$$
\begin{aligned}
a &\leq 0.3\,d, \\
t &\leq 0.2\,a, \\
\tan\beta &\leq 0.1.
\end{aligned}
$$

According to these suggested conditions we will use the following set of parameters in all calculations

$$
\begin{aligned}
d &= 2 \text{ m}, \quad a = 0.2 \text{ m}, \quad t = 0.03 \text{ m}, \\
d_1 &= 4 \text{ m}, \quad d_2 = 4 \text{ m}, \quad \beta = 3°.
\end{aligned}
\tag{6.6}
$$

Several possible approaches for modelling of concrete structures can be considered in practice: non-linear material models, including creep and shrinkage of a concrete; time

dependent models; linear elastic models, etc. In this study of a concrete hinge we will work only in the framework of a linear elastic model, which is a simplified model of a real concrete structure.

Following [Morgenthal & Olney 2014] we will introduce now basic engineering formulae for calculation of a concrete hinge. This model is confined to the throat area and has the following main assumptions:

- the effective area accommodating the throat behaviour and responsible for allowing the hinge rotation extends $\frac{a}{2}$ to either side of the throat line, where a is the throat width;

- bilinear stress-strain behaviour of the concrete is assumed: compression behaviour is linear but not tensile strength is accounted for.

Let us consider a vertical load N and a moment M acting on top of a hinge. In this case for a cracked hinge we obtain a linear stress distribution in the throat region defined by

$$\sigma_r^{(c)} = \frac{2N}{3a(\frac{1}{2} - m)b},\tag{6.7}$$

where b is the along-throat length, m is non-dimensionalised eccentricity which is given by

$$m = \frac{M}{a\,N}.$$

The stress $\sigma_r^{(c)}$ corresponds to a peak stress at the "right" side in the throat for a cracked hinge. Another important characteristic is the linearised rotation of the hinge (see Fig. 6.15) which is calculated as follows

$$r = \tan\alpha = \frac{8\,N}{9\,a\,b\,E_{cm}(1 - 2m)^2},$$

which at the limit of $m = \frac{1}{3}$ gives

$$r_{\lim} = \frac{8\,N}{a\,b\,E_{cm}},\tag{6.8}$$

where E_{cm} is the initial tangent modulus. The limit case corresponds to a crack which goes until the middle of the throat region.

After numerical simulations we will compare the obtained results with the results obtained by formulae (6.7) and (6.8). But before the calculations we have to convert the load N and the moment M to boundary conditions for the Lamé equation. Fig. 6.16 shows the design model for a hinge.

The boundary conditions are defined as follows:

$$\begin{cases} \mathbf{u} = 0, & \text{on} \quad \Gamma_u, \\ \sigma_n = 0, & \text{on} \quad \Gamma_n, \\ \sigma_n = 0, & \text{on} \quad \Gamma_c, \\ \sigma_n = q(x), & \text{on} \quad \Gamma_p, \end{cases}\tag{6.9}$$
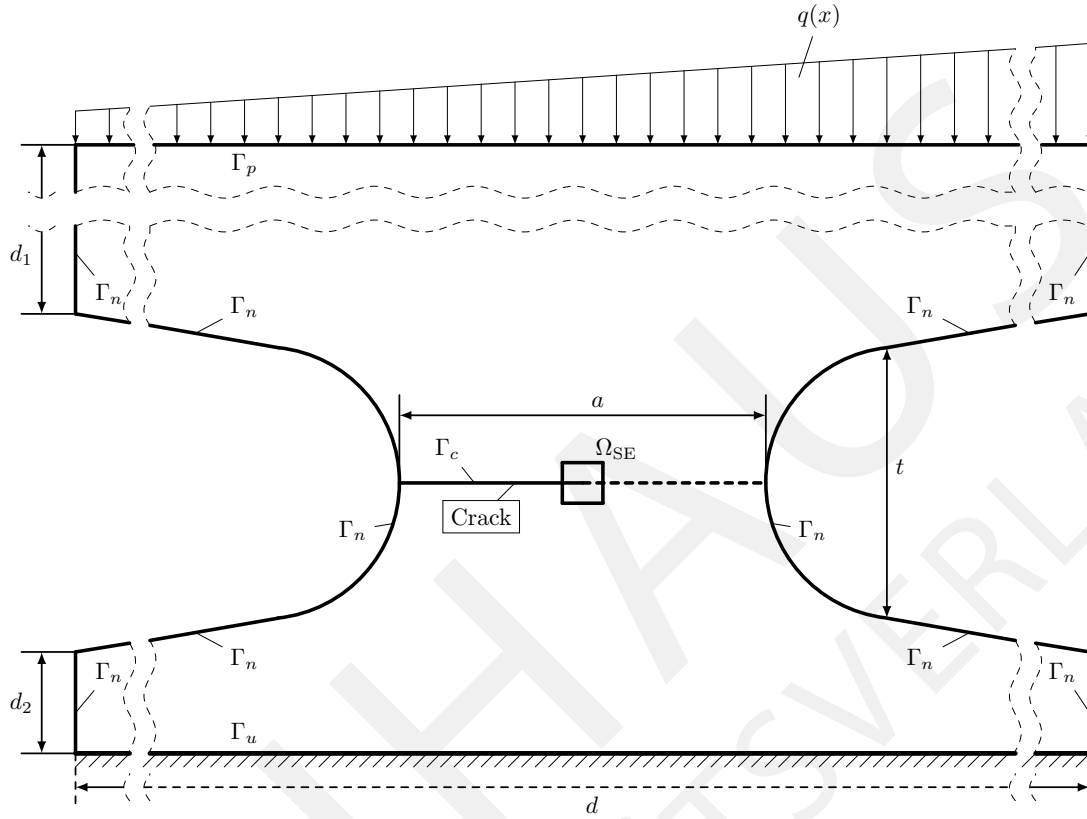
141

Figure 6.16: Design model for a concrete hinge

where the linear load function $q(x)$ is constructed from the stresses σ_{left} and σ_{right} which are calculated as follows

$$\sigma_{left} = -|N| + \frac{M}{\omega'}, \qquad \sigma_{right} = -|N| - \frac{M}{\omega'}, \tag{6.10}$$

where

$$\omega' = \frac{d^2}{6},$$

and the moment M can be calculated from the load N by using

$$M = \frac{|N|\, a}{3}.$$

We will perform all calculations for the concrete $C60$ with the material parameters

$$E_{cm} = 38.9 \cdot 10^9 \ \text{N/m}^2, \quad \nu = 0.2.$$

We take the following value for the vertical load N

$$N = -10.0 \ \text{MN}.$$

142

Taking $b = 1$ m and $m = \frac{1}{3}$ corresponding to the critical case we obtain

$$
\begin{aligned}
\sigma_r^{(c)} &= -200 \text{ M Pa}, & M &= 0.66 \text{ MN m}, \\
\sigma_{left} &= -9 \text{ MN/m}^2, & \sigma_{right} &= -11 \text{ MN/m}^2, \\
r_{\lim} &= -0.010282 \approx -0.58915°,
\end{aligned}
\tag{6.11}
$$

where the minus sign for the rotation angle means that rotation is in clockwise direction. The function $q(x)$ has the following form

$$
q(x) = \frac{x + \frac{d}{2}}{d} \left(\sigma_{right} - \sigma_{left} \right) + \sigma_{left}, \quad x \in \left[-\frac{d}{2}, \frac{d}{2} \right].
\tag{6.12}
$$

The load function in this form contains not only a linear part of load, but also a constant load. The constant load will lead to a contact problem with free boundary conditions on the crack faces, which is outside of the scope of this work. Since the throat stresses in front of the crack tip and the rotation of a hinge are not influenced by the constant load, we remove the constant part from the function $q(x)$. Finally we obtain the following loading function

$$
q(x) = \frac{x + \frac{d}{2}}{d} \left(\sigma_{right} - \sigma_{left} \right), \quad x \in \left[-\frac{d}{2}, \frac{d}{2} \right].
\tag{6.13}
$$

According to the chosen values (6.11) we obtain the following load function

$$
q(x) = -x - 1 \text{ MN/m}^2, \quad x \in \left[-\frac{d}{2}, \frac{d}{2} \right].
\tag{6.14}
$$

We will perform all calculations for the hinge with four coupling elements and with a global refinements of a whole finite element mesh. For the basis functions we consider the case of half-integer powers represented only by the leading term $r^{\frac{1}{2}}$. We perform a series of simulations applying refinements of the finite element mesh, particularly in the throat region. We start the calculation with 1520 degrees of freedom, in this case a mesh in the throat region is rather coarse (see Fig. 6.17). The last considered mesh contains 16928 degrees of freedom, Fig. 6.18 shows the meshing in the throat region for this case.

As we have mentioned above one of our main interests in the modelling of the concrete hinge is to investigate the stress distribution in front of the crack tip (the dashed line in Fig. 6.16). For all of the considered meshes the corresponding stresses are plotted with respect to the normalised length in Fig. 6.19. These curves are obtained by calculating the normal stresses over the elements lying in front of the crack tip. Near the crack tip the normal stresses are calculated over the analytical element, and the sign ∞ in Fig. 6.19 indicates that the stresses go to infinity at the crack tip due to the singularity.

The red curves correspond to the first three meshes where the throat region is not yet refined properly. The blue curves show the results for the meshes with a finer mesh in the throat region. As we can see from the Fig. 6.19 even in the case of a coarse mesh in the throat region one can obtain results which are comparable to finer meshes, except the peak stress in the right side of the throat. For the first considered mesh (Fig. 6.17)
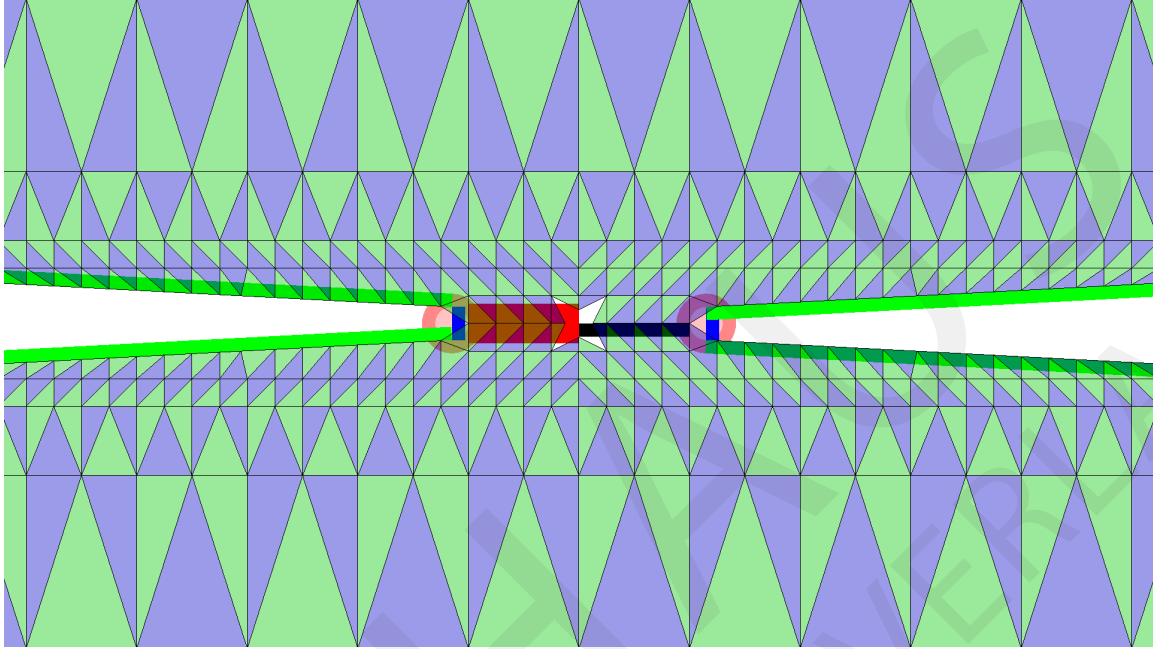
Figure 6.17: Mesh in the throat region in the case of 1520 degrees of freedom
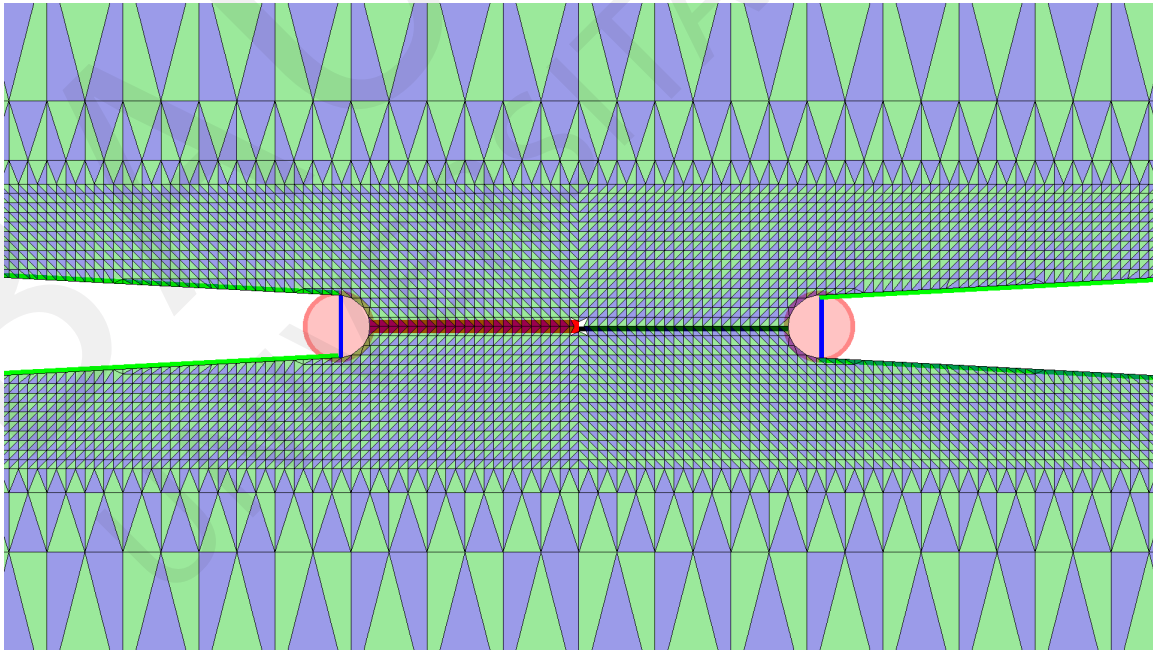

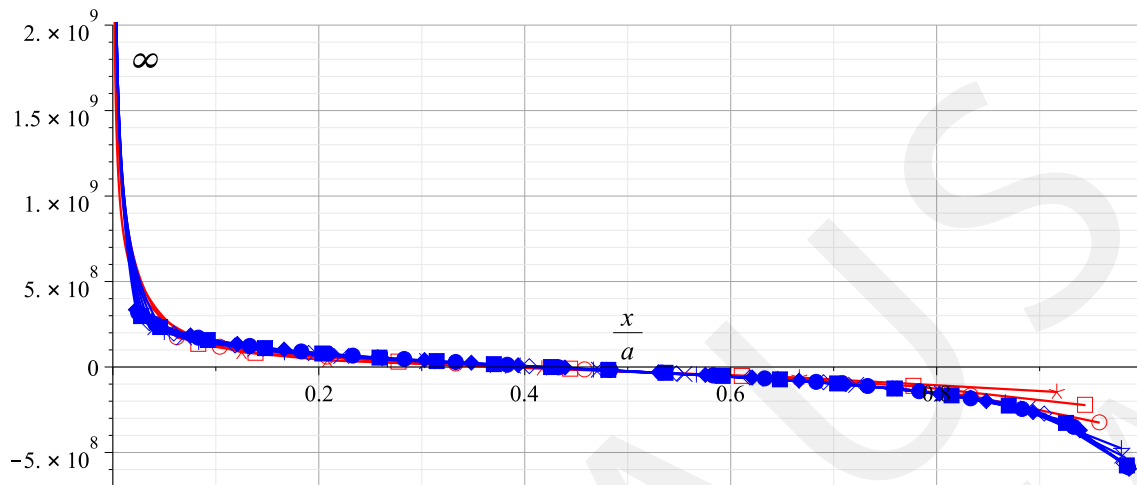Figure 6.18: Mesh in the throat region in the case of 16928 degrees of freedom

Figure 6.19: Normal stresses σ_{22} in front of the crack tip. All considered meshes

the peak stress is closed to the prediction from the engineering model (6.11), but with a refinement they stabilising to the higher value of $-600 \, \mathrm{M \, Pa}$.

Fig. 6.20 shows the normal stresses in front of the crack tip for the five most refined meshes. As we can see from the figure the curves do not change significantly any more. Thus we can say that we obtained the optimal level for refinement in the throat region to get stabilised results for the normal stresses in front of the crack tip. From this result one can also conclude that for the investigation of the stresses in the throat region 9004 degrees of freedom will be sufficient. The number of degrees of freedom is really low for such a big structure as a bridge column. But we have to underline, that our interests are to investigate the normal stresses in front of the crack tip and the rotation angle of a hinge. For deeper analysis of bridge column one definitely needs a proper refinement in the whole domain.
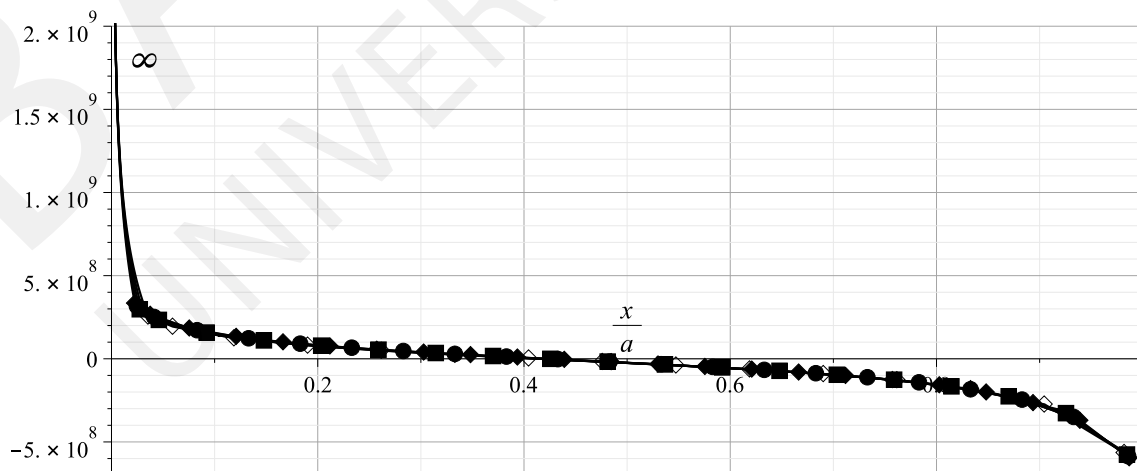

Figure 6.20: Normal stresses σ_{22} in front of the crack tip. Five the most refined meshes

145

Finally we show the normal stress curve for the finest mesh corresponding to 16928 degrees of freedom, see Fig. 6.21. All of the presented curves show the stress distributions coinciding with the expectations from engineering practice: we have infinite stresses at the crack tip and a high compression stress (peak stress) on the right part of the throat. Due to the special element we can obtain the correct asymptotic behaviour for stresses at the crack tip in the framework of the linear elastic fracture mechanics.
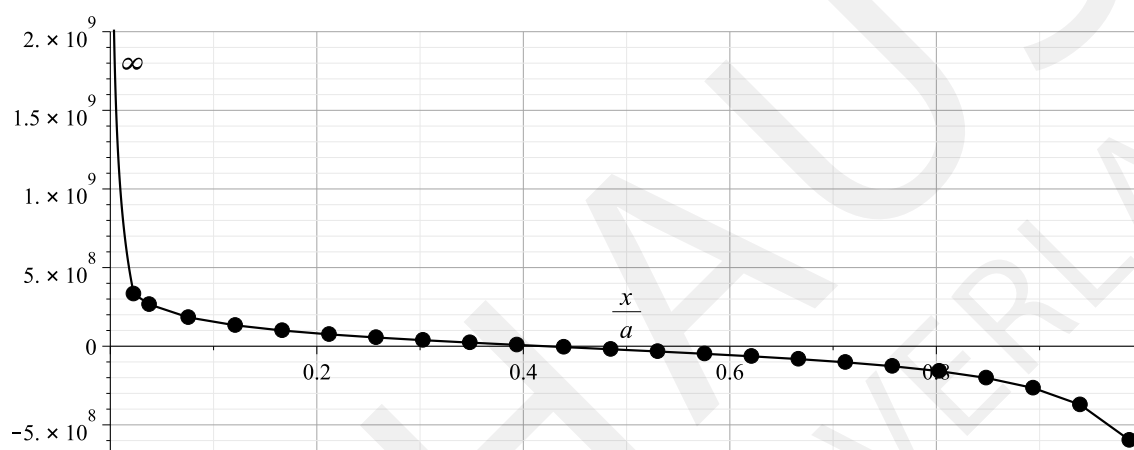

Figure 6.21: Normal stresses σ_{22} in front of the crack tip for the finest mesh, 16928 degrees of freedom

Finally we would like to present results according to study of the rotation angle of a concrete hinge. In our study we have calculated the rotation angle with respect to four lines, the corresponding angles $\alpha_i, i = 1, 2, 3, 4$ are shown in Fig. 6.22. The idea of considering four angles is to try to find a level of refinement when hinge stops to rotate as a rigid body. Because in the engineering model the rotation of a hinge is considered as a rigid body rotation. But in reality, particularly for columns of high height, one cannot expect that due a possible compression of column during deformation process. This compression can be observed with a certain level of refinement in the column. Therefore consider four angles which are calculated after the deformation process, and when we observe that they do not show similar results one can conclude that hinge doesn't rotate any more as a rigid body.

Fig. 6.23 shows the obtained results for the rotation angle. We use the following notations for the lines:

— α_1, angle calculated along the left line of the upper column;

- - - α_2, angle calculated along the central line of the upper column;

-·-· α_3, angle calculated along the right line of the upper column;

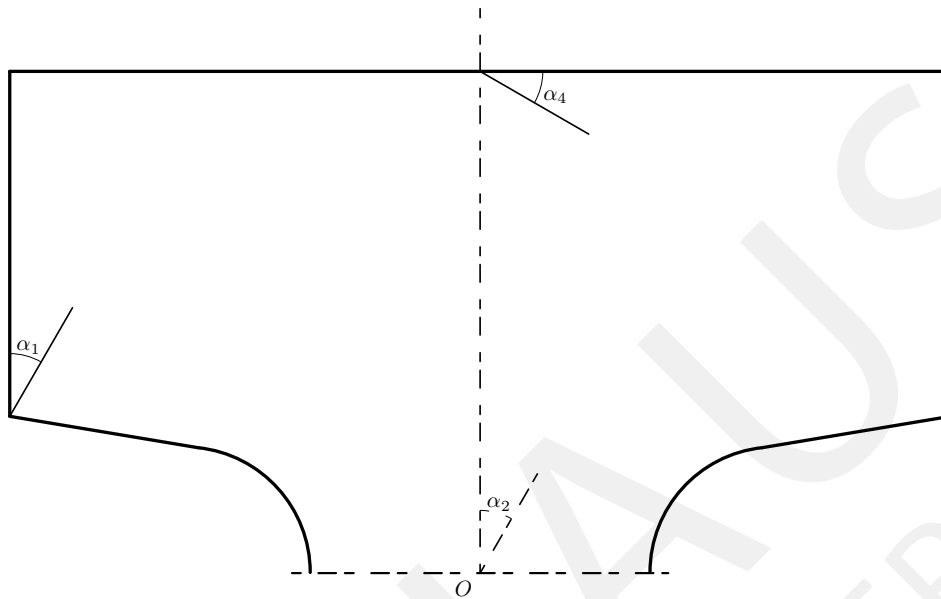······ α_4, angle calculated along the top line of the upper column.
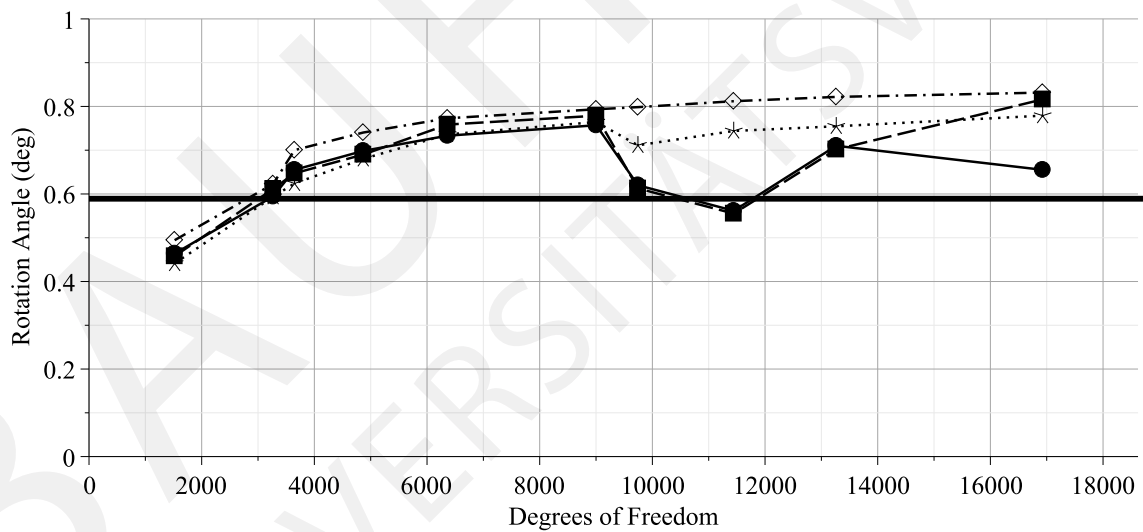
146

Figure 6.22: Four rotation angles used for calculations

Figure 6.23: Rotation angles α_1, α_2, α_3, α_4 calculated in degrees

As we can see from Fig. 6.23 up to 9004 degrees of freedom all angles α_i, $i = 1, 2, 3, 4$ are very closed to each over. But after the refinement with 9004 degrees of freedom we see that the values of the considered angles vary significantly from each other. One can conclude that in the first levels of refinement the hinge was rotating as a rigid body, but after the level of 9004 degrees of freedom one can say that the compression of the upper column is present in the finite element model. This observation has to be checked with more numerical simulations for different levels of refinement in the column.

147

The mean value of the rotation angle for 9004 degrees of freedom is

$$\alpha = -0.0134989 \approx -0.77343°.$$

The obtained value is higher than the value predicted by the model of Leonhardt (6.11) (thick line in Fig. 6.23). This observation coincides with the results for the peak stress in the throat region, which is also higher than predicted by the engineering model. To judge on quality of these two models one can perform more numerical tests, particularly by using some well-established commercial software, perform some physical experiments to validate the considered models of a hinge, or one can try to construct the reference solution for a linear elastic hinge applying the Schwarz-Christoffel mapping (3.28), which we have introduced in Chapter 3.

Fig. 6.24 shows the Schwarz-Christoffel mapping of a concrete hinge to the unit disk. In this case we approximate the curved parts in the throat region by straight lines, and after a certain refinement it gives an accurate representation of the curve. But in general case one can construct the mapping function for a polygon which has arcs as boundaries, see for example [Bjørstad & Grosse 1987, Howell 1993]. After the mapping to the unit disk we need to solve a Riemann-Hilbert boundary value problem in the unit disk. A detailed description of a transformation of a boundary value problem of linear elasticity to a Riemann-Hilbert boundary value problem is given in [Mußchelischwili 1971]. The construction of the reference solution for a concrete hinge is not yet finished task and will be considered as a next step of this research.
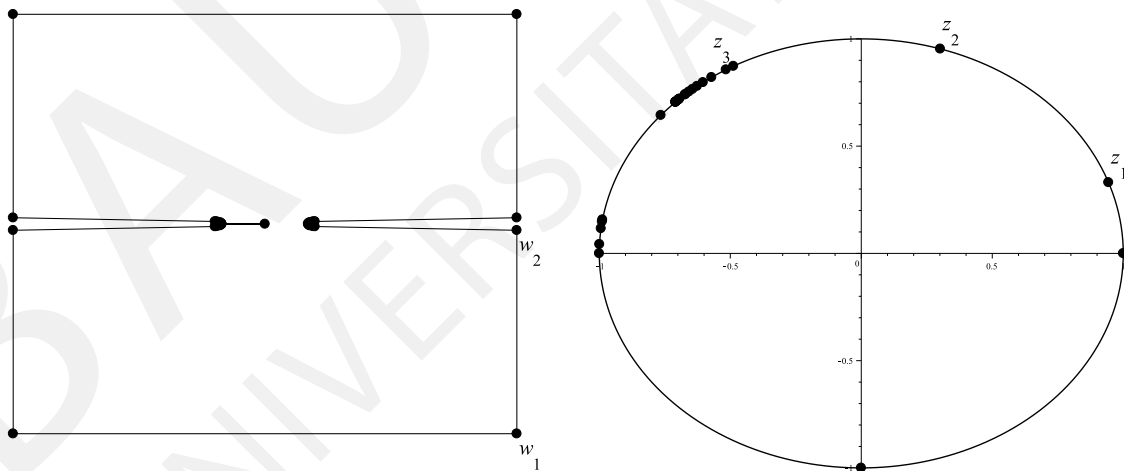

Figure 6.24: The Schwarz-Christoffel mapping of a concrete hinge to the unit disk

Chapter 7

Summary and conclusions

7.1 Summary

The goal of this thesis was to study a coupling between an analytical and a numerical solution for boundary value problems with a singularity. The problem of such a coupling comes from the fact that the analytical solution near the singularity is a purely analytical function, but the finite element solution is based on a piecewise polynomial. Therefore at the interface between the two solutions the displacement field has jumps. To overcome this problem we have introduced the new approach to obtain a continuous coupling between the analytical and the finite element solution.

To get the desired C^0 continuity we have introduced a special type of finite elements, the so-called coupling elements $\mathbb{T}$, which provide the continuity to the analytical element $\mathbb{A}$ and to the standard CST elements T. In Chapter 4 we have discussed in detail the procedure for the coupling. The interpolation problem at the interface Γ_{AD} arising in this construction was proved in Chapter 4 for an arbitrary number of the interpolation nodes. This result is a basis for the convergence analysis of the proposed method.

Additionally in Chapter 4 we have discussed a strategy how to construct a finite element mesh with a special element Ω_{SE}, which contains the analytical element $\mathbb{A}$, the coupling elements $\mathbb{T}$, and several CST elements. The main point was to propose a strategy for a refinement with an increasing number of the interpolation nodes, i.e. of the coupling element. In this strategy we used a criterion based on the shape parameter of the coupling elements. This idea allows to avoid too narrow triangles with the refinement. Finally we have proposed a strategy for numbering of the finite element mesh with the special element.

Finally in Chapter 4 we have shown how to construct the shape functions for the finite element approximation for the analytical element $\mathbb{A}$ and for the coupling elements $\mathbb{T}$. The obtained shape functions of the coupling elements $\mathbb{T}$ are the truncated analytical solution at the interface Γ_{AD} and are linear functions on the boundary with CST elements.

In Chapter 5 we have performed the numerical analysis of the proposed method. We distinguish two different strategies for the error estimation: the first strategy is based on the global refinement of the whole finite element mesh; the second strategy is based on

the idea of a fixed radius of the analytical element $\mathbb{A}$ and an increasing number of the interpolation nodes. We have proven both strategies separately.

The first strategy is similar to the classical ideas of the theory of the finite element method. But in our case we have to take care that due to construction the coupling elements cannot be considered as affine-equivalent elements to each other. To overcome this difficulty we consider the coupled element $\mathbb{T}\mathbb{A} = \mathbb{A} \cup \mathbb{T}$ in Ω_{SE} as the one element in the triangulation, and this element can be considered as the affine-equivalent to a reference coupled element. Additionally, since the coupled element $\mathbb{T}\mathbb{A}$ contains a singularity inside, we need to assure that the Sobolev embedding theorems are satisfied anyway. Due to the fact that we are interested to obtain the estimates in $W^{1,q}(\Omega)$ to satisfy the embedding $W^{2,p}(\hat{\mathbb{T}\mathbb{A}}) \hookrightarrow W^{1,q}(\hat{\mathbb{T}\mathbb{A}})$ we need to reduce the regularity p for the functions over the coupled element $\mathbb{T}\mathbb{A}$. After taking care about these problems we can apply the standard theorems of the finite element method to get the estimates.

The second strategy requires more advanced technique, since the standard theory of the finite element method cannot work in the case of an element of a fixed size. The fact of a fixed size element is close to the domain decomposition methods, but the principle idea behind the proposed method is different. The idea of the domain decomposition methods is based on the alternative method of Schwarz, which leads to an iterative procedure for the construction of the solution. But in the proposed method the global boundary value problem is solved without formulation of an additional problem in the domain Ω_{A}. Thus the proposed method is still the finite element method. Therefore we need to proposed a new strategy for the error estimation.

Due to the fixed radius of the analytical element $\mathbb{A}$ a global refinement by a scaling factor is not an appropriate choice in this case. Instead of such a global refinement we can increase the number of the coupling elements around, i.e. we increase the number of the interpolation nodes in the corresponding interpolation problem at the interface Γ_{AD}. This idea leads us to the question of the approximation by interpolation, and moreover since the values at the interpolation nodes are calculated by finite element approximation, we obtain the interpolation problem with not exact right hand side.

To estimate the error of the interpolation problem with not exact right hand side we split this error into the error of the exact interpolation and the coupling error. The error of the exact interpolation is estimated by using the classical theory of the approximation of an analytic function by its interpolating polynomial. To apply this theory we need to perform several preliminary steps, which are necessary due to the fact that the interpolation function in our case is not a polynomial. In these steps we use the proof of the main interpolation theorem from Chapter 4. To get the final estimate we use geometrical properties of the domain Ω.

The coupling error is estimated by using the alternative proof of the main interpolation theorem, which is presented in Chapter 5. The idea of this proof is based on a transformation of the original interpolation problem to an interpolation problem with a Vandermonde matrix F. The transformation is realised by using the transformation matrix M. In this case the estimation of the coupling error is based on estimates for the spectral norms of M^{-1} and F^{-1}. Due to a structure of the matrix M one can easily

calculate the spectral norm of M^{-1}, but the Vandermonde matrix F requires more effort. To get the estimate for F^{-1} we use a connection to the Discrete Fourier Transform and by the introduction of two additional matrices one can obtain the bound for the minimal and maximal eigenvalues of the matrix F^{-1}.

Finally, Chapter 6 shows first numerical experiments performed by the proposed method. The first numerical experiment is a test example with the known exact solution from the linear elastic fracture mechanics. The obtained results show that all considered cases converge to the exact solution, but total error depends on the quality of the approximation near the singularity.

The second example in Chapter 6 is a realistic example from the engineering practice. We consider a real size concrete hinge containing a crack in the throat region. For the concrete hinge we perform several simulations with different levels of refinement in the throat region. Our main interests in this study were to investigate the normal stress distribution in front of the crack tip, and to calculate the rotation angle of a hinge. The obtained results for the normal stresses show a stabilising behaviour after a certain level of the refinement in the throat region. The obtained results show qualitatively good behaviour, but the calculated values of the peak stress and of the rotation angle are higher than predicted by the engineering model.

7.2 Conclusions

The task of constructing a continuous coupling between an analytical and a numerical solution for boundary value problems with a singularity was remaining unsolved for many years. In this thesis we have proposed a new strategy which leads to the desired continuity between the two solutions. Instead of working only with numerical simulations we have proven all important steps for the proposed C^0 continuous coupling.

The main interpolation theorem, which is the basis of the continuous coupling, was proved in two ways, which were used in the error estimation process. The constructed proofs show difficulties which one has to face by working with the basis functions different to the standard set of the well-studied functions.

The error estimation proposed in the thesis considers two strategies. The most interesting case is the second strategy – the case of a fixed radius of the analytical element. This case is a new step in the finite element theory, because the classical theory cannot work for elements of a fixed size. Moreover, this strategy allows to define clearly the coupling error, which can be used to assess the quality of the coupling. To our knowledge this is the first mathematical attempt to assess the quality of a such coupling.

The considered numerical examples show promising results and confirm the potential of the proposed method. The adaptivity of the proposed method is one the most important ingredients for a practical use of the method. The possibilities to choose different combinations of the basis functions, vary the number of the coupling elements, vary the radius of the analytical element, underline the potential provided by the construction of the continuous coupling.

7.3 Open questions for future research

The work which has been done on the thesis clearly show the next steps in the research regarding to the proposed method.

One of a possible directions is to study more the coupling error: one can try to obtain the optimal node distribution to minimize the coupling error. Perhaps one needs to think about an alternative error estimate which will lead to a sharper bound.

Other possible strategies for the refinement of the special element have to be studied. Instead of using the shape parameter criterion one can fix the angle opposite to the curve edge for each refinement. One can ask a question about the optimal refinement: to find a strategy which will lead to the lower computational cost and will provide an easy way for a global or a local refinement.

To perform more numerical simulations with different versions of the method one needs to think about an efficient implementation of the proposed scheme. The implementation which was used in the thesis was motivated by scientific interest to make only first numerical simulations, because before finishing the theory of the method one cannot start to program it efficiently. But now one can start to think about higher-level programming languages and efficient algorithms.

Based on the results of simulation one can try to proof a general existence of the optimal combination between integer and half-integer powers. For some more specific examples one can try to find this combination and to prove it.

After clarifying the theoretical question one needs to make a comparison of the proposed method with the known numerical methods, like X-FEM, FEM, GFEM, etc. This comparison should be done on a test example and on a realistic example of a concrete hinge. To judge about the results for the hinge one needs to finish first the work in the direction of the Schwarz-Christoffel mapping for the hinge.

Finally one needs to start thinking about a possible generalisation of the proposed method 3D problems. In this case the exact solution will be based on the generalised Kolosov-Muskhelishvili formulae, but one needs to think carefully about a shape of the coupling elements. Because the fracture process in 3D is much more complicated than in 2D, and the method should be able to provide a certain flexibility in it.

Bibliography

[Adams & Fournier 2003] R.A. Adams, J.J.F. Fournier, *Sobolev spaces*, Elsevier B.V., 2003.

[Adams 1975] Robert A. Adams, *Sobolev spaces*, Academic Press, New York, 1975.

[Anderson 2005] T.L. Anderson, *Fracture mechanics. Fundamentals and applications*, Taylor & Francis Group, 2005.

[Argyris 1954-1955] J.H. Argyris, *Energy theorems and structural analysis, part I: General theory*, Aircraft engineering 26, 27.

[Babuška et al. 1996] I. Babuška and J.M. Melenk, *The partition of unity finite element method: Basic theory and applications.* Computational methods in applied mechanical engineering.139, 1996.

[Babuška et al. 2004] I. Babuška, U. Banerjee, J.E. Osborn, *Generalized finite element methods - main ideas, results and perspective.* International Journal of Computational Methods. Vol. 1, 2004.

[Bauch 1981] H. Bauch, *Approximationssätze für die Lösungen der Grundgleichung der Elastostatik.* Dissertation, Aachen, 1981.

[Belytschko et al. 2009] T. Belytschko, R. Gracie, G. Ventura, *A review of extended/generalized finite element methods for material modelling.* Modelling and Simulation in Materials Science and Engineering. Vol. 17, 2009.

[Bermúdez et al. 2007] A. Bermúdez, D. Gómez, M.C. Muñiz and P. Salgado, *A FEM/BEM for axisymmetric electromagnetic and thermal modelling of induction furnaces.* International Journal for Numerical Methods in Engineering. 71, 2007.

[Bieberbach 1964] L. Bieberbach, *Conformal mapping*, Chelsea Publishing Company, New-York, 1964.

[Bjørstad & Grosse 1987] Petter Bjørstad and Eric Grosse, *Conformal mapping of circular arc polygons*, SIAM, J. Sci. Stat. Comput, Vol. 8, No. 1, January 1987.

[Bock & Gürlebeck 2006] S. Bock, K. Gürlebeck, *A coupled Ritz-Galerkin approach using holomorphic and anti-holomorphic functions*. K. Gürlebeck and C. Könke eds. 17th *Conference on the Application of Computer Science and Mathematics in Architecture and Civil Engineering*, Weimar, Germany, 12-14 July 2006

[Bock & Gürlebeck 2009] S. Bock, K. Gürlebeck, *On a spatial generalization of the Kolosov-Muskhelishvili formular*. Mathematical Methods in the Applied Sciences, 32, 2009.

[Bock & Gürlebeck 2009] S. Bock, K. Gürlebeck, *On a polynomial basis generated from generalized Kolosov-Muskhelishvili formular*. Advances in Applied Clifford Algebras, 19, 2009.

[Bock 2009] S. Bock, *Über funktionentheoretische Methoden in der räumlichen Elastizitätstheorie*. Dissertation, 2009.

[Bock & Gürlebeck 2010] S. Bock, K. Gürlebeck, *On a generalized Appell system and monogenic power series*. Mathematical Methods in the Applied Sciences, 33, 2010.

[Bock et al. 2012] S. Bock, K. Gürlebeck, D. Legatiuk, *On the continuous coupling between analytical and finite element solutions*, Le Hung Son & Wolfgang Tutschke eds. *Interactions between real and complex analysis*, pp. 3 - 19. Science and Technics Publishing House, Hanoi, 2012.

[Bock et al. 2012] S. Bock, K. Gürlebeck, D. Legatiuk, *On a special finite element based on holomorphic functions*, AIP Conference proceedings 1479, 308, 2012.

[Bock et al. 2013] S. Bock, K. Gürlebeck, D. Legatiuk, *Convergence of the finite element method with holomorphic functions*. AIP Conference proceedings, 1558, 513, 2013.

[Bower 2010] Allan F. Bower, *Applied mechanics of solids*, Taylor and Francis Group, LLC, 2010.

[Brackx et al. 1982] F. Brackx, R. Delanghe & F. Sommen, *Clifford Analysis*, Pitman Publishing Inc., 1982.

[Brebbia & Dominguez 1992] C.A. Brebbia & J. Dominguez, *Boundary elements. An introductory course*, WITPress, Boston, 1992.

[Broek 1984] D. Broek, *Elementary engineering fracture mechanics*, Martinus Nijhoff Publishers, The Hague, 1984.

[Bubnov 1913] I.G. Bubnov, *Otzyv o sochineniyah professora Timoschenko (Review on works of professor Timoschenko)*, (in Russian) Sbornik instituta ingenernyh putei soobtscheniya, v. 81, Sankt-Petersburg, 1913.

[Borsuk & Kondratiev 2006] M. Borsuk, V. Kondratiev, *Elliptic boundary value problems of second order in piecewise smooth domains*, Elsevier B.V., 2006.

154

[Caçao et al. 2001] I. Caçao, K. Gürlebeck, H. Malonek, *Special monogenic polynomials and L_2-approximation*. Advances in Applied Clifford Algebras, 11, 2001.

[Caçao et al. 2004] I. Caçao, K. Gürlebeck, S. Bock, *Complete orthonormal systems of spherical monogenics – a constructive approach*. In *Methods of Complex and Clifford Analysis*, Son LH, Tutschke W, Jain S (eds), 2004.

[Ciarlet 1978] Philippe G. Ciarlet, *The finite element method for elliptic problems*, North-Holland Publishing Company, 1978.

[Ciarlet & Raviart 1971] P.G. Ciarlet, P.A. Raviart, *General Lagrange and Hermit interpolation in $\mathbb{R}^n$ with application to Finite Element Methods*, Archive. Rational mechanics. Anal, Vol. 46, 1971.

[Clough 1960] R.W. Clough, *The finite element method in plane stress analysis*, in Proceedings of the Second ASCE Conference on Electronic Computation, Pittsburg, Pennsylvania.

[Costabel & Dauge 2002] Martin Costabel and Monique Dauge, *Crack Singularities for General Elliptic Systems*. Mathematische Nachrichten, 235, 2002.

[Costabel & Stephan 1990] Martin Costabel and Ernst P. Stephan, *Coupling of finite and boundary element methods for an elastoplastic interface problem*. SIAM Journal on Numerical Analysis, 27, 1990.

[Courant 1943] R. Courant, *Variational methods for the solution of problems of equilibrium and vibrations*, Bull. Amer. Math. Soc. 49, 1943.

[Davis 1975] Philip J. Davis, *Interpolation and Approximation*, Dover Publications, Inc., 1975.

[Driscoll & Trefethen 2002] Tobin A. Driscoll, Lloyd N. Trefethen, *Scwarz-Christoffel mapping*, Cambridge University Press 2002.

[Ferreira 1999] Paulo J.S.G. Ferreira, *Superresolution, the recovery of missing samples and Vandermonde matrices on the unit circle*. Proceedings of the 1999 Workshop on Sampling Theory and Applications, Loen, Norway, 1999.

[Fleming et al. 1997] M. Fleming, Y.A. Chu, B. Moran and T. Belytschko, *Enriched element-free Galerkin methods for crack tip fields*, International journal for numerical methods in engineering, Volume 40, 1997.

[Fueter 1935] R. Fueter, *Die Funktionentheorie der Differentialgleichungen $\Delta u = 0$ und $\Delta\Delta u = 0$ mit vier reellen Variablen*. Commentarii Mathematici Helvetici, **7**: 307-330, 1935.

155

[Gaier 1964] Dieter Gaier, *Konstruktive Methoden der konformen Abbildung*, Springer Tracts in Natural Philosophy. Ergebnisse der angewandten Mathematik, Volume 3, 1964.

[Gaier 1987] Dieter Gaier, *Lecture on complex approximation*, Birkhäuser Boston Inc., 1987.

[Galerkin 1915] B.G. Galerkin, *Stergni i plastiny. Ryady v nekotoryh voprosah uprugogo ravnovesiya stergnei i plastin (Beams and plates. Series in some questions on elastic equilibrium of beams and plates)*, (in Russian) Vestnik ingenerov, v. 19, 1915.

[Gantmacher 1966] Felix R. Gantmacher, *Teoriya matric (Matrix theory)*, (in Russian) Nauka, 1966.

[Gerschgorin 1931] S. Gerschgorin, *Über die Abgrenzung der Eigenwerte einer Matrix*, Bulletin de L'académie des Sciences de L'URSS, 1931.

[Goursat 1898] K. Goursat, *Sur l'équation $\Delta\Delta u = 0$*, Bull. Soc. Math. France 26, 1898.

[Green & Zerna 1968] A.E. Green, W. Zerna, *Theoretical elasticity*, Oxford University Press, 1968.

[Grisvard 1985] P. Grisvard, *Elliptic problems in nonsmooth domains*, Pitman Publishing INC, 1985.

[Grisvard 1992] P. Grisvard, *Singularities in boundary value problems*, Springer-Verlag, 1992.

[Gürlebeck & Sprößig 1989] K. Gürlebeck and W. Sprößig, *Quaternionic analysis and elliptic boundary value problems*, Akademieverlag Berlin, Math. Research 56, 1989.

[Gürlebeck & Sprößig 1997] K. Gürlebeck and W. Sprößig, *Quaternionic and Clifford Calculus for Physicists and Engineers*, John Wiley & Sons, 1997.

[Gürlebeck et al. 2008] K. Gürlebeck, K. Habetha, W. Sprößig, *Holomorphic functions in the plane and n-dimensional spaces*, Birkhä ser, 2008.

[Gürlebeck & Legatiuk 2014] K. Gürlebeck and D. Legatiuk, *On the continuous coupling of finite elements with holomorphic basis functions*, "Hypercomplex Analysis: New perspectives and applications" in the series "Trends in Mathematics", ISBN: 978-3-319-08770-2, Birkhäuser, Basel, 2014.

[Howell 1993] Louis H. Howell, *Numerical conformal mapping of circular arc polygons*, Journal of Computational and Applied Mathematics 46, 1993.

[Hsiao et al. 2000] G.C. Hsiao, E. Schnack, W.L. Wendland, *Hybrid coupled finite–boundary element methods for elliptic systems of second order.* Computer Methods in Applied Mechanics and Engineering, 190, 2000.

[Hunter & Nachtergaele 2001] John K. Hunter, Bruno Nachtergaele, *Applied analysis*, World Scientific Publishing Co Pte Ltd, 2001.

[Ilyushin 1971] Ilyushin A.A., *Mekhanika sploshnoy sredy (Continuum mechanics)*, (in Russian) Moscow State University Press, Moscow, 1971.

[Ilyushin & Lensky 1959] Ilyushin A.A. and Lensky V.S., *Soptotivlenie materialov (Strength of Materials)*, (in Russian) State Press for Physical and Mathematical Literature, Moscow, 1959.

[Kober 1957] H. Kober, *Dictionary of conformal representations*, Dover Publications, 1957.

[Kolosov 1909] G.W. Kolosov, *About one application of the complex function theory to a problem of mathematical elasticity theory*, (in Russian) Yuriew (Dorpat), Dissertation, 1909.

[Kozlov et al. 1997] V.A. Kozlov, V.G. Maz'ya, J. Rossmann, *Elliptic boundary value problems in domain with point singularities*, American Mathematical Society, 1997.

[Kozlov et al. 2001] V.A. Kozlov, V.G. Maz'ya, J. Rossmann, *Spectral problems associated with corner singularities of solutions to elliptic equations*, American Mathematical Society, 2001.

[Kravchenko 2003] Vladislav V. Kravchenko, *Applied quaternionic analysis*, Heldermann Verlag, 2003.

[Kravchenko & Shapiro 1996] Vladislav V. Kravchenko & Michael V. Shapiro, *Integral representation for spatial models of mathematical physics*, Addison Wesley Longman Limited, 1996.

[Lavrentev & Shabat 1987] M.A. Lavrentev, B.V. Shabat, *Metody teorii funktsij kompleksnogo peremennogo (Methods of the complex function theory)* (in Russian), Moscow, Nauka, 1987.

[Legatiuk et al. 2012] D. Legatiuk, S. Bock, K. Gürlebeck, *The problem of coupling between analytical solution and finite element method.* K. Gürlebeck, T. Lahmer and F. Werner eds. 19th *Conference on the Application of Computer Science and Mathematics in Architecture and Civil Engineering*, Weimar, Germany, 04-06 July 2012.

[Legatiuk et al. 2013] D. Legatiuk, K. Gürlebeck, G. Morgenthal, *Modelling of concrete hinges through coupling of analytical and finite element solutions.* Bautechnik Sonderdruck, ISSN 0932-8351, A 1556, 2013.

[Leonhardt 1986] F. Leonhardt, *Vorlesungen über Massivbau. Teil 2. Sonderfälle der Bemessung im Stahlbetonbau*, Springer-Verlag, 1986.

[Leonhardt & Reimann 1965] F. Leonhardt, H. Reimann, *Betongelenke. Versuchsbericht, Vorschläge zur Bemessung und konstruktiven Ausbildung*, Deutscher Ausschuss für Stahlbeton. Heft 175, Berlin 1965.

[Levin et al. 1978] D. Levin, N. Papamichael and A. Sideridis, *The Bergman kernel method for the numerical conformal mapping of simply connected domains*. Bautechnik Sonderdruck, J. Inst. Maths Applics., 22, 1978.

[Liebowitz 1968] H. Liebowitz, *Fracture, an advanced treatise. Volume II: Mathematical fundamentals*, Academic Press, 1968.

[Lions 1988] P.L. Lions, *On the Schwarz alternating method I*. In Domain Decomposition Methods, SIAM, 1988.

[Lions 1989] P.L. Lions, *On the Schwarz alternating method II*. In Domain Decomposition Methods, SIAM, 1989.

[Lions 1990] P.L. Lions, *On the Schwarz alternating method III*. In Domain Decomposition Methods, SIAM, 1990.

[Lurie 1965] A.I. Lurie, *Theory of elasticity*, Foundations of engineering mechanics, Springer-Verlag Berlin Heidelberg, 2005. (translated from Russian)

[Malonek 1990] H. Malonek, *Power series representation for monogenic functions in $\mathbb{R}^{m+1}$ based on a permutational product*. Complex Variables, 15, 1990.

[Malvern 1969] Lawrence E. Malvern, *Introduction to the mechanics of a continuous medium*,Prentice-Hall Inc., 1969.

[Markushevich 1967] A.I. Markushevich, *Teoriya analyticheskih functiy. Tom I: Nachala teorii (Theory of analytic function. Volume I: Beginning of theory)* (in Russian), Nauka, 1967.

[Marx & Schacht 2010] S. Marx, G. Schacht, *Gelenke in Massivbau*, Beton- und Stahlbetonbau 105 (2010), Heft 1.

[Maz'ya & Soloview 2010] V.G. Maz'ya, A.A. Soloview, *Boundary integral equations on contour with peaks*, Birkhäuser, 2010.

[Melenk 1995] Jens Markus Melenk, *On Generalized Finite Element Method*, Dissertation, 1995.

[Melenk 1997] J.M. Melenk and I. Babuška, *Approximation with harmonic and generalized harmonic polynomials in the partition of unity method*, Comput. Assist. Mech. Eng. Sci., 1997.

[Michlin 1970] S.G. Michlin, *Variationnye metody v matematicheskoi fisike (Variational methods in mathematical physics)*, (in Russian) Nauka, Moscow, 1970.

[Moisil & Théodoresco 1931] Gr.C. Moisil et N. Théodoresco, *Fonctions holomorphes dans L'espace*, Docteurs és sciences, á Paris, 1931.

[Morais & Le 2010] J. Morais and H.T. Le, *Orthogonal Appell systems of monogenic functions in the cylinder*. Mathematical Methods in the Applied Sciences, 34, 2011.

[Morgenthal & Olney 2014] Guido Morgenthal and Peter Olney, *Concrete hinges and integral bridge piers*. Submitted to ASCE Journal of Bridge Engineering, 2014.

[Mußchelischwili 1971] N.I. Mußchelischwili, *Einige Grundaufgaben der mathematischen Elastizitätstheorie*, VEB Fachbuchverlag Leipzig, 1971.

[Nehari 1952] Z. Nehari, *Conformal mapping*, Dover Publications, New York, 1952.

[Neuber 1934] H. Lurie, *Ein neuer Ansatz zur Lösung räumlicher Probleme der Elastizitätstheorie*, Journal of Applied Mathematics and Mechanics 14, 1934.

[Oden 1972] J.T. Oden, *Finite Elements of Nonlinear Continua*, McGraw-Hill, New York, 1972.

[Papkovich 1932] P.F. Papkovich, *Solution Générale des équations differentielles fondamentales d'élasticité exprimée par trois fonctions harmoniques*. Compt. Rend. Acad. Sci. Paris 195, 1932.

[Patrault et al. 2014] D. Weisz-Patrault, S. Bock, K. Gürlebeck, *Three-dimensional elasticity based on quaternion-valued potentials*. International Journal of Solids and Structures, 6, 2014.

[Phillips & Taylor 1996] G.M.M. Phillips, Peter J. Taylor, *Theory and applications of numerical analysis*, Elsevier Science & Technology Books, 1996.

[Piltner 1982] R. Piltner, *Spezielle finite Element mit Löchern, Ecken und Rissen unter Verwendung von analytischen Teillösungen*, Dissertation, 1982.

[Piltner 1985] R. Piltner, *Special finite elements with holes and internal cracks*, International journal for numerical methods in engineering, Volume 21, 1985.

[Piltner 2003] R. Piltner, *The derivation of special purpose element functions using complex solution representation*, Computer Assisted Mechanics and Engineering Sciences, Vol. 10, No. 4, 2003.

[Piltner 2008] R. Piltner, *Some remarks on finite elements with an elliptic hole*, Finite elements in analysis and design, Volume 44, Issues 12-13, 2008.

[Riemann 1851] Bernhard Riemann, *Grundlagen für eine allgemeine Theorie der Functionen einer veränderlichen complexen Grösse*, Inauguraldissertation, Göttingen, 1851.

159

[Ritz 1909] W. Ritz, *Über eine neue Methode zur Lösung gewisser Variationsprobleme der mathematischen Physik*, Journal für die Reine und Angewandte Mathematik, Volume 135, 1909.

[Rössle 2000] Andreas Rössle, *Corner singularities and regularity of weak solutions for the two-dimensional Lamé equations on domains with angular points*. Journal of Elasticity, 60, 2000.

[Schwarz 1890] *Gesammelte Mathematische Abhandlungen von H.A. Schwarz. Zweiter Band*, Verlag von Julius Springer, 1890.

[Smith et al. 1996] Barry F. Smith, Petter E. Bjørstad, William D. Gropp, *Domain Decomposition. Parallel multilevel methods for elliptic partial differential equations*, Cambridge University Press, 1996.

[Schumaker 2007] Larry Schumaker, *Spline Functions on Triangulation*, Cambridge University Press, 2007.

[Sokolnikoff 1946] I.S. Sokolnikoff, *Mathematical theory of elasticity*, McGraw-Hill Book Company, Inc., New York, 1946.

[Sobolev 1988] S.L. Sobolev, *Nekotorye primeneniya funktionalnogo analisa v matematicheskoi fisike (Some applications of functional analysis in mathematical physics)*, (in Russian) third edition, Nauka, Moscow, 1988.

[Strouboulis et al. 2001] T. Strouboulis, K. Copps, I. Babuška, *Computation Mechanics Advances. The Generalized finite element method*. Computer methods in applied mechanics and engineering, 190, 2001.

[Timoshenko & Goodier 1951] Timoshenko S. and Goodier J.N., *Theory of elasticity*, McGraw-Hill Book Company, 1951.

[Trefethen 2013] Lloyd N. Trefethen, *Approximation Theory and Approximation Practice*, SIAM, 2013.

[Turner et al. 1956] M.J. Turner, R.W. Clough, H.C. Martin, L.J. Topp, *Stiffness and deflection analysis of complex structures*, J. Aero. Sci. 23.

[Westergaard 1939] H.M. Westergaard, *Bearing pressure and cracks*, Journal of Applied Mechanics 6 (1939), pp. 49-53.

[Wloka et al. 1995] J.T. Wloka, B. Rowley, B. Lawruk, *Boundary value problems for elliptic systems*, Cambridge University Press, 1995.

[Zienkiewicz & Taylor 2000] O.C. Zienkiewicz & R.L. Taylor, *The Finite Element Method. Volume I: Basis*, Fifth Edition, Butterworth, Heinemann, 2000.

[Zienkiewicz 1971] O.C. Zienkiewicz, *The Finite Element Method in Engineering Science*, McGraw-Hill, London, 1971.

[Zienkiewicz et al. 1977] O.C. Zienkiewicz, D.W. Kelly and P. Bettes, *The coupling of the finite element method and boundary solution procedures*, International Journal for Numerical Methods in Engineering, 11, 1977.

Ehrenwörtliche Erklärung

Ich erkläre hiermit ehrenwörtlich, dass ich die vorliegende Arbeit ohne unzulässige Hilfe Dritter und ohne Benutzung anderer als der angegebenen Hilfsmittel angefertigt habe. Die aus anderen Quellen direkt oder indirekt übernommenen Daten und Konzepte sind unter Angabe der Quelle gekennzeichnet.

Weitere Personen waren an der inhaltlich-materiellen Erstellung der vorliegenden Arbeit nicht beteiligt. Insbesondere habe ich hierfür nicht die entgeltliche Hilfe von Vermittlungs- bzw. Beratungsdiensten (Promotionsberater oder anderer Personen) in Anspruch genommen. Niemand hat von mir unmittelbar oder mittelbar geldwerte Leistungen für Arbeiten erhalten, die im Zusammenhang mit dem Inhalt der vorgelegten Dissertation stehen.

Die Arbeit wurde bisher weder im In- noch im Ausland in gleicher oder ähnlicher Form einer anderen Prüfungsbehörde vorgelegt.

Ich versichere ehrenwörtlich, dass ich nach bestem Wissen der reine Wahrheit gesagt und nichts verschwiegen habe.

Ort, Datum   Unterschrift